

Role of TRP Channels in Experimental Cell Mediated Immunity

By

P SANJAI KUMAR

LIFE11201404006

**National Institute of Science Education and Research,
Bhubaneswar**

*A thesis submitted to the
Board of Studies in Life Sciences
In partial fulfillment of requirements
for the Degree of*

DOCTOR OF PHILOSOPHY

of

HOMI BHABHA NATIONAL INSTITUTE



June, 2021

Homi Bhabha National Institute¹

Recommendations of the Viva Voce Committee

As members of the Viva Voce Committee, we certify that we have read the dissertation prepared by P Sanjai Kumar entitled “Role of TRP channels in experimental cell mediated immunity” and recommend that it may be accepted as fulfilling the thesis requirement for the award of Degree of Doctor of Philosophy.

Chairman – Dr. Chandan Goswami

Date: 25/06/2021



Guide / Convener – Dr. Subhasis Chattopadhyay

Date:

18/06/2021



External member – Dr. Sanjib Kar

Date: 28/06/2021



Examiner – Prof. Anirban Basu

Date: 29/06/2021



Member 1 – Dr. Asima Bhattacharyya

Date: 25/06/2021



Member 2 – Dr. Harapriya Mohapatra

Date: 18/06/2021



Final approval and acceptance of this thesis is contingent upon the candidate's submission of the final copies of the thesis to HBNI.

I/We hereby certify that I/We have read this thesis prepared under my/our direction and recommend that it may be accepted as fulfilling the thesis requirement.

Date: 28/06/2021

Place: NISER, Bhubaneswar



Dr. Subhasis Chattopadhyay

Ph.D. Supervisor

STATEMENT BY AUTHOR

This dissertation has been submitted in partial fulfilment of requirements for an advanced degree at Homi Bhabha National Institute (HBNI) and is deposited in the Library to be made available to borrowers under rules of the HBNI.

Brief quotations from this dissertation are allowable without special permission, provided that accurate acknowledgement of source is made. Requests for permission for extended quotation from or reproduction of this manuscript in whole or in part may be granted by the Competent Authority of HBNI when in his or her judgment the proposed use of the material is in the interests of scholarship. In all other instances, however, permission must be obtained from the author.

P. Sanjai Kumar
P Sanjai Kumar

DECLARATION

I, hereby declare that the investigation presented in the thesis has been carried out by me. The work is original and has not been submitted earlier as a whole or in part for a degree / diploma at this or any other Institution / University.

P. Sanjai Kumar
P Sanjai Kumar

LIST OF PUBLICATIONS

Journal Publications:

a. Published:

1. Inhibition of transient receptor potential vanilloid 1 (TRPV1) channel regulates chikungunya virus infection in macrophages. # **Kumar PS**, Nayak TK, Mahish C, Sahoo SS, Radhakrishnan A, De S, Datey A, Sahu RP, Goswami C, Chattopadhyay S, Chattopadhyay S. Arch Virol. 2021 Jan;166(1):139-155. doi: 10.1007/s00705-020-04852-8.
2. Transient receptor potential ankyrin1 channel is endogenously expressed in T cells and is involved in immune functions. Sahoo SS, Majhi RK, Tiwari A, Acharya T, # **Kumar PS**, Saha S, Kumar A, Goswami C, Chattopadhyay S. Biosci Rep. 2019 Sep 20;39(9):BSR20191437. doi: 10.1042/BSR20191437.
3. VIPER regulates naive T cell activation and effector responses: Implication in TLR4 associated acute stage T cell responses. Sahoo SS, Pratheek BM, Meena VS, Nayak TK, **Kumar PS**, Bandyopadhyay S, Maiti PK, Chattopadhyay S. Sci Rep. 2018 May 8;8(1):7118. doi: 10.1038/s41598-018-25549-8.
4. P38 and JNK Mitogen-Activated Protein Kinases Interact with Chikungunya Virus Non-structural Protein-2 and Regulate TNF Induction During Viral Infection in Macrophages. Nayak TK, Mamidi P, Sahoo SS, **Kumar PS**, Mahish C, Chatterjee S, Subudhi BB, Chattopadhyay S, Chattopadhyay S. Front Immunol. 2019 Apr 12;10:786. doi: 10.3389/fimmu.2019.00786.

b. Communicated/ Under preparation:

1. Elevation of TRPV1 expression on T cells during experimental immunosuppression. # **Kumar PS**, Mukherjee T, Khamaru S, Jupiter Nanda Kishore D, Chawla S, Sahoo S S, Chattopadhyay S. (Communicated).

2. Transient receptor potential ankyrin 1 (TRPA1) regulates Chikungunya virus infection in macrophages.
Kumar PS, Radhakrishnan A, De S, Chattopadhyay S, Chattopadhyay S. (Manuscript under preparation).
 3. Transient Receptor Potential (TRP) - Calcium axis in Viral Pathogenesis TRP-Ca²⁺ Gateway.
Kumar PS, Radhakrishnan A, De S, Chattopadhyay S, Chattopadhyay S. (Review article, Manuscript under preparation).
- # **Pertaining to thesis**

Conference proceedings:

1. Nayak TK, **Kumar PS**, Mahish C, Bandyopadhyay S, Chattopadhyay S, Chattopadhyay S. Analysis of Altered Host Cell Immunity of Macrophages during Chikungunya Virus (CHIKV) Infection, *in vitro*. “International Congress of Cell Biology”- CCMB Jan 27-31, 2018, Hyderabad, India (P217).
2. **Kumar PS**, Sahoo SS, Nayak TK, Bandyopadhyay S, Chattopadhyay S. TLR-4 Signalling Inhibitory Peptide, VIPER, Regulates T cell Activation and Effector Responses. “XLII All India Cell Biology Conference”-BITS Pilani, Dec 21-23, 2018, Goa, India. (P161).

P. Sanjai Kumar
P Sanjai Kumar

Dedicated to my family.....

ACKNOWLEDGEMENTS

I extend my profound gratitude to my mentor and Ph.D. supervisor, **Dr. Subhasis Chattopadhyay**, School of Biological Sciences (SBS), NISER, for his enthusiasm, persistent encouragement, constructive criticisms, timely advice and guidance during the course of my entire Ph.D. work. I would like to appreciate my guide for his patience while correcting my thesis and manuscripts in detail. I would also like to specially mention that the timely discourse of holy Bhagwat Gita, creative idioms and aphorisms from him really inspired my thought processes and decision making.

I want to avail myself this opportunity to express my sincerest gratitude to my doctoral committee (DC) members, **Dr. Sanjib Kar** (NISER, Bhubaneswar), **Dr. Chandan Goswami** (NISER, Bhubaneswar), **Dr. Asima Bhattacharyya** (NISER, Bhubaneswar) and **Dr. Harapriya Mohapatra** (NISER, Bhubaneswar) for their support and valuable scientific suggestions during my entire Ph.D. tenure. I sincerely thank **Dr. Chandan Goswami** for his help and guidance in my TRP channel work. I sincerely appreciate **Dr. Saurabh Chawla** (NISER, Bhubaneswar) for his help and support while doing animal experiments.

It gives me immense pleasure to extend my cordial gratitude to **Dr. Soma Chattopadhyay** (ILS, Bhubaneswar) for her constant help, motivation and moral support, which helped in the smooth completion of my work. I shall always remain indebted to her for imparting me the scientific skills and emotional support during my difficult times. Honestly, it was an honor working with her.

I would also like to thank all funding agencies (DAE, DST, CSIR and DBT) for financial support and fellowship during the Ph.D. I would also like to acknowledge both academic and non-academic SBS office staff for their support and co-operation.

I sincerely thank all my current and former lab members, **Dr. Tapas Kumar Nayak**, **Dr. Belluru M. Pratheek**, **Dr. Subhransu Sekhar Sahoo**, **Dr. Pradeep Kumar Singh**, **Dr. Saumya Bandyopadhyay**, and my juniors **Chandan**, **Tathagatha**, **Somlata**, **Megha**, **Jupiter** and **Manas**. My deepest appreciation to my outstanding junior, **Anukrishna** for helping me with experimental work and hours of manuscript/thesis editing. I am also thankful to my wonderful friends in NISER for their support and encouragement during difficult times. I am grateful to **Pragyesh**, **Durga**, **Dinesh**, **Himani**, **Soumya**, **Pratiksha** and **Bushra** for giving me the best times in NISER.

I would like to express my heartfelt gratitude to my family for their support and inspiration at each and every step of life. I thank my loving parents, **Mr. P Ananda Rao** and **Ms. P Uma Maheswari** and caring sister, **Ms. P Karuna Kumari**, for always believing in me. I am gratified to my wife **Ms. Sweta Smita Pani** for her constant moral and emotional support during my Ph.D. tenure.

Finally, I blissfully thank the Almighty God for his blessings on me.

P. Sanjai Kumar
P Sanjai Kumar

CONTENTS

SUMMARY	1
List of Abbreviations	3
List of Figures	9
List of Tables	11
1 Introduction	13
1.1 Introduction to the immune system	13
1.2 Innate immune system	13
1.3 Adaptive immune system	14
1.4 Components of an immune system.....	15
1.5 Transient receptor potential (TRP) channel.....	16
1.6 Transient receptor potential vanilloid 1 (TRPV1).....	16
1.7 Transient receptor potential ankyrin 1 (TRPA1).....	17
1.8 Chikungunya Virus (CHIKV)	17
1.9 B16F10 culture supernatant (B16F10-CS).....	18
1.10 FK506 (Tacrolimus)	18
2 Review of Literature	21
2.1 History of TRP channels.....	21
2.2 Diversity in TRP superfamily.....	22
2.3 Structure of TRP channels	26
2.3.1 TRPC	26
2.3.2 TRPV	27

2.3.3	TRPM	28
2.3.4	TRPA	28
2.3.5	TRPP and TRPML.....	29
2.4	TRPV1 and TRPA1 channels in macrophages.....	30
2.4.1	TRPV1	31
2.4.2	TRPA1	32
2.5	Role of TRPV1 and TRPA1 channels in T-lymphocytes.....	33
2.5.1	TRPV1	34
2.5.2	TRPA1	35
2.6	TRP channels and Virus infections	38
2.7	TRP channels in immune supression.....	43
3	Hypothesis and specific objectives.....	45
3.1	Hypothesis	46
3.2	Specific Objectives	46
4	Materials and Methods.....	47
4.1	Materials	48
4.1.1	Cell lines and virus	48
4.1.2	Animals.....	48
4.1.3	Antibodies:.....	48
4.1.4	Chemicals, reagents, and modulators:.....	50
4.1.5	Buffers and other reagents composition.....	53
4.1.6	Kits.....	54
4.2	Methods	54

4.2.1	CHIKV infection in macrophages	54
4.2.2	Splenocyte isolation.....	55
4.2.3	T cell purification	55
4.2.4	Flow cytometry (FC)	56
4.2.5	MTT assay	57
4.2.6	Plaque assay.....	57
4.2.7	Time-of-addition assay	57
4.2.8	Real-time RT-PCR	58
4.2.9	Immunocytochemistry (ICC).....	58
4.2.10	ELISA	59
4.2.11	Western blot.....	60
4.2.12	7-AAD staining.....	60
4.2.13	Calcium Imaging	60
4.2.14	Statistical analysis.....	61
5.	Results.....	64
5.1	Regulatory role of TRPV1 in CHIKV infection	64
5.1.1	CHIKV upregulates TRPV1 expression in macrophages.....	64
5.1.2	Assessment of TRPV1 antibody specificity	65
5.1.3	Cell viability assay for macrophages in the presence of TRPV1 modulators	66
5.1.4	TRPV1 regulates CHIKV infection.....	67
5.1.5	TRPV1 regulates CHIKV viral titer	70
5.1.6	TRPV1 modulates the early phases of the CHIKV life-cycle	70

5.1.7	TRPV1 modulates the CHIKV-induced pro-inflammatory cytokine response in host macrophages	73
5.1.8	Pro-inflammatory cytokine response in macrophages treated with TRPV1 modulators	74
5.1.9	Expression and nuclear localization of pNF- κ B (p65) in CHIKV-infected macrophages, in presence or absence of TRPV1 modulators	75
5.1.10	TRPV1 modulates Ca ²⁺ influx in macrophages.....	77
5.2	Regulatory role of TRPA1 in CHIKV infection	80
5.2.1	CHIKV upregulates TRPA1 expression in macrophages.....	80
5.2.2	Assessment of TRPA1 antibody specificity	82
5.2.3	Cell viability assay for macrophages in the presence of TRPA1 modulators	82
5.2.4	TRPA1 regulates CHIKV infection.....	83
5.2.5	TRPA1 regulates CHIKV viral titer	86
5.2.6	TRPA1 modulates the early phases of the CHIKV life-cycle	87
5.2.7	TRPA1 modulates the CHIKV-induced pro-inflammatory cytokine response in host macrophages	88
5.2.8	TRPA1 modulates Ca ²⁺ influx during CHIKV infection in macrophages	89
5.3	Regulatory role of TRPA1 in T cell activation.....	92
5.3.1	TRPA1 expression in mouse T cells.....	92
5.3.2	TRPA1 regulates T cell activation.....	93
5.3.3	TRPA1 modulates T cell effector cytokine response	95
5.3.4	TRPA1 modulates Ca ²⁺ influx during T cell activation	95
5.4	Regulatory role of TRPV1 in experimental T cell immunosuppression.....	98
5.4.1	TRPV1 expression in mouse T cells.....	98

5.4.2	Cell viability assay for T cells in the presence of B16F10-CS, 5'-IRTX and FK506	99
5.4.3	Upregulation of TRPV1 during immune-activation and immunosuppression .	100
5.4.4	Modulation of cytokine response in immunosuppressed T cells.....	102
5.4.5	Modulation of intracellular Ca ²⁺ via TRPV1 channel	103
6.	Discussion	106
7.	Future Directions and Implications	116
	BIBLIOGRAPHY	117
	PUBLICATIONS	152

List of Figures

Figure 1	Phylogenetic tree of the evolutionary relationship between the TRP channels	25
Figure 2	Structure and subcellular domains of TRP channels	30
Figure 3	CHIKV upregulates TRPV1 expression in macrophages	65
Figure 4	Assessment of TRPV1 antibody specificity	66
Figure 5	Percentage of cell viability via MTT assay	67
Figure 6	TRPV1 regulates CHIKV infection.....	69
Figure 7	TRPV1 regulates CHIKV viral titer	70
Figure 8	TRPV1 modulates early phases of the CHIKV life-cycle.....	72
Figure 9	TRPV1 modulates the CHIKV-induced pro-inflammatory cytokine response in host macrophages	73
Figure 10	TRPV1 modulators alone cannot induce pro-inflammatory cytokine response in host macrophages	74
Figure 11	Expression and nuclear localization of pNF- κ B (p65) in CHIKV-infected macrophages, in presence or absence of TRPV1 modulators	76
Figure 12	TRPV1 modulates Ca ²⁺ influx in macrophages.....	78
Figure 13	CHIKV upregulates TRPA1 expression in macrophages	81
Figure 14	Assessment of TRPA1 antibody specificity	82
Figure 15	Percentage of cell viability via MTT assay	83
Figure 16	TRPA1 regulates CHIKV infection.....	85
Figure 17	TRPA1 regulates CHIKV infection.....	86
Figure 18	TRPA1 modulates early phases of the CHIKV life-cycle.....	87
Figure 19	TRPA1 modulates the CHIKV-induced pro-inflammatory cytokine response in host macrophages	88
Figure 20	TRPA1 modulates Ca ²⁺ influx during CHIKV infection in macrophages	90

Figure 21 TRPA1 expression in mouse T cells	92
Figure 22 TRPA1 regulates T cell activation	94
Figure 23 TRPA1 modulates T cell effector cytokine response	95
Figure 24 TRPA1 regulates TCR mediated calcium influx.....	96
Figure 25 TRPV1 expression in purified mouse T cells.....	99
Figure 26 T cell viability in the presence of B16F10-CS, 5'-IRTX and FK506.....	99
Figure 27 Upregulation of TRPV1 during both immune-activation and immune-suppression.....	101
Figure 28 Modulation of cytokine response in immunosuppressed T cells.....	102
Figure 29 Modulation of intracellular Ca ²⁺ via TRPV1 channel.....	103
Figure 30 Proposed working model depicting the functional role of TRPV1 in CHIKV-infected macrophages.	112
Figure 31 Proposed working model depicting the functional role of TRPA1 in CHIKV-infected macrophages.	113
Figure 32 Model depicting the relationship between TRPA1 and Ca ²⁺ in T cell activation.	113
Figure 33 Model depicting the relationship between TRPV1 expression and Ca ²⁺ levels in both activated and immuno-suppressed T cells	114

List of Tables

Table 1: Functional roles of TRP channels in macrophages and T lymphocytes	36
Table 2: TRP channels in diverse viral infections	41
Table 3: Details of antibodies used	48
Table 4: Details of chemicals used	50
Table 5: Details of buffers used	53

CHAPTER # 7

Future Directions

and

Implications

7. Future Directions and Implications

Transient receptor potential (TRP) channels are comparatively novel receptors functionally expressed on various immune cells, including macrophage and T cells. TRP channels are now known to be associated with different disease conditions and can modulate macrophage and T cell effector functions. This study examined the TRP channel's regulatory effect in macrophage and T cell functions. However, the signaling cascade associated with TRP channels is still not elucidated for the active designing of TRP-specific therapeutic strategies for the effective treatment of diseases associated with altered effector functions. Moreover, a comparative study ascertaining the TRP channel's functional role can also be tested in various experimental disease model systems *in vivo*, to further confirm their functional roles in various immune cells. Interestingly, the TRP channels are also known to be functionally expressed as heteromers (hybrid TRP channels formed of two different TRP channel families). It would be fascinating to test the properties and signaling cascades associated with these TRP channels and their functional contribution towards effector cell functions. Moreover, these TRP channels are known to be expressed on both the surface as well as intracellularly in cells. In this study, we have inspected the functional role of surface expressed TRP channels only. It would be enthralling to test the function of intracellularly expressed TRP channels and investigate TRP channel's functional association with other immune receptors such as Toll-like receptors (TLRs), RIG-I-like receptors (RLRs) and NOD-like receptors. In the future, the pharmacological intervention of TRP channels may have profound implications in developing better strategies for effective pain management and in a plethora of disease conditions.

SUMMARY

Transient receptor potential (TRP) channels are a class of non-selective, polymodal gated and cationic channel superfamily. TRP channels mediate the transmembrane flux of cations down their electrochemical gradient. These channels conduct both monovalent and divalent cations, such as Na^+ , Mg^{2+} and Ca^{2+} . Based on the homology of amino acid sequences, mammalian TRP channels has been classified into six sub-families namely TRPC (canonical), TRPV (vanilloid), TRPA (ankyrin), TRPM (melastatin), TRPML (mucolipin) and TRPP (polycystin). Mammalian TRP superfamily comprises of 28 members. Functionally TRP channels are involved in several cellular functions, including excitation, transcription, proliferation, migration, differentiation, stress responses and cell death.

TRPV1 and TRPA1 are reported to act as transducers and amplifiers of pain and inflammation. Both TRPV1 and TRPA1 have been attributed to be associated with various disease and injury states, such as inflammatory bowel disease, neurogenic inflammation, cancer pain, skin inflammation, pancreatic inflammation, lung inflammation, neurogenic inflammation and airway hyperresponsiveness. Moreover, recent evidence suggests that both TRPV1 and TRPA1 mutually control the transduction of inflammation-induced noxious stimuli.

In the current study, we have observed that both TRPV1 and TRPA1 are functionally expressed on mouse macrophage cell line, RAW 264.7 and in mouse primary splenic T cells. In macrophages, the putative role of TRPV1 and TRPA1 during CHIKV infection in macrophages was explored. Additionally, CHIKV-induced effector response was investigated. Further, the potential role of TRPV1 and TRPA1 channels in calcium influx during CHIKV infection was also studied. Similarly, in T cells also the probable role of TRPA1 in immune-activation and TRPV1 in immunosuppression was examined. Additionally, T cell effector responses during immune-activation and immunosuppression were also investigated. Further,

the possible role of TRPA1 and TRPV1 channels in T cell immune responses was also studied.

The key findings of this study are:

1. TRPV1 was found to regulate CHIKV infection in macrophages. Inhibition of TRPV1 via 5'-IRTX and activation of TRPV1 via RTX either decreases or increases CHIKV infection, respectively. Additionally, TRPV1 was found to regulate early phases of the CHIKV life-cycle, i.e., viral binding and entry. TRPV1 was also found to modulate the pNF- κ B (p65) and hence the pro-inflammatory cytokine responses as well. Finally, TRPV1 was found to functionally contribute towards Ca^{2+} influx during CHIKV infection.
2. TRPA1 was found to regulate CHIKV infection in macrophages. Activation of TRPA1 via AITC and inhibition of TRPA1 via HC-030031 either decreases or increases CHIKV infection, respectively. Additionally, TRPA1 was found to regulate early phases of the CHIKV life-cycle, i.e., viral binding and entry. TRPA1 was also found to modulate the pro-inflammatory cytokine responses. Finally, TRPA1 was found to modulate Ca^{2+} influx during CHIKV infection. It is noteworthy that TRPA1 plays an opposing role to TRPV1 during CHIKV infection in macrophages.
3. TRPA1 was found to regulate T cell activation. Inhibition of TRPA1 by A967079 inhibits T cell activation. Inhibition of TRPA1 was also found to downregulate the T cell pro-inflammatory cytokine responses. Moreover, TRPA1 was also found to functionally contribute towards Ca^{2+} influx during T cell activation.
4. TRPV1 was found to regulate experimental immunosuppression in T cells. TRPV1 was found to be upregulated in immunosuppressed T cells (via FK506 or B16F10-CS). Subsequently, we observed an immediate rise in intracellular Ca^{2+} levels in FK506 and a progressive increase in B16F10-CS treated T cells as compared to ConA or TCR treated T cells. Further, it was observed that the total intracellular Ca^{2+} levels markedly decreased in the presence of TRPV1 inhibitor 5'-IRTX.

CHAPTER # 1

Introduction

1 Introduction

1.1 Introduction to the immune system

The immune system is defined as a complex network of diverse cells, an array of defense proteins and molecules working synchronously to protect the host from invading microorganisms, cancer and abnormal physiological conditions. The immune system's main functions include identification of foreign antigens, detection of the threat level, execution of necessary action to either neutralize or destroy it, protection against its host system malfunctioning and going rogue ¹. The immune system forms the line of defense, but it is also the overwatch. This vast complex network has been subdivided into many parts based on the components and the functions it executes. The immune system is classified mainly into two branches, the innate and the adaptive immune systems. Although each part of the immune system has a distinct function, its interconnection is critical for its efficient functioning and homeostasis ¹⁻³.

1.2 Innate immune system

Innate immune responses are largely dependent on the specific molecular patterns of the invading organism or the specific signal which the system can recognize as non-self or dangerous. It acts as the first line of defense combating pathogens and other immune-stimulating agents. The patterns identified by the innate immune receptors are known as pathogen-associated molecular patterns (PAMPs), which are unique to a specific type of pathogens ^{4,5}. Molecules on bacterial surfaces and viral DNAs are some examples. The innate immune system can also recognize various signals other than from pathogens, including tissue injury and toxins which are referred as danger-associated molecular patterns (DAMPs) ^{1,3,4}. The immune receptors against PAMPs and DAMPs are widely expressed in innate immune cells such as macrophages, monocytes, dendritic cells and neutrophils. One of the most important innate immune receptors for pathogen-specific responses are Toll-

like receptor proteins (TLRs), which are expressed in plants, invertebrates, and vertebrate animals. Vertebrate immune systems are rich in various other proteins, such as complement proteins, which help neutralize toxins and microbes. These blood proteins work synchronously to get rid of the pathogen through a series of complex pathways, finally disrupting pathogen membranes, making them more susceptible to phagocytosis and producing an inflammatory response⁵³. Another critical role of innate immunity is to pass the information (via APCs) about the invading pathogenic micro-organisms to the adaptive immune system. Innate immune cells such as dendritic cells and macrophages are considered as a bridge between the innate and adaptive systems². Even though the innate immune system comprises the features like distinguishing self and non-self, immediate immune responses, specific inheritance in the genome, and interaction with a broad spectrum of molecular structures, the immunological memory by the innate immune system is still not explained or appropriately understood¹.

1.3 Adaptive immune system

The adaptive immune system is highly selective and capable of recognizing and selectively eliminating the specific foreign antigens and molecules. The antigen presentation from the innate immune cells educates the adaptive immune cells and then a series of appropriate responses are triggered. The adaptive immune system comprises various immune cells, such as B and T- Lymphocytes, derived from bone marrow and thymus, respectively. The T and B cell diversity is the outcome of a rapid gene rearrangement called the VDJ recombination. Based on the functions and the cellular processes involved, the adaptive immune system is further classified as cell-mediated immunity and humoral immunity¹⁻³.

The collective immune responses executed by T lymphocytes, including the immunological synapse formation with antigen-presenting cells, clonal selection, clonal expansion, cytokine production, coupled innate immune activation, and stimulation of the humoral immunity, are a few of the collective cell-mediated immune responses. T lymphocytes

can be further classified into helper T cells (Th-CD4 positive) and cytotoxic T cells (T_C -CD8 positive). Helper T cells finely tune which cytokines will allow the immune system to be most useful or beneficial to the host, whereas cytotoxic T cells help in clearing out infected or dysfunctional cells via perforin and granzymes. Th1 tends to produce pro-inflammatory responses responsible for clearing intracellular parasites and for autoimmune diseases. Th2 mediates the activation and maintenance of the antibody-mediated immune responses. The regulatory T cells are a sub-population of T cells that maintain tolerance to self-antigens and prevent autoimmune diseases. Additionally, depletion of Tregs elicits autoimmunity and further augments immune responses to non-self antigens. Humoral immunity is an antibody-mediated immune response produced by B lymphocytes. Antibodies produced are essential in eliminating the specific pathogens through opsonization, neutralization, activation of NK cells, complement activation, in accordance with the nature of the pathogen ¹⁻³.

1.4 Components of an immune system

In an overview, the immune system is comprised of various organs, cells, and secreted molecules. The primary (bone-marrow and thymus) and secondary (spleen and lymph nodes) lymphoid organs serve in the production and differentiation of immune cells. The immune system cells range from the innate immune cells such as neutrophils, basophils, eosinophils, monocytes, macrophages, and dendritic cells to adaptive immune cells such as T and B lymphocytes. Some cells, such as $\gamma\delta$ -T cells and natural killer cells (NKT) cells, are considered part of both innate and adaptive immune systems. Among these cells, the dendritic cells, macrophages, and B cells possess the unique ability to present antigens to the T helper cells effectively, called professional antigen-presenting cells. Upon encountering immunogenic signals, the immune system's cells may secrete various proteins, including cytokines and chemokines, such as interleukins, transforming growth factors and tumor necrosis factor. These protein molecules facilitate various immunological processes including proliferative signalling

and chemotaxis of other immune cells. Similarly, other secreted proteins in blood serum such as complement proteins and antibodies help in immediate responses against invading pathogens or harmful signals ^{1,3,5,6}.

1.5 Transient receptor potential (TRP) channel

The transient receptor potential (TRP) channels are a superfamily of proteins with more than 30 cationic channels which are distributed to 7 subfamilies and two groups based on their sequence and topological differences. Even though these channel members possess a unique genomic identity that accounts for their diversity, many conserved sequences have been profoundly identified ^{7,8}. The seven subfamilies of TRP channels named TRPC (Canonical), TRPA (Ankyrin), TRPM (Melastatin), TRPV (Vanilloid), TRPP (Polycystin) and TRPML (Mucolipin) are found to be diversely distributed in both excitable and non-excitable vertebrate cells, contributing to various essential cellular functions. On the other hand, TRPN (NOMPC) is reported to be an exclusion to vertebrate systems and is exclusively found in insects only ^{7,9-12}. TRP channels are distributed between the plasma membrane and subcellular membranes of various organelles serving as non-selective cation currents, such as $[Na^+]_i$, $[Mg^{2+}]_i$, $[Ca^{2+}]_i$, and membrane voltage (V_m) across the membranes ^{9,13,14}. These non-selective TRP cation channels are reported to be polymodal sensors of many extracellular and intracellular signals, including temperature, physical stress, and various ligands. TRP channels carry out functions including cellular division, migration, differentiation, stress responses, apoptosis and have been explicitly reported to play crucial roles in cell signaling as well ^{15,16,17}.

1.6 Transient receptor potential vanilloid 1 (TRPV1)

Transient receptor potential vanilloid 1 (TRPV1) is a polymodal receptor and acts as a non-selective, calcium-permeable, cation channel. It belongs to the vanilloid cation channel subfamily comprising of 6 members, namely TRPV1-V6 ^{12,18}. TRPV1 is the only TRPV family member sensitive to vanilloid ligands, the rest of the members of the TRPV subfamily are non-

sensitive to vanilloid compounds ¹⁹. These cation channels are very well distributed across various cells of the nervous system, including both central and peripheral nervous systems, sensory epithelial tissues and cells of immune systems playing essential roles in cell function. TRPV1, the founding member of the TRPV subfamily, is found to be an active molecular sensor to differential temperature, noxious substances, and pain modalities ²⁰⁻²³. TRPV1 is evidently described to be involved in inflammatory bowel disease (IBD), allergic asthma, colitis, arthritis, hypersensitivity, chronic obstructive pulmonary disease (COPD), and various auto-immune diseases ²³⁻²⁹.

1.7 Transient receptor potential ankyrin 1 (TRPA1)

TRPA1 is a calcium-permeable, cationic channel with polymodal activation properties and is the sole member of the TRPA family. TRPA1 acts as a sensor for pain, cold and itch. The mammalian transient receptor potential ankyrin family is characterized by nearly 14 Ankyrin repeats in their N-terminus domain ⁷. TRPA subfamily has been recognized as cold sensors and the mammalian TRPA1 are reported to have an activation temperature of 17°C ³⁰. TRPA1 channels are widely distributed in various sensory and non-sensory cells and contribute to distinct cellular functions and are reported to play pivotal roles in hearing and mechanosensation ^{31,32}. Similar to the other TRP channels, TRPA1 channels are known to be polymodal as they can be activated by a wide array of stimuli such as temperature, noxious substances, mechanical pressure and PLC mediated receptors ³³⁻³⁵. TRPA1 has been reported to be associated with neuronal inflammation, neuropathic pain, kidney injury, TNBS colitis, complex regional pain syndrome type-1, inflammatory bowel disease and chronic obstructive pulmonary disease (COPD) ³⁶⁻⁴⁷.

1.8 Chikungunya Virus (CHIKV)

Chikungunya virus (CHIKV), an alphavirus with an enveloped positive-sense ssRNA genome, belongs to the *Togaviridae* family. CHIKV is reported to have a lytic life cycle within

macrophages, epithelial cells, endothelial cells, and primary fibroblast as the main host cells. The Chikungunya virus is reported to be transmitted through *Aedes aegypti* and *Aedes albopictus*, the two well-known mosquito vectors. The genome of CHIKV consists of four non-structural (nsP1-nsP4) and five structural proteins (E1-E3, capsid and 6K). The envelope proteins E1/E2 have been well identified to play an essential role in receptor-mediated endocytosis and various innate immune responses. The replication phase of CHIKV is cytopathic and induces inflammation and pain but is susceptible to Type I and II interferons⁴⁸. The outbreak of E1: A226V mutant CHIKV in 2008 has been a big catastrophe in India's coastal areas as it is rapidly spread through the vector *Aedes albopictus*. Yet, no efficacious vaccines or antiviral therapies are available to this date.

1.9 B16F10 culture supernatant (B16F10-CS)

B16F10 is a murine transplantable melanoma that has served as an excellent model system for human melanoma. B16F10 tumor cell line is a useful tool to examine metastasis, solid tumor formation and tumor progression. The B16F10 culture supernatant (B16F10-CS) has been effectively used in various immune-suppressive studies. Recent studies on the B16F10-CS with mouse splenic mononuclear lymphocytes have evidently described the effect of the B16F10-CS in immune suppression as the inflammatory cytokine levels were significantly reduced. The components of a B16F10-CS are yet to be explored, yet a number of recent studies highlight its immunosuppressive nature in diverse immune cells, namely B cells, T cells, macrophages and neutrophils⁴⁹⁻⁵¹.

1.10 FK506 (Tacrolimus)

FK506 is a powerful macrolactam, a natural product which is produced by several *Streptomyces* species^{52,53}. FK506 is commonly used in clinical procedures, particularly during organ transplantation, for its immunosuppressive ability and is also known as Tacrolimus. It has been extensively studied in various inflammatory and pathophysiology model systems^{54,55}.

The administration of FK506 has been known to suppress T cell activation and proliferation. Moreover, FK506 disrupts signaling cascades mediated by calcium-dependent serine/threonine protein phosphatase and calcineurin (CaN). Tacrolimus forms a complex with FK506 binding protein (FKBP12), which further interacts with CaN and interferes with the activity of nuclear factors of activated T cells (NFAT), a set of transcription factors in the regulation of lymphokine gene expressions ⁵⁶⁻⁵⁸. The protein FKBP12 binds with FK506 and disrupts the interaction of FKBP12 with ryanodine receptors (RyR) and IP₃ receptors. Additionally, the administration of FK506 is also known to induce calcium flux through RyR in various cells ⁵⁸.

CHAPTER # 2
Review of Literature

2 Review of Literature

2.1 History of TRP channels.

The transient receptor potential channels have acted as a salient tool in understanding sensory physiology, including taste, hearing, smell, touch, physical stress, and temperature⁵⁹⁻⁶⁴. These non-selective TRP cation channels have been reported to be actively participating in an array of cellular functions, including excitation, migration, proliferation, transcription, differentiation, cell death and stress responses¹⁵⁻¹⁷. In 1969, Cosens and Manning, first reported the TRP-mutant in *Drosophila melanogaster*. Under low-light conditions, these “light-defective” mutants, presumably behaves as phototactically positive in T-maze but are visually impaired and behave as blind in an optomotor apparatus⁶⁵. These mutants also show transient response in electroretinogram (ERG) rather than the sustained response in “wild types”⁶⁶. Later Baruch Minke, named these channels as TRP according to the responses in ERG⁶⁷. In 1989, Craig Montell later cloned TRP genes and predicted TRP proteins structural similarity with various other channels⁶⁸. In 1992, Roger Hardie and Barunch Minke identified TRP channels as ion channels that opens in response to light stimulation⁶⁹.

The TRP channel's role in conducting calcium ions across the plasma membrane was still a mystery, as in the initial days, the theory was strong that the TRP channels could not be sensitive to light. Later studies with *Drosophila melanogaster* photoreceptor cells were adequate in eliminating this theory⁵⁹. The light-induced calcium influx studies with *trp* mutant cells have reduced intracellular calcium influx, which marked the beginning of TRP-mediated calcium influx studies^{66,68}. Studies with the voltage-clamp technique in the later era have provided enough support for the TRP-induced calcium influx, yet the quantum bump in *trp* mutant with the exposure to light was still inconclusive⁶⁷. This quantum bump was later explained by the presence of TRP-like (TRPL) proteins in *Drosophila* mutants. Finally, the TRP-mediated calcium influx was explicitly confirmed with Roger Hardie's studies in

Drosophila flies⁶⁹⁻⁷². The mutation of the Aspartate residue at the 621st position of TRP channels at their selectivity filter markedly diminished the photoreceptor cell's calcium sensitivity compared to the wild-type fly, which provided extensive information about the non-selective nature and cation conduction of the TRP channels^{59,73}.

The mammalian homolog of TRP gene was identified by Lutz Birnbaumer in 1995⁷⁴. This first report of complete characterization of the TRPC1 gene was revolutionary in the field of mammalian cation channels and later succeeding reports on the existence of conserved TRP channel genes from nematodes to humans addressed the roles of TRP channels apart from the insect photoreceptors^{74,75}. Further, reports on the mammalian TRPC1 paved the path to numerous discoveries on various other TRP channels and their functions. TRPM2 and TRPM7 were reported to be fused to enzyme domains that pioneered the TRP channel discoveries in various biochemical reactions. Later, the chanzyme TRPM6 was reported to be associated with TRPM7 in executing significant roles in hypomagnesemia and hypocalcemia⁷⁶⁻⁸¹. In 1997, the mammalian TRPV1 was discovered by Michael Caterina *et al.* and this discovery turned out to be the most important in the history of TRP channels as these capsaicin receptor channels helped in understanding the functions of TRPV1 in sensory physiology and cellular functions⁸²⁻⁸⁴.

2.2 Diversity in TRP superfamily

The discovery of the mammalian TRP canonical (TRPC) channels harbored the TRP field's scientific community's attention. Consequently, the following decade was allied with several findings in TRP channels, including new TRP channel members and their association and function relationship in various aspects of cellular functions¹⁵⁻¹⁷. These discoveries have enumerated the TRP channels to 28 members in vertebrates^{60,61}. The TRP channels have been classified into seven subfamilies and two groups based on their sequence similarity⁸⁵. The founding member of the TRP superfamily was termed the transient receptor potential canonical

or classical and the rest of the families were termed after the original designation or on the name of the stimuli, the first discovered member has been actively found responding^{60,85}.

The TRP subfamilies are grouped into two based on the sequence similarities and their topological differences. The seven subfamilies are named as TRPC (canonical), TRPV (vanilloid), TRPA (ankyrin), TRPML (mucolipin), TRPM (melastatin), TRPP (polycystin), and TRPN (NOPMC) (Figure 1). The first group is composed of five subfamilies which bear the highest sequence similarity to the founding member TRPC. This group includes TRPC, TRPA, TRPV, TRPM, and TRPN^{86,79}. All the members in group 1 except for the TRPN are expressed in various mammalian cells, integrating their function in sensory and subcellular signaling. In contrast, the TRPN is expressed in insects and only in some vertebrates, such as zebrafish¹⁰⁻¹². The members of this group possess a similar topology in their pore loop, ankyrin repeats, and TRP box 1 and 2, which attributes to the TRP domain in the intracellular domains. Group 2 is comprised of TRPP and TRPML, which are considered to be ancient as they are extended from yeast to mammals⁸⁵. The group 2 channels are considered to be distantly related to the group 1 channels. These channels share sequence homology and a conserved topology of having a large loop separating the first two transmembrane segments⁸⁷.

The subfamilies share sequence similarity and evolutionary relationships among their members. The TRPC subfamily consists of six members named TRPC1-TRPC7. All mammalian TRPC proteins are activated through protein kinase C (PKC) and associated with PKC-mediated calcium influx^{86,88,89}.

The TRPV channels are primarily found to be sensitive to vanilloid compounds and they share sequence similarity of 25% with the canonical channels^{82,85}. The founding member of this subfamily, the TRPV1, was reported to be activated by a vanilloid compound capsaicin and thus given the name transient receptor potential vanilloid channels^{87,90}. Apart from the

capsaicin, TRPV1 channels are known to be sensitive to various other stimuli such as heat and chemicals, including endocannabinoid, anandamide, camphor, and pungent compounds like piperine in black pepper and allicin in garlic ^{33,82,91-93}. There are six members in this subfamily named as TRPV1-TRPV6, and all of these channels are well-reported calcium-permeable channels ^{60,85,90,94,95}. Among these channels, TRPV4 has been attributed as an osmolarity sensor and TRPV6 has been reported to be associated with CRAC channel ^{94,96}.

TRPM, another important member of group 1, shares 20% sequence similarities to TRPC ⁸⁵. Members of this subfamily are enumerated to 8 as TRPM1-M8. TRPM channels are reported to be expressed in an array of cells, such as neurons, melanoma cells, hepatocytes, splenocytes, bone marrow cells and lung epithelial cells ^{79,97-100}. These channels are known to act as active sensors of ADP-ribose, ATP, osmolarity changes and are sensitive to cold and menthol ⁹⁹⁻¹⁰².

TRPA channels are characterized by a large number of ankyrin repeats in their N terminus domain and consist of a single member, TRPA1 ⁸⁵. TRPA1 is attributed to be a calcium conductor and are found to be sensitive to cold stimuli, mustard oil, cannabinoids, and PLC ^{30,33,35,101-103}. Like TRPA, the TRPN subfamily comprises a single member of TRPN1 and a higher number of ankyrin repeats at the N-terminus. These channels are expressed in invertebrates like worms, insects and few vertebrates such as zebrafish ^{7,9-12}. Their expression in higher vertebrates is yet to be discovered. TRPN channels are attributed to being mechanically gated ^{85,104}.

Group 2 members such as TRPP and TRPML share a sequence that is highly variant from group 1. The members of the TRPP sub-family are enumerated to 5 as TRPP1-P5. TRPP channels are known to be actively expressed in benign tumor cells and modulated by various cell-derived molecules such as PIP₂ and EGF ¹⁰⁵. TRPP channels are reported to be associated

with fluid flow and actin cytoskeleton^{85,105–108}. Similar to TRPP, the TRPML subfamily is evolutionarily distant from group 1 and encodes three different variants, such as TRPML1, TRPML2, and TRPML3. These channels are reported to be expressed in lysosomes and late endolysosomal compartments^{109–111}. TRPML1 is attributed as monovalent cation channels such as H⁺ and Na⁺ and thus, it is known to be sensitive to pH^{60,109–113}.

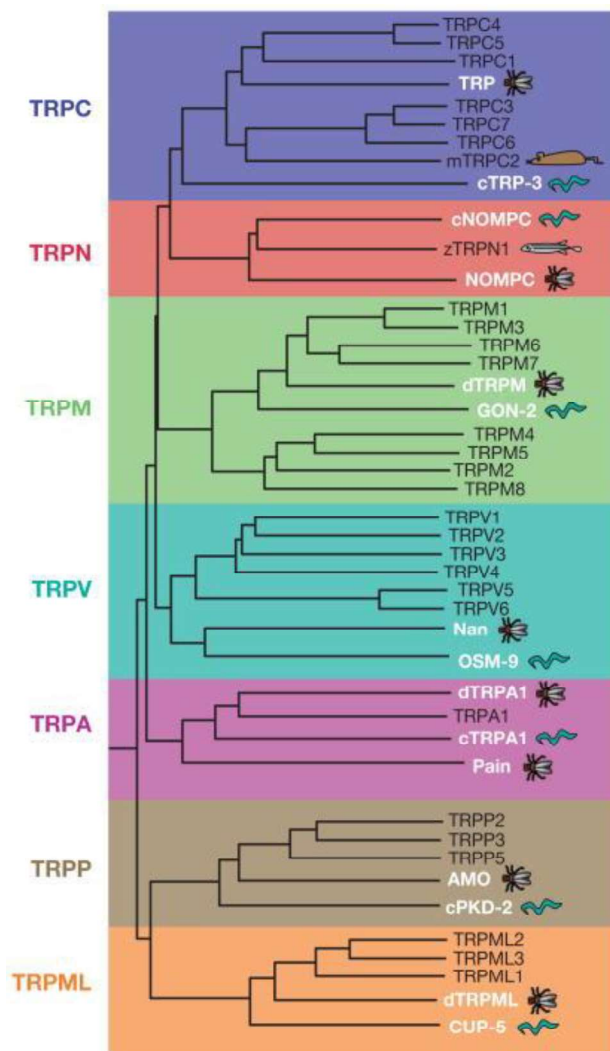


Figure 1 Phylogenetic tree of the evolutionary relationship between the TRP channels

The dendrogram tree of TRPs channels in vertebrates including humans, mouse, zebrafish. Other invertebrates including *C. elegans* and *Drosophila* is also included (Source: 60).

2.3 Structure of TRP channels

The TRP channels are similar to other voltage-gated ion channels^{114,115}. TRP channels follow six transmembrane segments typical architecture, with intracellular N and C termini¹¹⁶⁻¹¹⁸. Irrespective of the common features, TRP channels show high degrees of diversity in cation selectivity and activation mechanisms^{9,117}. The 6TM structure of the TRP channel consists of two distinct structural and functional units with the C and N termini in the cytoplasmic domain and a pore in between TM5 and TM6 with diverse functional subcellular domains (Figure 2). Segment 1 (S1) to segment 4 (S4) forms a structure that acts as an anchor and voltage sensor, while the S5 and S6 form the conduction pore⁹. Cationic selectivity of TRP channels is critically dependent on the conserved domains, which function as a selectivity filter in each channel. Most of the TRP channels have a conserved calcium selectivity filter, whereas TRPM4 and TRPM5 were discovered to be calcium-dependent monovalent cation channels¹¹⁹. Even though the TRP channels architecture is conserved across the superfamily, families of the two groups differ based on their sequence homology and topology. Except for TRPM, all the families in group 1 have conserved N-terminal ankyrin repeats, where the three members of the TRPM have C-terminal enzyme domain repeats, called chanzymes^{9,117}. The two sub-families of group 2, TRPPs and TRPML. TRPs have a shared sequence homology in segments and a large loop between the first two transmembrane domains¹¹⁴. Even though TRP channels share a typical architecture, the pore properties, subcellular domains, and affinity towards various cations differ significantly. The N termini and C termini subcellular domains of TRP subfamilies vary throughout the superfamily as these domains account for their cellular signaling and sensory functions^{9,114,117}.

2.3.1 TRPC

The transient receptor potential canonical channels subfamily is considered multifaceted for their cation selectivity within the sub-family¹²⁰. TRPC4 and TRPC5 are

attributed as non-selective for monovalent and divalent cations, whereas the rest of the members are reported specific towards divalent cations^{121–123}. Unlike many other TRP channels, members of TRPC channels do not share the homology at transmembrane segments 5 and 6 to bacterial potassium channels^{117,124}. The TRPC1 channels have been shown to form 8 alpha-helix loops and out of them, only six are known to be membrane-spanning. One of the non-membrane spanning helix is found to be located in the pore-forming region with a paucity of negatively charged amino acids^{125–127}. Studies with TRPC1 and C5 pore-forming loop and their specific residues have suggested that the channel selectivity is regulated by the aspartate and glutamate residues at the distal part of the pore entrance¹²⁵. The point mutation of these residues has been reported to significantly reduce the calcium sensitivity but not the Na⁺ sensitivity of TRPC1 and TRPC5 channels¹²⁶.

2.3.2 TRPV

Transient receptor potential vanilloid channels are well known for their sequence similarities to various other cation channels. Members of this family, such as TRPV1, 2, 3, and 4, are permeable to Ca²⁺ ions with a low affinity to monovalent cations. The PCa : PNa ratios of these channels range from 1 to 10, while the TRPV5 and six channels are highly calcium-selective with a PCa: PNa ratio of 100 or more^{124,128,129}. TRPV5 and TRPV6 channels show a minor affinity towards protons and other monovalent cations (Na⁺ ~ Li⁺ > K⁺ > Cs⁺). At a micromolar range of calcium concentration, these channels are highly selective to monovalent cations. In contrast, higher calcium concentration leads to blockade of monovalent cation permeability and enhanced selectivity towards divalent cations such as calcium^{130–132}.

TRP channels subcellular domains include six ankyrin repeats at N terminus, a TRP box and PDZ amino acid motif binding PDZ domains at C terminus, conserved throughout the subfamily¹³³. TRPV channels are known for their highly selective pore properties among the TRP superfamily and these channels share a sequence similarity at the selectivity filter to

bacterial potassium channels (KcsA, with the sequence TXXTXGYGD)^{115,128,134}. A point mutation in the aspartate residues in the selectivity filter has been reported to be reducing the affinity to voltage-dependent cations such as Ca²⁺ and Na⁺. The pore properties and affinity of the channels are mainly determined by the GM(L)GD sequence motif at the putative pore region for TRPV1, 2, 3 and 4 channels^{115,124,135}. Similar point mutations had minimal effect on the TRPV5 and V6 channels. Further studies have indicated that the pore properties of TRPV5 and V6 are determined by a ring of four aspartate residues at the selectivity filter¹³⁶⁻¹³⁸.

2.3.3 TRPM

Transient receptor potential melastatin channels comprise eight members with differential selectivity to cations¹³⁹. Among TRPM channels superfamily, the TRPM4 and M5 possess the uniqueness that they are impermeable to Ca²⁺ while TRPM2, M3 and M8 are relatively permeable to Ca²⁺, and TRPM6 and M7 are known to have a higher affinity to Ca²⁺. TRPM channels share limited sequence homology to the bacterial KcsA and TRPV¹⁴⁰. Further, the TM5 to TM6 sequences are highly conserved among the TRPM family members¹⁴¹⁻¹⁴³. It has been reported that the pore, loop and helix of TRPM channels consists of hydrophobic amino acid stretch followed by aspartate repeats, which account for their selectivity filter¹⁴³.

2.3.4 TRPA

Transient receptor potential ankyrin channel follows a similar structure to TRPV and KcsA channels with a minute difference at the helix amino acids forming the selectivity filter and two acidic amino acids at the putative pore-forming loop^{133,144}. These channel's subcellular domains comprise 17 ankyrin repeats at N-terminus and a coiled-coil domain at the C-terminus. TRPA1 channels form a heteromeric assembly with six transmembrane segments and a putative pore loop segment between the 5th and 6th transmembrane segments. Human TRPA1 channels are considered to have a pore loop of 8.2 Å. The aspartate residue at the pore's

opening (D915) is considered the constriction point of the channels, which accounts for the selectivity towards the divalent cations^{145,146}. These channels shows a PCa:PNa = 0.8 to 1.4. The aspartate amino acids (D915) at the pore-forming loop and the glutamate amino acids (E920, E924, E930) at the channels outer opening have been shown to regulate the cation specificity, as the point mutation at these selected regions significantly diminished the cation permeability^{144,146,147}.

2.3.5 TRPP and TRPML

TRPP2 forms homomeric channels and is also reported to heteromers with other TRP subfamilies, including TRPV4 and TRPC1¹⁴⁸. The intracellular domain of TRPP proteins comprises 16 PKD residues in a coiled-coil structure, which is essential for their functionality and heteromeric complex formation. Apart from this coiled-coil domain, TRPP channels are embedded with EF-hand, canonical Ca²⁺-binding domain in TRPP1/PKD2, and endoplasmic reticulum retention signal at the C- terminus, while the N-terminus is devoid of such domains^{117,133}. All three members of the TRPP family have been reported to have a PCa: PNa value in a range of 1-5, indicating that they are highly selective towards calcium¹¹⁴.

Similarly, the TRPML family is also well known for its moderate calcium selectivity. Members of this family are pH sensitive and reported to have a close association with two-pore channels¹⁴⁹. These channel's subcellular domains lack specialized domains except for an endoplasmic reticulum retention signal at the C- terminus while the N terminus remains empty, similar to TRPP channels^{9,114,117,133}. TRPML channels possess a low sequence similarity to TRPV or KcsA channels and thus, it employs a differing selectivity filter with a PCa:PNa \leq 1. The selectivity filter and pore properties of this TRPML channel are yet to be explored¹¹⁴. Recent studies on point mutation in TRPML channels have revealed that loss of function point mutations at T232P, F408del and F465L have impaired the channel's function and calcium selectivity. In contrast, the gain of function mutation at A419P has induced an intracellular

robust calcium influx. These studies indicate that the tryptophan and alanine residues may have a significant role in the channel properties of TRPML^{150,151}.

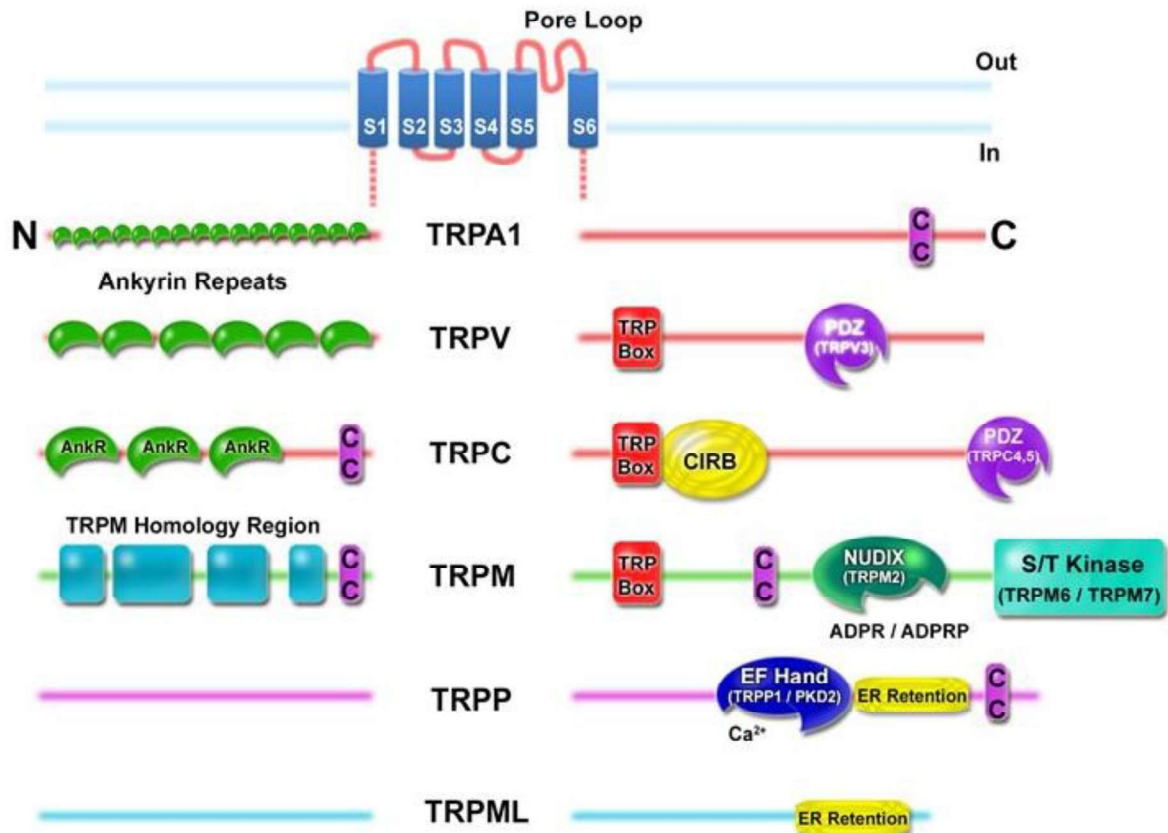


Figure 2 Structure and subcellular domains of TRP channels

Structurally, TRP channels possess a predicted 6TM topology with S5 and S6 forming a pore-loop. The intracellular N- and C- termini and the diverse functional domains for each subfamily are indicated (Source: 152).

2.4 TRPV1 and TRPA1 channels in macrophages

TRP channels are found to play important regulatory roles in many of the immune functions and diverse functional roles in an array of immune cells, such as lymphocytes, dendritic cells, T cells, monocytes and macrophages^{153–156}. Macrophages, the phagocytic innate immune cells, express several TRP channels such as TRPA1, TRPV1, TRPV2, TRPC1, TRPC6, TRPM2, TRPM4 and TRPM7^{44,157–159}. The list of functional TRP channels expressed

on macrophages is summarized in Table 1. Under various pathophysiological conditions, TRPV1 and TRPA1 channels have been reported to play an immense role in macrophage activation, migration and effector responses, such as cytokine production and nitric oxide production^{38,39}.

2.4.1 TRPV1

Transient receptor potential vanilloid channels are an essential contributor to the survival and proper functioning of macrophages^{160,161}. TRPV1 functional and pathophysiological roles in various macrophage-model systems have been actively explored. Further, TRPV1 has also been found to be involved in macrophage polarization. Activation of TRPV1 via capsaicin has been reported in polarizing M1 macrophages to M2 macrophages. Conversely, inhibition of TRPV1 by capsazepine downregulated the M2 polarisation in macrophages¹⁶². TRPV1 has also been attributed to neovascularization. Activation of TRPV1 has been found to induce collateral vessel growth (arteriogenesis) in rat hind limbs¹⁶³. Additionally, TRPV1 has been found to be regulating critical macrophage function such as phagocytosis. A recent study on a sepsis model of cecal ligation and puncture (CLP) has shown that the ablation of TRPV1 resulted in impaired bacterial clearance and phagocytosis in LPS-stimulated TRPV1 KO mice compared to its WT (wild-type) mice and the functional inhibition of TRPV1 through antagonist administration resulted in macrophage population with dysfunctional phagocytosis. Similarly, studies with TRPV1 KO models have evidently reported that TRPV1 deletion may impair the macrophage-defense mechanisms^{39,161,164}. Moreover, TRPV1 has also been found to be involved in diverse pathophysiology. A physiological dose of oral capsaicin prevented auto-immunity induced via P2-peptide in experimental autoimmune neuritis (EAN) model in Lewis rat¹⁶⁵. A recent report showed that preserving the expression and function of TRPV1 may prevent renal ischemia-reperfusion (I/R) in diet-induced obese mice by reducing renal macrophage infiltration and reducing pro-

inflammatory cytokine response¹⁶⁶. Moreover, it has been found that after renal I/R injury, TRPV1-positive nerves degeneration leads to exacerbation of salt-induced hypertension and tissue injury in rats via macrophages¹⁶⁷. Recently, it has been reported that injection of complete Freund's adjuvant in the hind paw produces mechanical and thermal hyperalgesia in mouse. In TRPV1 knock-out mice, direct injection of C5a did not produce any thermal hyperalgesia. This study highlights the importance of macrophage-to-neuron signaling in pain processing and the involvement of TRPV1 in cross-cellular communication^{168,169}. Interestingly, TRPV1 has also been reported to be associated with other receptors such as TLRs. It has been reported that TRPV1 and TLR4 work in conjunction in an autoimmune model of acute gout attack¹⁷⁰.

2.4.2 TRPA1

TRPA1 has been attributed to diverse functional roles in monocyte/macrophage activation, migration and secretion of various immune molecules^{41,42,44-47,171,172}. It has been found that TRPA1 regulates macrophage phenotype plasticity and in the possible regulation of atherosclerosis¹⁷³. TRPA1 has also been found actively in promoting neovascularization. During corneal wound healing, transactivation by vascular endothelial growth factor receptors (VEGFR) of TRPA1 contributes to mediating neovascularization and macrophage infiltration in cauterization corneal mouse wound healing model¹⁷⁴. Like TRPV1, TRPA1 has also been accredited in various pain modalities. It has been found that type II angiotensin II receptor (AT2R) in macrophages triggers intercellular redox communications via TRPA1 channels¹⁷⁵. Further, it has been reported that mechanical or cold allodynia in the hind limb of chronic post-ischemia pain (CPIP) was reduced in *Trpa1*^{-/-} mice and transiently after administration of TRPA1 agonists⁴³. Further, knocking out TRPA1 has also been found to exacerbate injury and inflammation, providing protection. It has been found that in *Trpa1*^{-/-} mice, the proinflammatory cytokine and receptors are markedly overexpressed in the kidneys.

Activation of murine macrophages with phorbol 12-myristate 13-acetate (PMA) downregulated TRPA1 gene expression⁴⁶. Another similar study has shown that following renal ischemia-reperfusion injury (IRI), *Trpa1*^{-/-} mice developed alleviated acute kidney injury (AKI) symptoms. Additionally, *Trpa1*^{-/-} mouse kidneys displayed increased M1 macrophage infiltration¹⁷⁶. Further, in the atopic dermatitis (AD) model, reduced dermal mast cell infiltration, Th2 cytokines, proinflammatory cytokines, and macrophage infiltration were observed in the TRPA1^{-/-} mice as compared to the WT. Moreover, AD-like symptoms were also alleviated by TRPA1 antagonist HC-030031 in mice¹⁷⁷. Recently, another report has shown that the inhibition of TRPA1 may protect THP-1 derived macrophages from lysophosphatidylcholine (LPC)-induced injury¹⁷⁸. Similarly, a recent report has shown that during colitis, the TRPA1 is upregulated which exerts various protective roles by decreasing proinflammatory neuropeptides, cytokines and chemokines.⁴⁴

2.5 Role of TRPV1 and TRPA1 channels in T-lymphocytes

Calcium is one of the key regulators of T-lymphocytes, and it is extensively reported that calcium is essential for T cell development, maturation, effector functions and cytokine release^{179,180}. A wide array of calcium channels such as CRAC, RyR channels, L-type calcium channels and various TRP channels are reported to be functionally expressed on T lymphocytes¹⁷⁹⁻¹⁸¹. These channel's functional inhibition impairs or abolishes the T cell development and effector functions in various experimental model systems. TRP channels are regarded as an essential contributor to T cell calcium influx. Members of this cation channel superfamily are expressed in T lymphocytes modulating their functions^{38,39}. Mammalian T lymphocytes express several TRP channels, including TRPC1, TRPC3, TRPC5 and TRPC6 from the canonical subfamily, TRPM2, TRPM4 and TRPM7 from the melastatin subfamily, TRPV1, TRPV5 and TRPV6 from the vanilloid subfamily and TRPA1 from the ankyrin subfamily^{38,39}. The canonical TRP channels play an essential role in TCR signaling, proliferation, and T

lymphocyte's autoimmune suppression. Recent studies described the SOCE role of TRPC1 in CD4⁺ lymphocytes as TRPC1 and C3 are functionally associated with STIM1 and the ORAI driven calcium influx in T cells¹⁸²⁻¹⁸⁴. The role of TRPM channels in various T cells has been extensively explored over the years. TRPM2 and M4 channels are reported to be associated with a wide array of T lymphocyte functions such as proliferation, cytokine release and IL-2 modulation^{182,185-187}. These channels are also essential for T cell development in the thymus and fas-mediated apoptosis¹⁸⁸. Additionally, T cell-specific TRPM7 deletion in *Trpm7*^{-fl} (*Ick-Cre*) mice have significantly reduced the thymic T cell development through the progressive loss of medullary thymic tissue¹⁸⁹. The list of functional TRP channels expressed on T cells is summarized in Table 1.

Similarly, TRP channel's vanilloid and ankyrin subfamily has been profoundly expressed on the T lymphocytes population. Their critical roles in T cell survival, maturation, activation and effector functions have been extensively reported over the recent years.

2.5.1 TRPV1

Transient receptor potential vanilloid channels are an essential contributor for T cell's survival and proper functioning^{38,39}. TRPV1 functional and pathophysiological roles in various T cell-model systems have been actively explored. Thymocytes from KO mice displayed autophagy and proteasome dysfunction leading to increased apoptosis and reduced double-positive thymocytes. Additionally, in peripheral blood and spleen, a reduction in CD8⁺ and CD4⁺ T cells has been observed as compared to WT mice¹⁹⁰. TRPV1 has also been found to be essential for T cell activation. It has been observed that TCR induces Ca²⁺ influx via the TRPV1 channel. Inhibition of TRPV1 led to reduced T cell activation and effector cytokine responses^{36,191}. Additionally, TRPV1 channels are also attributed in several T cell-associated pathophysiology. Recently, it has been found that TRPV1 is involved in CD4⁺ T cells in allergic rhinitis. *Trpv1*^{-/-} and chemical inhibition reduced the Th2/Th17 cytokines compared to

WT mice ¹⁹². In Rheumatoid arthritis (RA) model, it was reported that knockout of TRPV1 displayed attenuated RA pain ¹⁹³. A recent study on TRPV1 channels in CD4⁺ cells has documented evidence of constitutive expression of TRPV1 in mice and human peripheral blood mononuclear cells (PBMCs) and Jurkat cells. Patch-clamp studies confirmed that the TRPV1 is functional in these cells as capsaicin-induced calcium currents were observed in wild-type cells, while it is absent in TRPV1 mutant strains. Upon T cell activation, an independent calcium influx apart from the conventional store-operated calcium entry was registered, which was markedly reduced in TRPV1 KO cells ^{190,194}. Further studies suggested that the TRPV1 channels are a component of the TCR signaling complex, as it is actively recruited to the TCR cluster via the Src family of tyrosine kinase-dependent pathway. Additionally, the p38 and JNK activation pathways are also reported to be impaired in TRPV1 KO cells compared to the WT cells ¹⁹⁰.

2.5.2 TRPA1

Similar to TRPV1, the transient receptor ankyrin channels are also reported to affect T cell activation and effector responses ^{20,38,39} significantly. Recent studies have reported that TRPA1 is endogenously expressed on CD4⁺ T cells and their essential role in regulating the Th1 biased inflammatory responses ¹⁹⁵. TRPA1 channels have displayed protective functions in an experimental colitis model, as their abolishment has increased Th1 effector responses such as IFN production ¹⁹⁶. In a similar study, *Il10^{-/-}Trpa1^{-/-}* mice, the colitis was accelerated and exacerbated with an increased Th1 biased, inflammatory responses ^{36,197}. Further studies have concluded that the colitis exacerbation in *Il10^{-/-}Trpa1^{-/-}* mice was due to the cytokine IFN but not IL-17A. Further, upon TCR activation, *Il10^{-/-}Trpa1^{-/-}* mice T cells displayed diminished calcium influx. Additionally, the genetic or pharmacological ablation of TRPV1 in these mice rescued the elevated calcium influx and associated inflammatory cytokine responses in colitis ³⁶.

Table 1: Functional roles of TRP channels in macrophages and T lymphocytes

TRP channels	Immune cells	Function	References
TRPM1	T lymphocyte	Modulate calcium entry	Inada et al., 2006
TRPM2	Macrophages	Cytokine production, Calcium entry, ROS production	Di et al., 2012; Gelderblom et al., 2014; Yamamoto et al., 2008
	T lymphocytes	Proliferation, Cytokine release, Development	Guse et al., 1999; Magnone et al., 2012; Wenning et al., 2011
TRPM4	Macrophages	Cytokine production, phagocytosis	Billeter et al., 2014
	T lymphocytes	Inhibition of IL-2, Cytokine production	Wenning et al., 2011; Yamamoto et al., 2008
TRPM7	T lymphocytes	Apoptosis	Jin et al., 2008
TRPV1	Macrophages	Activation, Cytokine production, Phagocytosis,	Elizabeth S. Fernandes et al., 2012; Guptill et al., 2011, Tóth et al., 2014

		Migration	
	T lymphocytes	Activation, Inflammation, TCR signalling	Bertin et al., 2016; Majhi et al., 2015
TRPV2	Macrophages	Migration, Phagocytosis, Cytokine production	Heiner et al., 2003; Link et al., 2010
TRPV5	T lymphocytes	Calcium entry	Vassilieva et al., 2013
TRPV6	T lymphocytes	Calcium entry, proliferation	Vassilieva et al., 2013
TRPC1	T lymphocytes	Activation, Calcium entry	Medic et al., 2013; Wenning et al., 2011
TRPC3	Macrophages	Development, Polarization, Apoptosis	Solanki, Dube, Tano, Birnbaumer, & Vazquez, 2014; Tano et al., 2011
	T lymphocytes	TCR signalling, Proliferation	Wenning et al., 2011
TRPC5	T lymphocytes	Autoimmune- suppression	J. Wang et al., 2009
TRPA1	Macrophages	Inhibition of Nitric oxide,	Romano, Borrelli, Fasolino, Capasso, Piscitelli, Cascio, et al., 2013

	T lymphocytes	Activation, cytokine release	Gouin, et al., 2017
TRPML1	T lymphocytes	Immune suppression	Zhang, et al., 2019
TRPM8	T lymphocytes	Immune suppression	Arcas, et al., 2019

2.6 TRP channels and Virus infections

Viruses hijack the host cellular machinery and employ tailored calcium fluxes in host cells to meet their own life-cycle necessities such as viral adsorption, infection, spread and persistence^{198,199}. Studies have shown that viruses employ a range of diverse calcium channels such as VOCCs, CRACs, L-type channels, VGCCs, SOCCs, and other ligand-gated calcium channels such as IP3Rs, RyR and TRP channels to meet their calcium requisite²⁰⁰⁻²⁰⁵

Transient receptor potential channels are recently reported to show association to various virus infections helping the virus in multiple phases of their life-cycle. The tailored calcium influx through the surface and intracellular TRP channels play an essential role in viral infections. Association of TRPV1, TRPV4, TRPA1, TRPM8, TRPML1, TRPML2 and TRPML3 channels with a plethora of viruses has been reported over the years²⁰⁶⁻²⁰⁹. A recent study on the respiratory syncytial virus (RSV), measles virus (MV) and human rhinovirus (HRV) infection in various host cells such as primary human bronchial epithelial cells (HBE), BEAS-2B, dIMR-32, human neuroblastoma cells and PBECs, have shown the association of endogenous host TRPA1, TRPV1 and TRPM8 channels with the virus^{206,207}. TRPM8 channels were upregulated following the viral infection, and the upregulation was more prominent during the later phases of the virus infections, indicating that TRPM8 may have a role in the virus replication²⁰⁷. Another temperature-sensitive channel, TRPV4, has also exhibited an

association with virus infections such as dengue, hepatitis C, and Zika viruses in human Huh7 cells. TRPV4 channels modulate the virus replication mechanism by regulating the DEAD-box RNA helicase, DDX3X²⁰⁹.

Similarly, the transient receptor potential mucolipin-1 (TRPML1) channel was associated with HIV-induced accumulation of sphingomyelin and amyloid- β peptides (A β) clearance in the lysosome of CNS neurons. TRPML1 activation through an agonist has displayed an accelerated clearance of the accumulated calcium, sphingomyelin and amyloid- β peptides (A β) from the neurons in infected host²¹⁰. Other mucolipin subfamily members, such as TRPML2 and TRPML3 are shown to play a crucial role in an array of RNA virus infections such as influenza A virus, yellow fever virus and zika virus. TRPML2 and TRPML3 channels are found to be augmenting the virus infections in immortalized STAT1^{-/-} human skin-derived fibroblasts²⁰⁸. Further analysis has shown that the TRPML channels are profoundly expressed in the endolysosomal compartments and associated to the virus vesicular trafficking at the entry phase, which in turn helps the virus to escape the endolysosomal compartment^{211,212}. The list of TRP channels associated with diverse viruses is summarized in Table 2.

2.6.1.1 TRPV1

TRPV1 and acid-sensing ion channel receptor 3 (ASIC3) are found to be upregulated during infection with respiratory syncytial virus (RSV) and measles virus (MV) in respiratory sensory neuronal and airway epithelial cells. HRV infection in dIMR-32 and lung fibroblast show significant early and short upregulation of TRPV1 at 4 hpi²⁰⁷. RSV and MV show IL-8 dependent upregulation in BEAS-2B cells and in primary bronchial epithelial cells (PBECs), where MV only shows IL-6 dependent upregulation in PBECs. These are considered important aspects for antagonist drug development against respiratory viruses²⁰⁶. Development of pruritus by upregulation of TRPV1 in neuronal cells by expression of TGR5, a bile acid membrane receptor of GPCR during Hepatitis C virus (HCV) infection, has been reported.

HCV induces STAT3 activation, which increases bioactive lipid mediators such as lysophosphatidic acid (LPA), which is associated with the expression of G protein-coupled receptors, including TRPV1 channels, which account for the HCV induced pruritus ²¹³.

Increased expression of TRPV1 is associated with herpes zoster skin disease associated with pain caused by reactivation of varicella-zoster virus (VZV). TRPV1 mediated pain responses in VZV infection are through chronic inflammation and peripheral nerve sensitization in epidermal cells. Antiviral medications accounted for an effective reduction in TRPV1 expression in epidermal cells, thereby reducing chronic pain, suggesting the direct role of TRPV1 in VZV infection ²¹⁴. Various viruses are being used as vectors for studying the effects of TRP channels under multiple conditions. Lentivirus is one such widely used vector system for multiple studies *in vitro* for HEK293 cell lines. Herpes simplex virus (HSV) vectors expressing TRPV1 channels in the host cell have been developed as an important tool for preventing virus replication ²¹⁵.

2.6.1.2 TRPA1

Respiratory viruses upregulate the TRP channel expression in differentiated sensory neurons of the human airway. Human rhinovirus (HRV), which account for common cold and chronic asthma, has also been shown to upregulate TRPA1 and TRPM8 primarily causing irritant induced airway reflexes ²⁰⁷. Infection of HRV in dIMR-32 and Wi lung fibroblast show significant early upregulation of TRPA1 at 2 hpi and was persistent upto 24 hpi whereas TRPM8 was upregulated in later phases. Viral induced soluble factors such as NGF, IL-6 and IL-8 were found to induce upregulation of TRPA1, which shows the early stage association of TRPA1 with virus ²⁰⁷.

Table 2: TRP channels in diverse viral infections

Ion channel	Virus	Host cell	Upregulated/ Downregulated	Reference
TRPV1	Respiratory syncytial virus (RSV)	Human neuroblastoma cells (SHSY5Y), PBEC, BEAS-2B, dIMR-32	Upregulated	Omar et al. 2017
		Primary human bronchial epithelial cells (HBE)	---	Harford et al. 2018
	Measles virus (MV)	Human neuroblastoma cells(SHSY5Y), PBEC, BEAS-2B, dIMR-32	Upregulated	Omar et al. 2017
	Human rhinovirus (HRV)	dMIR-32, human lung fibroblast(Wi-38), HEK cells	Upregulated	Abdullah et al. 2014
	Hepatitis C virus (HCV)	Primary Sensory neurons	---	Alhmada et al. 2017
	Herpes simplex virus-2 (HSV-2)	CD-1 males, DRG neurons	---	Cabrera et al. 2016
	Herpes simplex virus-1 (HSV-1)	Male Sprague-Dawley rats	---	Kitagawa et al. 2013
	Herpes Simplex virus (HSV)	Vero	---	Reinhart et al. 2016

	Varicella zoster virus (VZV)	Human epidermal keratinocytes	Upregulated	Han et al. 2016
TRPV4	Dengue (DENV), Hepatitis C (HCV), Zika (ZIKV)	Human Huh7 cells	---	Donate-Macian et al. 2018
TRPA1	Respiratory syncytial virus (RSV)	Human neuroblastoma cells(SHSY5Y), PBEC, BEAS-2B, dIMR-32	Upregulated	Omar et al. 2017
	Human rhinovirus (HRV)	dMIR-32, human lung fibroblast(Wi-38), HEK cells	Upregulated	Abdullah et al. 2014
	Measles virus (MV)	Human neuroblastoma cells(SHSY5Y), PBEC, BEAS-2B, dIMR-32	Upregulated	Omar et al. 2017
TRPM8	Human rhinovirus (HRV)	dMIR-32, human lung fibroblast(Wi-38), HEK cells	Upregulated	Abdullah et al. 2014
TRPML1	Human immunodeficiency virus (HIV)	Hippocampal neurons (C57BL/6 mutant gp120/APP/PS1) and SHSY5Y	---	Bae et al. 2014

TRPML2	Zika virus (ZIKV), Equine arteritis virus (EAV) Yellow fever virus (YFV), Influenza A virus (IAV), Dengue virus (DENV)	immortalized STAT1 ^{-/-} human skin-derived fibroblasts	Upregulated	Rinkenberger and Schoggins 2018
TRPML3	Influenza A virus (IAV)	immortalized STAT1 ^{-/-} human skin-derived fibroblasts	Upregulated	Rinkenberger and Schoggins 2018

2.7 TRP channels in immune suppression.

Even though the functional role of TRP channels in inflammation and associated immune responses are well reported, the functional association of TRP channels in immunosuppression is yet to be established^{44,45,172,216,217}. Various immunosuppressive agents, FK506 and cyclosporin, are reported to induce a rise in intracellular calcium levels^{58,218–223}. A few of these immunosuppressants, such as rapamycin and tacrolimus are now associated with TRP channels. Rapamycin is a potent immunosuppressant and is widely used in clinical settings to prevent organ transplant rejection and treat certain types of cancer. It has been demonstrated that rapamycin directly activates TRPML1, found in lysosomes triggering Ca²⁺ influx. Additionally, *in vitro* binding assays have shown that rapamycin directly binds to TRPML1. In TRPML1-deficient cells or in the presence of TRPML1 inhibitors, all the rapamycin effects were abolished²²⁴. Like rapamycin, tacrolimus is also a potent immunosuppressant being widely used during organ transplantation. In this study, it has been

demonstrated that TRPM8 is the pharmacological target of tacrolimus. Tacrolimus was found to evoke an intracellular rise in calcium influx in cultured mouse DRG neurons. In TRPM8-deficient cells or in the presence of TRPM8 inhibitors, all the tacrolimus effects were abolished²²⁵. Together, it seems TRPML1 and TRPM8 channels act as molecular targets of the immunosuppressant rapamycin and tacrolimus.

CHAPTER # 3

Hypothesis

and

Specific Objectives

3.1 Hypothesis

There might be differential functional surface expression of TRP channels during immune-activation and immuno-suppression.

3.2 Specific Objectives

1. To study the surface expression and frequencies of TRP channels on T cells and macrophages.
2. To investigate the surface expression and frequencies of TRP channels on T cells and macrophages associated to immune-activation and immuno-suppression.
3. To investigate the altered CMI responses associated to TRP channels directed functional regulation towards T cells and macrophages.

CHAPTER # 4

Materials and Methods

4.1 Materials

4.1.1 Cell lines and virus

The RAW 264.7 (ATCC® TIB-71™), a mouse macrophage cell line was grown in RPMI-1640 (Himedia, Mumbai, India) medium supplemented with 10% heat-inactivated fetal bovine serum (PAN Biotech, Aidenbach, Germany), L-glutamine and penstrep antibiotics at 37°C in a humidified incubator with 5% CO₂. Vero cells (an African green monkey kidney epithelial cell line), were grown in DMEM (Himedia, Mumbai, India) supplemented with 10% heat-inactivated fetal bovine serum, L-glutamine and penstrep antibiotics at 37°C in a humidified incubator with 5% CO₂.

The Vero cells and the Indian outbreak strain of CHIKV (DRDE-06, accession no. EF210157.2) were kind gifts from Dr. Manmohan Parida, Defence Research and Development Establishment (DRDE), Gwalior, India.

4.1.2 Animals

8-10 weeks old either BALB/C or C57BL/6 mice (male or female) were used in the present studies. All mice were supplied from the in-house animal facility of the National Institute of Science Education and Research (NISER). Mice were maintained in 12h light/dark cycle with standard rodent chow and water ad libitum. All the experiments were approved by Institute, according to the guidelines set by the Committee for the Purpose of Control and Supervision of Experiments on Animals (CPCSEA).

4.1.3 Antibodies:

Table 3: Details of antibodies used

SI. No.	Antibodies (Concentration/dilution)	Company	Catalog no./Clone
1	α -mouse CD90.2 APC (0.025 μ g/sample)	Tonbo biosciences, CA, USA	20-0903- U100/30-H12
2	α -mouse CD25 PE	BD Biosciences,	553866/PC61

	(0.1 µg/sample)	CA, USA	
3	α-mouse CD69 PE (0.1 µg/sample)	BD Biosciences, CA, USA	553237/H1.2F3
4	α-mouse CD69 FITC (0.1 µg/sample)	Tonbo biosciences, CA, USA	35-0691- U100/H1.2F3
5	Mouse IgG1 Isotype control	Abgenex India Pvt. Ltd. BBS, India	10- 101/MOPC31C
6	<i>In vivo</i> Ready™ α-mouse CD28 (1 µg/ml)	Tonbo Biosciences, CA, USA	40-0281- U100/37.51
7	Anti-Mouse CD3 (2 µg/ml)	Tonbo Biosciences, CA, USA	40-0032- U500/17A2
8	Isotype control APC (0.05 µg/sample)	BD Biosciences, CA, USA	553932
9	Isotype control PE (0.05 µg/sample)	BD Biosciences, CA, USA	559841
10	Anti-TRPV1 polyclonal antibody (1:200)	Alomone Lab, Jerusalem, Israel	ACC-030 0.2 ml
11	Anti-TRPA1 polyclonal antibody (1:200)	Alomone Lab, Jerusalem, Israel	ACC-037 0.2 ml
12	F(ab') ₂ -Goat anti-Rabbit IgG (H+L) Cross- Adsorbed Secondary Antibody, Alexa Fluor 488	Invitrogen, CA, USA	A-11070
13	HRP-goat anti-mouse IgG (1:3000)	BD Biosciences, CA, USA	554002/NA
14	HRP-goat anti-rabbit IgG (1:3000)	BD Biosciences, CA, USA	554021/NA

15	phospho-NF- κ B-p65 (Ser536)	Invitrogen, CA, USA	MA5-15160
----	-------------------------------------	------------------------	-----------

4.1.4 Chemicals, reagents, and modulators:

Table 4: Details of chemicals used

Sl. No.	Chemicals	Company	Catalog no.
1	Bovine serum albumin fraction-V	Himedia Laboratories Pvt. Ltd., Mumbai, India	GRM105-100G
2	Triton X-100	Sigma Aldrich, MO, USA	MB031-500ML
3	Sodium deoxycholate	Sigma Aldrich, MO, USA	D6750-25G
4	SDS (sodium dodecyl sulfate)	Sigma Aldrich, MO, USA	L6026
5	2-mercaptoethanol	Sigma Aldrich, MO, USA	63689
6	PhosStop TM (phosphatase inhibitors cocktail)	Sigma Aldrich, MO, USA	04906837001
7	Complete EDTA-free Protease inhibitor	Sigma Aldrich, MO, USA	05892970001
8	Bromophenol blue	Sigma Aldrich, MO, USA	114391
9	Crystal violet	Sigma Aldrich, MO, USA	C6158
10	Bis-Acrylamide	Himedia Laboratories Pvt. Ltd., Mumbai, India	MB005-250G
11	Glycine	Himedia Laboratories Pvt. Ltd., Mumbai, India	MB013-1KG
12	Sodium chloride	Himedia Laboratories Pvt. Ltd., Mumbai, India	GRM031-1KG

13	Tris base	Himedia Laboratories Pvt. Ltd., Mumbai, India	TC072-1KG
14	Sodium azide	Himedia Laboratories Pvt. Ltd., Mumbai, India	GRM123-100G
15	EDTA	Himedia Laboratories Pvt. Ltd., Mumbai, India	R066-500ML
16	Glycerol	Himedia Laboratories Pvt. Ltd., Mumbai, India	MB060-500ML
17	Sulphuric acid (H ₂ SO ₄)	Himedia Laboratories Pvt. Ltd., Mumbai, India	AS016-500ML
18	Tween-20	Himedia Laboratories Pvt. Ltd., Mumbai, India	GRM156-500G
19	Ammonium persulfate (APS)	Bio-Rad, CA, USA	161-0700
20	HPLC grade Methanol	Himedia Laboratories Pvt. Ltd., Mumbai, India	AS061-2.5L
21	Paraformaldehyde	Himedia Laboratories Pvt. Ltd., Mumbai, India	GRM-3660- 500GM
22	Acrylamide	Himedia Laboratories Pvt. Ltd., Mumbai, India	MB068-1KG
23	Antibiotic solution 100x liquid (10000 U Penicillin+ 10 mg Streptomycin)	Himedia Laboratories Pvt. Ltd., Mumbai, India	A001A-5x100ML
24	10X Phosphate Buffered Saline	Himedia Laboratories Pvt. Ltd., Mumbai, India	TL1032-500ML

25	HiGlutaXL™ RPMI-1640	Himedia Laboratories Pvt. Ltd., Mumbai, India	AL060G
26	TEMED	Himedia Laboratories Pvt. Ltd., Mumbai, India	MB026-100ML
27	Fetal Bovine Serum (FBS), Australian origin	PAN Biotech, Aidenbach, Germany	P30-1302
28	10x RBC lysis buffer	Himedia Laboratories Pvt. Ltd., Mumbai, India	R075-100ML
29	20X TMB/H ₂ O ₂	Bangalore Genei, Bangalore, India	62160118010A
30	Trypan blue	Himedia Laboratories Pvt. Ltd., Mumbai, India	TC193
31	Concanavalin A	Sigma Aldrich, MO, USA	C0412-5MG
32	RTX	Sigma Aldrich, MO, USA	R8756-1MG
33	5'-IRTX	Sigma Aldrich, MO, USA	I9281-1MG
34	DMEM	PAN Biotech, Aidenbach, Germany	P04-01550
35	HC-030031	Sigma Aldrich, MO, USA	H4415-10MG
36	AITC	Sigma Aldrich, MO, USA	36682-1G
37	DMSO	Himedia Laboratories Pvt. Ltd., Mumbai, India	TC185-250ML
38	Methylcellulose	Sigma Aldrich, MO, USA	M0387-250g

39	FcR blocking reagent, mouse	Macs Miltenyi Biotech, Gladbach, Germany	130-092-575
40	Fluo-4 AM	Invitrogen, CA, USA	F14217
41	Crystal violet	Sigma Aldrich, MO, USA	C6158

4.1.5 Buffers and other reagents composition

Table 5: Details of buffers used

Sl. No.	Buffers and other reagents	Composition
1	RIPA lysis buffer (Radio Immunoprecipitation Assay buffer)	150 mM sodium chloride, 0.1% SDS (sodium dodecyl sulphate) (w/v), 1.0% NP-40 (v/v), 0.5% sodium deoxycholate (w/v), 50 mM Tris, adjust to pH 8.0
2	2x Laemmli buffer	4% SDS (w/v), 10% 2-mercaptoethanol (v/v), 20% glycerol (v/v), 0.125 M Tris HCl, 0.004% bromophenol blue (w/v), adjust to pH 6.8
3	1x TGS or SDS-PAGE running buffer	25 mM Tris base, 190 mM glycine, 0.1% SDS (w/v)
4	1x Transfer buffer	25 mM Tris base, 190 mM glycine, 20% HPLC grade methanol (v/v)
5	4% Paraformaldehyde (PFA)	1x PBS (pH 7.4-7.6), 4% paraformaldehyde (w/v)
6	Blocking reagent Western blotting	3% BSA fraction-V in TBST
7	Tris-buffered saline (TBS)	0.0153 M Trizma HCl, 0.147 M NaCl in ultrapure water (Milli Q), pH adjusted to 7.6 by HCl

8	Tris-buffered saline Tween-20 (TBST)	0.05% (v/v) Tween-20 in 1x TBS
9	Permeabilization buffer (ICS)	0.5% BSA (w/v), 0.1% saponin (w/v), 0.01% NaN ₃ (w/v), 1x PBS, (pH 7.2)
10	Blocking buffer (ICS)	1% BSA (w/v), 0.1% saponin (w/v), 0.01% NaN ₃ (w/v), 1x PBS, (pH 7.2)
11	Methylcellulose media (plaque assay)	Complete DMEM media, 2% Methylcellulose (w/v)

4.1.6 Kits

EZcount™ MTT cell assay kit was purchased from Himedia Laboratories Pvt. Ltd, (Mumbai, India). Mouse T cell purification kit (Catalog no.11413D) was purchased from Invitrogen (Carlsbad, CA, USA). OptEIA™ ELISA kits for cytokines IL-2, IFN- γ , TNF and IL-6 were purchased from BD Biosciences (San Jose, CA, USA).

4.2 Methods

4.2.1 CHIKV infection in macrophages

RAW 264.7 cells were infected with CHIKV (DRDE-06) at a multiplicity of infection (MOI) 5, as described previously^{226,227}. 0.5×10^6 cells were seeded in 6 well plate in complete RPMI-1640 and placed in an incubator for 20 hours. Next, the media is removed and washed thrice with 1X PBS. CHIKV diluted in serum-free RPMI is added to the cells and placed in the incubator at 37°C. Manual shaking at every 15 minutes is performed to prevent cells from drying up for 2 hours. Next, the virus is pipetted out, washed thrice with 1X PBS and RPMI-1640 media is added. Then, the cells are harvested at either 8 or 12 hpi.

To examine TRP modulators effects during CHIKV infection, macrophages were pre-treated for 2 hours before CHIKV infection, during CHIKV infection and after infection at 0

hpi till the harvesting time-point. DMSO was used as solvent control. The remaining protocol was followed as mentioned above.

4.2.2 Splenocyte isolation

Spleen was collected from either BALB/c or C57BL/6 mice aseptically, as described previously^{191,196}. Using a syringe plunger, the spleen was disrupted through a 70 μ m cell strainer in complete RPMI-1640 media. Next, splenocytes were centrifuged at 350g for 5 minutes at 4°C. After centrifugation, the supernatant was slowly decanted and the pellet was broken down by gentle tapping. RBCs were lysed by 1X RBC lysis buffer (Himedia, Mumbai, India) with 1-minute incubation. For neutralization, an equal volume of 1X PBS or media was added and washed twice at 350g for 5 minutes at 4°C. Splenocytes were later suspended in complete RPMI-1640 media and placed in an incubator.

4.2.3 T cell purification

T cells were purified using dynabeadsTM untouchedTM mouse T cells kit from Invitrogen (Carlsbad, CA, USA), as described previously^{191,196}. 50×10^6 splenocytes were suspended in 500 μ l of isolation buffer (2mM EDTA + 2% FBS + 1X PBS) supplemented with additional 100 μ l of FBS. Next, a biotinylated antibody cocktail was added to the cells and incubated in ice for 20 minutes. After incubation, cells were washed with excess isolation buffer and centrifuged at 350g for 5 minutes at 4°C. The supernatant was decanted and cells were added with streptavidin-conjugated magnetic beads for 15 minutes at room temperature with gentle mixing. After 15 minutes, an extra isolation buffer was added and gently pipetted and placed on a magnet for 2 minutes. The clear solution containing purified T cells was collected in another tube and centrifuged at 350g for 5 minutes at 4°C. Purified T cells were resuspended in complete RPMI-1640 media. The purity of T cells was found to be $\geq 95\%$ via Flow cytometry

4.2.4 Flow cytometry (FC)

For quantification of cell markers, flow cytometry was performed, as described previously^{191,226}. For cell surface staining, cells were suspended in FACS buffer (1% BSA, 0.01% NaN₃, 1X PBS). Antibody cocktail is added to the cells and incubated for 30 minutes on ice. Next, washing is performed by FACS buffer and cells are centrifuged at 350g for 5 minutes at 4°C. In the case of unconjugated primary antibodies, fluorochrome-conjugated secondary antibody (1:1000) is added and incubated for 30 minutes on ice followed by washing. Finally, cells are resuspended in FACS buffer containing 1% paraformaldehyde (w/v) and stored at 4°C until acquisition.

For intracellular staining (ICS), the cells were fixed with 4% paraformaldehyde (w/v) for 10 minutes at room temperature. The fixed cells were permeabilized via saponin-based permeabilization buffer (0.5% BSA + 0.1% saponin + 0.01% NaN₃ + 1X PBS), followed by blocking with 1% BSA in permeabilization buffer for 30 minutes at room temperature. Using permeabilization buffer, the cells were washed and incubated with primary antibodies for 30 minutes at RT. After incubation, fixed cells are washed twice with permeabilization buffer. In the case of unconjugated primary antibody, fluorochrome-conjugated secondary antibody (1:1000) is diluted in the permeabilization buffer and incubated for another 30 minutes, followed by two washes with permeabilization buffer. For acquisition via Flow cytometry, the cells were resuspended in FACS buffer and stored at 4°C.

For isotype control, mouse IgG and rabbit IgG, as appropriate, were used. To prevent any non-specific binding of Fc receptors in macrophages, FcR blocking reagent (Miltenyi Biotech, Germany) was used at a concentration of 1:20. The cells were acquired using Flow cytometer (BD FACSCalibur™ or BD FACSFortessa™).

4.2.5 MTT assay

To determine the cellular viability of RAW 264.7 cells in presence of TRPV1 modulators, 5'-IRTX and RTX, an MTT assay using an EZcount™ MTT Cell Assay Kit (Himedia, Mumbai, India) was used, as described previously²²⁶. 5×10^3 cells were seeded in a flat-bottom, 96 well plate and placed in an incubator at 37°C. After 24 hours, the media was removed and the TRPV1 modulators were added to each well in triplicate. As a solvent control, DMSO was used. After 24 hours of treatment, media was removed and were treated with fresh RPMI media containing 10% MTT (v/v). For formazan crystal formation, cells were placed in the incubator for more 2 hours. A 100 µl of solubilization buffer was added to each well followed by incubation for 15 minutes at room temperature. Absorbance was measured at 570 nm, using a microplate reader (Bio-Rad, CA, USA) and the percentage of viable cells was calculated in comparison to DMSO control cells.

4.2.6 Plaque assay

To determine the viral titer, a plaque assay was performed, as described elsewhere²²⁶. 0.15×10^6 Vero cells were seeded in a 24 well plate to attain upto 100% confluency. Next, the various dilutions of cell culture supernatants were used to infect Vero cells. After infection, Vero cells were washed thrice with 1X PBS and complete DMEM containing methylcellulose (2% w/v) is overlaid on the cells and maintained in an incubator for 4-5 days, till the visible plaques are formed. Then, the cells are fixed with 4% paraformaldehyde at RT. Next, the cells are washed gently with distilled water to remove DMEM containing methylcellulose and stained with crystal violet. The plaques were counted manually under white light.

4.2.7 Time-of-addition assay

To determine which stage of the CHIKV life cycle does the TRP modulators affect, a time-of-addition experiment was performed, as described elsewhere²²⁸. In this assay, TRP modulators were added to the host cells at different time points relative to the addition of

CHIKV. A total of four different conditions were set up namely, (i) pre-during-post (TRP modulators were added 2 hours before CHIKV infection, during CHIKV infection and post CHIKV infection at 0 hpi) (ii) pre-during (TRP modulators were added 2 hours prior to CHIKV infection and during CHIKV infection only, no TRP modulators were used post-infection) (iii) post at 0 hpi (TRP modulators were added after CHIKV infection at 0 hpi) and (iv) post at 4 hpi (TRP modulators were added after CHIKV infection at 4 hpi). The cell-free supernatants were collected at 12 hpi. The viral titer was quantified by either plaque assay or qRT-PCR by amplifying the viral E1 gene.

4.2.8 Real-time RT-PCR

qRT-PCR was performed as described elsewhere²²⁹. Using 140 µl of CHIKV-infected supernatant, viral RNA was extracted, using a QIAamp Viral RNA Mini Kit (QIAGEN, Hilden, Germany). Using random hexamers, 1 µg of viral RNA was used to prepare cDNA by using a PrimeScript 1st Strand cDNA Synthesis Kit (Takara, Kusatsu, Japan). This cDNA was amplified for the viral E1 gene by RT-PCR (Applied Biosystems QuantStudio 3), using the primers F (5'-TGC CGT CAC AGT TAA GGA CG-3'), R (5'-CCT CGC ATG ACA TGT CCG -3') and a MESA GREEN qPCR MasterMix Plus for SYBR Assay, No ROX (Eurogentec, Belgium). A standard curve for Ct values was prepared by using six tenfold serial dilutions of the E1 gene^{230,231}. This E1 gene was cloned in the plasmid pBiEx. The percentage of copy number/ml was calculated from the corresponding Ct values.

4.2.9 Immunocytochemistry (ICC)

RAW 264.7 cells were seeded on sterile coverslips and infected with CHIKV (MOI=5) as described elsewhere²³². At time-points 8 and 12 hpi, cells were fixed with 4% paraformaldehyde for 15 minutes at RT. Next, cells were permeabilized by blocking buffer (3% BSA in 1X PBS) + 0.2% Triton X-100 for 10 minutes at RT. After permeabilization, cells were washed thrice with 1X PBS for 10 minutes. Then, blocking was carried out for 1 hour at

RT. Next, cells were incubated with primary antibodies for 1 hour at RT. After washing, the cells are incubated with secondary antibody for 1 hour at RT followed by washing with 1X PBS. DAPI was used as a nuclear stain. To reduce photobleaching, the coverslips were mounted with antifade (Invitrogen, CA, USA). Fluorescence images were acquired, using a 63X objective. Finally, images were analysed using the ImageJ software.

4.2.10 ELISA

To estimate the cytokine levels in cell-free culture supernatants, Sandwich ELISA was performed, using a BD OptEIA™ kit (BD Biosciences, CA, USA) for TNF, IL-6, IFN- γ and IL-2 as described previously^{226,233}. 96 well, medi-binding strip immune-plates (SPL Life Sciences, Korea) were used. Capture antibodies diluted in coating buffer (vol. 100 μ l) were dispensed into each well and incubated at 4°C overnight with a plate sealant. Next, each well is aspirated and washed three times with 300 μ l of wash buffer (1X PBS with 0.05% Tween-20). Next, plates are incubated with 300 μ l/well of assay diluent (1X PBS with 10% FBS) and incubated at room temperature for 1 hour. After incubation, washing is performed three times with wash buffer. Standards are serially diluted as recommended in the kit and samples are also diluted as desired and added to the corresponding well. After incubation for 2 hours, washing is performed five times with wash buffer. The detection antibody + streptavidin HRP reagent (working detector) is added to all the wells and incubated for 1 hour at room temperature with a plate sealer. Next, the plate is washed with wash buffer for seven times and incubated with substrate solution (TMB/H₂O₂ diluted in H₂O) in the dark without a plate sealer. The reaction develops blue color. After 5-30 minutes, by adding 50 μ l of stop solution (2N H₂SO₄), the reaction was stopped. The reading was immediately taken at 450 nm by Bio-Rad iMark™ microplate absorbance reader. The cytokine concentration (pg/ml) was calculated in comparison with the corresponding standard curve.

4.2.11 Western blot

To assess the protein expression levels in CHIKV-infected macrophages, Western blot was performed as described previously^{226,227}. Mock and CHIKV-infected macrophages treated with different TRP modulators were harvested and lysed with RIPA buffer supplemented with protease and phosphatase inhibitor cocktail (Roche, Mannheim, Germany). 30 µg of protein was loaded in each well and subjected to 10% SDS-PAGE and blotted to polyvinylidene fluoride (PVDF) membrane (Millipore, MA, USA). After blocking with 3% BSA for 1 hour at RT, overnight incubation at 4°C with primary antibody was carried out. The membranes were washed with TBST followed by addition of HRP-conjugated secondary antibody. Finally, chemiluminescence was detected by Bio-Rad Gel Doc.

4.2.12 7-AAD staining

Purified mouse T cells were incubated with two-fold serial dilution of B16F10-CS, 5'-IRTX and FK506 for 36 hours. Next, cells were washed with 1X PBS and stained with 7-AAD. Cells were then immediately acquired in Flow cytometer (BD LSRFortessa™, BD Biosciences). The analysis was performed by the software Flowjo V10.7.1.

4.2.13 Calcium Imaging

Cells are stained with calcium-sensitive dye, Fluo-4 AM (Invitrogen, CA, USA), 2 µM for 30 minutes and incubated at 37°C with 5% CO₂, as described previously¹⁹¹. To remove any excess dye, cells were washed twice with 1X PBS. After de-esterification, the cells were placed in a live cell chamber and stimulated with specific reagents alone or in combinations as per experimental conditions. Accordingly, the fluo-4 AM intensity was assessed by either via flow cytometry or fluorescence-based microplate reader or confocal microscopy. Using the GraphPad Prism 7.0 (GraphPad Software Inc., San Diego, CA, USA), the time-lapse kinetics of calcium influx were plotted.

4.2.14 Statistical analysis

The comparison between the groups was performed by either student t-test, one-way ANOVA or two-way ANOVA. Using GraphPad Prism 7.0 (GraphPad Software Inc., San Diego, CA, USA), statistical analysis was performed. Data are presented as the mean \pm SD. Data presented are representative of three independent experiments. $p \leq 0.05$ is considered as statistically significant difference between the groups (ns, non-significant, * $p \leq 0.05$, ** $p \leq 0.01$, *** $p \leq 0.001$).

CHAPTER # 5

Results

**Regulatory role of TRPV1 in
CHIKV infection**

5. Results

5.1 Regulatory role of TRPV1 in CHIKV infection

Several viral infections such as varicella-zoster virus (VZV), herpes simplex virus type 2 (HSV-2), hepatitis C virus (HCV), measles virus (MV), respiratory syncytial virus (RSV) and human rhinovirus (HRV) infection upregulate TRPV1 levels in host cells^{206,207,214,234–236}. Additionally, TRPV1 has also been reported to play vital roles in host-pathogen interactions, including viral binding, entry and replication^{206,207,214}. Further, TRPV1 has also been associated with post-viral infection pain and inflammation as well^{206,207,214,234–236}. The current study provides evidence that TRPV1 regulates CHIKV infection in macrophages. Further, the regulatory role of TRPV1 in host-pathogen interactions, effector cytokine response, pNF- κ B (p65) expression and nuclear localisation, and calcium influx were also investigated.

5.1.1 CHIKV upregulates TRPV1 expression in macrophages

TRPV1 has been reported to be upregulated during various viral infections^{206,207,214,234–236}. Thus, the surface expression levels of TRPV1 was assessed in CHIKV-infected macrophages. For CHIKV infection, RAW 264.7 cells were infected with CHIKV at MOI 5 and the viral proteins (nsP2 and E2) and TRPV1 expression at both 8 and 12 hpi were quantified by Flow cytometry. As reported earlier, the highest CHIKV protein-positive cells were found at 8 hpi (nsP2: 7.74 ± 1.01 ; E2: 14.66 ± 1.09). At 12 hpi (nsP2: 4.87 ± 1.01 ; E2: 11.15 ± 0.85), a marginal decrease in CHIKV protein-positive cells were found. (Figure 3A). Further, it was observed that in CHIKV-infected macrophages, TRPV1 expression levels significantly increased as compared to mock cells at both 8 hpi (mock: 43.147 ± 1.48 ; CHIKV: 51.13 ± 1.32) and 12 hpi (mock: 47.22 ± 1.58 ; CHIKV: 64.79 ± 0.52) (Figure 3B). Simultaneous detection of viral proteins and TRPV1 expression could not be performed because of saponin. TRPV1 is closely associated with cholesterol in plasma membrane^{237–239}. Since saponin creates transient pores in the plasma membrane by removing cholesterol, it leads to membrane loss and

consequently loss of TRPV1 signal^{240–243}. These findings suggest that TRPV1 is upregulated during CHIKV infection in a time-dependent manner.

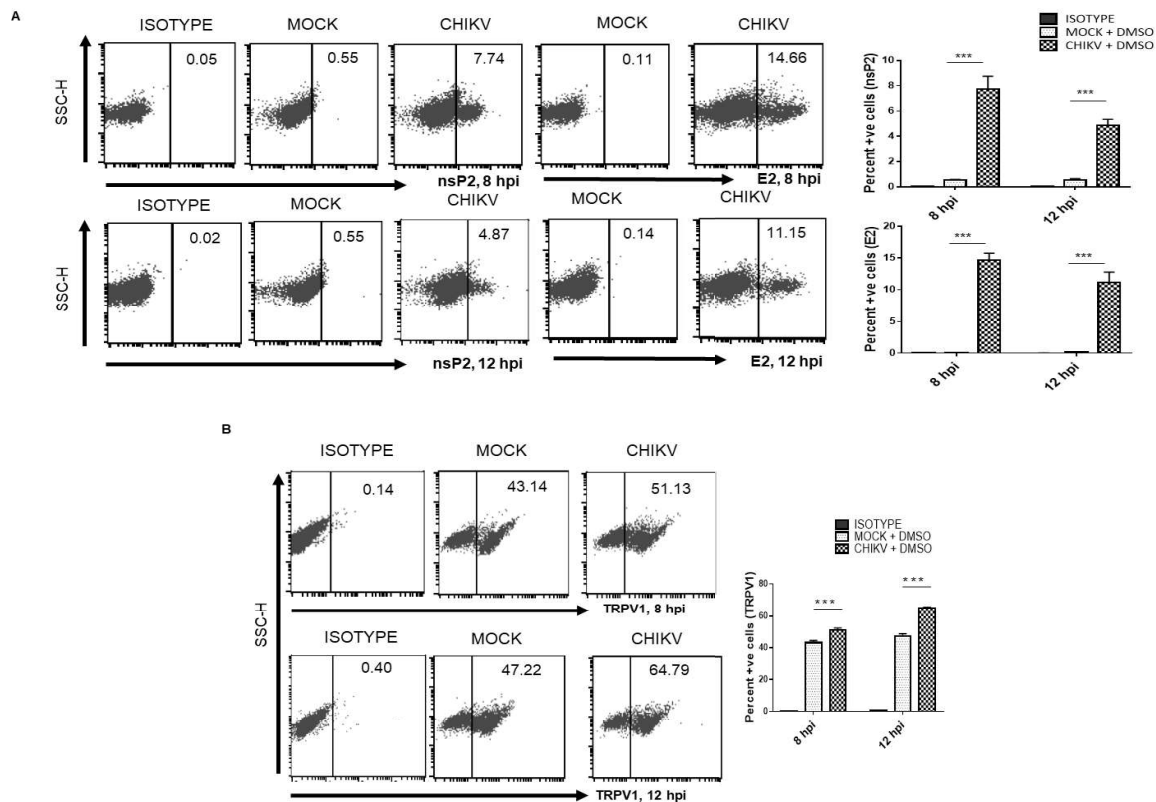


Figure 3 CHIKV upregulates TRPV1 expression in macrophages

RAW 264.7 cells were infected with CHIKV at an MOI of 5, harvested at 8 and 12 hpi and finally acquired by Flow cytometry (FC). (A) FC dot-plot analysis showing the percentage of cells positive for the viral proteins nsP2 and E2 with representative bar diagram. (B) FC analysis depicting TRPV1 expression in CHIKV- infected RAW 264.7 cells with representative bar diagram. Data represents the mean \pm SD of three independent experiments. $P < 0.05$ were considered statistically significant (* * *, $p < 0.001$).

5.1.2 Assessment of TRPV1 antibody specificity

TRPV1 antibody is polyclonal in origin. Hence, the specificity of the TRPV1 antibody was assessed via Flow cytometry (FC), using a control blocking peptide antigen¹⁹¹. RAW 264.7 cells were stained with TRPV1 antibody in the presence or absence of the blocking peptide. As anticipated, it was found that the percentage of cells that were positive for TRPV1

decreased in a dose-dependent manner from 42.21 ± 3.90 to 7.75 ± 2.74 in the presence of 1X control blocking peptide antigen, and it decreased further to 2.03 ± 0.69 in the presence of 3X control blocking peptide antigen, confirming the specificity of the TRPV1 antibody in RAW 264.7 cells (Figure 4).

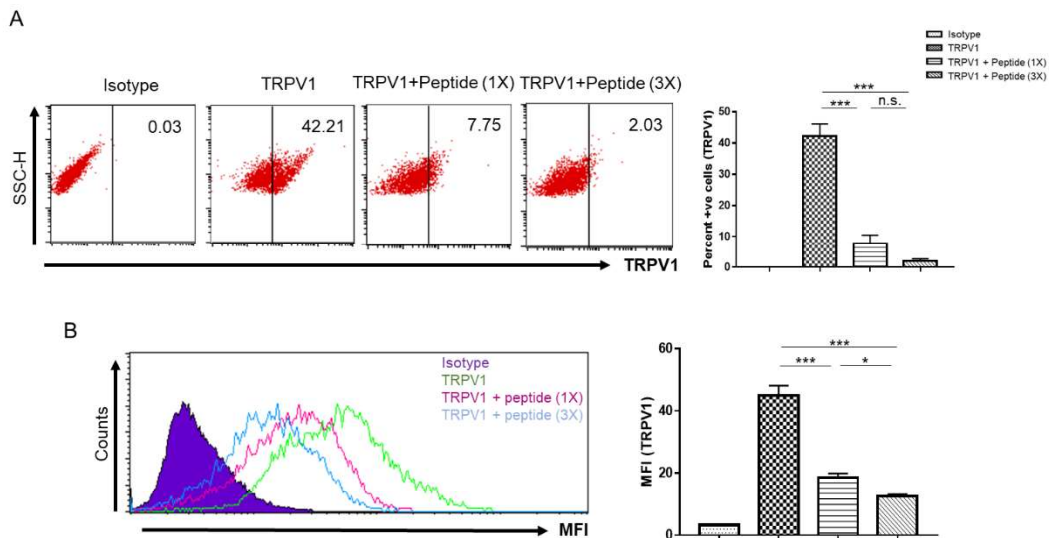


Figure 4 Assessment of TRPV1 antibody specificity

FC analysis depicting TRPV1 expression in RAW 264.7 cells, in presence or absence of control blocking peptide antigen as dot plot (upper panel) and MFI (lower panel) representing TRPV1 expression in isotype (purple filled), TRPV1 (green), TRPV1 + blocking peptide (1X) (pink) and TRPV1 + blocking peptide (3X) (blue) along with representative bar diagram. Data represents the mean \pm SD of three independent experiments. $P < 0.05$ were considered statistically significant (ns, non-significant; *, $p < 0.05$; ***, $p < 0.001$).

5.1.3 Cell viability assay for macrophages in the presence of TRPV1 modulators

TRPV1 specific functional modulators, 5'-IRTX and RTX were used in this study 191,192,244. To determine the cellular cytotoxicity of 5'-IRTX and RTX, an MTT assay was performed. The drugs, 5'-IRTX ($0.625 \mu\text{M}$ to $160 \mu\text{M}$) and RTX ($0.08 \mu\text{M}$ to $10 \mu\text{M}$) were two-fold serially diluted. DMSO was used as solvent control. It was observed that the percentage of cell viability for $0.625 \mu\text{M}$ of 5'-IRTX and RTX was $\sim 97\%$ and $\sim 100\%$,

respectively (Figure 5). A similar observation has also been reported earlier as well ^{245–247}.

Hence for further experiments, 0.625 μM of 5'-IRTX and RTX were used.

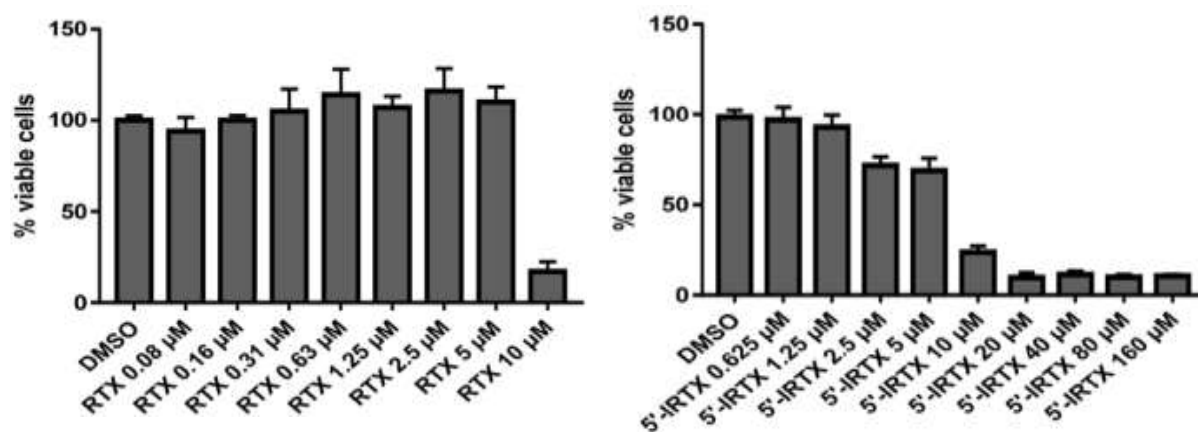


Figure 5 Percentage of cell viability via MTT assay

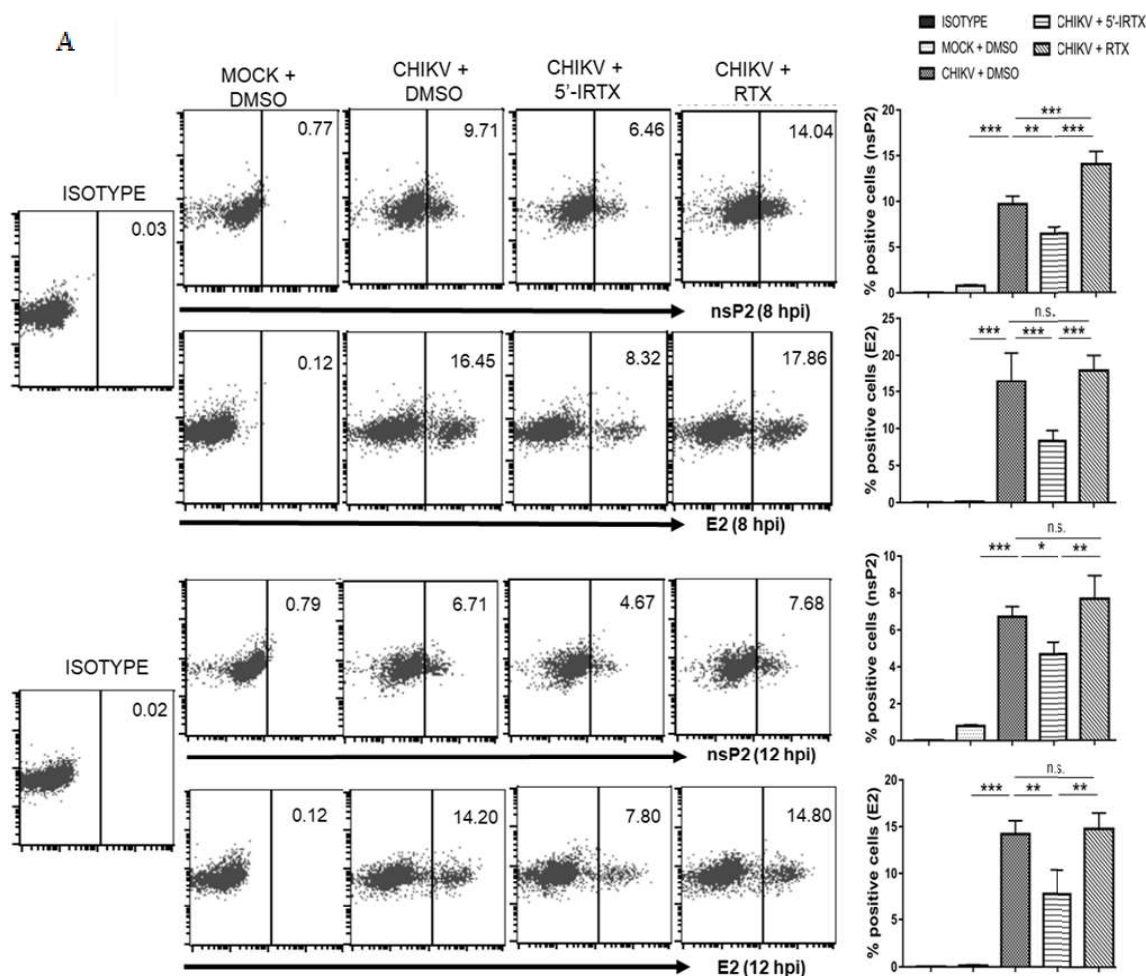
Bar diagram showing the percentage of viable RAW 264.7 cells treated with two-fold serially diluted concentrations of RTX (left panel) and 5'-IRTX (right panel) as compared to the DMSO (solvent control, as determined by MTT assay. Data represents the mean \pm SD of three independent experiments.

5.1.4 TRPV1 regulates CHIKV infection

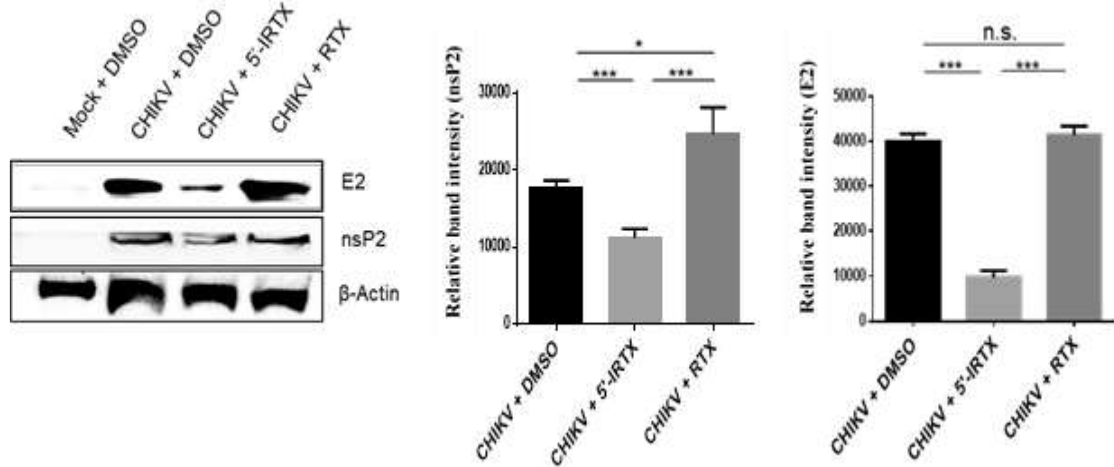
TRPV1 has been reported to regulate various viral infections, including varicella-zoster virus (VZV), herpes simplex virus type 2 (HSV-2), hepatitis C virus (HCV), measles virus (MV), respiratory syncytial virus (RSV) and human rhinovirus (HRV) ^{206,207,214,234–236}. However, no such role of TRPV1 in CHIKV infection has been reported. To determine whether pharmacologically regulating TRPV1 functioning via 5'-IRTX or RTX can also regulate CHIKV infection in macrophages, RAW 264.7 cells were infected with CHIKV in the presence of TRPV1 modulators. Flow cytometric analysis revealed that in the presence of 5'-IRTX, the percentage of CHIKV positive cells (nsP2: 6.46 ± 0.72 ; E2: 8.32 ± 1.41) decreased whereas, in the presence of RTX, the percentage of CHIKV positive cells (nsP2: 14.04 ± 1.38 ; E2: 17.86 ± 2.05) increased as compared to CHIKV+DMSO control (nsP2: 9.71 ± 0.86 ; E2: 16.45 ± 3.87) (Figure 6A). Similarly, Western blot analysis has shown that E2 and nsP2 have significantly decreased in the presence of 5'-IRTX as compared to CHIKV+DMSO control. However, in

RTX-treated cells, only nsP2 expression was significantly increased (Figure 6B). These findings suggest that TRPV1 may regulate CHIKV infection in macrophages.

Subsequently, the TRPV1 expression levels were also quantified in 5'-IRTX or RTX treated CHIKV-infected macrophages. A significant change was observed only in CHIKV + DMSO (8 hpi: 50.16 ± 2.55) as compared to Mock + DMSO (8 hpi: 41.92 ± 1.09). However, no significant change was observed in the presence of 5'-IRTX (8 hpi: 55.7 ± 2.43) and RTX (8 hpi: 52.01 ± 3.21 ; treated CHIKV-infected macrophages as compared to CHIKV + DMSO (Figure 6C). Taken together, these results indicate that upon CHIKV infection in macrophages, surface TRPV1 levels increase significantly. Although TRPV1 modulators can modulate CHIKV infection, no significant change in TRPV1 expression levels was observed, since the TRPV1 modulators used in this study are functional modulators.



B



C

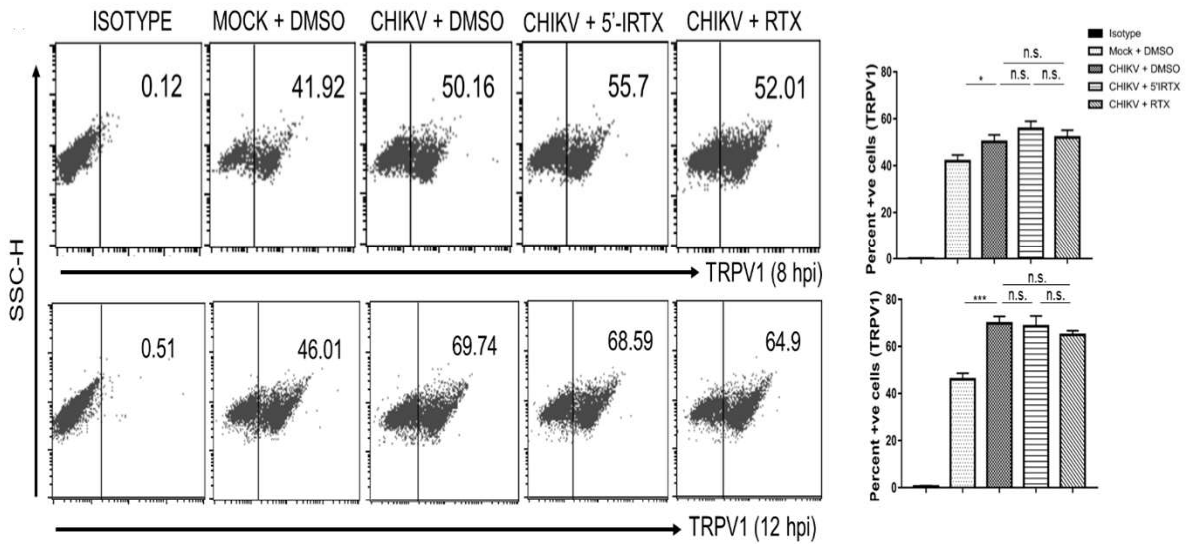


Figure 6 TRPV1 regulates CHIKV infection

The RAW 264.7 cells were treated with either TRPV1 modulators or DMSO. (A) FC dot-plot showing percentage of positive cells for viral proteins, nsP2 or E2 (8 and 12 hpi) with either 5-IRTX or RTX treated CHIKV-infected macrophages with representative bar diagram (B) Western blot analysis showing viral proteins, E2 and nsP2 levels at 8 hpi. The bar diagram below shows relative band intensities of nsP2 and E2. (C) Representative FC dot-plot depicting percent positive cells for TRPV1 at 8 hpi and 12 hpi with its corresponding bar diagram. Data represents the mean \pm SD of three independent experiments. P < 0.05 were considered statistically significant (ns, non-significant; * p < 0.05; *** p < 0.001).

5.1.5 TRPV1 regulates CHIKV viral titer

To determine whether TRPV1 regulates CHIKV viral titer, a plaque assay was performed^{226,248}. Cell-free supernatants containing the infectious viral particles from the experiments were collected and stored at -80°C. CHIKV viral titer significantly decreased in the presence of 5'-IRTX to $3.33 \times 10^6 \pm 6.66 \times 10^5$ (0.57-fold) and conversely increased in the presence of RTX to $1.13 \times 10^7 \pm 1.15 \times 10^6$ (1.96 fold) as compared to CHIKV + DMSO control ($5.77 \times 10^6 \pm 7.69 \times 10^5$) (Figure 7). This result indicates that TRPV1 also regulates CHIKV viral titer.

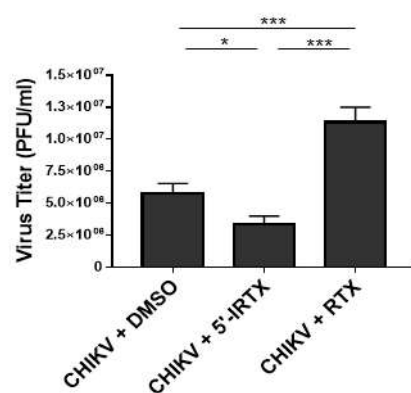


Figure 7 TRPV1 regulates CHIKV viral titer

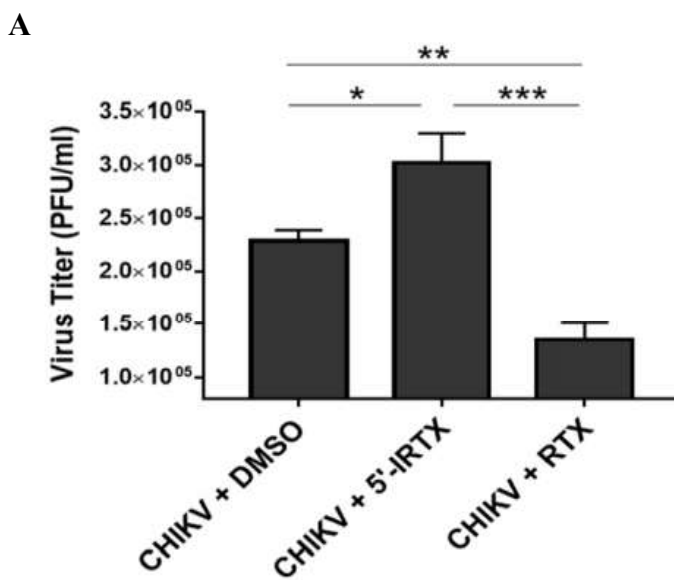
The RAW 264.7 cells were treated with either DMSO or TRPV1 modulators. As determined by plaque assay, bar diagram showing viral plaque-forming units (PFU/ml), from the supernatants of CHIKV-infected macrophages at 12 hpi treated with either 5'-IRTX, RTX or DMSO as control. Data represents the mean \pm SD of three independent experiments. $P < 0.05$ were considered statistically significant (* $p < 0.05$; * * * $p < 0.001$).

5.1.6 TRPV1 modulates the early phases of the CHIKV life-cycle

TRPV1 has been widely reported to affect various viral life-cycle stages such as adsorption, entry and replication^{206,207,214}. To determine which phase of the CHIKV life-cycle does TRPV1 affects, we performed a plaque assay from supernatants (collected after CHIKV infection, containing unbound virus) and time-of-addition studies.

To perform plaque assay, supernatants containing the unbound virus after CHIKV infection were used. It was observed that a significantly higher viral titer was present in 5'-IRTX treated CHIKV-infected macrophages ($3.02 \times 10^5 \pm 2.7 \times 10^4$ PFU/ml, 32% more than DMSO only). In contrast, a significantly lower viral titer in RTX treated CHIKV-infected macrophages ($1.35 \times 10^5 \pm 1.5 \times 10^4$ PFU/ml, 40.77% less than DMSO only) as compared to CHIKV + DMSO control ($2.28 \times 10^5 \pm 1.01 \times 10^4$) (Figure 8A). These findings suggest that the viral adsorption and/or entry decreases in the presence of 5'-IRTX and increases in RTX presence during CHIKV infection in macrophages.

Next, the time-of-addition assay as described in Methods depicted that the addition of TRPV1 modulators with respect to virus addition profoundly affects the CHIKV viral copy number. The CHIKV infection significantly altered in the presence of TRPV1 modulators in the “Pre+During+Post” and “Pre+During” conditions. The percentage of CHIKV infection in the presence of 5'-IRTX reduced significantly to 13.79% and 47.29% in “Pre+During+Post” and “Pre+During” respectively as compared to the corresponding CHIKV + DMSO control. Conversely, the percentage of CHIKV infection in the presence of RTX increased to 130% and 110% in “Pre+During+Post” and “Pre+During”, respectively as compared to CHIKV + DMSO control. In the presence of TRPV1 modulators, both at “post 0 hpi” or “post at 4 hpi”, a non-



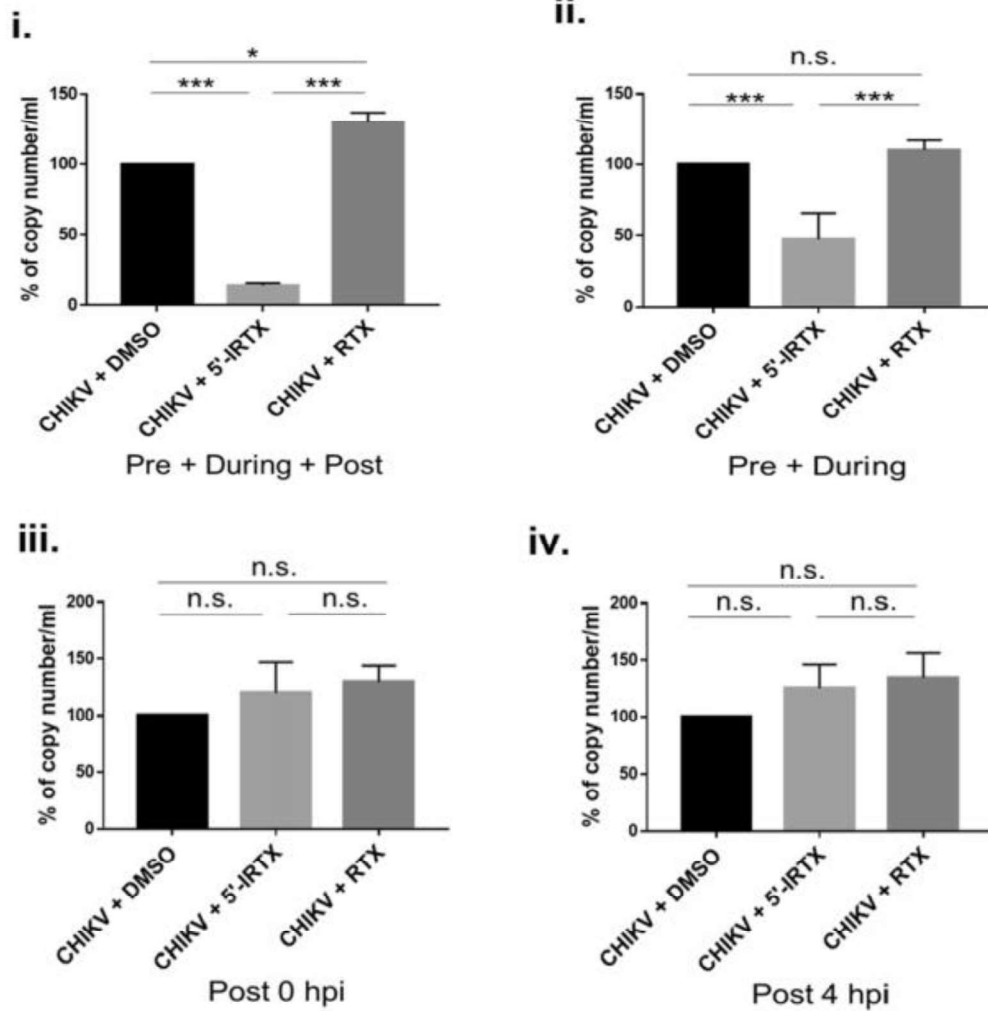
B

Figure 8 TRPV1 modulates early phases of the CHIKV life-cycle

RAW 264.7 cells were pre-treated with 5'-IRTX, RTX or DMSO for 2 h prior to CHIKV addition. After CHIKV adsorption to the cells, the unbound virus in the left-over supernatant was collected and plaque assay was performed. (A) Bar diagram depicting the number of viral plaque-forming units (PFU/ml) derived from left-over supernatant from the TRPV1 treated CHIKV-infected macrophages. (B) CHIKV infection was carried out in RAW 264.7 cells by adding TRPV1 modulators in different phases of CHIKV addition to RAW 264.7 cells like pre + during + post (i), pre + during (ii), post at 0 hpi (iii) and post at 4 hpi (iv). Real-time RT-PCR was performed for viral gene (E1) expression. Data are expressed in the percentage of copy number/ml normalized to CHIKV + DMSO. Data represents the mean \pm SD of three independent experiments. $P < 0.05$ were considered statistically significant (ns, non-significant; * $p < 0.05$; ** $p < 0.01$; *** $p < 0.001$).

significant change in CHIKV infection was observed (Figure 8B). Taken together, these results suggest that the TRPV1 might affect the early phases of the CHIKV viral life-cycle i.e., viral adsorption and/or entry.

5.1.7 TRPV1 modulates the CHIKV-induced pro-inflammatory cytokine response in host macrophages

CHIKV has been widely reported to induce robust pro-inflammatory cytokine response in host macrophages ^{226,227,249–251}. To quantitate the secreted cytokines during CHIKV infection, we performed sandwich ELISA. As expected, the cytokines TNF and IL-6 were markedly upregulated during CHIKV infection at both 8 and 12 hpi.

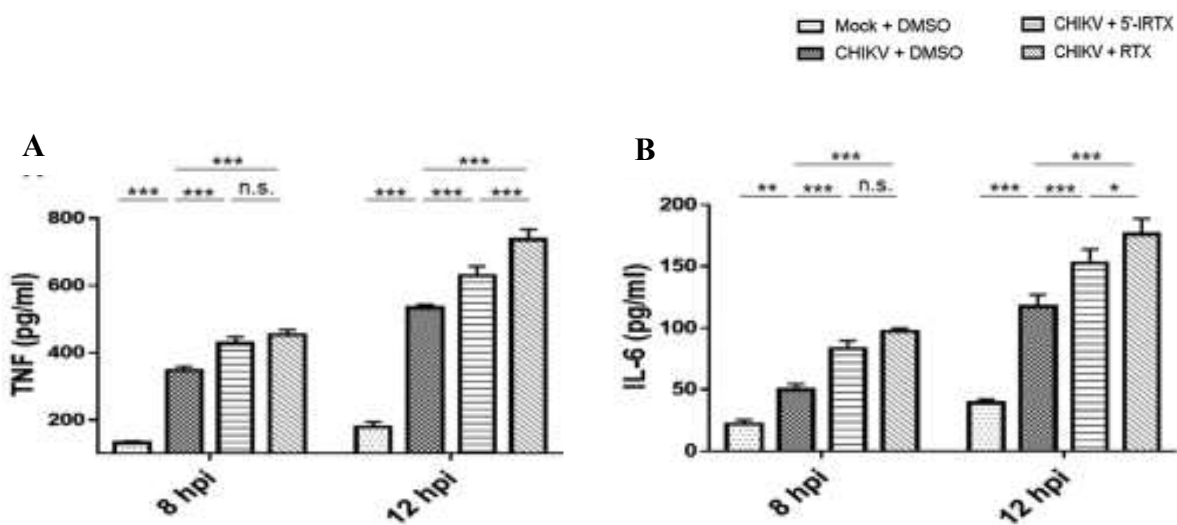


Figure 9 TRPV1 modulates the CHIKV-induced pro-inflammatory cytokine response in host macrophages

Sandwich ELISA was performed from the cell-free supernatants collected from the CHIKV-infected macrophages. Bar diagram showing the amount of secreted (pg/ml) at both 8 and 12 hpi (A) TNF and (B) IL-6. Data represent the mean \pm SD of three independent experiments. Data represents the mean \pm SD of three independent experiments. $P < 0.05$ were considered statistically significant (ns, non-significant; * $p < 0.05$; ** $p < 0.01$; *** $p < 0.001$).

In RTX-treated CHIKV-infected macrophages, the cytokine TNF and IL-6 were further significantly upregulated as compared to CHIKV + DMSO control. Unprecedentedly, in 5'-

IRTX treated CHIKV-infected macrophages, the cytokines TNF and IL-6 were also significantly upregulated as compared to CHIKV + DMSO control, albeit lesser than CHIKV + RTX (Figure 9). These results suggest that the RTX-treated CHIKV-infected macrophages produces the maximum upregulation in cytokine responses as compared to CHIKV + DMSO control. Surprisingly, pro-inflammatory cytokine response was also found to be increased in 5'-IRTX treated CHIKV-infected macrophages.

5.1.8 Pro-inflammatory cytokine response in macrophages treated with TRPV1 modulators

To determine whether TRPV1 modulators alone can induce cytokine response in macrophages, we performed a sandwich ELISA. We observed that both 5'-IRTX and RTX did not induce any change in TNF and IL-6 levels at both 8 and 12 hpi as compared to mock cells (Figure 10). These findings indicate that TRPV1 modulators alone cannot induce any change in both TNF and IL-6 levels in macrophages.

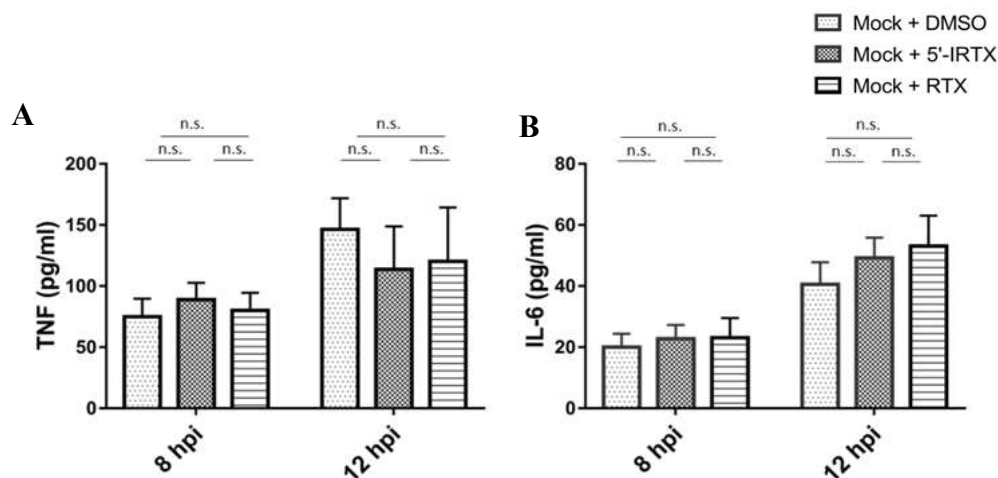


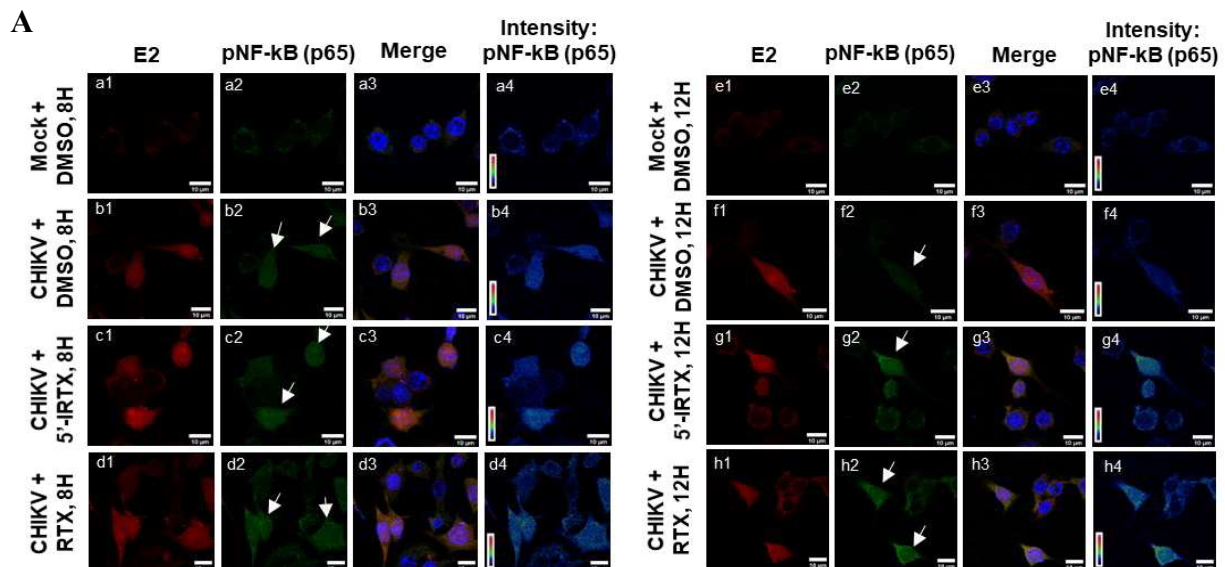
Figure 10 TRPV1 modulators alone cannot induce pro-inflammatory cytokine response in host macrophages

RAW 264.7 cells were treated with TRPV1 modulators. Sandwich ELISA was performed from the cell-free supernatants collected from the RAW 264.7 cells at both 8 and 12 hours. Graphical bar diagram depicting the amount of secreted TNF (A) and IL-6 (B) in 5'-IRTX or RTX treated mock macrophages.

Data represents the mean \pm SD of three independent experiments. $P < 0.05$ were considered statistically significant (ns, non-significant).

5.1.9 Expression and nuclear localization of pNF- κ B (p65) in CHIKV-infected macrophages, in presence or absence of TRPV1 modulators

NF- κ B is a protein complex involved in various cellular processes, including transcription, cell survival, cytokine and chemokine production^{26,252,253}. Its phosphorylated form (pNF- κ B) plays a central role in inflammation. To determine the discrepancy in the cytokine production of 5'-IRTX treated CHIKV-infected macrophages, we assessed the pNF- κ B (p65) expression and nuclear localization via Immunofluorescence and Flow cytometry. Immunofluorescence studies reveal that CHIKV infection-induced pNF- κ B expression and nuclear localization at both 8 and 12 hpi as compared to mock cells. In RTX-treated CHIKV-infected macrophages, the pNF- κ B levels reached maximum elevation. Similarly, in 5'-IRTX treated CHIKV-infected macrophages, the pNF- κ B expression was also elevated as compared to CHIKV-infected macrophages, albeit lesser than the RTX treated CHIKV-infected macrophages (Figure 11 A, B).



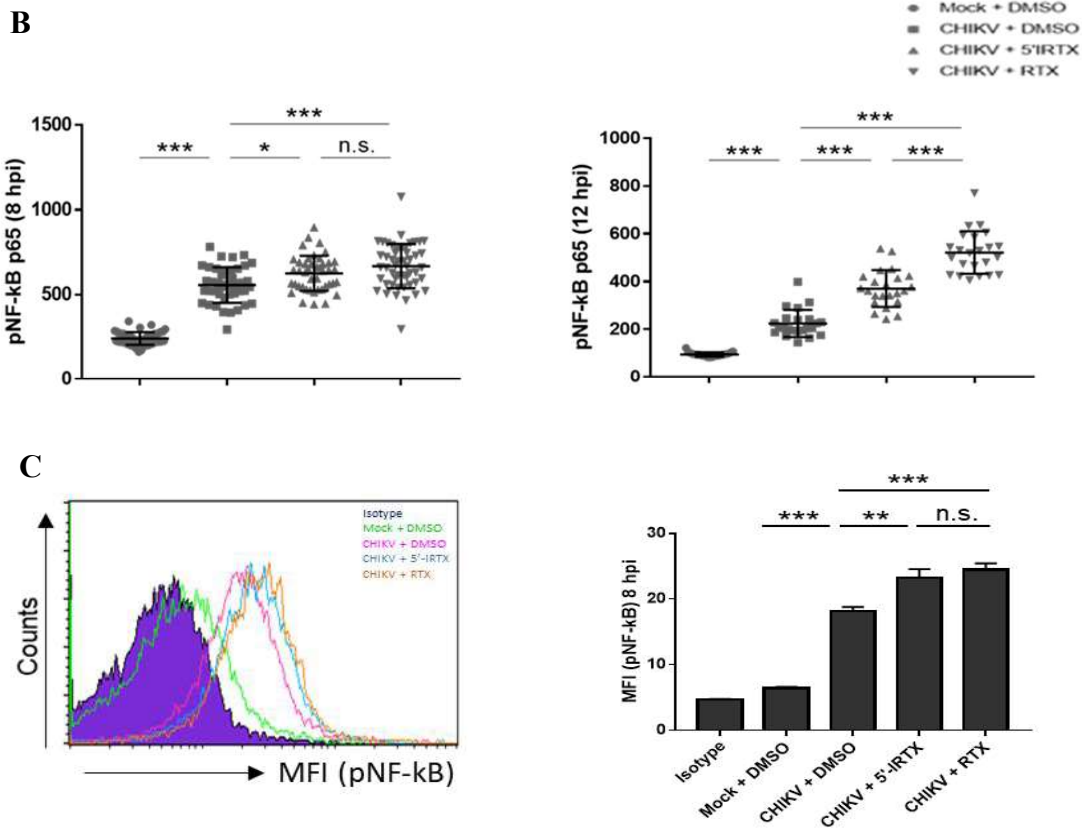


Figure 11 Expression and nuclear localization of pNF-κB (p65) in CHIKV-infected macrophages, in presence or absence of TRPV1 modulators

pNF-κB (p65) expression and nuclear localisation was studied by Immunofluorescence at both (A) 8 hpi (left panel) and 12 hpi (right panel) and Flow cytometry at 8 hpi. CHIKV infected macrophages in presence or absence of TRPV1 modulators were stained with CHIKV E2 monoclonal (red) (a1, b1, c1, d1 and e1, f1, g1, h1). The immunofluorescence images show the nuclear localisation of pNF-κB (p65) (green) (a2, b2, c2, d2 and e2, f2, g2, h2) in CHIKV-infected macrophages as compared to mock. Nuclei were stained with DAPI (a3, b3, c3, d3 and e3, f3, g3, h3). pNF-κB levels in rainbow scale (a4, b4, c4, d4 and e4, f4, g4, h4). Mock cells are used as negative control. (B) Scatter plot showing pNF-κB (p65) intensity at 8 hpi (left panel) and 12 hpi (right panel) in TRPV1 modulator treated CHIKV-infected macrophages. (C) FC histogram plot depicting MFI of pNF-κB (p65) at 8 hpi in TRPV1 modulator treated CHIKV-infected macrophages. with representative bar diagram. Data represents the mean \pm SD of three independent experiments. $P < 0.05$ were considered statistically significant (ns, non-significant; * $p < 0.05$; ** $p < 0.01$; *** $p < 0.001$).

The flow cytometry data at 8 hpi is also in agreement with the above results (Figure 11C). Taken together, these results suggest that the pNF- κ B levels markedly increase in 5'-IRTX treated CHIKV-infected macrophages as compared to CHIKV-infected macrophages, which might explain the discrepancy in cytokine response in 5'-IRTX treated CHIKV-infected macrophages.

5.1.10 TRPV1 modulates Ca²⁺ influx in macrophages

TRPV1 is a non-selective calcium-permeable cation channel ^{254–257}. Here, we have assessed the functional contribution of TRPV1 in Ca²⁺ influx during CHIKV infection in macrophages. The macrophages were stained with Ca²⁺ sensitive dye fluo 4-AM ^{258,259}. The addition of Ca²⁺ solution only did not induce any Ca²⁺ influx indicating that the Ca²⁺ solution is not triggering any non-specific change in Ca²⁺ levels. Next, upon the addition of 5'-IRTX, we observed a slight reduction in fluo-4 intensity. Further, we observed a robust increase in fluo-4 intensity upon treatment with RTX indicating Ca²⁺ influx via TRPV1 channels. Similarly, upon treatment with CHIKV, we observed an increase in Ca²⁺ influx, indicating that CHIKV binding to host macrophages induces Ca²⁺ influx. Next, upon the addition of CHIKV+5'-IRTX, we observed that the Ca²⁺ influx has reduced. Conversely, upon treatment with CHIKV+ RTX, the fluo-4 intensity increased maximum (Figure 12A). To further quantify the above results, we have estimated the area under the curve (AUC). The estimated AUC values for different treatments were: -99.28 a.u. (calcium solution), -55.6 a.u. (5'-IRTX), +128.2 a.u. (RTX), +94.03 a.u. (CHIKV + DMSO), -14.14 a.u. (CHIKV + 5'-IRTX), and +179.4 a.u. (CHIKV + RTX) (Figure 12B). These results suggest that TRPV1 regulates Ca²⁺ influx during CHIKV infection in macrophages.

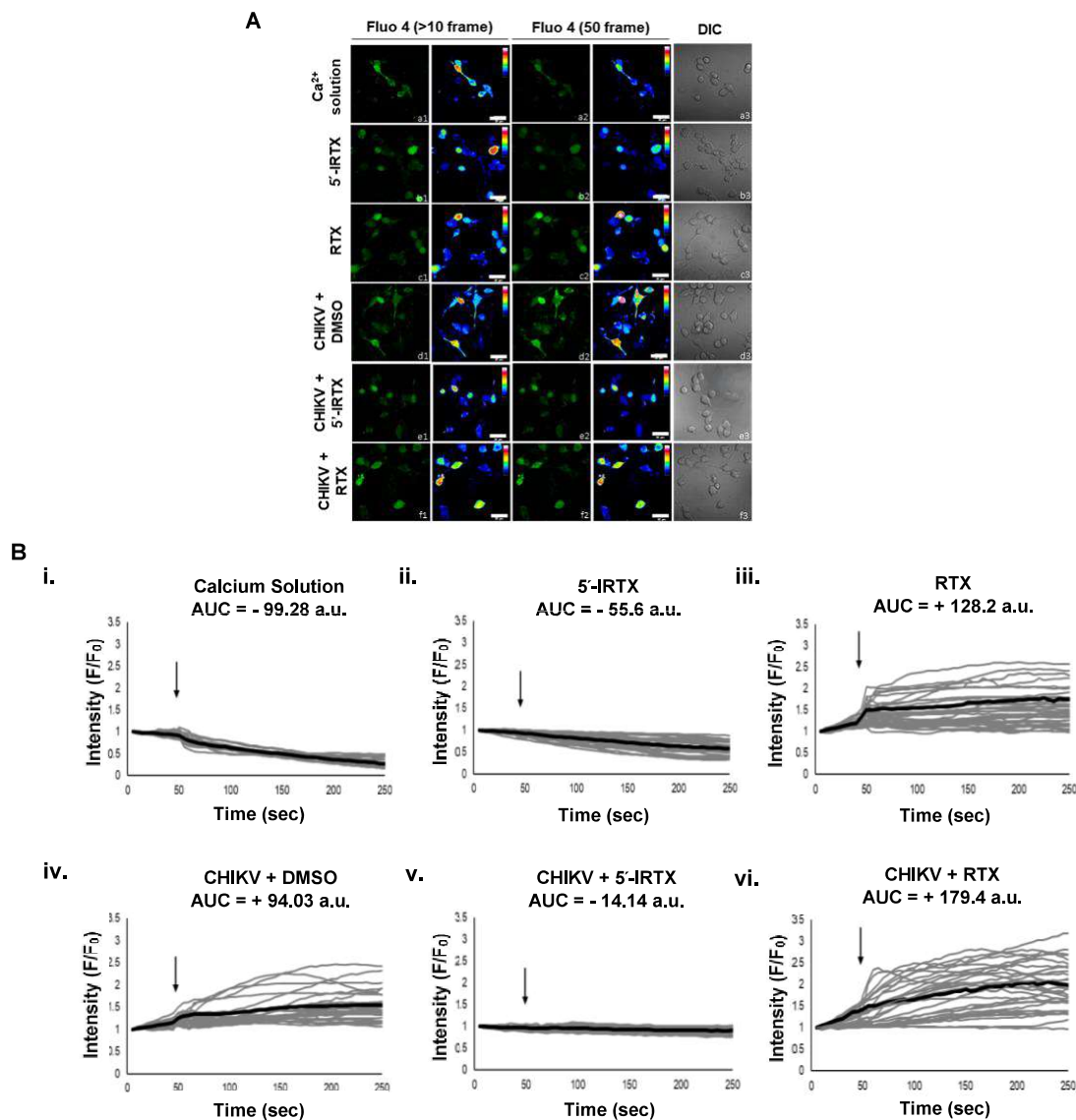


Figure 12 TRPV1 modulates Ca²⁺ influx in macrophages

RAW 264.7 cells were stained with Fluo-4 AM, a calcium-sensitive dye. (A) Fluo-4 (>10 frame) refers to fluorescence before the addition of reagent at 10th frame and fluo-4 (50 frame) refers to fluorescence level at 50th frame. The treatment conditions from top to bottom order is as Mock + Ca²⁺ solution (a1, a2, a3), TRPV1 inhibitor (5'-IRTX) only (b1, b2, b3), TRPV1 activator (RTX) only (c1, c2, c3), CHIKV + DMSO (d1, d2, d3), CHIKV + 5'-IRTX (e1, e2, e3) and CHIKV + RTX (f1, f2, f3). Using the pseudo 16 color, the fluorescence intensities are represented (White and black represent the highest and lowest intracellular Ca²⁺ levels, respectively). (B) Time-lapse kinetics of intracellular calcium influx treated with (i) Ca²⁺ solution (ii) 5'-IRTX (iii) RTX (iv) CHIKV (v) CHIKV + 5'-IRTX (vi) CHIKV + RTX. The intensity (F/F₀) of each cell is represented in grey lines and the average in black lines. The black arrows indicate the time of addition of a specific reagent. Representative data is of three independent experiments.

**Regulatory role of TRPA1 in
CHIKV infection**

5.2 Regulatory role of TRPA1 in CHIKV infection

Like TRPV1, TRPA1 has also been reported to be upregulated during several viral infections, including human rhinovirus (HRV), respiratory syncytial virus (RSV) and measles virus (MV)^{206,207}. TRPA1 has also been known to play vital roles in viral binding, entry and replication^{206,207}. Further, TRPA1 has also been found to be associated with pain and inflammation^{31,43,45,47,260–263}. The current study provides evidence that TRPA1 regulates CHIKV infection in macrophages. Further, the regulatory role of TRPA1 in host-pathogen interactions, effector cytokine response and calcium influx were also investigated.

5.2.1 CHIKV upregulates TRPA1 expression in macrophages

TRPA1 has been reported to be actively involved in various inflammatory diseases, such as, inflammatory bowel disease, neurogenic inflammation, skin inflammation, bone-cancer pain, pancreatic inflammation, lung inflammation and airway hyperresponsiveness^{195,197,217,261,262}. Furthermore, it has also been testified to be upregulated during diverse viral infections as well^{206,207}. Thus, the TRPA1 surface expression levels was assessed in CHIKV-infected macrophages. For CHIKV infection, RAW 264.7 cells were infected with CHIKV at MOI 5 and the viral proteins (nsP2 and E2) and TRPA1 expression at 8 hpi were quantified by Flow cytometry. It was observed that CHIKV viral proteins (nsP2: 8.85 ± 0.73 ; E2: 15.97 ± 0.75) significantly increased as compared to mock cells (nsP2: 0.70 ± 0.30 ; E2: 0.52 ± 0.53) (Figure 13A). Further, it was observed that in CHIKV-infected macrophages, TRPA1 expression levels significantly increased as compared to mock cells at 8 hpi (mock: 36.17 ± 1.21 ; CHIKV: 46.17 ± 2.25) (Figure 13B). Simultaneous detection of viral proteins and TRPA1 expression could not be performed because of saponin. TRPA1 is closely associated with cholesterol in plasma membrane^{217,264,265}. Since saponin creates transient pores in the plasma membrane by removing cholesterol, it leads to membrane loss and consequently loss of TRPA1

signal^{240–243}. These findings suggest that TRPA1 is upregulated during CHIKV infection in a time-dependent manner.

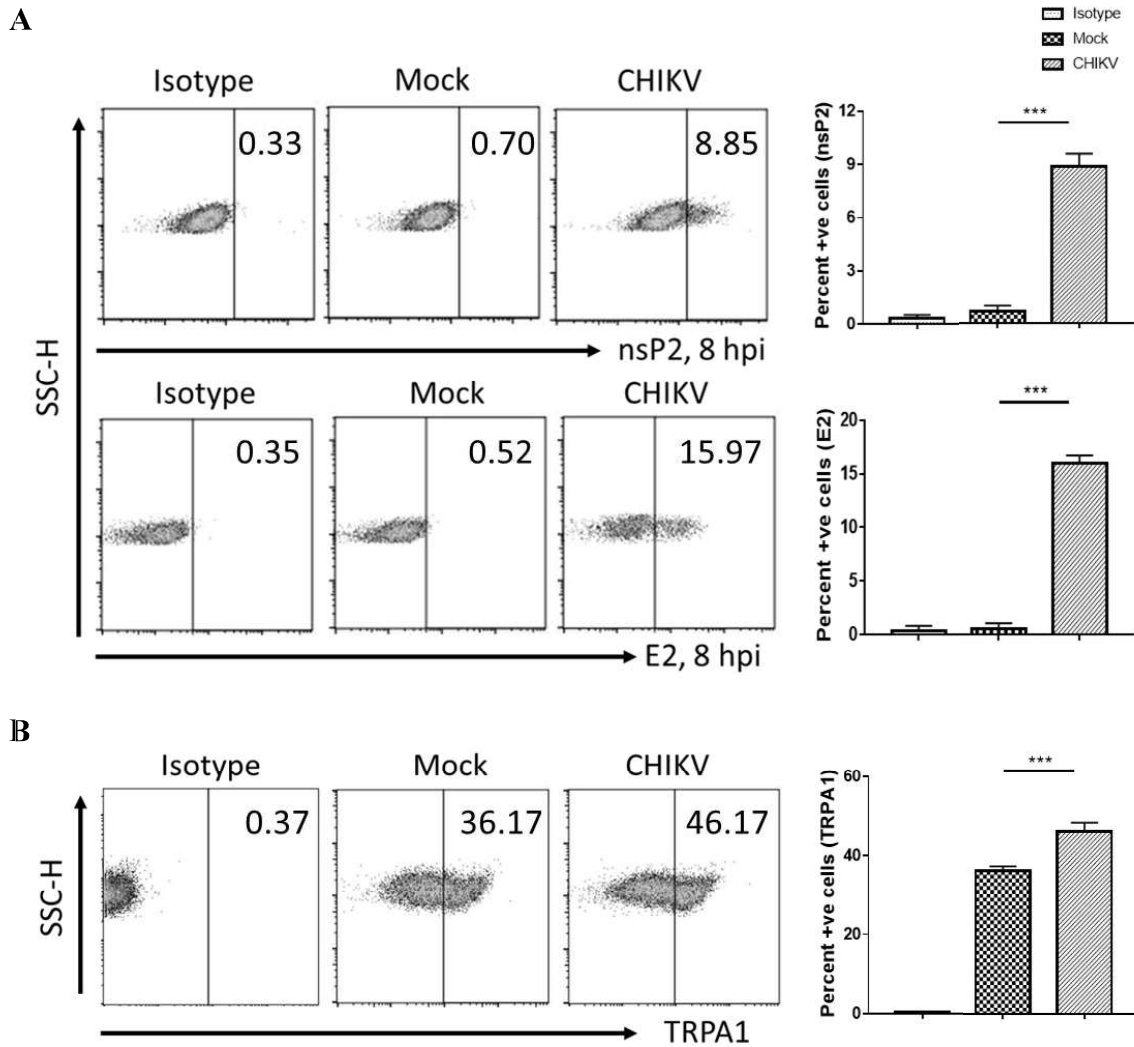


Figure 13 CHIKV upregulates TRPA1 expression in macrophages

RAW 264.7 cells were infected with CHIKV at an MOI of 5 and analyzed for viral proteins, nsP2 and E2 via Flow cytometry (FC) at both 8 and 12 hpi. (A) FC dot-plot depicting the percentage of cells positive for the viral proteins nsP2 (upper panel) and E2 (lower panel) in CHIKV-infected macrophages along with representative bar diagram. (B) FC analysis showing increased TRPA1 expression in CHIKV-infected RAW 264.7 cells with representative bar diagram. Data represents the mean \pm SD of three independent experiments. $P < 0.05$ were considered statistically significant (***, $p < 0.001$).

5.2.2 Assessment of TRPA1 antibody specificity

TRPA1 antibody is polyclonal in origin²⁶⁶. Using a control blocking peptide antigen the specificity of the TRPA1 antibody in RAW 264.7 was assessed via FC. RAW 264.7 cells were stained with TRPA1 antibody in the presence or absence of the blocking peptide. As expected, it was found that the percentage of cells that were positive for TRPV1 decreased in a dose-dependent manner from 35.17 ± 1.21 to 2.50 ± 0.79 (1X control blocking peptide antigen) and further reduced to 0.83 ± 0.28 (3X control blocking peptide antigen), confirming the specificity of the TRPA1 antibody (Figure 14).

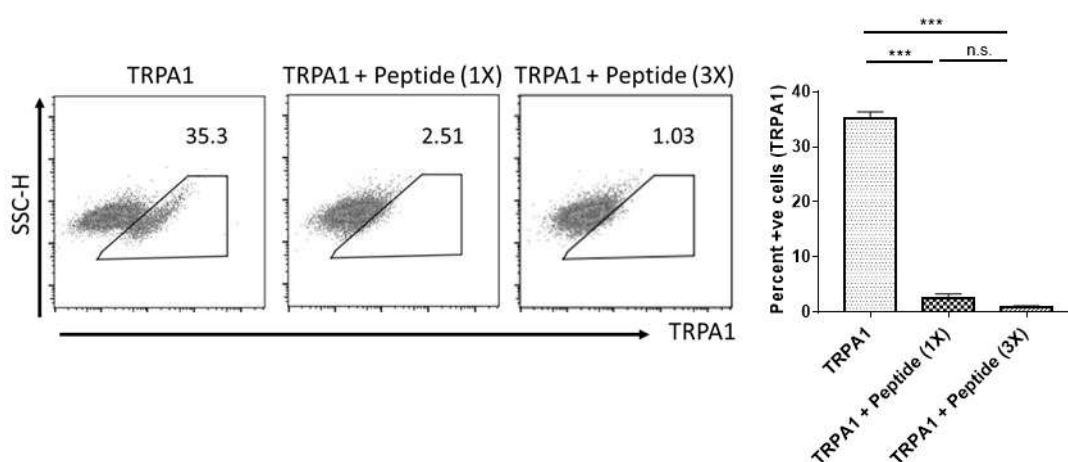


Figure 14 Assessment of TRPA1 antibody specificity

FC analysis depicting TRPA1 expression in RAW 264.7 cells, in presence or absence of control blocking peptide antigen as dot plot. Data represents the mean \pm SD of three independent experiments. $P < 0.05$ were considered statistically significant (ns, non-significant; * * *, $p < 0.001$).

5.2.3 Cell viability assay for macrophages in the presence of TRPA1 modulators

TRPA1 specific functional modulators, HC-030031 and AITC were used²⁶⁷⁻²⁶⁹. To determine the cellular cytotoxicity of HC-030031 and AITC in macrophages, an MTT assay was performed. The drugs, HC-030031 (2.5 μ M to 80 μ M) and AITC (2.5 μ M to 80 μ M) were two-fold serially diluted. DMSO was used as solvent control. It was observed that the percentage of cell viability for 10 μ M of HC-030031 and AITC was $\sim 93\%$ and $\sim 100\%$,

respectively (Figure 15). Hence for further experiments, 10 μ M of HC-030031 and AITC were used.

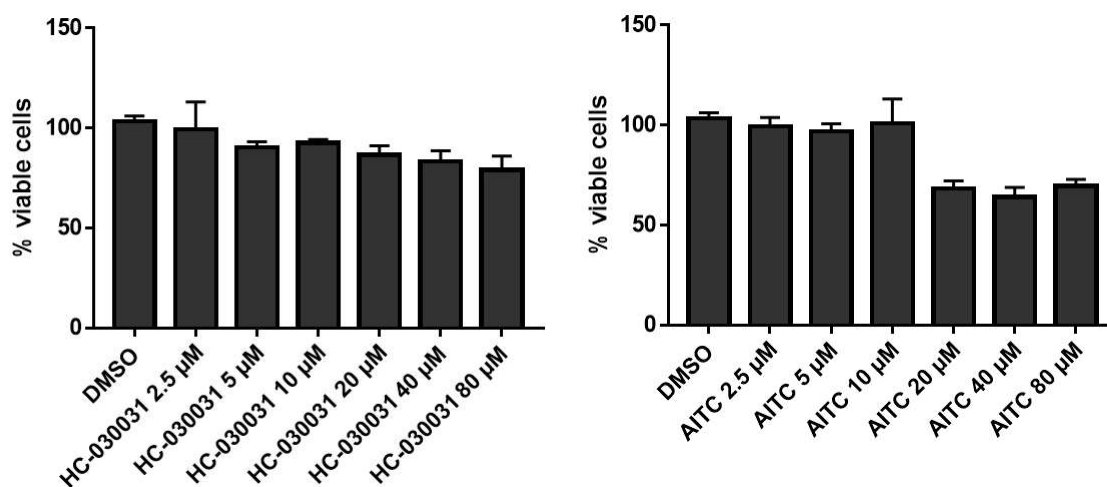


Figure 15 Percentage of cell viability via MTT assay

Bar diagram depicting the percentage of viable RAW 264.7 cells treated with two-fold serially diluted concentrations of HC-030031 (left panel) and AITC (right panel) with respect to the solvent control (DMSO), as determined by MTT assay. Data represents the mean \pm SD of three independent experiments.

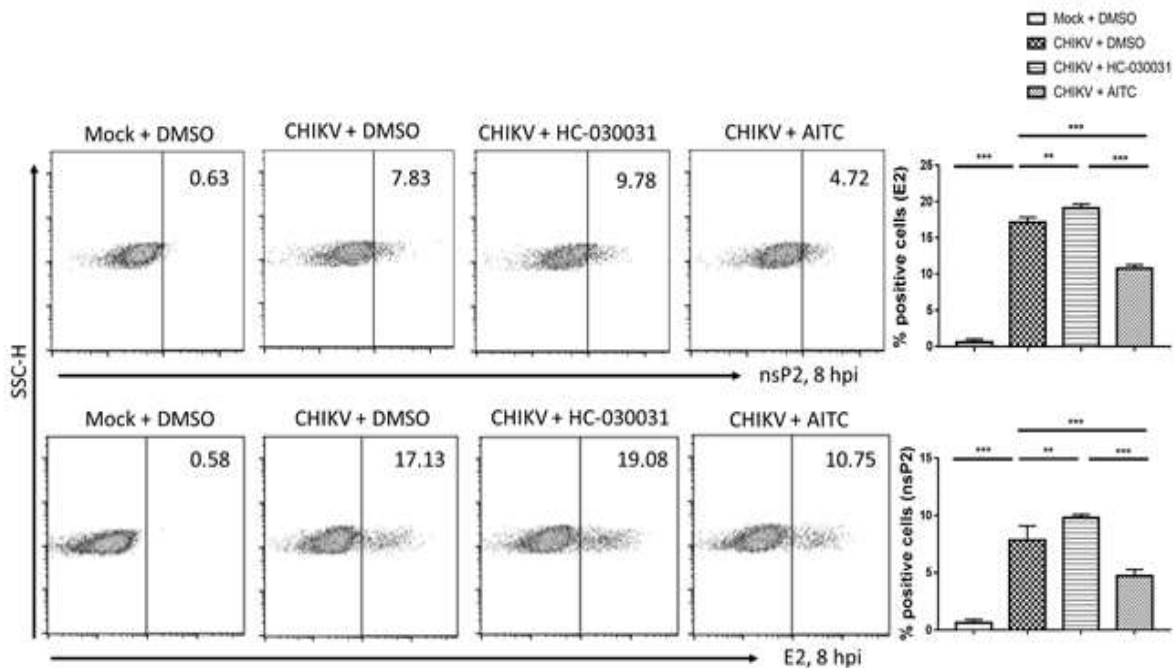
5.2.4 TRPA1 regulates CHIKV infection

TRPA1 has been reported to regulate various viral infections, including respiratory syncytial virus (RSV), measles virus (MV), and human rhinovirus (HRV)^{206,207}. However, no such role of TRPA1 in CHIKV infection has been reported. To ascertain whether TRPA1 regulates CHIKV infection, RAW 264.7 cells were infected with CHIKV in the presence of TRPA1 modulators (HC-030031 or AITC). Flow cytometric analysis revealed that in presence of HC-030031, CHIKV percentage positive cells (nsP2: 9.78 ± 0.27 ; E2: 19.08 ± 0.57) increased whereas in presence of AITC, the CHIKV percentage positive cells (nsP2: 4.72 ± 0.55 ; E2: 10.75 ± 0.5) decreased as compared to CHIKV+DMSO control (nsP2: 7.83 ± 1.23 ; E2: 17.13 ± 0.68) (Figure 16A, i). Similarly, at 12 hpi, CHIKV percentage positive cells in presence of HC-030031 (nsP2: 7.45 ± 0.31 ; E2: 15.07 ± 1.67) increased whereas in presence

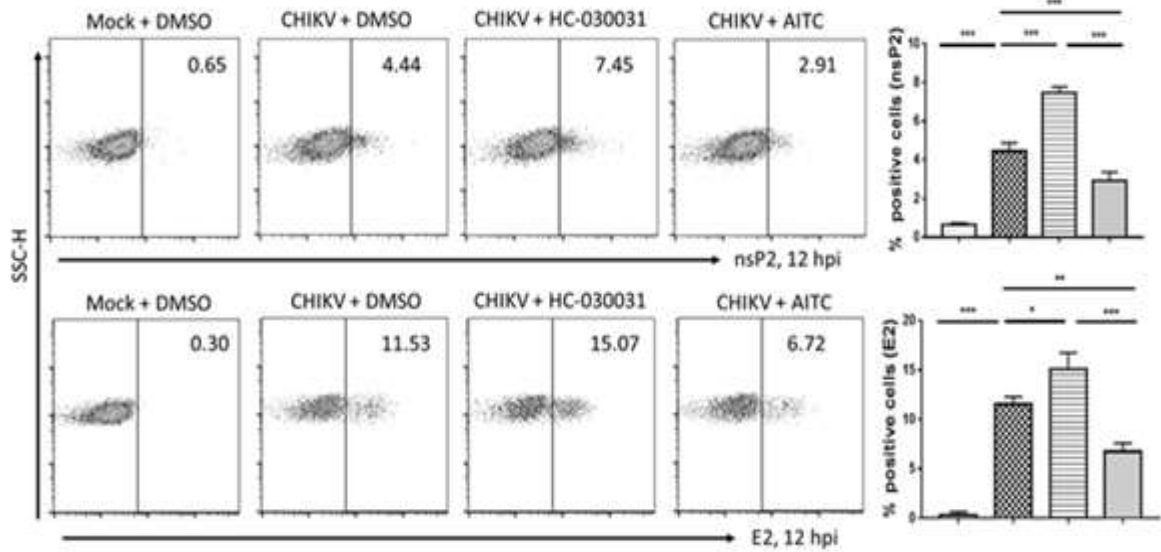
of AITC, the CHIKV percentage positive cells (nsP2: 2.91 ± 0.46 ; E2: 6.72 ± 0.86) decreased as compared to CHIKV+DMSO control (nsP2: 4.44 ± 0.43 ; E2: 11.53 ± 0.75) (Figure 16A, ii). Taken together, these findings suggest that TRPA1 may regulate CHIKV infection in macrophages.

Subsequently, the TRPA1 expression levels were also quantified in CHIKV-infected macrophages treated with TRPA1 modulators. In CHIKV + DMSO (8hpi: 45.05 ± 2.55 ; 12hpi: 54.37 ± 1.41), a significant change was observed as compared to Mock + DMSO (8hpi: 35.4 ± 1.09 ; 12hpi: 44.6 ± 1.45). However, no significant change was observed in presence of HC-030031 (8hpi: 44.1 ± 2.43 ; 12hpi: 55.73 ± 2.06) and AITC (8hpi: 45.55 ± 2.31 ; 12hpi: 54.63 ± 3.20) treated CHIKV-infected macrophages as compared to CHIKV + DMSO (Figure 16C). Taken together, these results indicate that upon CHIKV infection in macrophages, surface TRPA1 levels increase significantly. Although TRPA1 modulators can modulate CHIKV infection, no significant change in TRPA1 expression levels was observed since the TRPA1 modulators used in this study are functional modulators.

A
i



ii.



B

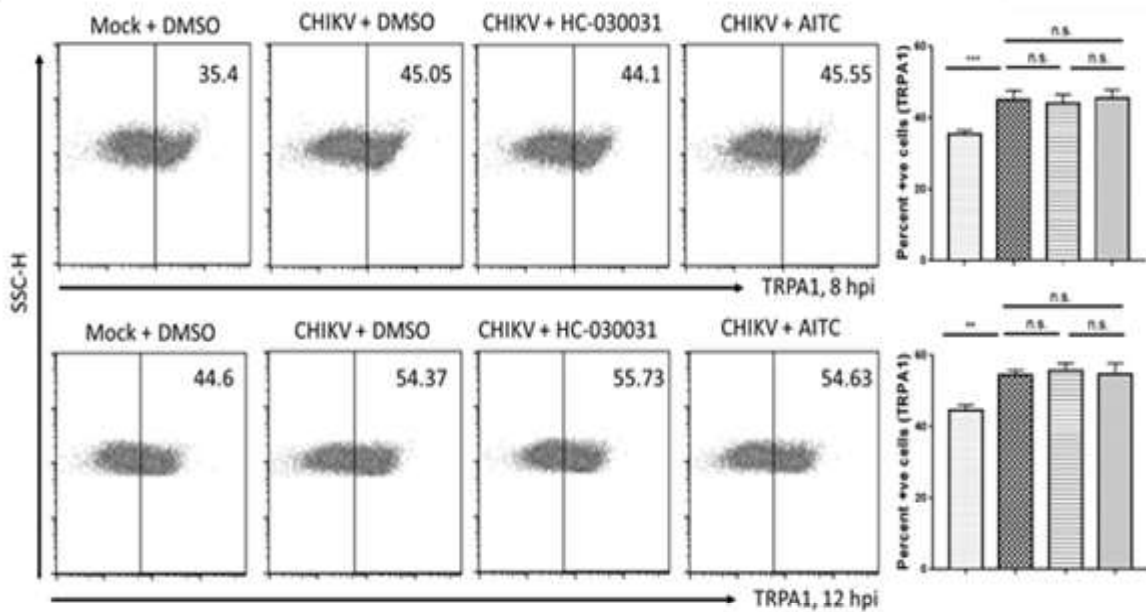


Figure 16 TRPA1 regulates CHIKV infection

The RAW 264.7 cells were treated with either DMSO or TRPA1 modulators, HC-030031 or AITC at both 8 and 12 hpi. (A) Representative FC dot plot depicting percent positive cells for viral proteins, nsP2 (i) and E2 (ii) with either HC-030031 or AITC treatment. (B) Representative FC dot plot depicting percent positive cells for TRPA1 in CHIKV-infected macrophages treated with TRPA1 modulators. Data represents the mean \pm SD of three independent experiments. $P < 0.05$ were considered statistically significant (ns, non-significant; * $p < 0.05$; ** $p < 0.01$; *** $p < 0.001$).

5.2.5 TRPA1 regulates CHIKV viral titer

To determine whether TRPA1 regulates CHIKV viral titer, a plaque assay was performed as mentioned elsewhere^{226,248}. Cell-free supernatants containing the infectious viral particles from the experiments were collected and stored at -80°C. CHIKV viral titer significantly increased in the presence of HC-030031 to $2.32 \times 10^8 \pm 2 \times 10^7$ (1.33-fold) and conversely decreased in presence of AITC to $1.36 \times 10^8 \pm 1.9 \times 10^7$ (0.78-fold) as compared to CHIKV + DMSO control ($1.74 \times 10^8 \pm 1.5 \times 10^7$) (Figure 17). This result indicates that TRPA1 also regulates CHIKV viral titer.

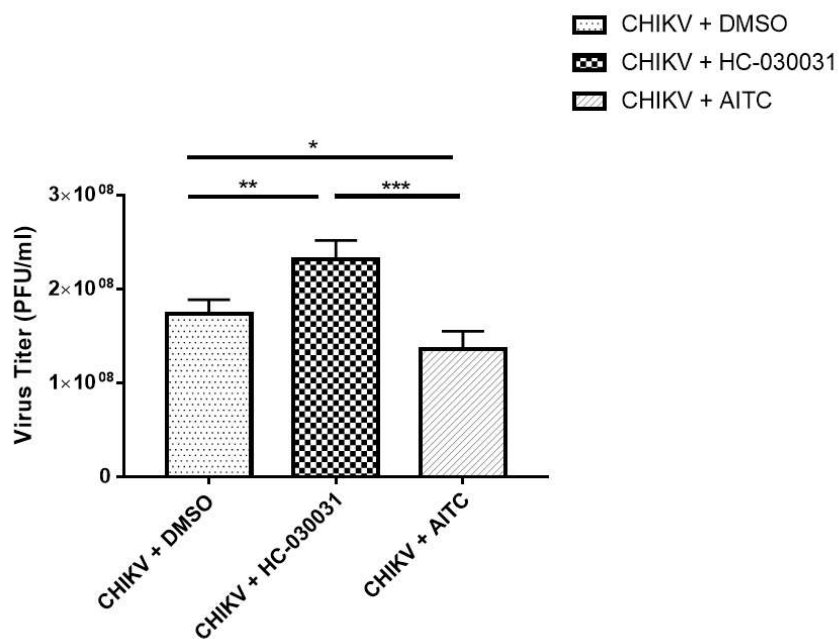


Figure 17 TRPA1 regulates CHIKV infection

The RAW 264.7 cells were treated with either DMSO or TRPA1 modulators, HC-030031 or AITC. Bar diagram showing viral plaque-forming units (PFU/ml), as determined by plaque assay from CHIKV-infected macrophages with HC-030031 or AITC treatment at 12 hpi. Data represents the mean \pm SD of three independent experiments. $P < 0.05$ were considered statistically significant (ns, non-significant; * $p < 0.05$; ** $p < 0.01$; *** $p < 0.001$).

5.2.6 TRPA1 modulates the early phases of the CHIKV life-cycle

TRPA1 has been widely reported to affect various viral life-cycle stages such as adsorption, entry and replication^{206,207}. To determine which phase of the CHIKV life-cycle does TRPA1 affect, we performed time-of-addition studies. The time-of-addition assay as described in Methods showed that the addition of TRPA1 modulators with respect to the CHIKV addition profoundly affects the CHIKV titer estimated via plaque assay from culture supernatants at 12 hpi. CHIKV infection significantly altered in the presence of TRPA1 modulators in the “Pre+During+Post” and “Pre+During” conditions. The percentage of CHIKV infection in presence of HC-030031 increased significantly to 30.92% and 36.79% in “Pre+During+Post” and “Pre+During”, respectively as compared to the corresponding CHIKV + DMSO control. Conversely, the percentage of CHIKV infection in the presence of AITC decreased to 27.22% and 25.47% in “Pre+During+Post” and “Pre+During” respectively as compared to the corresponding control (CHIKV + DMSO). At “post 0 hpi”, a non-significant change in CHIKV infection was observed (Figure 18). Taken together, these results suggest that the TRPA1 may affect the early phases of the CHIKV viral life-cycle i.e., viral adsorption and/or entry.

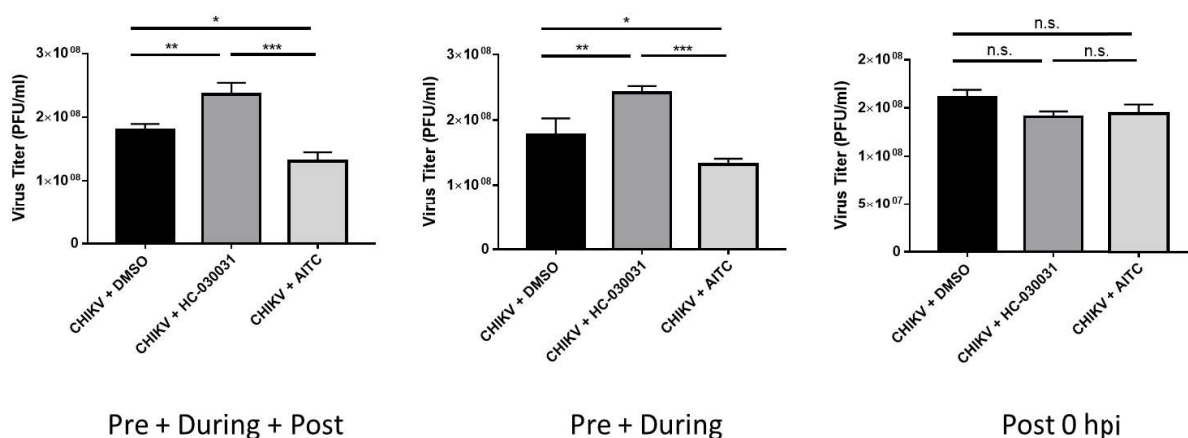


Figure 18 TRPA1 modulates early phases of the CHIKV life-cycle

CHIKV infection was carried out in RAW 264.7 cells by adding TRPA1 modulators, HC-030031 or AITC in different phases of CHIKV infection like (i) pre + during + post, (ii) pre + during and (iii) post

at 0 hpi. Data are expressed in plaque-forming units (PFU/ml) and represented as mean \pm SD of three independent experiments. $P < 0.05$ were considered statistically significant (ns, non-significant; * $p < 0.05$; ** $p < 0.01$; *** $p < 0.001$).

5.2.7 TRPA1 modulates the CHIKV-induced pro-inflammatory cytokine response in host macrophages

CHIKV has been widely reported to induce robust pro-inflammatory cytokine response in host macrophages^{226,227,249–251}. To quantitate the secreted cytokines during CHIKV infection, we performed sandwich ELISA.

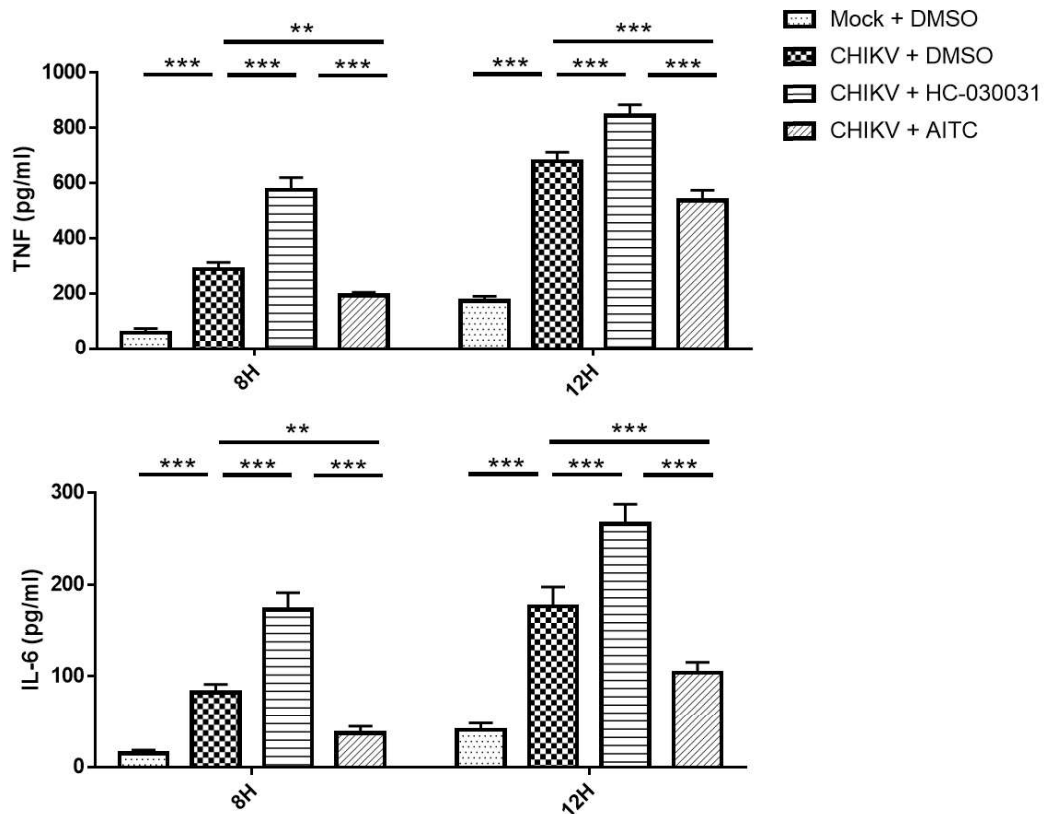


Figure 19 TRPA1 modulates the CHIKV-induced pro-inflammatory cytokine response in host macrophages

The cell-free supernatants from CHIKV-infected macrophages were collected at 8 and 12 hpi. Sandwich ELISA was performed to determine the levels of the pro-inflammatory cytokine. Bar diagram depicting the amount of (A) TNF and (B) IL-6 secreted in mock-treated and HC-030031 or AITC-treated CHIKV-infected macrophages in pg/ml. Data represents the mean \pm SD of three independent experiments. $P < 0.05$ were considered statistically significant (* $p < 0.01$; *** $p < 0.001$).

As expected, the cytokines TNF and IL-6 were markedly upregulated during CHIKV infection at both 8 and 12 hpi. In HC-030031 treated CHIKV-infected macrophages, the cytokine TNF and IL-6 were further significantly upregulated as compared to CHIKV + DMSO control. Similarly, in AITC treated CHIKV-infected macrophages, the cytokines TNF and IL-6 were significantly downregulated as compared to CHIKV + DMSO control (Figure 19). These results suggest that upon TRPA1 inhibition or activation, the pro-inflammatory response either increased or decreased respectively in CHIKV-infected macrophages as compared to CHIKV + DMSO control, respectively.

5.2.8 TRPA1 modulates Ca²⁺ influx during CHIKV infection in macrophages

TRPA1 is a non-selective calcium-permeable cation channel. Here, we have assessed the functional contribution of TRPA1 in Ca²⁺ influx during CHIKV infection in macrophages. The macrophages were stained with Ca²⁺ sensitive dye fluo 4-AM. The addition of Ca²⁺ solution did not induce any Ca²⁺ influx, indicating that the Ca²⁺ solution does not trigger any non-specific change in Ca²⁺ levels. Next, upon the addition of HC-030031, we observed a slight reduction in fluo-4 intensity. Further, upon treatment with AITC, we observed a robust increase in fluo-4 intensity indicating Ca²⁺ influx via TRPA1 channels. Similarly, upon treatment with CHIKV, we observed an increase in Ca²⁺ influx, indicating that CHIKV binding to host macrophages induces Ca²⁺ influx. Next, upon the addition of CHIKV + HC-030031, we observed that the Ca²⁺ influx has reduced. Conversely, upon treatment with CHIKV + AITC, the fluo-4 intensity increased to maximum (Figure 20). To further quantify the above results, we have estimated the area under the curve (AUC). The estimated AUC values for different conditions were ionomycin (+1756 a.u.), HC-030031 (-316.4 a.u.), AITC (+447.8 a.u.), CHIKV + DMSO (+383.6 a.u.), CHIKV + HC-030031 (+282.4 a.u.), and CHIKV + AITC (+952.4 a.u.) (Figure 20). These results indicate that TRPA1 plays a regulatory role in regulating Ca²⁺ influx during CHIKV infection in macrophages.

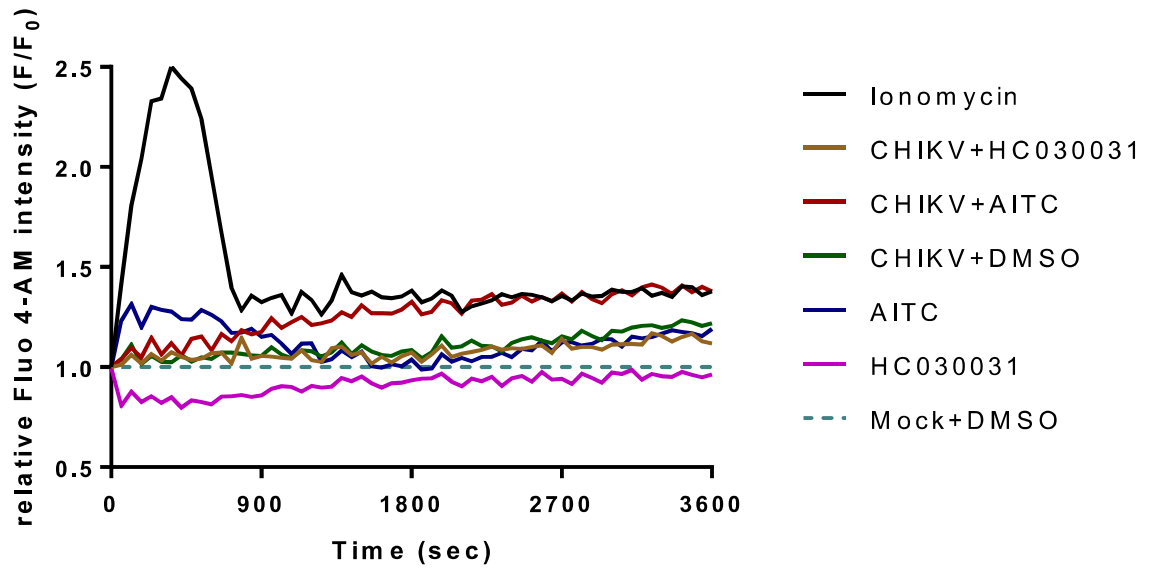


Figure 20 TRPA1 modulates Ca²⁺ influx during CHIKV infection in macrophages

RAW 264.7 cells were treated with Fluo-4 AM, a calcium-sensitive dye. The intensity (F/F₀) was estimated for 60 minutes and the varying treatment conditions were Mock + DMSO (dotted blue), HC-030031 only (pink), AITC only (blue), CHIKV + DMSO (green), CHIKV + AITC (red), CHIKV + HC-030031 (yellow) and Ionomycin (black). Representative data is of three independent experiments.

Regulatory role of TRPA1 in T cell activation

5.3 Regulatory role of TRPA1 in T cell activation

Recently, several TRP channels, including TRPV1, TRPV4 and TRPM8, have been attributed to T cell activation^{191,270,98,99}. All these TRP channels are reported to contribute immensely towards the calcium influx required during T cell activation. Moreover, it has been reported that the unavailability of Ca^{2+} in T cells leads to inadequate activation of T cells and its associated effector functions²⁷¹⁻²⁷³. Additionally, signaling molecules such as PKC, NFAT, NF- κ B, JNK and calmodulin-dependent kinase also requires Ca^{2+} for their function^{181,274,275}. Accordingly, in the current study, the possible role of TRPA1 in T cell activation was explored. Moreover, inflammatory cytokines response and subsequent Ca^{2+} influx was also investigated.

5.3.1 TRPA1 expression in mouse T cells

A number of TRP channels are expressed on T cells^{191,194,270,276}. In order to determine whether TRPA1 is expressed on T cells, Flow cytometry was performed. It was observed that ~37.8 % of resting T cells were positive for TRPA1 and upon TCR activation, TRPA1 levels increases to 60.1% (Figure 21). These results suggest that TRPA1 is expressed on T cells.

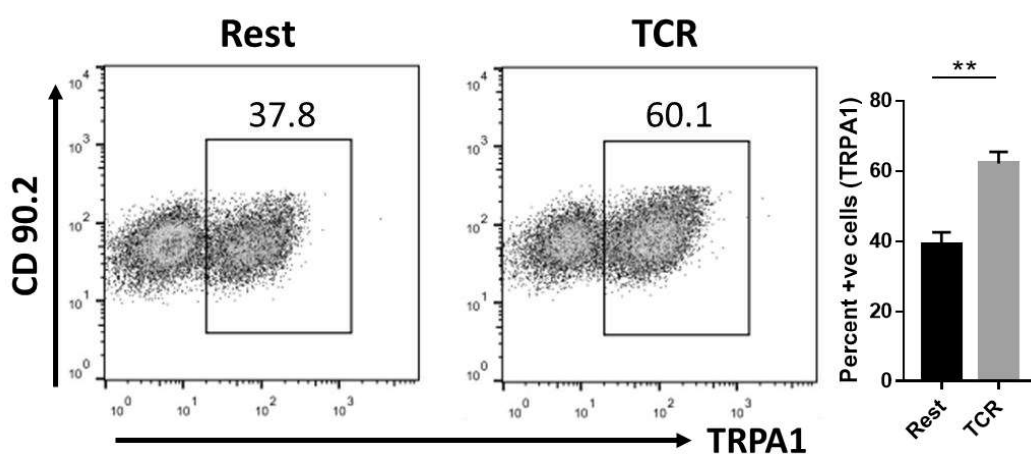


Figure 21 TRPA1 expression in mouse T cells

Purified T cells were activated by TCR and stained with the α -TRPA1 antibody. In TCR-treated T cells, the surface TRPA1 expression levels markedly increased as compared to resting T cells. Data represents the mean \pm SD of three independent experiments. $P < 0.05$ were considered statistically significant (* * $p < 0.01$).

Additionally, TRPA1 antibody specificity was tested by using control blocking peptide antigen as mentioned elsewhere ¹⁹¹. Consequently, T cells were stained with α -TRPA1 antibody in the presence or absence of the 1X control blocking peptide. It was observed that the percentage of TRPA1 positive cells significantly reduced from ~38% to ~2% in the presence of 1X control blocking peptide antigen. Similarly, it was observed that in TCR-activated T cells, the TRPA1 levels reduced from ~60% to ~2%, as shown below. These results indicate that the TRPA1 antibody is highly specific towards the TRPA1 antigen in T cells.

Experimental conditions	Frequency of TRPA1 (%)	
	(-) blocking peptide	(+) blocking peptide
Resting T cells	~ 38	~2
TCR activated T cells	~ 60	~2

5.3.2 TRPA1 regulates T cell activation

In order to determine whether TRPA1 regulates T cell activation, we assessed the levels of CD69 and CD25 in TCR mediated T cell activation in A-967079 (TRPA1 inhibitor) pre-treated T cells via Flow cytometry. It was observed that in A-967079 pre-treated and TCR stimulated T cells, CD69 (CD4: 14.47 ± 3.83 , CD8: 13.11 ± 3.02) and CD25 (CD4: 12.86 ± 2.19 , CD8: 12.29 ± 1.58) levels significantly reduced as compared to control TCR activated T cells in both CD4 (CD69: 41.71 ± 2.6 , CD25: 46.3 ± 2.53) and CD8 (CD69: 60.5 ± 4.58 , CD25: 55.02 ± 4.18) T cells (Figure 22). These results indicate that TRPA1 plays a functional role in T cell activation.

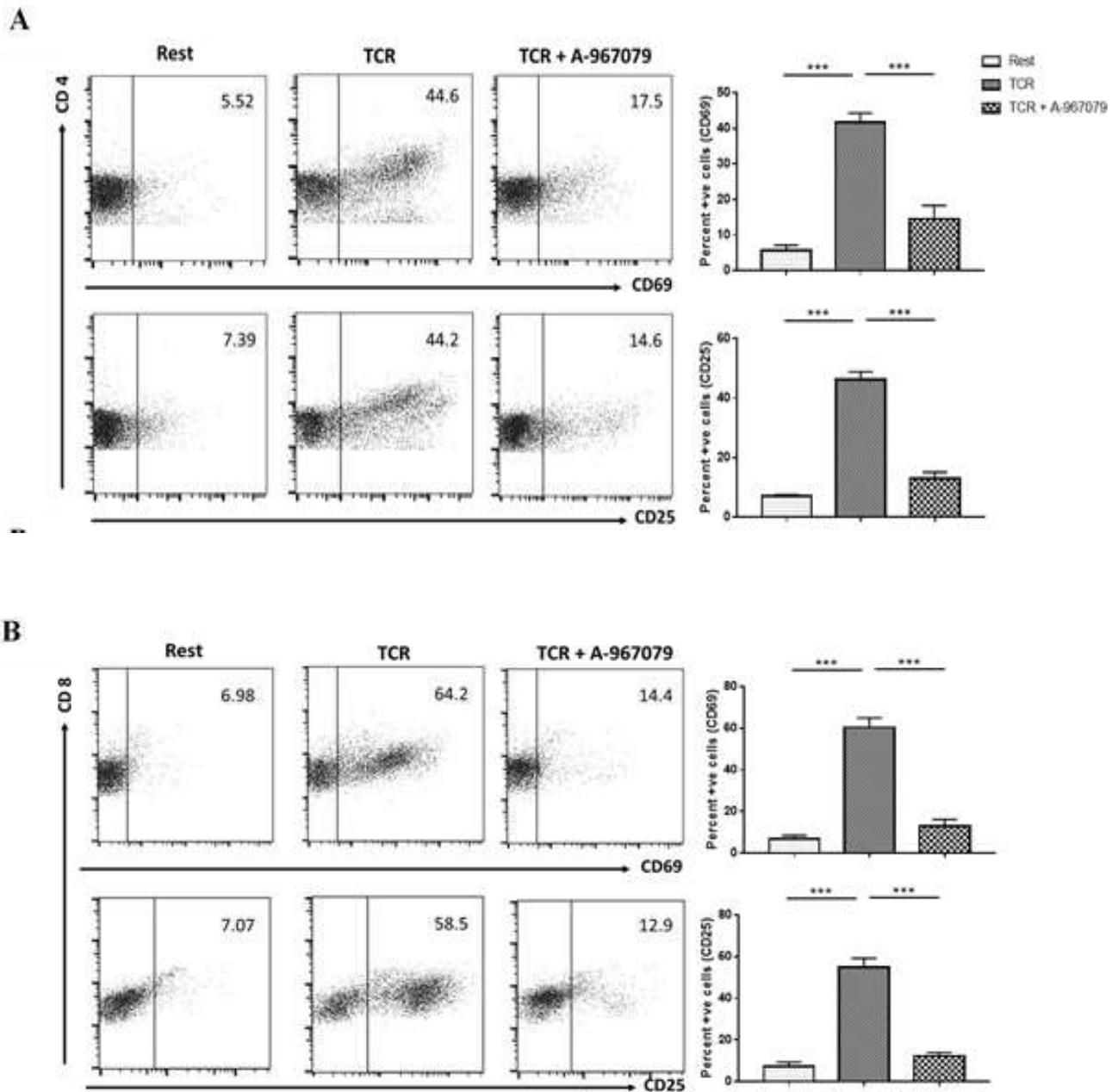


Figure 22 TRPA1 regulates T cell activation

Purified T cells were either activated with TCR or pre-treated with A-967079 and stimulated with TCR. Additionally, the T cells were also stained for Th cells (A) and T_C cells (B). The T cell activation markers (CD69 and CD25) were upregulated in TCR-activated T cells. Conversely, in T cells pre-treated with A-967079 and later stimulated with TCR, the CD69 and CD25 levels markedly decreased. Data represents the mean \pm SD of three independent experiments. $P < 0.05$ were considered statistically significant (* * * $p < 0.001$).

5.3.3 TRPA1 modulates T cell effector cytokine response

T cell activation is known to induce a robust effector or pro-inflammatory cytokine response^{191,270}. Hence, to determine any change in effector cytokine response in immunosuppressed T cells, sandwich ELISA was performed as studied elsewhere^{191,233}.

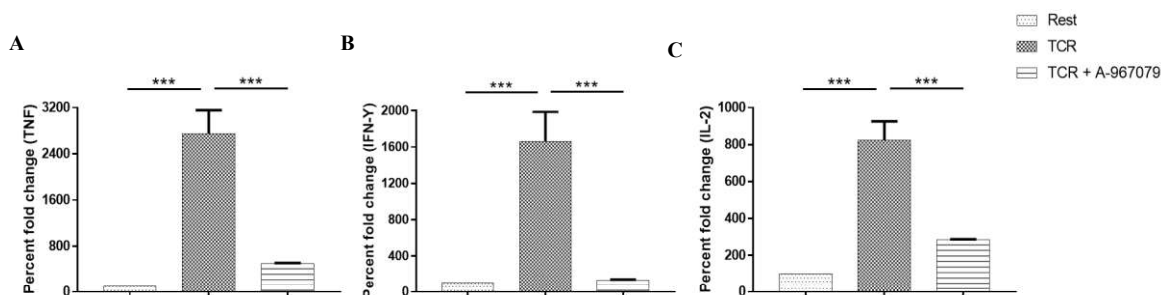


Figure 23 TRPA1 modulates T cell effector cytokine response

Cell-free supernatant was collected at 36 h and sandwich ELISA was performed to determine the level of cytokines. Data are expressed in the percentage of fold change. Bar diagram showing the amount of secreted (A) TNF, (B) IFN- γ and (C) IL-2 in T cells. Data represents the mean \pm SD of three independent experiments. $P < 0.05$ were considered statistically significant (***) $p < 0.001$.

The estimated IL-2, IFN- γ and TNF levels decreased in A-967079 pre-treated T cells stimulated with TCR as compared to TCR activated T cells (Figure 23). These results suggest the TRPA1 functional role in pro-inflammatory cytokine production in T cells.

5.3.4 TRPA1 modulates Ca^{2+} influx during T cell activation

A number of TRP channels are reported to contribute immensely towards the calcium influx required during T cell activation^{60,91,98}. To assess whether TRPA1 also contributes towards the TCR-mediated rise in intracellular Ca^{2+} levels, we performed Ca^{2+} influx studies. We observed that the application of TCR beads led to an immediate increase in TCR-mediated Ca^{2+} influx in T cells as compared to resting T cells. Conversely, A967079 pre-treated T cells stimulated with TCR led to reduced Ca^{2+} influx as compared to TCR activated T cells (Figure 24). These results indicate that the TRPA1 channel might contribute to the calcium influx required during T cell activation.

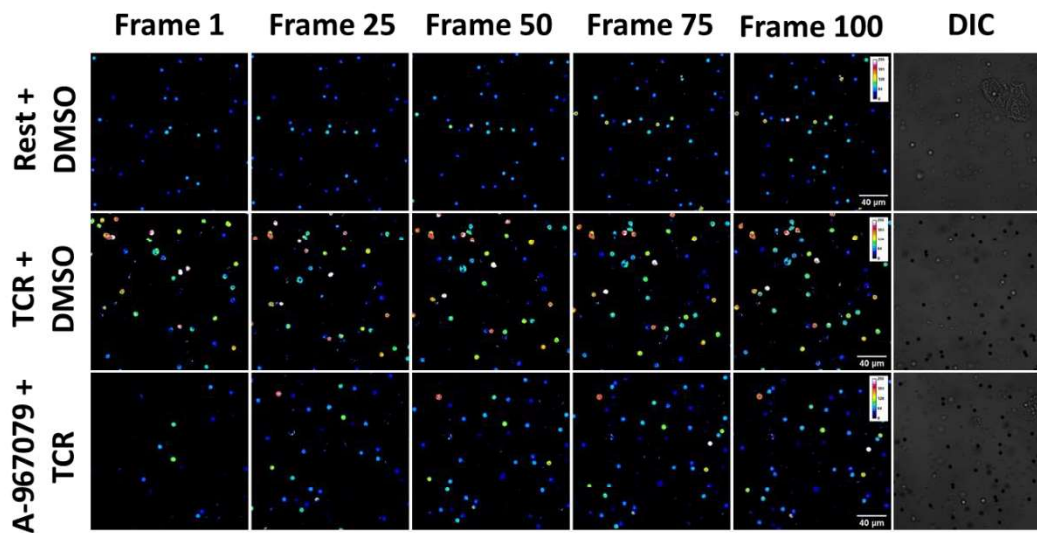


Figure 24 TRPA1 regulates TCR mediated calcium influx

Purified T cells were stained with Fluo 4-AM, a calcium-sensitive dye, as mentioned in the methods. Next, T cells were activated with TCR beads or pre-treated with A-967079 and stimulated with TCR beads. T cells treated with TCR beads show a rise in intracellular Ca^{2+} levels. Conversely, in T cells pre-treated with A-967079 and later stimulated with TCR, the intracellular Ca^{2+} levels were reduced as compared to TCR-activated T cells. Representative data is of three independent experiments.

Regulatory role of TRPV1 in experimental T cell immunosuppression

5.4 Regulatory role of TRPV1 in experimental T cell immunosuppression

Recently, the functional role of TRPV1 in T cell activation has been established^{191,194,276}. Further, TRPV1 has also been reported to affect T cell effector cytokine responses and contribute to the Ca²⁺ influx associated with T cell activation^{191,194,276}. On the other hand, many immunosuppressive agents, such as, FK506 and cyclosporin, have also been reported to immediately induce rise in intracellular Ca²⁺ levels^{58,218–223}. However, the potential contribution of TRPV1 in the increase of intracellular calcium levels during immunosuppression has not been investigated. Accordingly, in this study, the probable functional role of TRPV1 in experimental immunosuppression via FK506 or B16F10-CS was investigated. Further, FK506 or B16F10-CS driven down-regulation in T cell activation, inflammatory cytokine responses and subsequent Ca²⁺ influx was also explored.

Accordingly, in the current study, the probable role of TRPV1 during experimental immunosuppression was explored. Moreover, FK506 or B16F10-CS driven regulation in T cell activation, inflammatory cytokines response and subsequent Ca²⁺ influx was also investigated.

5.4.1 TRPV1 expression in mouse T cells

T cells express several TRP channels, including TRPV1, TRPV4, TRPA1 and TRPM8^{36,191,270,277}. To determine the levels of TRPV1 expression in purified T cells, we performed Flow cytometry. The TRPV1 percent positive cells were 15.63 ± 1.25 compared to an isotype control (0.49 ± 0.18) (Figure 25). Additionally, TRPV1 antibody specificity was tested by using blocking peptide antigen. Consequently, T cells were stained with α -TRPV1 antibody in the presence or absence of the blocking peptide. It was observed that the percentage of TRPV1 positive cells significantly reduced from 15.63 ± 1.25 to 3.86 ± 0.34 in the presence of 1X control blocking peptide antigen and further reduced to 1.30 ± 0.06 in the presence of 3X control blocking peptide antigen (Figure 25). These findings suggest the expression of TRPV1

on the surface of T cells and the α -TRPV1 antibody is high specificity towards the TRPV1 antigen in T cells.

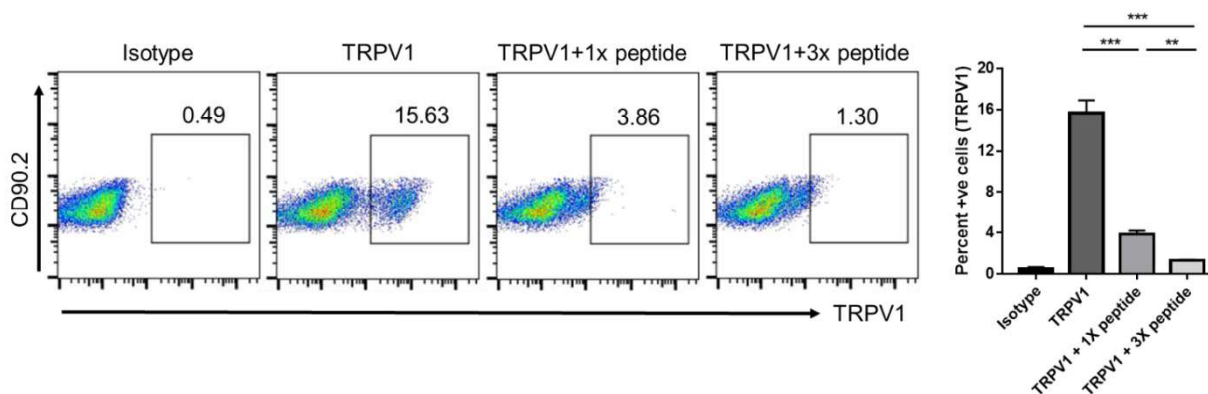


Figure 25 TRPV1 expression in purified mouse T cells

Resting T cells were stained with anti-TRPV1 antibody for 30 mins in FACS buffer followed by secondary antibody staining and acquired via Flow cytometry (FC). Representative FC images showing TRPV1 expression in resting T cells. TRPV1 antibody specificity is shown in the presence or absence of control blocking peptide as dot-plot. Data represents the mean \pm SD of three independent experiments. $P < 0.05$ were considered statistically significant ($**p < 0.01$; $***p < 0.001$).

5.4.2 Cell viability assay for T cells in the presence of B16F10-CS, 5'-IRTX and FK506

To determine the percentage of cell viability in the presence of B16F10-CS, 5'-IRTX and FK506, 7-AAD staining was performed as mentioned in methods.

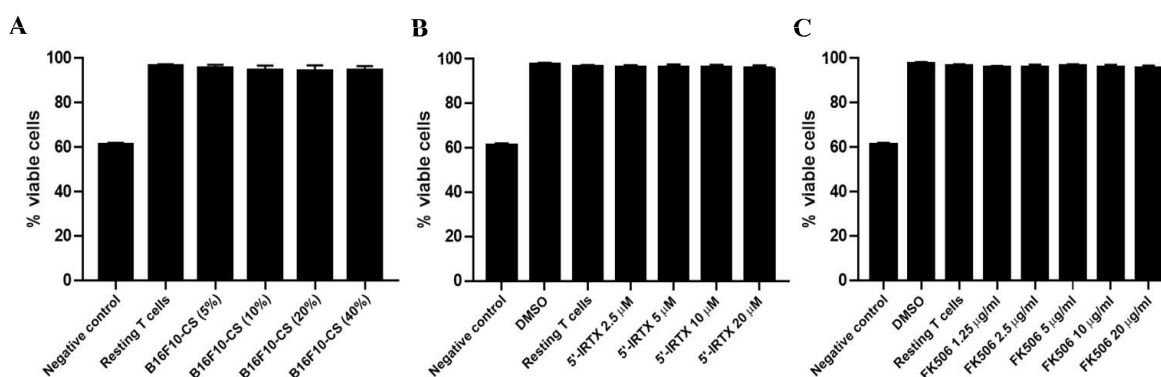


Figure 26 T cell viability in the presence of B16F10-CS, 5'-IRTX and FK506

Bar diagram showing the percentage of viable T cells (7-AAD negative) treated with different concentrations of B16F10-CS (A), 5'-IRTX (B) and FK506 (C) with respect to the solvent control (DMSO), as determined by 7-AAD staining. The data shown are representative of three independent experiments.

All the reagents were two-fold serially diluted. DMSO was used as solvent control, as applicable. It was observed that the percentage of cell viability was at least ~ 95% in all the concentrations of reagents tested (Figure 26). Accordingly, for further experiments, the desired concentration of each reagent has been chosen.

5.4.3 Upregulation of TRPV1 during immune-activation and immunosuppression

TRPV1 has been reported to play a functional role in T cell activation and its effector responses^{191,194}. To assess the T cell activation status during immunosuppression, early T cell activation marker, CD69 and late T cell activation marker, CD25, were analyzed via FC. For immunosuppression, FK506 or B16F10-CS pre-treated T cells were stimulated with either TCR or ConA. Upon Flow cytometric analysis, we observed that both CD69 and CD25 decreased in pre-treated T cells with either FK506 (CD69: 24.2 ± 5.36 , CD25: 13.51 ± 10.65) or B16F10-CS (CD69: 34.37 ± 3.85 , CD25: 18.18 ± 12.94) stimulated with ConA as compared to ConA activated T cells (CD69: 60.23 ± 9.64 , CD25: 56.03 ± 13.51). Similarly, we observed that both CD69 and CD25 decreased in pre-treated T cells with either FK506 (CD69: 8.19 ± 1.93 , CD25: 5.03 ± 2.92) or B16F10-CS (CD69: 19.43 ± 2.45 , CD25: 20.87 ± 5.31) stimulated with TCR as compared to TCR activated T cells (CD69: 41.43 ± 3.37 , CD25: 31.44 ± 4.21) (Figure 27 A, B).

Subsequently, the TRPV1 percent positive cell expression levels were also quantified in immunosuppressed T cells. Surprisingly, the TRPV1 expression levels increased significantly in FK506 (26.9 ± 1.11) or B16F10-CS (23.97 ± 1.04) treated T cells as compared to resting T cells (16.5 ± 0.52). Additionally, the TRPV1 expression levels were found to be increased in FK506 (34.53 ± 0.86) or B16F10-CS (33.77 ± 0.85) pre-treated T cells stimulated with ConA as compared to ConA activated T cells (28.83 ± 1.19). Similarly, the TRPV1 expression levels also increased in FK506 (33.97 ± 0.77) or B16F10-CS (36.1 ± 1.31) pre-

treated T cells stimulated with TCR as compared to TCR activated T cells (30.07 ± 0.20) (Figure 27C).

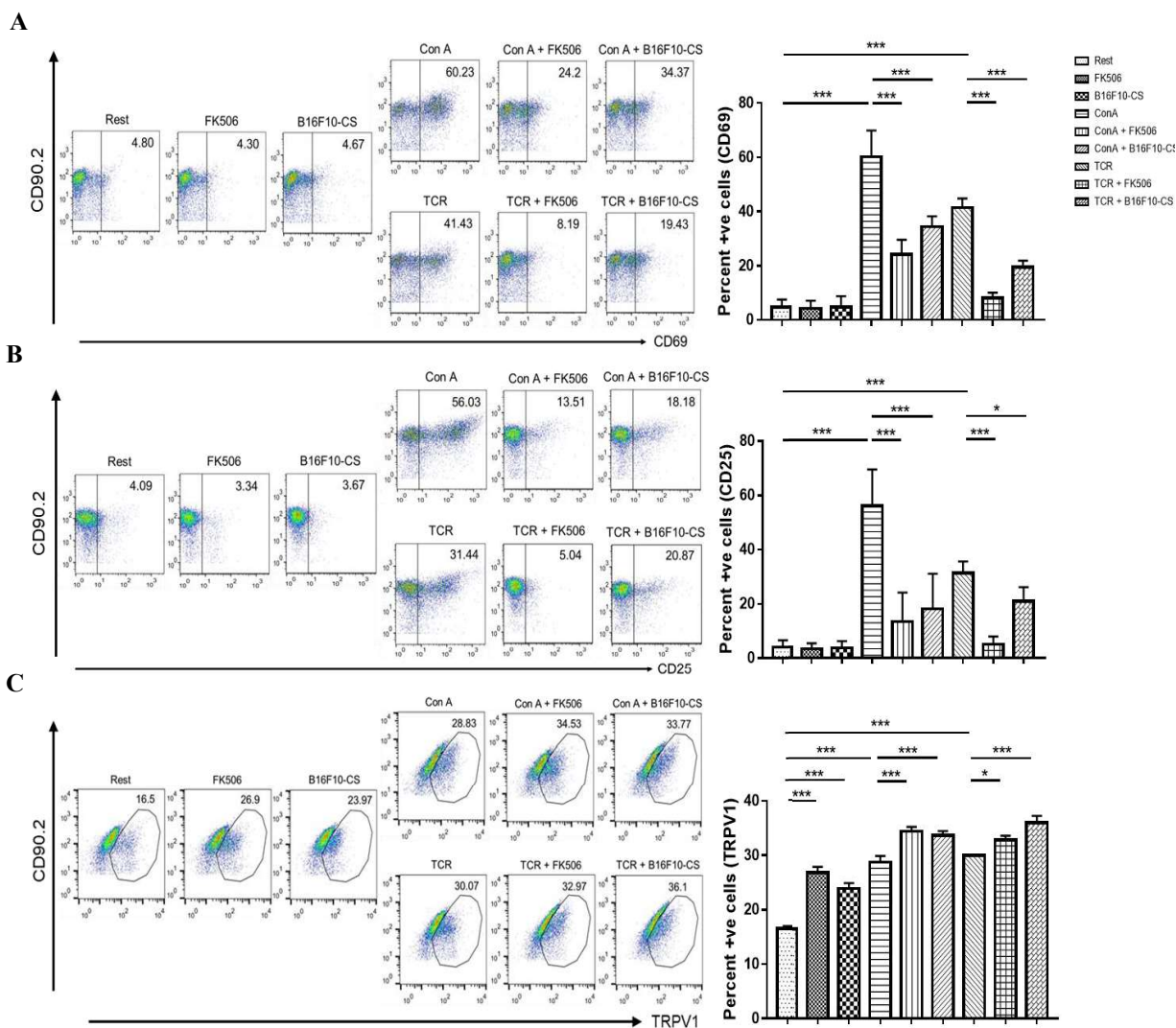


Figure 27 Upregulation of TRPV1 during both immune-activation and immune-suppression

FK506 or B16F10-CS pre-treated T cells were stimulated with either ConA or TCR. Representative FC dot-plot depicting T cell activation markers (A) CD69 and (B) CD25 along with its corresponding bar diagram. (C) Dot-plot representing TRPV1 expression showing rest, FK506, B16F10-CS, ConA, ConA + FK506, ConA + B16F10-CS, TCR, TCR + FK506, TCR + B16F10-CS along with bar diagram. Data represents the mean \pm SD of three independent experiments. $P < 0.05$ were considered statistically significant (* $p < 0.05$; ** $p < 0.01$; *** $p < 0.001$).

As reported earlier, the TRPV1 expression levels significantly increased in ConA or TCR activated T cells as compared to resting T cells. These results indicate that although surface TRPV1 expression levels increase in ConA or TCR activated T cells, it reaches to maximum levels in immunosuppressed T cells stimulated with either ConA or TCR, signifying the potential role of TRPV1 in immunosuppression.

5.4.4 Modulation of cytokine response in immunosuppressed T cells

T cell activation is known to induce a robust pro-inflammatory cytokine response^{191,194}. On the contrary, immunosuppressed T cells stimulated with ConA or TCR respond via attenuated effector cytokine response. Hence, to determine any change in effector cytokine response in immunosuppressed T cells, a sandwich ELISA was performed.

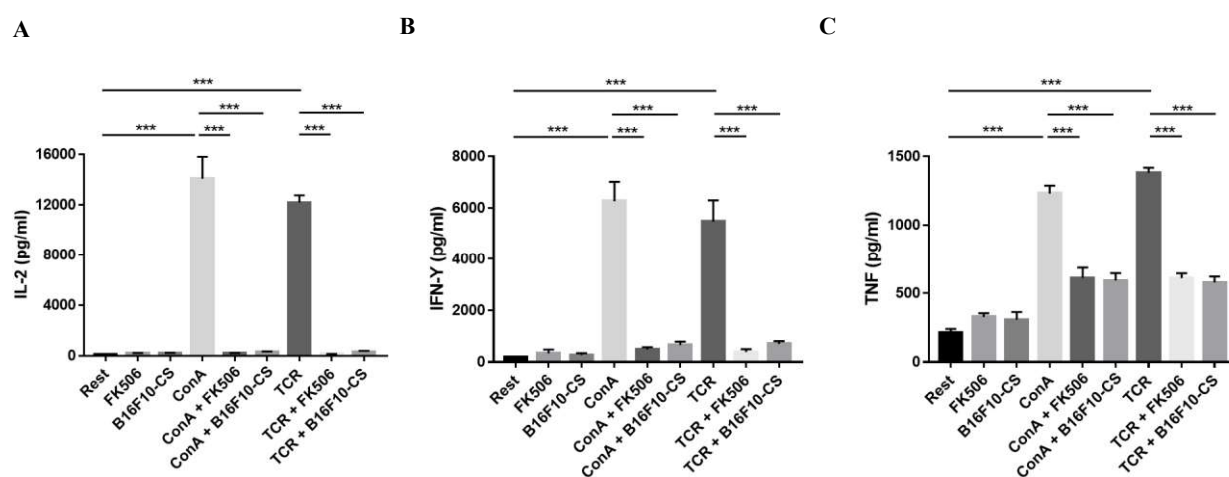


Figure 28 Modulation of cytokine response in immunosuppressed T cells

FK506 or B16F10-CS pre-treated T cells stimulated either with ConA or TCR. The supernatant was collected at 36h and sandwich ELISA was performed to quantitate secreted cytokines, such as, (A) IL-2, (B) IFN-γ and (C) TNF. Data represents the mean ± SD of three independent experiments. $P < 0.05$ were considered statistically significant ($p < 0.001$).

The estimated pro-inflammatory cytokine responses, including IL-2, IFN-γ and TNF decreased in FK506 or B16F10-CS pre-treated T cells stimulated with ConA as compared to ConA activated T cells. Similarly, these cytokines also decreased in FK506 or B16F10-CS pre-treated T cells stimulated with TCR as compared to TCR activated T cells (Figure 28).

Altogether, these results suggest that both FK506 or B16F10-CS pre-treated T cells stimulated with either ConA or TCR show decreased T cell activation cytokines response as compared to ConA or TCR activated T cells.

5.4.5 Modulation of intracellular Ca²⁺ via TRPV1 channel

Activation of various immune cells has been marked with a rise in intracellular Ca²⁺ levels^{191,194}. On the other hand, a number of immunosuppressive agents, such as, FK506 and cyclosporin, have also been reported to immediately induce a rise in intracellular Ca²⁺ levels^{36,191,270,277}. To determine whether immunosuppressive FK506 or B16F10-CS triggers increased accumulated intracellular Ca²⁺ levels via TRPV1 channels, cells were stained with the calcium-sensitive dye, Fluo 4-AM and the changes in intensities were measured via Flow cytometry

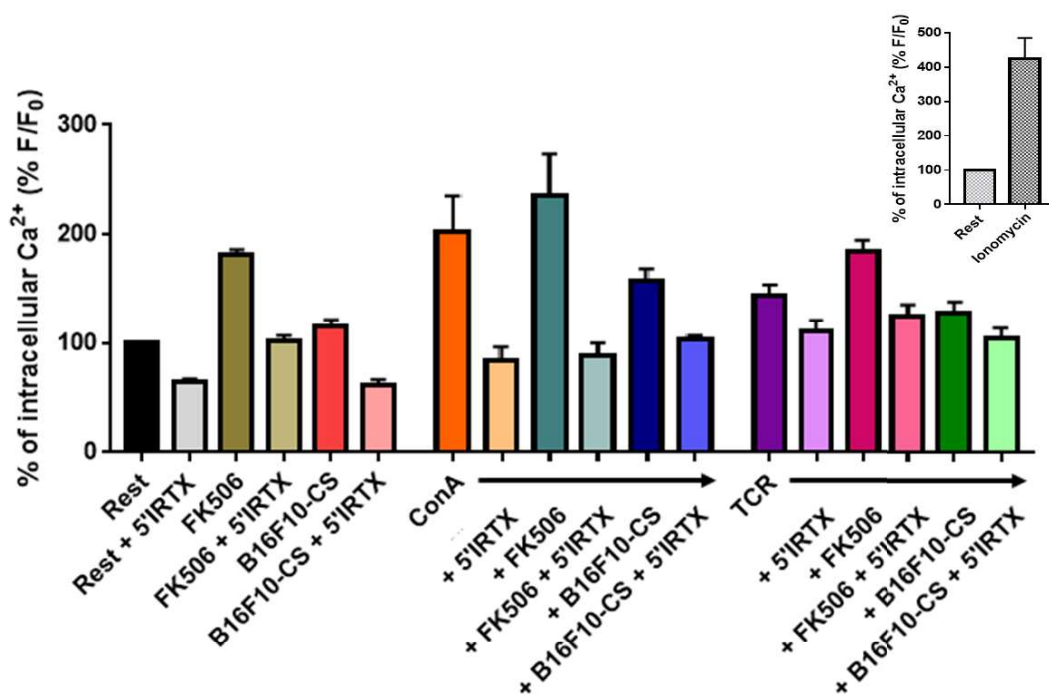


Figure 29 Modulation of intracellular Ca²⁺ via TRPV1 channel

T cells were stained with Fluo-4 AM, a calcium-sensitive dye. The accumulated intracellular Ca²⁺ was represented as a percentage normalized to resting control. All the experimental conditions were divided into two sets. The first subset of T cells were treated as per the experimental conditions whereas the other subset of T cells were pre-treated with 5'IRTX followed by further treatment as per experimental

conditions. In the inset, ionomycin-treated T cells exhibited the rise in intracellular Ca^{2+} levels (positive control). Each column represents three independent experiments.

Accordingly, T cells were stained with fluo-4AM, a calcium-sensitive dye. Next, T cells were pre-treated with TRPV1 inhibitor, 5'-IRTX followed by varying experimental conditions as mentioned. It was observed that in FK506 or B16F10-CS conditions, the fluo-4 AM intensity increased indicating robust calcium influx. Conversely, in the corresponding 5'-IRTX treated conditions, the fluo-4 AM intensity drastically decreased indicating lower intracellular Ca^{2+} levels. Similarly, in T cells pre-treated with FK506 and stimulated with either ConA or TCR, the intracellular Ca^{2+} increased markedly. Conversely, in the corresponding 5'-IRTX treated conditions, the fluo-4 AM intensity drastically decreased indicating lower intracellular Ca^{2+} levels. Similarly, in T cells pre-treated with B16F10-CS and stimulated with either ConA or TCR, the intracellular Ca^{2+} increased modestly as compared to resting cells. Conversely, in the corresponding 5'-IRTX treated conditions, the fluo-4 AM intensity drastically decreased indicating lower intracellular Ca^{2+} levels. The figure inset depicts the treatment of T cells with ionomycin used as a positive control. (Figure 29). These results highlight that the TRPV1 channel contributes to elevated intracellular Ca^{2+} levels during immune activation and immunosuppression.

CHAPTER # 6

Discussion

6. Discussion

TRPV1 and TRPA1 channels are members of the TRP superfamily of structurally related, Ca²⁺ permeable channels with polymodal activation properties^{10,12,60}. Formerly, TRPV1 and TRPA1 channels have been attributed in the field of thermo-sensitive pain responses, especially in the context of neurophysiological responses^{278–281}. Interestingly, it has been found that TRPV1 is co-expressed with TRPA1 in sensory neurons and both integrate a variety of noxious stimuli^{195,280–285}. Current studies indicate that the TRPV1 and TRPA1 channels might operate in the immunological context as well. Several recent reports suggest that these TRP channels are also functionally expressed on immune cells, including macrophages, T cells, B cells, NK cells and dendritic cells^{23,39,276,286,287}. The current study provides the first evidence that the TRPV1 and TRPA1 may functionally regulate CHIKV infection in macrophages and regulate T cell functions during both immune activation and suppression.

TRPV1 and TRPA1 have been reported to be markedly upregulated during several viral infections, including herpes simplex virus-2 (HSV-2), varicella-zoster virus (VZV), herpes simplex virus-1 (HSV-1), hepatitis C virus (HCV), human rhinovirus (HRV), measles virus (MV) and respiratory syncytial virus (RSV)^{206,207,214,235,236}. TRPV1 and TRPA1 have been reported to play a pivotal role in critical host-pathogen interactions, such as viral binding, viral entry, viral replication, viral exit and egress^{206,207}. In this study, it has been demonstrated for the first time that the TRPV1 and TRPA1 are markedly upregulated during CHIKV infection in macrophages. Upon treatment with either TRPV1 or TRPA1 modulators, the CHIKV infection was also modulated. In the presence of TRPV1 inhibitor (5'-IRTX) or TRPA1 activator (AITC), CHIKV infection decreased. Conversely, in the presence of a TRPV1 activator (RTX) or TRPA1 inhibitor (HC-030031), CHIKV infection increased. Moreover, the quantification of viral titer via plaque assay has also shown a similar trend. However, TRPV1

and TRPA1 expression levels did not alter in CHIKV-infected macrophages in the presence of TRPV1 or TRPA1 modulators. Since the modulators used in this study are functional modulators, which may modulate TRP channels functional activity rather than affecting the TRP channel expression^{191,288}. These findings suggest that both TRPV1 and TRPA1 play a regulatory role during CHIKV infection in macrophages. Further, TRPV1 and TRPA1 were found to play an opposing role in CHIKV-infected macrophages. Nevertheless, further investigation is warranted to understand the relationship among TRPV1, TRPA1, host cell immunity and CHIKV together.

Additionally, TRPV1 has also been found to be associated with the nociceptive and pro-inflammatory role in various disease and injury states, such as arthritis, diabetic neuropathy, cancer, urinary bladder infection, non-erosive reflux disease (NERD) and gastro-oesophageal reflux disease (GERD)^{21,28,289–292}. However, recent reports have suggested a differential role of TRPV1. It has been found that the abrogation of TRPV1 expression enhances the pro-inflammatory responses in various model systems, including cardiovascular system, sepsis, dermatitis, salt hypertension and renal inflammation^{161,293–297}. In the current study, we have also observed that CHIKV infection in the presence of 5'-IRTX decreased yet the pro-inflammatory cytokine response increased compared to CHIKV control. To further investigate the apparent discrepancy in cytokine responses, the expression and nuclear localization of pNF- κ B (p65) has been studied. pNF- κ B (p65) is the well-characterized subunit and reported to play vital roles in cellular activation and transcription events^{26,252,253}. Immunofluorescence and Flow cytometry assays have shown that in CHIKV-infected macrophages, pNF- κ B (p65) was induced and translocated to the nucleus as compared to mock cells. In the presence of TRPV1 modulators, the expression and nuclear translocation of pNF- κ B (p65) was further enhanced as compared to CHIKV control. The above findings suggest that both constitutive inhibition or

activation of TRPV1 may lead to enhanced pNF- κ B (p65), thus leading to increased pro-inflammatory cytokine response.

Like TRPV1, TRPA1 has also been reported to act as a transducer and amplifier of pain and inflammation^{31,43,45,47,260–263}. TRPA1 has been found to be associated with various disease and injury states, such as inflammatory bowel disease, neurogenic inflammation, skin inflammation, bone-cancer pain, pancreatic inflammation, lung inflammation and airway hyperresponsiveness^{195,197,217,261,262}. In the present study, we have observed that the CHIKV infection in presence of HC-030031 increases and the pro-inflammatory cytokine response also increased as compared to CHIKV control. On the contrary, the CHIKV infection in the presence of AITC decreased and the pro-inflammatory cytokine response was also reduced as compared to CHIKV control.

A number of TRP channels, including TRPV1, TRPA1, TRPV4, TRPML1, TRPML2, TRPML3 and TRPM8, have been demonstrated to regulate various phases of the viral life-cycle^{206–208,214}. TRPV1 and TRPA1 have been reported to regulate viral binding and entry in diverse viruses such as, respiratory syncytial virus (RSV), human rhinovirus (HRV) and measles virus (MV)^{206,207}. To determine which phase of the CHIKV life-cycle does TRPV1 and TRPA1 affects, we have performed time-of-addition studies. We observed that the TRP modulators affect CHIKV infection most effectively in the “pre+during+post” set-up followed by the “pre+during” set-up. TRP modulators were found to be ineffective at “post 0 hpi” and “post 4 hpi”. These findings suggest that both TRPV1 and TRPA1 channels regulate the early stages of CHIKV life-cycle, i.e., viral binding and entry as reported in other viral model systems as well^{206,207}.

Viruses are adept in tailoring their calcium requirements during viral adsorption, infection, spread and persistence^{205,298–301}. It has been reported that viral adsorption and entry are accompanied by calcium influx at plasma membrane^{200,205,302–305}. Since TRP channels are

Ca²⁺ permeable channels, we further explored whether CHIKV binding to host macrophages in the presence of TRP modulators can modulate differential Ca²⁺ influx, thereby affecting the CHIKV infection. We observed that the application of CHIKV to host macrophages induced Ca²⁺ influx. In the presence of TRPV1 and TRPA1 activator, Ca²⁺ influx increased and conversely decreased in the presence of TRPV1 and TRPA1 inhibitor as compared to CHIKV control. These results suggest that TRP modulators can regulate Ca²⁺ influx and thereby can affect the CHIKV early stages, i.e., viral adsorption and entry.

TRPV1 and TRPA1 are found to be functionally expressed on T cells ^{36,191,192,194}. Additionally, TRPV1 and TRPA1 are reported to be functionally expressed as heteromers ³⁰⁶⁻³⁰⁸. In the current study, it has been observed that during T cell activation by ConA or TCR, TRPA1 levels significantly increased in mouse T cells. A-967079, a TRPA1 inhibitor, pre-treated T cells stimulated by TCR have significantly downregulated T cell activation (CD69 and CD25). These results are similar to the functional role of TRPV1 and TRPV4 in T cell activation as reported elsewhere ^{191,194}. Further, these results highlight that TRPA1 is crucial for T cell activation.

T cell activation is associated with robust cytokine response ^{191,233,270}. Th1 cytokines, such as IFN- γ , IL-2 and TNF, were upregulated during T cell activation. In the current study, we have observed that the cytokines IFN- γ , IL-2 and TNF were also upregulated during T cell activation via TCR. Further, upon pre-treatment with A-967079 and TCR stimulation, the cytokine levels reduced significantly. These findings indicate that the TRPA1 activation is pivotal during T cell activation for optimum effector responses.

T cell activation is marked with calcium influx leading to a rise in intracellular Ca²⁺ levels ^{191,309-313}. Increased intracellular Ca²⁺ levels trigger various cellular signaling events vital for optimum T cell activation and effector responses ³¹⁴⁻³¹⁸. Upon ConA or TCR treatment, an immediate calcium influx was observed. TCR stimulated T cells pre-treated with TRPA1

inhibitor, A-967079, displayed reduced Ca^{2+} influx and lower intracellular Ca^{2+} levels. These results indicate that TRPA1 immensely contributes towards Ca^{2+} influx during T cell activation and consequently for optimum T cell activation and effector responses.

Although the functional role of TRPV1 in T cells during immune activation is very well reported, its role in immunosuppression has not been studied previously^{191,192,194}. It was observed that the treatment of T cells with FK506 or B16F10-CS enhanced surface TRPV1 expression as compared to resting T cells. Moreover, TRPV1 expression markedly increased in immunosuppressed T cells stimulated with either TCR or ConA as compared to corresponding TCR or ConA control.

Intracellular calcium signaling plays a crucial role in cellular processes, including activation, migration, proliferation and differentiation^{181,219,275,319–324}. Resting T cells maintain low cytosolic calcium either by extruding calcium to the extracellular environment or by sequestering in the endoplasmic reticulum^{181,254,325}. It has been earlier reported that T cell activation is marked with a rise in intracellular Ca^{2+} levels. In the current study, we have observed that intracellular Ca^{2+} levels also increase during immunosuppression. Treatment of T cells with either FK506 or B16F10-CS increased intracellular Ca^{2+} levels as compared to resting T cells. A similar increase in intracellular Ca^{2+} levels was also reported in other non-immune models as well^{58,218–223}.

TRPV1 functional modulation via 5'-IRTX further validates the FK506 or B16F10-CS driven rise in intracellular Ca^{2+} levels in T cells. It has been observed that T cells treated with FK506 or B16F10-CS have shown an increase in cytosolic Ca^{2+} as compared to resting T cells control. Moreover, pre-treatment with 5'-IRTX has led to a marked decrease in cytosolic Ca^{2+} accumulation. Next, in FK506 treated T cells, either in the presence or absence of ConA or TCR, the cytosolic Ca^{2+} levels increased and pre-treatment with 5'-IRTX has led to a marked decrease in cytosolic Ca^{2+} levels. Similarly, in B16F10-CS treated T cells, either in the

presence or absence of ConA or TCR, the cytosolic Ca^{2+} levels increased modestly yet lesser than corresponding ConA or TCR controls. Moreover, pre-treatment with 5'-IRTX has led to a marked decrease in cytosolic Ca^{2+} levels. These findings indicate that both FK506 or B16F10-CS employ a similar rise in cytosolic Ca^{2+} levels yet induce different immunosuppression levels. Further, these results also suggest that during both immune-activation and immunosuppression, the TRPV1 may be the key Ca^{2+} channel playing an important role in elevating cytosolic Ca^{2+} levels in T cells. Mechanistically, a rise in intracellular Ca^{2+} has been reported to activate CaMKK2, which in return can induce immunosuppression. Moreover, *in vivo* studies show deletion of CaMKK2 inhibits tumor growth³²⁶. Further studies are warranted for an in-depth mechanism between increased cytosolic Ca^{2+} and induction of immunosuppressive environment.

The current study focused on the functional roles of TRPV1 and TRPA1 during immune activation and immunosuppression in both macrophages and T cells. In macrophages, TRPV1 has been found to act as a pro-inflammatory channel where activation or inhibition of the TRPV1 channel has either increased or decreased CHIKV infection. The relationship between TRPV1 and CHIKV infection in macrophages is schematically plotted as a model in Figure 30. Similarly, TRPA1 has been found to act as an anti-inflammatory channel in macrophages where activation or inhibition of the TRPA1 channel has either decreased or increased CHIKV infection. The relationship between TRPA1 and CHIKV infection in macrophages is schematically plotted as a model in Figure 31. TRPV1 and TRPA1 play opposing roles during CHIKV infection in macrophages. Interestingly, in T cells, TRPA1 has been found to act as a pro-inflammatory channel regulating T cell activation and its effector responses. The current understanding of the relationship between TRPA1 and T cell activation is schematically summarized in the working model shown in Figure 32. Although TRPV1 has been earlier reported as a pro-inflammatory channel in T cells, its dual role as an anti-inflammatory channel

has been established. The current understanding of the relationship between TRPV1 and T cell immunosuppression is schematically summarized in the working model shown in Figure 33. TRPV1 and TRPA1 may play entirely diverse functional roles in different host and model systems. These findings may also have broader implications for understanding the role of TRPV1, TRPA1 and Ca^{2+} in various pathophysiological conditions, such as inflammatory, immunosuppressive and autoimmune diseases as well.

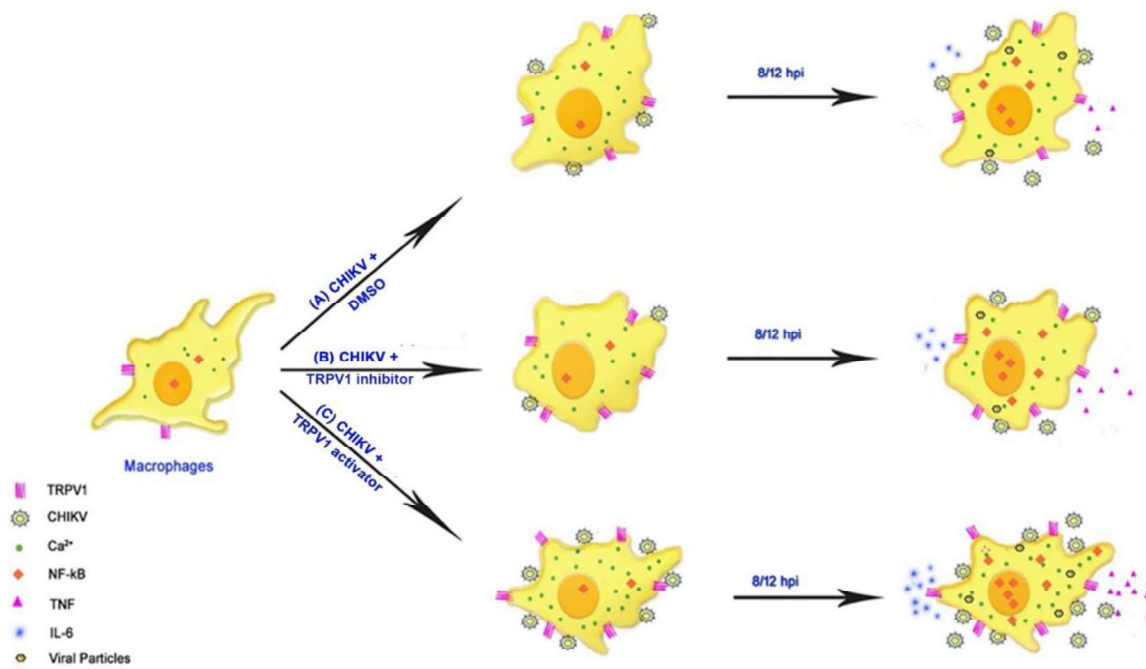


Figure 30 Proposed working model depicting the functional role of TRPV1 in CHIKV-infected macrophages.

TRPV1 is expressed on the surface of macrophages. (A) Upon CHIKV adsorption, TRPV1 channels get triggered and facilitate Ca^{2+} influx in macrophages and entry. (B) Upon treatment with the TRPV1 inhibitor, the TRPV1 channel is blocked, leading to attenuated Ca^{2+} entry into the macrophages, leading to a lower viral entry. Interestingly, TNF and IL-6 production increased as compared to CHIKV+DMSO control. (C) Upon treatment with the TRPV1 activator, the TRPV1 channel gets triggered and facilitates heightened Ca^{2+} influx in macrophages and viral entry, thereby resulting in elevated TNF and IL-6 responses.

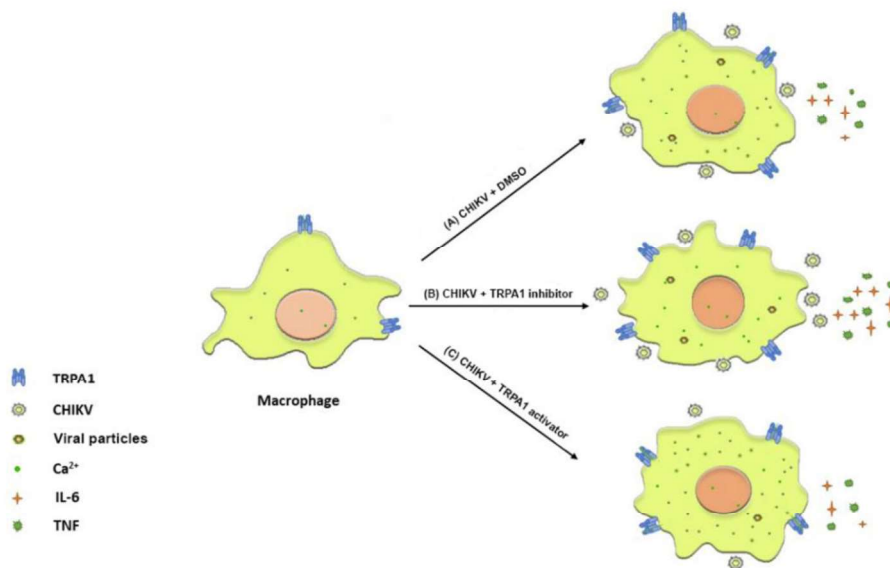


Figure 31 Proposed working model depicting the functional role of TRPA1 in CHIKV-infected macrophages.

TRPA1 is expressed on the surface of macrophages. (A) Upon CHIKV infection, TRPA1 channels get activated, facilitating Ca²⁺ influx in macrophages. (B) Upon treatment with the TRPA1 inhibitor, the TRPA1 channel gets inactivated and consequently, the CHIKV infection and pro-inflammatory cytokine response increases as compared to control CHIKV + DMSO. (C) Upon treatment with the TRPA1 activator, the TRPA1 channel gets activated, which leads to lower CHIKV infection and thus, the pro-inflammatory cytokine response also decreases.

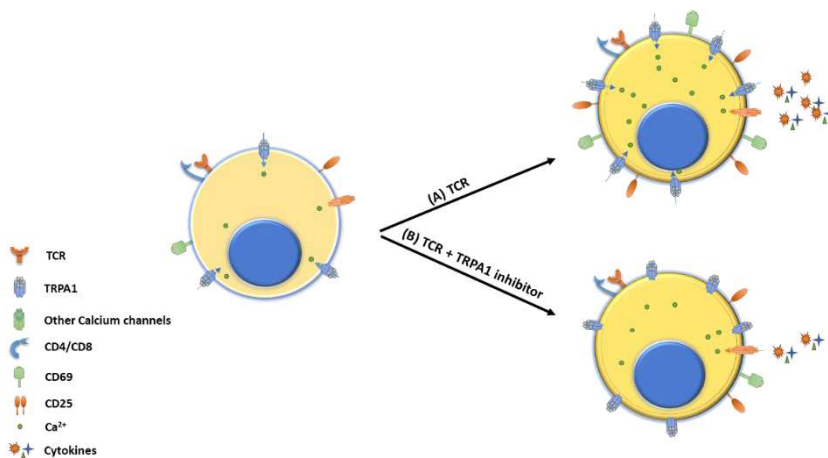


Figure 32 Model depicting the relationship between TRPA1 and Ca²⁺ in T cell activation.

TRPA1 is expressed on the surface of T cells. (A) Upon T cell activation via TCR, Ca²⁺ influx is induced via various Ca²⁺ channels, including TRPA1 leading to T cell activation and downstream effector

cytokine response. (B) In TRPA1 inhibitor, pre-treated T cells stimulated with TCR, the Ca^{2+} influx via TRPA1 is abolished and consequent downstream effector cytokine response is also attenuated.

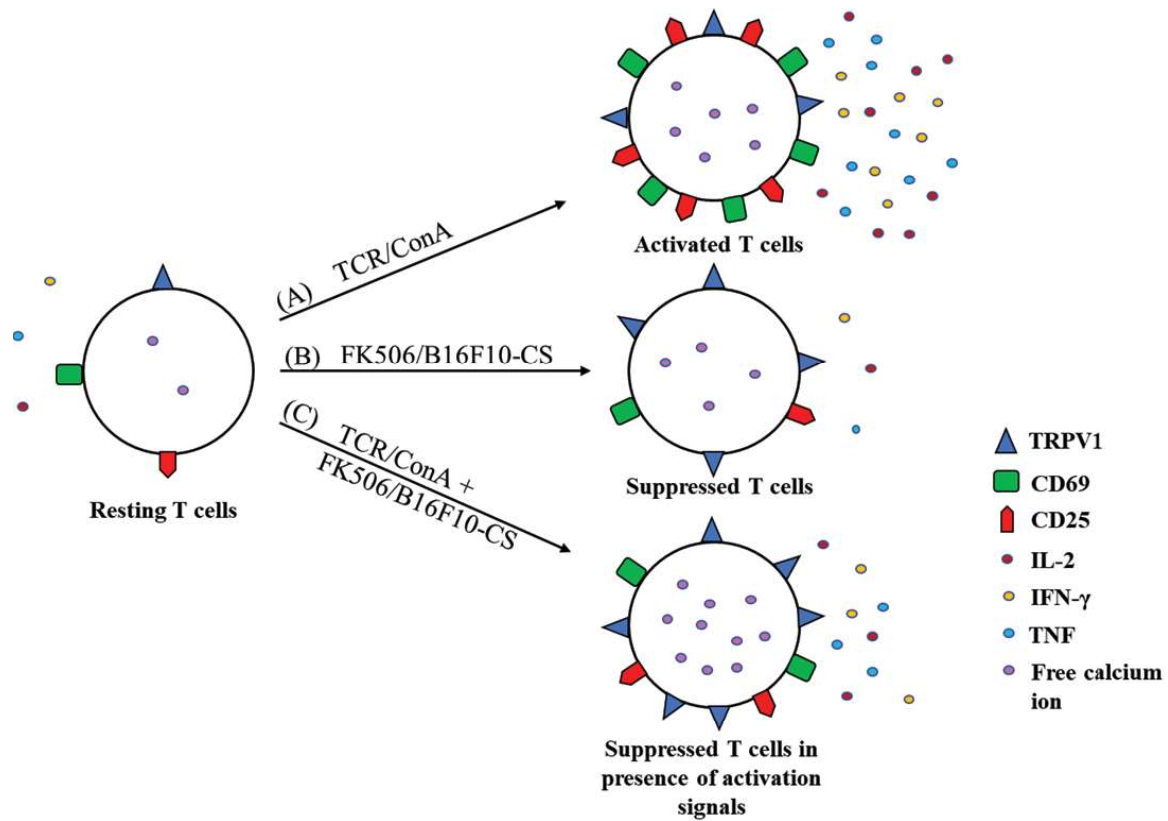


Figure 33 Model depicting the relationship between TRPV1 expression and Ca^{2+} levels in both activated and immuno-suppressed T cells

Resting T cells maintain basal levels of TRPV1 expression and cytosolic Ca^{2+} . (A) Upon activation with either ConA or TCR, both cytosolic Ca^{2+} and TRPV1 expression are upregulated along with robust effector cytokine responses. (B) Upon treatment with immunosuppressive FK506 or B16F10-CS, both TRPV1 expression and cytosolic Ca^{2+} markedly increased. (C) Immunosuppressed T cells shows reduced activation as well as effector cytokine response. However, immunosuppressed T cells exhibit significantly higher TRPV1 expression and cytosolic Ca^{2+} .

CHAPTER # 7

Future Directions

and

Implications

7. Future Directions and Implications

Transient receptor potential (TRP) channels are comparatively novel receptors functionally expressed on various immune cells, including macrophage and T cells. TRP channels are now known to be associated with different disease conditions and can modulate macrophage and T cell effector functions. This study examined the TRP channel's regulatory effect in macrophage and T cell functions. However, the signaling cascade associated with TRP channels is still not elucidated for the active designing of TRP-specific therapeutic strategies for the effective treatment of diseases associated with altered effector functions. Moreover, a comparative study ascertaining the TRP channel's functional role can also be tested in various experimental disease model systems *in vivo*, to further confirm their functional roles in various immune cells. Interestingly, the TRP channels are also known to be functionally expressed as heteromers (hybrid TRP channels formed of two different TRP channel families). It would be fascinating to test the properties and signaling cascades associated with these TRP channels and their functional contribution towards effector cell functions. Moreover, these TRP channels are known to be expressed on both the surface as well as intracellularly in cells. In this study, we have inspected the functional role of surface expressed TRP channels only. It would be enthralling to test the function of intracellularly expressed TRP channels and investigate TRP channel's functional association with other immune receptors such as Toll-like receptors (TLRs), RIG-I-like receptors (RLRs) and NOD-like receptors. In the future, the pharmacological intervention of TRP channels may have profound implications in developing better strategies for effective pain management and in a plethora of disease conditions.

BIBLIOGRAPHY

1. Janeway, C. *Immunobiology 5 : the immune system in health and disease*. (2001).
2. Uzman, A. Molecular biology of the cell (4th ed.): Alberts, B., Johnson, A., Lewis, J., Raff, M., Roberts, K., and Walter, P. *Biochemistry and Molecular Biology Education* **31**, 212–214 (2003).
3. Punt J, Owen JA, Stranford SA, Jones PP, K. J. *Kuby Immunology*. (2019).
4. Biron, C. A. Chapter 4 - Innate Immunity: Recognizing and Responding to Foreign Invaders—No Training Needed. in *Viral Pathogenesis (Third Edition)* (eds. Katze, M. G., Korth, M. J., Law, G. L. & Nathanson, N.) 41–55 (Academic Press, 2016).
doi:<https://doi.org/10.1016/B978-0-12-800964-2.00004-5>.
5. Kumar, H., Takeda, K. & Akira, S. Toll-Like Receptors. in *Encyclopedia of Biological Chemistry* (eds. Lennarz, W. J. & Lane, M. D.) 190–194 (Elsevier, 2004).
doi:<https://doi.org/10.1016/B0-12-443710-9/00729-8>.
6. Merle, N. S., Noe, R., Halbwachs-Mecarelli, L., Fremeaux-Bacchi, V. & Roumenina, L. T. Complement System Part II: Role in Immunity. *Frontiers in Immunology* **6**, 257 (2015).
7. Flockerzi, V. *et al.* for the Superfamily of TRP Cation Channels The TRP superfamily includes a diversity of non-voltage-. **9**, 229–231 (2002).
8. Ramsey, I., Delling, M. & Clapham, D. An introduction to TRP channels. *Annual review of physiology* **68**, 619–647 (2006).
9. Gaudet, R. TRP channels entering the structural era. *Journal of Physiology* **586**, 3565–3575 (2008).
10. Gees, M., Colsoul, B. & Nilius, B. The role of transient receptor potential cation channels in Ca²⁺ signaling. *Cold Spring Harbor perspectives in biology* **2**, a003962–a003962 (2010).
11. Vay, L., Gu, C. & McNaughton, P. A. The thermo-TRP ion channel family: Properties

- and therapeutic implications. *British Journal of Pharmacology* **165**, 787–801 (2012).
12. Clapham, D. E. TRP channels as cellular sensor. *Nature* **426**, 517–524 (2003).
 13. Yang, F., Ma, L., Cao, X., Wang, K. & Zheng, J. Divalent cations activate TRPV1 through promoting conformational change of the extracellular region. *The Journal of General Physiology* **143**, 91–103 (2014).
 14. Ramirez, G. *et al.* Ion Channels and Transporters in Inflammation: Special Focus on TRP Channels and TRPC6. *Cells* **7**, 70 (2018).
 15. Smani, T., Shapovalov, G., Skryma, R., Prevarskaya, N. & Rosado, J. A. Biochimica et Biophysica Acta Functional and physiopathological implications of TRP channels. *BBA - Molecular Cell Research* **1853**, 1772–1782 (2015).
 16. Pla, A. F. & Gkika, D. Emerging role of TRP channels in cell migration: From tumor vascularization to metastasis. *Frontiers in Physiology* **4 NOV**, 1–13 (2013).
 17. Sukumaran, P., Schaar, A., Sun, Y. & Singh, B. B. Functional role of TRP channels in modulating ER stress and Autophagy. *Cell Calcium* **60**, 123–132 (2016).
 18. Clapham, D. E., Julius, D., Montell, C. & Schultz, G. International Union of Pharmacology. XLIX. Nomenclature and structure-function relationships of transient receptor potential channels. *Pharmacological reviews* **57**, 427–450 (2005).
 19. Nilius, B. & Owsianik, G. The transient receptor potential family of ion channels. *Genome Biology* vol. 12 (2011).
 20. Fernandes, E. S., Fernandes, M. A. & Keeble, J. E. The functions of TRPA1 and TRPV1: Moving away from sensory nerves. *British Journal of Pharmacology* **166**, 510–521 (2012).
 21. Facer, P. *et al.* Differential expression of the capsaicin receptor TRPV1 and related novel receptors TRPV3, TRPV4 and TRPM8 in normal human tissues and changes in traumatic and diabetic neuropathy. *BMC Neurology* **7**, 1–12 (2007).

22. Lishko, P. V., Procko, E., Jin, X., Phelps, C. B. & Gaudet, R. The Ankyrin Repeats of TRPV1 Bind Multiple Ligands and Modulate Channel Sensitivity. *Neuron* **54**, 905–918 (2007).
23. Omari, S. A., Adams, M. J. & Geraghty, D. P. TRPV1 Channels in Immune Cells and Hematological Malignancies. in *Advances in Pharmacology* vol. 79 173–198 (Elsevier Inc., 2017).
24. Devesa, I. *et al.* Role of the transient receptor potential vanilloid 1 in inflammation and sepsis. *Journal of Inflammation Research* **4**, 67–81 (2011).
25. Marrone, M. C. *et al.* TRPV1 channels are critical brain inflammation detectors and neuropathic pain biomarkers in mice. *Nature Communications* **8**, (2017).
26. Yoshida, A. *et al.* TRPV1 is crucial for proinflammatory STAT3 signaling and thermoregulation-associated pathways in the brain during inflammation. *Scientific Reports* **6**, 26088 (2016).
27. Boyd, S., Parikh, N., Chu, E., Peleato, B. & Eckstein, J. Distributed optimization and statistical learning via the alternating direction method of multipliers. *Foundations and Trends in Machine Learning* vol. 3 1–122 (2010).
28. Silva, R. O. *et al.* Role of TRPV1 receptor in inflammation and impairment of esophageal mucosal integrity in a murine model of nonerosive reflux disease. *Neurogastroenterology and Motility* **30**, 1–8 (2018).
29. Toledo-Mauriño, J. J. *et al.* The Transient Receptor Potential Vanilloid 1 Is Associated with Active Inflammation in Ulcerative Colitis. *Mediators of Inflammation* **2018**, 1–7 (2018).
30. Story, G. M. *et al.* ANKTM1, a TRP-like Channel Expressed in Nociceptive Neurons, Is Activated by Cold Temperatures. *Cell* **112**, 819–829 (2003).
31. Nagata, K., Duggan, A., Kumar, G. & García-Añoveros, J. Nociceptor and hair cell

- transducer properties of TRPA1, a channel for pain and hearing. *Journal of Neuroscience* **25**, 4052–4061 (2005).
32. Holt, J. R., Kwan, K. Y., Lin, S. & Vollrath, M. A. TRPA1 is a candidate for the mechanosensitive transduction channel of vertebrate hair cells.
 33. Macpherson, L. J. *et al.* The Pungency of Garlic : Activation of TRPA1 and TRPV1 in Response to Allicin. **15**, 929–934 (2005).
 34. Jordt, S., Bautista, D. M., Chuang, H., Meng, I. D. & Julius, D. Mustard oils and cannabinoids excite sensory nerve fibres through the TRP channel ANKTM1. **427**, (2004).
 35. Bandell, M. *et al.* Noxious Cold Ion Channel TRPA1 Is Activated by Pungent Compounds and Bradykinin. *Neuron* **41**, 849–857 (2004).
 36. Bertin, S. *et al.* The TRPA1 ion channel is expressed in CD4+ T cells and restrains T-cell-mediated colitis through inhibition of TRPV1. *Gut* **66**, 1584–1596 (2016).
 37. Engel, M. A. *et al.* TRPA1 and Substance P Mediate Colitis in Mice. 1346–1358 (2011) doi:10.1053/j.gastro.2011.07.002.
 38. Parenti, A., De Logu, F., Geppetti, P. & Benemei, S. What is the evidence for the role of TRP channels in inflammatory and immune cells? *British Journal of Pharmacology* **173**, 953–969 (2016).
 39. Khalil, M. *et al.* Functional role of transient receptor potential channels in immune cells and epithelia. *Frontiers in Immunology* **9**, 1–7 (2018).
 40. Kochukov, M. Y. *et al.* Thermosensitive TRP ion channels mediate cytosolic calcium response in human synoviocytes. **1043**, 424–433 (2006).
 41. Romano, B. *et al.* The cannabinoid TRPA1 agonist cannabichromene inhibits nitric oxide production in macrophages and ameliorates. (2013) doi:10.1111/bph.12120.
 42. Facchinetti, F. *et al.* a , b -Unsaturated Aldehydes in Cigarette Smoke Release

- Inflammatory Mediators from Human Macrophages. doi:10.1165/rcmb.2007-0130OC.
43. De Logu, F. *et al.* Macrophages and Schwann cell TRPA1 mediate chronic allodynia in a mouse model of complex regional pain syndrome type I. *Brain, behavior, and immunity* **88**, 535–546 (2020).
 44. Kun, J. *et al.* Upregulation of the Transient Receptor Potential Ankyrin 1 Ion Channel in the Inflamed Human and Mouse Colon and Its Protective Roles. *PLoS ONE* **9**, e108164 (2014).
 45. Trevisan, G. *et al.* TRPA1 mediates trigeminal neuropathic pain in mice downstream of monocytes/macrophages and oxidative stress. *Brain* **139**, 1361–1377 (2016).
 46. Ma, S., Zhang, Y., He, K., Wang, P. & Wang, D. H. Knockout of TRPA1 exacerbates angiotensin II-induced kidney injury. *American journal of physiology. Renal physiology* **317**, F623–F631 (2019).
 47. De Logu, F. *et al.* Schwann cell TRPA1 mediates neuroinflammation that sustains macrophage-dependent neuropathic pain in mice. *Nature Communications* **8**, 1–16 (2017).
 48. Mercer, J. & Greber, U. F. Virus interactions with endocytic pathways in macrophages and dendritic cells. *Trends in Microbiology* **21**, 380–388 (2013).
 49. Zhou, M. *et al.* Tumor-released autophagosomes induce IL-10- producing B cells with suppressive activity on T lymphocytes via TLR2-MyD88-NF- κ B signal pathway. *Oncology* **5**, 1–14 (2016).
 50. Wen, Z. F. *et al.* Tumor cell-released autophagosomes (TRAPs) promote immunosuppression through induction of M2-like macrophages with increased expression of PD-L1. *Journal for ImmunoTherapy of Cancer* **6**, 1–16 (2018).
 51. Chen, Y.-Q. *et al.* *Journal for ImmunoTherapy of Cancer* **7**, 178 (2019).
 52. Beom, J. Y. *et al.* Biosynthesis of Nonimmunosuppressive FK506 Analogues with

- Antifungal Activity. *Journal of Natural Products* **82**, 2078–2086 (2019).
53. Dumont, F. J. FK506, an immunosuppressant targeting calcineurin function. *Current medicinal chemistry* **7**, 731–48 (2000).
 54. Haddad, E. M. *et al.* Cyclosporin versus tacrolimus for liver transplanted patients. *The Cochrane database of systematic reviews* CD005161 (2006)
doi:10.1002/14651858.CD005161.pub2.
 55. Naesens, M., Kuypers, D. R. J. & Sarwal, M. Calcineurin inhibitor nephrotoxicity. *Clinical journal of the American Society of Nephrology : CJASN* **4**, 481–508 (2009).
 56. Thomson, A. W., Bonham, C. A. & Zeevi, A. Mode of action of tacrolimus (FK506): molecular and cellular mechanisms. *Therapeutic drug monitoring* **17**, 584–91 (1995).
 57. Weiwad, M. *et al.* Comparative analysis of calcineurin inhibition by complexes of immunosuppressive drugs with human FK506 binding proteins. *Biochemistry* **45**, 15776–84 (2006).
 58. Bultynck, G. *et al.* Effects of the immunosuppressant FK506 on intracellular Ca²⁺ release and Ca²⁺ accumulation mechanisms. *Journal of Physiology* **525**, 681–693 (2000).
 59. Montell, C. The history of TRP channels, a commentary and reflection. *Pflügers Archiv - European Journal of Physiology* **461**, 499–506 (2011).
 60. Venkatachalam, K. & Montell, C. TRP Channels. *Annual Review of Biochemistry* **76**, 387–417 (2007).
 61. Damann, N., Voets, T. & Nilius, B. TRPs in Our Senses. *Current Biology* **18**, 880–889 (2008).
 62. Patapoutian, A. TRP Channels and Thermosensation. *Chemical Senses* **30**, i193–i194 (2005).
 63. Dhaka, A., Viswanath, V. & Patapoutian, A. Trp ion channels and temperature

- sensation. *Annual review of neuroscience* **29**, 135–61 (2006).
64. Chung, M.-K., Jung, S. J. & Oh, S. B. Role of TRP channels in pain sensation. *Advances in experimental medicine and biology* **704**, 615–36 (2011).
 65. Minke, B. The History of the Drosophila TRP Channel: The Birth of a New Channel Superfamily. *Journal of Neurogenetics* **24**, 216–233 (2010).
 66. Cosens, D. J. & Manning, A. Abnormal electroretinogram from a Drosophila mutant [30]. *Nature* **224**, 285–287 (1969).
 67. Minke, B., Wu, C. & Pak, W. L. Induction of photoreceptor voltage noise in the dark in Drosophila mutant. *Nature* **258**, 84–87 (1975).
 68. Montell, C. & Rubin, G. M. Molecular characterization of the Drosophila trp locus: A putative intergral membrane protein required for phototransduction. *Neuron* **2**, 1313–1323 (1989).
 69. Phillips, A. M., Bull, A. & Kelly, L. E. Identification of a Drosophila gene encoding a calmodulin-binding protein with homology to the trp phototransduction gene. *Neuron* **8**, 631–642 (1992).
 70. Niemeyer, B. A., Suzuki, E., Scott, K., Jalink, K. & Zuker, C. S. The Drosophila light-activated conductance is composed of the two channels TRP and TRPL. *Cell* **85**, 651–659 (1996).
 71. Reuss, H., Mojet, M. H., Chyb, S. & Hardie, R. C. In vivo analysis of the drosophila light-sensitive channels, TRP and TRPL. *Neuron* **19**, 1249–1259 (1997).
 72. Leung, H. T., Geng, C. & Pak, W. L. Phenotypes of trpl mutants and interactions between the transient receptor potential (TRP) and TRP-like channels in Drosophila. *The Journal of neuroscience : the official journal of the Society for Neuroscience* **20**, 6797–6803 (2000).
 73. Liu, C. H. *et al.* In vivo identification and manipulation of the Ca²⁺ selectivity filter in

- the *Drosophila* transient receptor potential channel. *The Journal of neuroscience : the official journal of the Society for Neuroscience* **27**, 604–615 (2007).
74. Zhu, X., Chu, P. B., Peyton, M. & Birnbaumer, L. Molecular cloning of a widely expressed human homologue for the *Drosophila* trp gene. *FEBS letters* **373**, 193–198 (1995).
 75. Wes, P. D. *et al.* TRPC1, a human homolog of a *Drosophila* store-operated channel. *Proceedings of the National Academy of Sciences of the United States of America* **92**, 9652–9656 (1995).
 76. Nadler, M. J. *et al.* LTRPC7 is a Mg.ATP-regulated divalent cation channel required for cell viability. *Nature* **411**, 590–595 (2001).
 77. Perraud, A. L. *et al.* ADP-ribose gating of the calcium-permeable LTRPC2 channel revealed by Nudix motif homology. *Nature* **411**, 595–599 (2001).
 78. Salkoff, L. Genetic and voltage-clamp analysis of a *Drosophila* potassium channel. *Cold Spring Harbor symposia on quantitative biology* **48 Pt 1**, 221–231 (1983).
 79. Sano, Y. *et al.* Immunocyte Ca²⁺ influx system mediated by LTRPC2. *Science (New York, N.Y.)* **293**, 1327–1330 (2001).
 80. Schlingmann, K. P. *et al.* Hypomagnesemia with secondary hypocalcemia is caused by mutations in TRPM6, a new member of the TRPM gene family. *Nature genetics* **31**, 166–170 (2002).
 81. Walder, R. Y. *et al.* Mutation of TRPM6 causes familial hypomagnesemia with secondary hypocalcemia. *Nature genetics* **31**, 171–174 (2002).
 82. Caterina, M. J. *et al.* The capsaicin receptor: a heat-activated ion channel in the pain pathway. *Nature* **389**, 816–824 (1997).
 83. Bandell, M., Macpherson, L. J. & Patapoutian, A. From chills to chilis: mechanisms for thermosensation and chemesthesis via thermoTRPs. *Current opinion in*

- neurobiology* **17**, 490–497 (2007).
84. Talavera, K., Nilius, B. & Voets, T. Neuronal TRP channels: thermometers, pathfinders and life-savers. *Trends in neurosciences* **31**, 287–295 (2008).
 85. Montell, C. The TRP Superfamily of Cation Channels. *Science Signaling* **2005**, re3–re3 (2005).
 86. Montell, C. *et al.* A unified nomenclature for the superfamily of TRP cation channels. *Molecular cell* **9**, 229–31 (2002).
 87. Zheng, J. Molecular mechanism of TRP channels. *Comprehensive Physiology* **3**, 221–42 (2013).
 88. Venkatachalam, K., Zheng, F. & Gill, D. L. Regulation of canonical transient receptor potential (TRPC) channel function by diacylglycerol and protein kinase C. *The Journal of biological chemistry* **278**, 29031–40 (2003).
 89. Vazquez, G., Bird, G. S. J., Mori, Y. & Putney, J. W. Native TRPC7 channel activation by an inositol trisphosphate receptor-dependent mechanism. *The Journal of biological chemistry* **281**, 25250–8 (2006).
 90. Montell, C. Physiology, phylogeny, and functions of the TRP superfamily of cation channels. *Science's STKE : signal transduction knowledge environment* **2001**, re1 (2001).
 91. Zygmunt, P. M. *et al.* Vanilloid receptors on sensory nerves mediate the vasodilator action of anandamide. *Nature* **400**, 452–7 (1999).
 92. McNamara, F. N., Randall, A. & Gunthorpe, M. J. Effects of piperine, the pungent component of black pepper, at the human vanilloid receptor (TRPV1). *British journal of pharmacology* **144**, 781–90 (2005).
 93. Xu, H., Blair, N. T. & Clapham, D. E. Camphor activates and strongly desensitizes the transient receptor potential vanilloid subtype 1 channel in a vanilloid-independent

- mechanism. *The Journal of neuroscience : the official journal of the Society for Neuroscience* **25**, 8924–37 (2005).
94. Yue, L., Peng, J. B., Hediger, M. A. & Clapham, D. E. CaT1 manifests the pore properties of the calcium-release-activated calcium channel. *Nature* **410**, 705–9 (2001).
 95. Liedtke, W. & Kim, C. Functionality of the TRPV subfamily of TRP ion channels: add mechano-TRP and osmo-TRP to the lexicon! *Cellular and molecular life sciences : CMLS* **62**, 2985–3001 (2005).
 96. Voets, T. *et al.* CaT1 and the Calcium Release-activated Calcium Channel Manifest Distinct Pore Properties. *Journal of Biological Chemistry* **276**, 47767–47770 (2001).
 97. Duncan, L. M. *et al.* Down-regulation of the novel gene melastatin correlates with potential for melanoma metastasis. *Cancer research* **58**, 1515–20 (1998).
 98. Grimm, C., Kraft, R., Sauerbruch, S., Schultz, G. & Harteneck, C. Molecular and functional characterization of the melastatin-related cation channel TRPM3. *The Journal of biological chemistry* **278**, 21493–501 (2003).
 99. Liu, D. & Liman, E. R. Intracellular Ca²⁺ and the phospholipid PIP₂ regulate the taste transduction ion channel TRPM5. *Proceedings of the National Academy of Sciences of the United States of America* **100**, 15160–5 (2003).
 100. Perraud, A. L. *et al.* ADP-ribose gating of the calcium-permeable LTRPC2 channel revealed by Nudix motif homology. *Nature* **411**, 595–9 (2001).
 101. McKemy, D. D., Neuhauser, W. M. & Julius, D. Identification of a cold receptor reveals a general role for TRP channels in thermosensation. *Nature* **416**, 52–8 (2002).
 102. Peier, A. M. *et al.* A TRP Channel that Senses Cold Stimuli and Menthol. *Cell* **108**, 705–715 (2002).
 103. Bautista, D. M. *et al.* TRPA1 mediates the inflammatory actions of environmental

- irritants and proalgesic agents. *Cell* **124**, 1269–82 (2006).
104. Walker, R. G., Willingham, A. T. & Zuker, C. S. A *Drosophila* mechanosensory transduction channel. *Science (New York, N.Y.)* **287**, 2229–34 (2000).
 105. Li, Y., Wright, J. M., Qian, F., Germino, G. G. & Guggino, W. B. Polycystin 2 interacts with type I inositol 1,4,5-trisphosphate receptor to modulate intracellular Ca²⁺ signaling. *The Journal of biological chemistry* **280**, 41298–306 (2005).
 106. Nauli, S. M. *et al.* Polycystins 1 and 2 mediate mechanosensation in the primary cilium of kidney cells. *Nature genetics* **33**, 129–37 (2003).
 107. González-Perrett, S. *et al.* Polycystin-2, the protein mutated in autosomal dominant polycystic kidney disease (ADPKD), is a Ca²⁺-permeable nonselective cation channel. *Proceedings of the National Academy of Sciences of the United States of America* **98**, 1182–7 (2001).
 108. Li, Q. *et al.* Alpha-actinin associates with polycystin-2 and regulates its channel activity. *Human molecular genetics* **14**, 1587–603 (2005).
 109. Soyombo, A. A. *et al.* TRP-ML1 regulates lysosomal pH and acidic lysosomal lipid hydrolytic activity. *The Journal of biological chemistry* **281**, 7294–301 (2006).
 110. Kiselyov, K. *et al.* TRP-ML1 Is a Lysosomal Monovalent Cation Channel That Undergoes Proteolytic Cleavage *. **280**, 43218–43223 (2005).
 111. Raychowdhury, M. K. *et al.* Molecular pathophysiology of mucopolipidosis type IV: pH dysregulation of the mucopolipin-1 cation channel. *Human molecular genetics* **13**, 617–27 (2004).
 112. Sun, M. *et al.* Mucopolipidosis type IV is caused by mutations in a gene encoding a novel transient receptor potential channel. *Human molecular genetics* **9**, 2471–8 (2000).
 113. Venkatachalam, K., Hofmann, T. & Montell, C. Lysosomal localization of TRPML3

- depends on TRPML2 and the mucopolidosis-associated protein TRPML1. *The Journal of biological chemistry* **281**, 17517–27 (2006).
114. Owsianik, G., Talavera, K., Voets, T. & Nilius, B. PERMEATION AND SELECTIVITY OF TRP CHANNELS. *Annual Review of Physiology* **68**, 685–717 (2006).
 115. Doyle, D. A. *et al.* The structure of the potassium channel: molecular basis of K⁺ conduction and selectivity. *Science (New York, N.Y.)* **280**, 69–77 (1998).
 116. Song, M. Y. & Yuan, J. X. J. Introduction to TRP channels: Structure, function, and regulation. in *Advances in Experimental Medicine and Biology* vol. 661 99–108 (Adv Exp Med Biol, 2010).
 117. Li, M., Yu, Y. & Yang, J. Structural biology of TRP channels. in *Advances in Experimental Medicine and Biology* vol. 704 1–23 (2011).
 118. Hellmich, U. A. & Gaudet, R. Structural biology of TRP channels. *Handbook of Experimental Pharmacology* **223**, 963–990 (2014).
 119. Balasubrahmanyam, K. & Janz, G. J. Water in melts: Raman spectral investigation of the molten Ca(NO₃)₂·4H₂O-KNO₃ system. *Journal of Solution Chemistry* **1**, 445–453 (1972).
 120. Vazquez, G., Wedel, B. J., Aziz, O., Trebak, M. & Putney, J. W. The mammalian TRPC cation channels. *Biochimica et Biophysica Acta (BBA) - Molecular Cell Research* **1742**, 21–36 (2004).
 121. Plant, T. D. & Schaefer, M. TRPC4 and TRPC5: receptor-operated Ca²⁺-permeable nonselective cation channels. *Cell calcium* **33**, 441–50.
 122. Philipp, S. *et al.* A mammalian capacitative calcium entry channel homologous to *Drosophila* TRP and TRPL. *The EMBO journal* **15**, 6166–71 (1996).
 123. Okada, T. *et al.* Molecular Cloning and Functional Characterization of a Novel

- Receptor-activated TRP Ca²⁺ Channel from Mouse Brain. *Journal of Biological Chemistry* **273**, 10279–10287 (1998).
124. Voets, T. & Nilius, B. The pore of TRP channels: trivial or neglected? *Cell Calcium* **33**, 299–302 (2003).
125. Dohke, Y., Oh, Y. S., Ambudkar, I. S. & Turner, R. J. Biogenesis and Topology of the Transient Receptor Potential Ca²⁺ Channel TRPC1. *Journal of Biological Chemistry* **279**, 12242–12248 (2004).
126. Liu, X., Singh, B. B. & Ambudkar, I. S. TRPC1 is required for functional store-operated Ca²⁺ channels: Role of acidic amino acid residues in the S5-S6 region. *Journal of Biological Chemistry* **278**, 11337–11343 (2003).
127. Obukhov, A. G. & Nowycky, M. C. A cytosolic residue mediates Mg²⁺ block and regulates inward current amplitude of a transient receptor potential channel. *The Journal of neuroscience : the official journal of the Society for Neuroscience* **25**, 1234–9 (2005).
128. Voets, T. *et al.* Molecular Determinants of Permeation through the Cation Channel TRPV4. *Journal of Biological Chemistry* **277**, 33704–33710 (2002).
129. Gunthorpe, M. J., Benham, C. D., Randall, A. & Davis, J. B. The diversity in the vanilloid (TRPV) receptor family of ion channels. *Trends in Pharmacological Sciences* **23**, 183–191 (2002).
130. van de Graaf, S. F. J., Hoenderop, J. G. J. & Bindels, R. J. M. Regulation of TRPV5 and TRPV6 by associated proteins. *American Journal of Physiology-Renal Physiology* **290**, F1295–F1302 (2006).
131. Vennekens, R. *et al.* Pore properties and ionic block of the rabbit epithelial calcium channel expressed in HEK 293 cells. *The Journal of physiology* **530**, 183–91 (2001).
132. Hoenderop, J. G. *et al.* Function and expression of the epithelial Ca(2+) channel

- family: comparison of mammalian ECaC1 and 2. *The Journal of physiology* **537**, 747–61 (2001).
133. Blair, N. T. *et al.* Transient Receptor Potential channels (version 2019.4) in the IUPHAR/BPS Guide to Pharmacology Database. *IUPHAR/BPS Guide to Pharmacology CITE* **2019**, (2019).
134. García-Martínez, C., Morenilla-Palao, C., Planells-Cases, R., Merino, J. M. & Ferrer-Montiel, A. Identification of an aspartic residue in the P-loop of the vanilloid receptor that modulates pore properties. *The Journal of biological chemistry* **275**, 32552–32558 (2000).
135. Zhou, Y., Morais-Cabral, J. H., Kaufman, A. & MacKinnon, R. Chemistry of ion coordination and hydration revealed by a K⁺ channel–Fab complex at 2.0 Å resolution. *Nature* **414**, 43–48 (2001).
136. Yang, J., Ellnor, P. T., Sather, W. A., Zhang, J.-F. & Tsien, R. W. Molecular determinants of Ca²⁺ selectivity and ion permeation in L-type Ca²⁺ channels. *Nature* **366**, 158–161 (1993).
137. Heinemann, S. H., Terlau, H., Stühmer, W., Imoto, K. & Numa, S. Calcium channel characteristics conferred on the sodium channel by single mutations. *Nature* **356**, 441–443 (1992).
138. Talavera, K. *et al.* Aspartate Residues of the Glu-Glu-Asp-Asp (EEDD) Pore Locus Control Selectivity and Permeation of the T-type Ca²⁺Channel α 1G. *Journal of Biological Chemistry* **276**, 45628–45635 (2001).
139. Huang, Y., Fliegert, R., Guse, A. H., Lü, W. & Du, J. A structural overview of the ion channels of the TRPM family. *Cell Calcium* **85**, 102111 (2020).
140. Liao, M., Cao, E., Julius, D. & Cheng, Y. Structure of the TRPV1 ion channel determined by electron cryo-microscopy. doi:10.1038/nature12822.

141. Hofmann, T., Chubanov, V., Gudermann, T. & Montell, C. TRPM5 is a voltage-modulated and Ca(2+)-activated monovalent selective cation channel. *Current biology : CB* **13**, 1153–8 (2003).
142. Nilius, B. *et al.* Voltage dependence of the Ca²⁺-activated cation channel TRPM4. *The Journal of biological chemistry* **278**, 30813–20 (2003).
143. Nilius, B. *et al.* The Selectivity Filter of the Cation Channel TRPM4. *Journal of Biological Chemistry* **280**, 22899–22906 (2005).
144. Paulsen, C. E., Armache, J.-P., Gao, Y., Cheng, Y. & Julius, D. Structure of the TRPA1 ion channel suggests regulatory mechanisms. *Nature* **520**, 511–517 (2015).
145. Christensen, A. P., Akyuz, N. & Corey, D. P. The Outer Pore and Selectivity Filter of TRPA1. *PLOS ONE* **11**, 1–23 (2016).
146. Cvetkov, T. L., Huynh, K. W., Cohen, M. R. & Moiseenkova-Bell, V. Y. Molecular Architecture and Subunit Organization of TRPA1 Ion Channel Revealed by Electron Microscopy*. *Journal of Biological Chemistry* **286**, 38168–38176 (2011).
147. Bobkov, Y. V, Corey, E. A. & Ache, B. W. The pore properties of human nociceptor channel TRPA1 evaluated in single channel recordings. *Biochimica et biophysica acta* **1808**, 1120–8 (2011).
148. Yu, Y. *et al.* Molecular mechanism of the assembly of an acid-sensing receptor ion channel complex. *Nature Communications* **3**, 1252 (2012).
149. Grimm, C., Hassan, S., Wahl-Schott, C. & Biel, M. Role of TRPML and two-pore channels in endolysosomal cation homeostasis. *The Journal of pharmacology and experimental therapeutics* **342**, 236–44 (2012).
150. Cheng, X., Shen, D., Samie, M. & Xu, H. Mucolipins: Intracellular TRPML1-3 channels. *FEBS Letters* **584**, 2013–2021 (2010).
151. Zeevi, D. A., Lev, S., Frumkin, A., Minke, B. & Bach, G. Heteromultimeric TRPML

- channel assemblies play a crucial role in the regulation of cell viability models and starvation-induced autophagy. *Journal of Cell Science* **123**, 3112–3124 (2010).
152. Transient Receptor Potential channels | Introduction | BPS/IUPHAR Guide to PHARMACOLOGY.
<https://www.guidetopharmacology.org/GRAC/FamilyIntroductionForward?familyId=78>.
153. Billeter, A. T. *et al.* TRPA1 mediates the effects of hypothermia on the monocyte inflammatory response. *Surgery* **158**, 646–654 (2015).
154. Billeter, A. T., Hellmann, J. L., Bhatnagar, A. & Polk, H. C. Transient receptor potential ion channels: Powerful regulators of cell function. *Annals of Surgery* **259**, 229–235 (2014).
155. Tóth, B. I., Oláh, A., Szöllösi, A. G. & Biró, T. TRP channels in the skin. *British journal of pharmacology* **171**, 2568–81 (2014).
156. Inada, H., Iida, T. & Tominaga, M. Different expression patterns of TRP genes in murine B and T lymphocytes. *Biochemical and biophysical research communications* **350**, 762–7 (2006).
157. Entin-Meer, M. *et al.* The transient receptor potential vanilloid 2 cation channel is abundant in macrophages accumulating at the peri-infarct zone and may enhance their migration capacity towards injured cardiomyocytes following myocardial infarction. *PloS one* **9**, e105055 (2014).
158. Schilling, T., Miralles, F. & Eder, C. TRPM7 regulates proliferation and polarisation of macrophages. *Journal of Cell Science* **127**, 4561–4566 (2014).
159. FONFRIA, E. *et al.* Tissue Distribution Profiles of the Human TRPM Cation Channel Family. *Journal of Receptors and Signal Transduction* **26**, 159–178 (2006).
160. Guptill, V. *et al.* Disruption of the transient receptor potential vanilloid 1 can affect

- survival, bacterial clearance, and cytokine gene expression during murine sepsis. *Anesthesiology* **114**, 1190–1199 (2011).
161. Fernandes, E. S. *et al.* TRPV1 Deletion Enhances Local Inflammation and Accelerates the Onset of Systemic Inflammatory Response Syndrome. *The Journal of Immunology* **188**, 5741–5751 (2012).
 162. Bok, E. *et al.* Modulation of M1/M2 polarization by capsaicin contributes to the survival of dopaminergic neurons in the lipopolysaccharide-lesioned substantia nigra in vivo. *Experimental & molecular medicine* **50**, 1–14 (2018).
 163. Zhao, S. *et al.* Effect and Molecular Mechanisms of Collateral Vessel Growth Mediated by Activation of Transient Receptor Potential Vanilloid Type 1. *Journal of vascular research* **57**, 185–194 (2020).
 164. Clark, N. *et al.* The transient receptor potential vanilloid 1 (TRPV1) receptor protects against the onset of sepsis after endotoxin. *The FASEB Journal* **21**, 3747–3755 (2007).
 165. Motte, J. *et al.* Capsaicin-enriched diet ameliorates autoimmune neuritis in rats. *Journal of neuroinflammation* **15**, 122 (2018).
 166. Zhong, B., Ma, S. & Wang, D. H. Knockout of TRPV1 Exacerbates Ischemia-reperfusion-induced Renal Inflammation and Injury in Obese Mice. *In Vivo* **34**, 2259–2268 (2020).
 167. Yu, S.-Q., Ma, S. & Wang, D. H. Ablation of TRPV1-positive nerves exacerbates salt-induced hypertension and tissue injury in rats after renal ischemia-reperfusion via infiltration of macrophages. *Clinical and experimental hypertension (New York, N.Y. : 1993)* **43**, 254–262 (2021).
 168. Shutov, L. P. *et al.* The complement system component C5a produces thermal hyperalgesia via macrophage-to-nociceptor signaling that requires NGF and TRPV1. *Journal of Neuroscience* **36**, 5055–5070 (2016).

169. Warwick, C. A., Shutov, L. P., Shepherd, A. J., Mohapatra, D. P. & Usachev, Y. M. Mechanisms underlying mechanical sensitization induced by complement C5a: the roles of macrophages, TRPV1, and calcitonin gene-related peptide receptors. *Pain* **160**, 702–711 (2019).
170. Rossato, M. F. *et al.* Monosodium urate crystal interleukin-1 β release is dependent on Toll-like receptor 4 and transient receptor potential V1 activation. *Rheumatology (Oxford, England)* **59**, 233–242 (2020).
171. Payrits, M., Helyes, Z., Szentagothai, J. & Sciences, A. E. Oestrogen-dependent up-regulation of TRPA1 and TRPV1 receptor proteins in the rat endometrium. 1–49 (2015).
172. Tian, C. *et al.* Transient Receptor Potential Ankyrin 1 Contributes to Lysophosphatidylcholine - Induced Intracellular Calcium Regulation and THP - 1 - Derived Macrophage Activation. *The Journal of Membrane Biology* (2019) doi:10.1007/s00232-019-00104-2.
173. Wang, Q. *et al.* TRPA1 regulates macrophages phenotype plasticity and atherosclerosis progression. *Atherosclerosis* **301**, 44–53 (2020).
174. Usui-Kusumoto, K. *et al.* Suppression of neovascularization in corneal stroma in a TRPA1-null mouse. *Experimental eye research* **181**, 90–97 (2019).
175. Shepherd, A. J. *et al.* Angiotensin II Triggers Peripheral Macrophage-to-Sensory Neuron Redox Crosstalk to Elicit Pain. *The Journal of neuroscience : the official journal of the Society for Neuroscience* **38**, 7032–7057 (2018).
176. Ma, S. & Wang, D. H. Knockout of Trpa1 exacerbates renal ischemia-reperfusion injury with classical activation of macrophages. *American journal of hypertension* (2020) doi:10.1093/ajh/hpaa162.
177. Zeng, D. *et al.* TRPA1 deficiency alleviates inflammation of atopic dermatitis by

- reducing macrophage infiltration. *Life sciences* **266**, 118906 (2021).
178. Tian, C. *et al.* Transient Receptor Potential Ankyrin 1 Contributes to Lysophosphatidylcholine-Induced Intracellular Calcium Regulation and THP-1-Derived Macrophage Activation. *The Journal of membrane biology* **253**, 43–55 (2020).
179. Oh-hora, M. & Rao, A. Calcium signaling in lymphocytes. *Current opinion in immunology* **20**, 250–8 (2008).
180. Feske, S., Skolnik, E. Y. & Prakriya, M. Ion channels and transporters in lymphocyte function and immunity. *Nature Reviews Immunology* **12**, 532–547 (2012).
181. Vig, M. & Kinet, J.-P. Calcium signaling in immune cells. *Nature Immunology* **10**, 21–27 (2009).
182. Wenning, A. S. *et al.* TRP expression pattern and the functional importance of TRPC3 in primary human T-cells. *Biochimica et biophysica acta* **1813**, 412–23 (2011).
183. Medic, N. *et al.* Knockout of the *Trpc1* gene reveals that TRPC1 can promote recovery from anaphylaxis by negatively regulating mast cell TNF- α production. *Cell Calcium* **53**, 315–326 (2013).
184. Wang, J. *et al.* Cross-linking of GM1 ganglioside by galectin-1 mediates regulatory T cell activity involving TRPC5 channel activation: possible role in suppressing experimental autoimmune encephalomyelitis. *Journal of immunology (Baltimore, Md. : 1950)* **182**, 4036–45 (2009).
185. Guse, A. H. *et al.* Regulation of calcium signalling in T lymphocytes by the second messenger cyclic ADP-ribose. *Nature* **398**, 70–73 (1999).
186. Magnone, M. *et al.* NAD⁺ levels control Ca²⁺ store replenishment and mitogen-induced increase of cytosolic Ca²⁺ by Cyclic ADP-ribose-dependent TRPM2 channel gating in human T lymphocytes. *The Journal of biological chemistry* **287**, 21067–81

- (2012).
187. Yamamoto, S. *et al.* TRPM2-mediated Ca²⁺ influx induces chemokine production in monocytes that aggravates inflammatory neutrophil infiltration. *Nature Medicine* **14**, 738–747 (2008).
 188. Lange, I. *et al.* TRPM2 Functions as a Lysosomal Ca²⁺-Release Channel in b Cells. *Science Signaling* **2**, ra23 (2009).
 189. Jin, J. *et al.* Deletion of Trpm7 Disrupts Embryonic Development and Thymopoiesis Without Altering Mg²⁺ Homeostasis. *Science* **322**, 756–760 (2008).
 190. Amantini, C. *et al.* The TRPV1 ion channel regulates thymocyte differentiation by modulating autophagy and proteasome activity. *Oncotarget* **8**, 90766–90780 (2017).
 191. Majhi, R. K. *et al.* Functional expression of TRPV channels in T cells and their implications in immune regulation. *FEBS Journal* **282**, 2661–2681 (2015).
 192. Samivel, R. *et al.* The role of TRPV1 in the CD4⁺ T cell-mediated inflammatory response of allergic rhinitis. *Oncotarget* **7**, 148–60 (2016).
 193. Hsieh, W.-S., Kung, C.-C., Huang, S.-L., Lin, S.-C. & Sun, W.-H. TDAG8, TRPV1, and ASIC3 involved in establishing hyperalgesic priming in experimental rheumatoid arthritis. *Scientific Reports* **7**, 8870 (2017).
 194. Bertin, S. *et al.* The ion channel TRPV1 regulates the activation and proinflammatory properties of CD4⁺T cells. *Nature Immunology* **15**, 1055–1063 (2014).
 195. Gouin, O. *et al.* TRPV1 and TRPA1 in cutaneous neurogenic and chronic inflammation: pro-inflammatory response induced by their activation and their sensitization. *Protein and Cell* **8**, 644–661 (2017).
 196. Sahoo, S. S. *et al.* Transient receptor potential ankyrin1 channel is endogenously expressed in T cells and is involved in immune functions. *Bioscience Reports* **39**, BSR20191437 (2019).

197. Csekő, K., Beckers, B., Keszthelyi, D. & Helyes, Z. Role of TRPV1 and TRPA1 Ion Channels in Inflammatory Bowel Diseases: Potential Therapeutic Targets? *Pharmaceuticals* **12**, 48 (2019).
198. Clapham, D. E. Calcium Signaling. *Cell* **131**, 1047–1058 (2007).
199. Zhou, Y., Frey, T. K. & Yang, J. J. Viral calciomics: Interplays between Ca²⁺ and virus. *Cell Calcium* **46**, 1–17 (2009).
200. Cheshenko, N. *et al.* HSV activates Akt to trigger calcium release and promote viral entry: novel candidate target for treatment and suppression. *The FASEB Journal* **27**, 2584–2599 (2013).
201. Brisac, C. *et al.* Calcium Flux between the Endoplasmic Reticulum and Mitochondrion Contributes to Poliovirus-Induced Apoptosis □. **84**, 12226–12235 (2010).
202. Lupescu, A. *et al.* Phospholipase A2 Activity-Dependent Stimulation of Ca²⁺ Entry by Human Parvovirus B19 Capsid Protein VP1 □. **80**, 11370–11380 (2006).
203. Lobeck, I. *et al.* Rhesus rotavirus VP6 regulates ERK-dependent calcium in flux in cholangiocytes. *Virology* **499**, 185–195 (2016).
204. Wang, S. *et al.* Screening of FDA-Approved Drugs for Inhibitors of Japanese Encephalitis Virus Infection. *Journal of Virology* **91**, (2017).
205. Fujioka, Y. *et al.* A Ca²⁺-dependent signalling circuit regulates influenza A virus internalization and infection. *Nature Communications* **4**, 2763 (2013).
206. Omar, S. *et al.* Respiratory virus infection up-regulates TRPV1, TRPA1 and ASIC3 receptors on airway cells. *PLoS ONE* **12**, 1–21 (2017).
207. Abdullah, H., Heaney, L. G., Cosby, S. L. & McGarvey, L. P. A. A. Rhinovirus upregulates transient receptor potential channels in a human neuronal cell line: implications for respiratory virus-induced cough reflex sensitivity. *Thorax* **69**, 46–54 (2014).

208. Rinkenberger, N. & Schoggins, J. W. Mucolipin-2 cation channel increases trafficking efficiency of endocytosed viruses. *mBio* **9**, 1–16 (2018).
209. Doñate-Macián, P. *et al.* The TRPV4 channel links calcium influx to DDX3X activity and viral infectivity. *Nature Communications* **9**, 1–13 (2018).
210. Bae, M. *et al.* Activation of TRPML1 Clears Intraneuronal A in Preclinical Models of HIV Infection. *Journal of Neuroscience* **34**, 11485–11503 (2014).
211. Staring, J., Raaben, M. & Brummelkamp, T. R. Viral escape from endosomes and host detection at a glance. *Journal of Cell Science* **131**, jcs216259 (2018).
212. Yamauchi, Y. & Helenius, A. Virus entry at a glance. *Journal of Cell Science* **126**, 1289–1295 (2013).
213. Alhmada, Y. *et al.* Hepatitis C virus-associated pruritus : Etiopathogenesis and therapeutic strategies. **23**, 743–750 (2017).
214. Han, S. B. *et al.* Transient receptor potential vanilloid-1 in epidermal keratinocytes may contribute to acute pain in herpes zoster. *Acta Dermato-Venereologica* **96**, 319–322 (2016).
215. Reinhart, B. *et al.* An HSV-based library screen identifies PP1 α as a negative TRPV1 regulator with analgesic activity in models of pain. *Molecular Therapy - Methods and Clinical Development* **3**, 16040 (2016).
216. Romano, B. *et al.* The cannabinoid TRPA1 agonist cannabichromene inhibits nitric oxide production in macrophages and ameliorates murine colitis. *British Journal of Pharmacology* **169**, 213–229 (2013).
217. Zhao, J.-F., Shyue, S.-K., Kou, Y. R., Lu, T.-M. & Lee, T.-S. Transient Receptor Potential Ankyrin 1 Channel Involved in Atherosclerosis and Macrophage-Foam Cell Formation. *International Journal of Biological Sciences* **12**, 812–823 (2016).
218. Cameron, A. M. *et al.* Immunophilin FK506 binding protein associated with inositol

- 1,4,5-trisphosphate receptor modulates calcium flux. *Proceedings of the National Academy of Sciences of the United States of America* **92**, 1784–1788 (1995).
219. Cameron, A. M. *et al.* Calcineurin associated with the inositol 1,4,5-trisphosphate receptor-FKBP12 complex modulates Ca²⁺ flux. *Cell* **83**, 463–472 (1995).
220. MacMillan, D. & McCarron, J. Regulation by FK506 and rapamycin of Ca²⁺ release from the sarcoplasmic reticulum in vascular smooth muscle: the role of FK506 binding proteins and mTOR. *British Journal of Pharmacology* **158**, 1112–1120 (2009).
221. Kanoh, S. *et al.* Effect of FK506 on ATP-induced intracellular calcium oscillations in cow tracheal epithelium. *American Journal of Physiology - Lung Cellular and Molecular Physiology* **276**, 891–899 (1999).
222. Van Acker, K. *et al.* The 12 kDa FK506-binding protein, FKBP12, modulates the Ca²⁺-flux properties of the type-3 ryanodine receptor. *Journal of Cell Science* **117**, 1129–1137 (2004).
223. Bielefeldt, K., Sharma, R. V., Whiteis, C., Yedidag, E. & Abboud, F. M. Tacrolimus (FK506) modulates calcium release and contractility of intestinal smooth muscle. *Cell Calcium* **22**, 507–514 (1997).
224. Zhang, X. *et al.* Rapamycin directly activates lysosomal mucolipin TRP channels independent of mTOR. *PLoS biology* **17**, e3000252 (2019).
225. Arcas, J. M. *et al.* The Immunosuppressant Macrolide Tacrolimus Activates Cold-Sensing TRPM8 Channels. *The Journal of neuroscience : the official journal of the Society for Neuroscience* **39**, 949–969 (2019).
226. Nayak, T. K. *et al.* Regulation of viral replication, apoptosis and pro-inflammatory responses by 17-aag during chikungunya virus infection in macrophages. *Viruses* **9**, (2017).
227. Nayak, T. K. *et al.* P38 and JNK Mitogen-Activated Protein Kinases Interact With

- Chikungunya Virus Non-structural Protein-2 and Regulate TNF Induction During Viral Infection in Macrophages. *Frontiers in Immunology* **10**, 1–15 (2019).
228. C, A.-U., Chen, M. & Hotta, H. Time-of-addition and Temperature-shift Assays to Determine Particular Step(s) in the Viral Life Cycle that is blocked by Antiviral Substances(s). *Bio-protocol* **8**, 1–12 (2018).
229. Saswat, T. *et al.* High rates of co-infection of Dengue and Chikungunya virus in Odisha and Maharashtra, India during 2013. *Infection, Genetics and Evolution* **35**, 134–141 (2015).
230. Siva Raghavendhar *et al.* Virus load and clinical features during the acute phase of Chikungunya infection in children. *PLoS ONE* **14**, 1–10 (2019).
231. Bartholomeusz, A. & Locarnini, S. Associated With Antiviral Therapy. *Antiviral Therapy* **55**, 52–55 (2006).
232. Chattopadhyay, S. S. *et al.* Development and characterization of monoclonal antibody against non-structural protein-2 of chikungunya virus and its applications. *Journal of Virological Methods* **199**, 86–94 (2014).
233. Sahoo, S. S. *et al.* VIPER regulates naive T cell activation and effector responses: Implication in TLR4 associated acute stage T cell responses. *Scientific reports* **8**, 7118 (2018).
234. Kitagawa, Y. *et al.* Orally administered selective TRPV1 antagonist, JTS-653, attenuates chronic pain refractory to non-steroidal anti-inflammatory drugs in rats and mice including post-herpetic pain. *Journal of pharmacological sciences* **122**, 128–137 (2013).
235. Cabrera, J. R., Viejo-Borbolla, A., Alcamí, A. & Wandosell, F. Secreted herpes simplex virus-2 glycoprotein G alters thermal pain sensitivity by modifying NGF effects on TRPV1. *Journal of Neuroinflammation* **13**, 1–9 (2016).

236. Harford, T. J., Rezaee, F., Scheraga, R. G., Olman, M. A. & Piedimonte, G. Asthma predisposition and respiratory syncytial virus infection modulate transient receptor potential vanilloid 1 function in children's airways. *Journal of Allergy and Clinical Immunology* **141**, 414-416.e4 (2018).
237. Liu, M., Huang, W., Wu, D. & Priestley, J. V. TRPV1, but not P2X3, requires cholesterol for its function and membrane expression in rat nociceptors. *European Journal of Neuroscience* **24**, 1–6 (2006).
238. Morales-Lázaro, S. L. & Rosenbaum, T. Cholesterol as a key molecule that regulates TRPV1 channel function. in *Advances in Experimental Medicine and Biology* vol. 1135 105–117 (2019).
239. Morales-Lázaro, S. L. *et al.* Inhibition of TRPV1 channels by a naturally occurring omega-9 fatty acid reduces pain and itch. *Nature Communications* **7**, (2016).
240. Lorent, J. H., Quetin-Leclercq, J. & Mingeot-Leclercq, M.-P. The amphiphilic nature of saponins and their effects on artificial and biological membranes and potential consequences for red blood and cancer cells. *Org. Biomol. Chem.* **12**, 8803–8822 (2014).
241. Sudji, I., Subburaj, Y., Frenkel, N., García-Sáez, A. & Wink, M. Membrane Disintegration Caused by the Steroid Saponin Digitonin Is Related to the Presence of Cholesterol. *Molecules* **20**, 20146–20160 (2015).
242. Chen, M., Balhara, V., Jaimes Castillo, A. M., Balsevich, J. & Johnston, L. J. Interaction of saponin 1688 with phase separated lipid bilayers. *Biochimica et Biophysica Acta (BBA) - Biomembranes* **1859**, 1263–1272 (2017).
243. Böttger, S. & Melzig, M. F. The influence of saponins on cell membrane cholesterol. *Bioorganic & Medicinal Chemistry* **21**, 7118–7124 (2013).
244. Shimizu, I., Iida, T., Horiuchi, N. & Caterina, M. J. 5-Iodoresiniferatoxin evokes

- hypothermia in mice and is a partial transient receptor potential vanilloid 1 agonist in vitro. *The Journal of pharmacology and experimental therapeutics* **314**, 1378–85 (2005).
245. Baboota, R. K. *et al.* Capsaicin Induces ““ Brite ”” Phenotype in Differentiating 3T3-L1 Preadipocytes. **9**, 1–12 (2014).
246. Takahashi, N. *et al.* Epithelial TRPV1 Signaling Cell Proliferation. 1141–1147 (2014) doi:10.1177/0022034514552826.
247. Tóth, B. I. *et al.* Transient receptor potential vanilloid-1 signaling as a regulator of human sebocyte biology. *Journal of Investigative Dermatology* **129**, 329–339 (2009).
248. Kumar, A., Mamidi, P., Das, I., Nayak, T. K. & Kumar, S. A Novel 2006 Indian Outbreak Strain of Chikungunya Virus Exhibits Different Pattern of Infection as Compared to Prototype Strain. **9**, (2014).
249. Tanabe, I. S. B., Tanabe, E. L. L., Santos, E. C. & Martins, W. V. Cellular and Molecular Immune Response to Chikungunya Virus Infection. **8**, 1–15 (2018).
250. Fox, J. M. & Diamond, M. S. Immune-Mediated Protection and Pathogenesis of Chikungunya Virus. (2016) doi:10.4049/jimmunol.1601426.
251. Venugopalan, A., Ghorpade, R. P. & Chopra, A. Cytokines in Acute Chikungunya. *PLoS ONE* **9**, e111305 (2014).
252. Tak, P. P. & Firestein, G. S. NF- κ B in defense and disease NF- κ B : a key role in inflammatory diseases. **107**, 7–11 (2001).
253. Lawrence, T. The nuclear factor NF-kappaB pathway in inflammation. *Cold Spring Harbor perspectives in biology* **1**, 1–10 (2009).
254. Trebak, M. & Kinet, J. P. Calcium signalling in T cells. *Nature Reviews Immunology* vol. 19 154–169 (2019).
255. Stueber, T. *et al.* Differential cytotoxicity and intracellular calcium-signalling

- following activation of the calcium-permeable ion channels TRPV1 and TRPA1. *Cell Calcium* **68**, 34–44 (2017).
256. Zhang, M., Ruwe, D., Saffari, R., Kravchenko, M. & Zhang, W. Effects of TRPV1 Activation by Capsaicin and Endogenous N-Arachidonoyl Taurine on Synaptic Transmission in the Prefrontal Cortex. *Frontiers in Neuroscience* **14**, (2020).
257. Lotteau, S., Ducreux, S., Romestaing, C., Legrand, C. & Van Coppenolle, F. Characterization of Functional TRPV1 Channels in the Sarcoplasmic Reticulum of Mouse Skeletal Muscle. *PLoS ONE* **8**, e58673 (2013).
258. Zumerle, S. *et al.* Intercellular Calcium Signaling Induced by ATP Potentiates Macrophage Phagocytosis. *Cell reports* **27**, 1-10.e4 (2019).
259. Papaioannou, N. E., Voutsas, I. F., Samara, P. & Tsitsilonis, O. E. A flow cytometric approach for studying alterations in the cytoplasmic concentration of calcium ions in immune cells following stimulation with thymic peptides. *Cellular Immunology* **302**, 32–40 (2016).
260. Bautista, D. M., Pellegrino, M. & Tsunozaki, M. TRPA1: A gatekeeper for inflammation. *Annual Review of Physiology* vol. 75 181–200 (2013).
261. Logashina, Y. A., Korolkova, Y. V., Kozlov, S. A. & Andreev, Y. A. TRPA1 Channel as a Regulator of Neurogenic Inflammation and Pain: Structure, Function, Role in Pathophysiology, and Therapeutic Potential of Ligands. *Biochemistry (Moscow)* vol. 84 101–118 (2019).
262. Xu, M. *et al.* TRPV1 and TRPA1 in lung inflammation and airway hyperresponsiveness induced by fine particulate matter (PM2.5). *Oxidative Medicine and Cellular Longevity* **2019**, (2019).
263. Meseguer, V. *et al.* TRPA1 channels mediate acute neurogenic inflammation and pain produced by bacterial endotoxins. *Nature Communications* **5**, 1–14 (2014).

264. Startek, J. B. *et al.* Mouse TRPA1 function and membrane localization are modulated by direct interactions with cholesterol. *eLife* **8**, (2019).
265. Startek, J. B. & Talavera, K. Lipid Raft Destabilization Impairs Mouse TRPA1 Responses to Cold and Bacterial Lipopolysaccharides. *International Journal of Molecular Sciences* **21**, 3826 (2020).
266. Conklin, D. J. *et al.* TRPA1 channel contributes to myocardial ischemia-reperfusion injury. *American Journal of Physiology - Heart and Circulatory Physiology* **316**, H889–H899 (2019).
267. Eid, S. R. *et al.* HC-030031, a TRPA1 selective antagonist, attenuates inflammatory- and neuropathy-induced mechanical hypersensitivity. *Molecular pain* **4**, 48 (2008).
268. Hassan, A.-A., Sleet, B., Cousins, Z. & Keating, C. D. TRPA1 Channel Activation Inhibits Motor Activity in the Mouse Colon. *Frontiers in neuroscience* **14**, 471 (2020).
269. Yap, J. M. G. *et al.* An inflammatory stimulus sensitizes TRPA1 channel to increase cytokine release in human lung fibroblasts. *Cytokine* **129**, 155027 (2020).
270. Acharya, T. K., Tiwari, A., Majhi, R. K. & Goswami, C. TRPM8 channel augments T cell activation and proliferation. *Cell Biology International* (2020) doi:10.1002/cbin.11483.
271. Birx, D. L., Berger, M. & Fleisher, T. A. The interference of T cell activation by calcium channel blocking agents. *The Journal of Immunology* **133**, (1984).
272. Nakabayashi, H., Komada, H., Yoshida, T., Takanari, H. & Izutsu, K. Lymphocyte calmodulin and its participation in the stimulation of T lymphocytes by mitogenic lectins. *Biology of the Cell* **75**, 55–59 (1992).
273. Watman, N. P., Crespo, L., Davis, B., Poiesz, B. J. & Zamkoff, K. W. Differential effect on fresh and cultured T cells of PHA-induced changes in free cytoplasmic calcium: Relation to IL-2 receptor expression, IL-2 production, and proliferation.

- Cellular Immunology* **111**, 158–166 (1988).
274. Ando, Y. *et al.* Concanavalin A-mediated T cell proliferation is regulated by herpes virus entry mediator costimulatory molecule. *In Vitro Cellular and Developmental Biology - Animal* **50**, 313–320 (2014).
275. Pang, B. *et al.* Differential pathways for calcium influx activated by concanavalin A and CD3 stimulation in Jurkat T cells. *Pflugers Archiv European Journal of Physiology* **463**, 309–318 (2012).
276. Bertin, S. & Raz, E. Transient Receptor Potential (TRP) channels in T cells. *Seminars in Immunopathology* **38**, 309–319 (2016).
277. Kume, H. & Tsukimoto, M. TRPM8 channel inhibitor AMTB suppresses murine T-cell activation induced by T-cell receptor stimulation, concanavalin A, or external antigen re-stimulation. *Biochemical and Biophysical Research Communications* **509**, 918–924 (2019).
278. Westlund, K. N., Kochukov, M. Y., Lu, Y. & McNearney, T. A. Impact of central and peripheral TRPV1 and ROS levels on proinflammatory mediators and nociceptive behavior. *Molecular Pain* **6**, (2010).
279. Lapointe, T. K. *et al.* TRPV1 sensitization mediates postinflammatory visceral pain following acute colitis. *American Journal of Physiology - Gastrointestinal and Liver Physiology* **309**, G87–G99 (2015).
280. Masuoka, T. *et al.* TRPA1 Channels Modify TRPV1-Mediated Current Responses in Dorsal Root Ganglion Neurons. *Frontiers in Physiology* **8**, 1–9 (2017).
281. Akopian, A. N., Ruparel, N. B., Jeske, N. A. & Hargreaves, K. M. Transient receptor potential TRPA1 channel desensitization in sensory neurons is agonist dependent and regulated by TRPV1-directed internalization. *Journal of Physiology* **583**, 175–193 (2007).

282. Hsu, C.-C. & Lee, L.-Y. Role of calcium ions in the positive interaction between TRPA1 and TRPV1 channels in bronchopulmonary sensory neurons. *Journal of Applied Physiology* **118**, 1533–1543 (2015).
283. Meng, J., Wang, J., Steinhoff, M. & Dolly, J. O. TNF α induces co-trafficking of TRPV1/TRPA1 in VAMP1-containing vesicles to the plasmalemma via Munc18-1/syntaxin1/SNAP-25 mediated fusion. *Scientific Reports* **6**, 1–15 (2016).
284. Kistner, K. *et al.* Systemic desensitization through TRPA1 channels by capsaizepine and mustard oil - A novel strategy against inflammation and pain. *Scientific Reports* **6**, 1–11 (2016).
285. Than, J. Y. X. L., Li, L., Hasan, R. & Zhang, X. Excitation and modulation of TRPA1, TRPV1, and TRPM8 channel-expressing sensory neurons by the pruritogen chloroquine. *Journal of Biological Chemistry* **288**, 12818–12827 (2013).
286. Cowan, A. & Editors, G. Y. *Transient Receptor Potential (TRP) Channels Handbook of Experimental Pharmacology Review*. vol. 226 (2015).
287. Dietrich, A. *Cells* 2019, 8, x; doi: FOR PEER REVIEW *Cells*. **8**, 413 (2019).
288. Elokely, K. *et al.* Understanding TRPV1 activation by ligands: Insights from the binding modes of capsaicin and resiniferatoxin. *Proceedings of the National Academy of Sciences* **113**, E137–E145 (2016).
289. Tsuji, F. & Aono, H. Role of transient receptor potential vanilloid 1 in inflammation and autoimmune diseases. *Pharmaceuticals* **5**, 837–852 (2012).
290. Szitter, I. *et al.* The role of transient receptor potential vanilloid 1 (Trpv1) receptors in dextran sulfate-induced colitis in mice. *Journal of Molecular Neuroscience* **42**, 80–88 (2010).
291. Messeguer, A., Planells-Cases, R. & Ferrer-Montiel, A. Physiology and pharmacology of the vanilloid receptor. *Current neuropharmacology* **4**, 1–15 (2006).

292. Alawi, K. & Keeble, J. The paradoxical role of the transient receptor potential vanilloid 1 receptor in inflammation. *Pharmacology and Therapeutics* **125**, 181–195 (2010).
293. Wang, Y. & Wang, D. H. Aggravated renal inflammatory responses in TRPV1 gene knockout mice subjected to DOCA-salt hypertension. *American Journal of Physiology-Renal Physiology* **297**, F1550–F1559 (2009).
294. Helyes, Z. *et al.* Role of transient receptor potential vanilloid 1 receptors in endotoxin-induced airway inflammation in the mouse. *Am J Physiol Lung Cell Mol Physiol* **292**, L1173–81 (2007).
295. Wang, Y. & Wang, D. H. TRPV1 ablation aggravates inflammatory responses and organ damage during endotoxic shock. *Clinical and Vaccine Immunology* **20**, 1008–1015 (2013).
296. Wang, Y. & Wang, D. H. Role of the transient receptor potential vanilloid type 1 channel in renal inflammation induced by lipopolysaccharide in mice. *American Journal of Physiology-Regulatory, Integrative and Comparative Physiology* **304**, R1–R9 (2013).
297. Zhong, B., Rubinstein, J., Ma, S. & Wang, D. H. Genetic ablation of TRPV1 exacerbates pressure overload-induced cardiac hypertrophy. *Biomedicine and Pharmacotherapy* **99**, 261–270 (2018).
298. Kraeft, S. K., Chen, D. S., Li, H. P., Chen, L. B. & Lai, M. M. C. Mouse hepatitis virus infection induces an early, transient calcium influx in mouse astrocytoma cells. *Experimental Cell Research* **237**, 55–62 (1997).
299. Yasui, H. *et al.* Selective inhibition of mitogen-induced transactivation of the HIV long terminal repeat by carboxyamidotriazole: Calcium influx blockade represses HIV-1 transcriptional activation. *Journal of Biological Chemistry* **272**, 28762–28770

- (1997).
300. Scherbik, S. V. & Brinton, M. A. Virus-Induced Ca²⁺ Influx Extends Survival of West Nile Virus-Infected Cells. *Journal of Virology* **84**, 8721–8731 (2010).
 301. Taverner, W. K. *et al.* Calcium Influx Caused by ER Stress Inducers Enhances Oncolytic Adenovirus Enadenotucirev Replication and Killing through PKC α Activation. *Molecular Therapy - Oncolytics* **15**, 117–130 (2019).
 302. Pando, V., Iša, P., Arias, C. F., Ló Pez, S. & López, S. Influence of calcium on the early steps of rotavirus infection. *Virology* **295**, 190–200 (2002).
 303. Chhibber, S., Kaur, T. & Kaur, S. Essential role of calcium in the infection process of broad-spectrum methicillin-resistant Staphylococcus aureus bacteriophage. *Journal of Basic Microbiology* **54**, 775–780 (2014).
 304. Musarrat, F., Jambunathan, N., Rider, P. J. F., Chouljenko, V. N. & Kousoulas, K. G. The Amino-terminus of HSV-1 Glycoprotein K (gK) is Required for gB Binding to Akt, Release of Intracellular Calcium and Fusion of the Viral Envelope with Plasma Membranes. *Journal of Virology* **92**, JVI.01842-17 (2018).
 305. Cheshenko, N. *et al.* TWtMe Herpes simplex virus triggers activation of calcium-signaling pathways. **163**, 283–293 (2014).
 306. Fischer, M. J. M. *et al.* Direct evidence for functional TRPV1/TRPA1 heteromers. *Pflugers Archiv European Journal of Physiology* **466**, 2229–2241 (2014).
 307. Weyer, A. D. & Stucky, C. L. Loosening Pain's Grip by Tightening TRPV1-TRPA1 Interactions. *Neuron* vol. 85 661–663 (2015).
 308. Staruschenko, A., Jeske, N. A. & Akopian, A. N. Contribution of TRPV1-TRPA1 interaction to the single channel properties of the TRPA1 channel. *Journal of Biological Chemistry* **285**, 15167–15177 (2010).
 309. Kaufmann, U. *et al.* Calcium Signaling Controls Pathogenic Th17 Cell-Mediated

- Inflammation by Regulating Mitochondrial Function. *Cell Metabolism* **29**, 1104–1118.e6 (2019).
310. Hyser, J. M., Utama, B., Crawford, S. E., Broughman, J. R. & Estes, M. K. Activation of the endoplasmic reticulum calcium sensor STIM1 and store-operated calcium entry by rotavirus requires NSP4 viroporin activity. *Journal of virology* **87**, 13579–88 (2013).
311. Liu, X. *et al.* T cell receptor-induced nuclear factor κ B (NF- κ B) signaling and transcriptional activation are regulated by STIM1- and Orai1-mediated calcium entry. *Journal of Biological Chemistry* **291**, 8440–8452 (2016).
312. Kim, K.-D. *et al.* Targeted calcium influx boosts cytotoxic T lymphocyte function in the tumour microenvironment. *Nature communications* **8**, 15365 (2017).
313. Sarkadi, B., Tordai, A., Homolya, L., Scharff, O. & Gárdos, G. Calcium influx and intracellular calcium release in anti-CD3 antibody-stimulated and thapsigargin-treated human T lymphoblasts. *The Journal of Membrane Biology* **123**, 9–21 (1991).
314. Wei, X. *et al.* Ca²⁺–Calcineurin Axis–Controlled NFAT Nuclear Translocation Is Crucial for Optimal T Cell Immunity in an Early Vertebrate. *The Journal of Immunology* **204**, 569–585 (2020).
315. Fenninger, F. *et al.* Mutation of an l-type calcium channel gene leads to t lymphocyte dysfunction. *Frontiers in Immunology* **10**, (2019).
316. Beesetty, P. *et al.* Inactivation of TRPM7 kinase in mice results in enlarged spleens, reduced T-cell proliferation and diminished store-operated calcium entry. *Scientific Reports* **8**, (2018).
317. Christo, S. N., Diener, K. R. & Hayball, J. D. The functional contribution of calcium ion flux heterogeneity in T cells. *Immunology and Cell Biology* **93**, 694–704 (2015).
318. Monaco, S., Jahraus, B., Samstag, Y. & Bading, H. Nuclear calcium is required for

- human T cell activation. *Journal of Cell Biology* **215**, 231–243 (2016).
319. Aghdasi, B. *et al.* Physiologic Regulator of the Cell Cycle. *Proceedings of the National Academy of Science* **98**, 2425–2430 (2001).
320. Feske, S. Calcium signalling in lymphocyte activation and disease. *Nature Reviews Immunology* **7**, 690–702 (2007).
321. Komada, H., Nakabayashi, H., Hara, M. & Izutsu, K. Early calcium signaling and calcium requirements for the IL-2 receptor expression and IL-2 production in stimulated lymphocytes. *Cellular Immunology* **173**, 215–220 (1996).
322. MacMillan, D. FK506 binding proteins: Cellular regulators of intracellular Ca²⁺ signalling. *European Journal of Pharmacology* **700**, 181–193 (2013).
323. Oh-hora, M. & Rao, A. Calcium signaling in lymphocytes. *Current Opinion in Immunology* vol. 20 250–258 (2008).
324. Wille, A. C. M. *et al.* Modulation of membrane phospholipids, the cytosolic calcium influx and cell proliferation following treatment of B16-F10 cells with recombinant phospholipase-D from *Loxosceles intermedia* (brown spider) venom. *Toxicon* **67**, 17–30 (2013).
325. Joseph, N., Reicher, B. & Barda-Saad, M. The calcium feedback loop and T cell activation: How cytoskeleton networks control intracellular calcium flux. *Biochimica et Biophysica Acta - Biomembranes* **1838**, 557–568 (2014).
326. Racioppi, L. *et al.* CaMKK2 in myeloid cells is a key regulator of the immune-suppressive microenvironment in breast cancer. *Nature Communications* **10**, 2450 (2019).

PUBLICATIONS



Inhibition of transient receptor potential vanilloid 1 (TRPV1) channel regulates chikungunya virus infection in macrophages

P. Sanjai Kumar¹ · Tapas K. Nayak^{1,2} · Chandan Mahish¹ · Subhransu S. Sahoo¹ · Anukrishna Radhakrishnan¹ · Saikat De² · Ankita Datey² · Ram P. Sahu¹ · Chandan Goswami¹ · Soma Chattopadhyay² · Subhasis Chattopadhyay¹ 

Received: 6 October 2019 / Accepted: 8 September 2020
© Springer-Verlag GmbH Austria, part of Springer Nature 2020

Abstract

Chikungunya virus (CHIKV), a virus that induces pathogenic inflammatory host immune responses, is re-emerging worldwide, and there are currently no established antiviral control measures. Transient receptor potential vanilloid 1 (TRPV1), a non-selective Ca²⁺-permeable ion channel, has been found to regulate various host inflammatory responses including several viral infections. Immune responses to CHIKV infection in host macrophages have been reported recently. However, the possible involvement of TRPV1 during CHIKV infection in host macrophages has not been studied. Here, we investigated the possible role of TRPV1 in CHIKV infection of the macrophage cell line RAW 264.7. It was found that CHIKV infection upregulates TRPV1 expression in macrophages. To confirm this observation, the TRPV1-specific modulators 5'-iodoresiniferatoxin (5'-IRTX, a TRPV1 antagonist) and resiniferatoxin (RTX, a TRPV1 agonist) were used. Our results indicated that TRPV1 inhibition leads to a reduction in CHIKV infection, whereas TRPV1 activation significantly enhances CHIKV infection. Using a plaque assay and a time-of-addition assay, it was observed that functional modulation of TRPV1 affects the early stages of the viral lifecycle in RAW 264.7 cells. Moreover, CHIKV infection was found to induce of pNF-κB (p65) expression and nuclear localization. However, both activation and inhibition of TRPV1 were found to enhance the expression and nuclear localization of pNF-κB (p65) and production of pro-inflammatory TNF and IL-6 during CHIKV infection. In addition, it was demonstrated by Ca²⁺ imaging that TRPV1 regulates Ca²⁺ influx during CHIKV infection. Hence, the current findings highlight a potentially important regulatory role of TRPV1 during CHIKV infection in macrophages. This study might also have broad implications in the context of other viral infections as well.

Introduction

Transient receptor potential (TRP) channels constitute a superfamily of ion channels that are non-selective, polymodal gated, and permeable to cations [1–4]. TRP channels can conduct an array of both monovalent and divalent cations, such as Na⁺, Mg²⁺, and Ca²⁺ [5, 6]. Based on amino acid sequence similarity, the mammalian TRP superfamily

is divided into six subfamilies: TRPC (canonical), TRPV (vanilloid), TRPM (melastatin), TRPA (ankyrin), TRPML (mucolipin), and TRPP (polycystin). In total, the mammalian TRP superfamily has 28 members [7–10]. TRP channels have been shown to be involved in a number of cellular functions, including cell division, proliferation, excitation, migration, transcription, differentiation, stress responses, and cell death [11–13].

Transient receptor potential cation channel subfamily V member 1 (TRPV1) is also known as vanilloid receptor 1 [14–16]. TRPV1 channels are widely distributed in the central and peripheral nervous systems as well as in various non-neuronal cells, where they act as molecular sensors to differential temperature, noxious substances, and pain modalities [14, 17–19]. In addition, TRPV1 is involved in various inflammatory conditions, such as in inflammatory bowel disease (IBD), cutaneous neurogenic inflammation, brain inflammation, allergic asthma, colitis, arthritis,

Handling Editor: Patricia Aguilar.

Electronic supplementary material The online version of this article (<https://doi.org/10.1007/s00705-020-04852-8>) contains supplementary material, which is available to authorized users.

✉ Soma Chattopadhyay
sochat.ils@gmail.com

✉ Subhasis Chattopadhyay
subho@niser.ac.in

Extended author information available on the last page of the article

hypersensitivity, chronic obstructive pulmonary disease (COPD), and autoimmune diseases [15, 19–24].

Recently, TRPV1 has been found to be significantly upregulated in numerous viral infections, including human rhinovirus (HRV), respiratory syncytial virus (RSV), measles virus (MV), hepatitis C virus (HCV), herpes simplex virus type 2 (HSV-2), herpes simplex virus type 1 (HSV-1), and varicella-zoster virus (VZV) infections [25–31]. It has been suggested that TRPV1 plays a pivotal role in host-pathogen interactions involved in virus binding, viral entry, and viral replication. Moreover, TRPV1 has been found to be closely associated with post-viral-infection pain and inflammation [25–31].

Chikungunya virus (CHIKV) is a positive-sense, single-stranded RNA virus belonging to the genus *Alphavirus*, family *Togaviridae*. Chikungunya is now considered a re-emerging disease, and it is endemic to Africa, India, China, and many parts of Asia [32, 33]. The symptoms of chikungunya fever (CHIKF) include high fever, nausea, vomiting, headache, rashes, polyarthralgia, and myalgia [34–36]. CHIKV infects a wide range of both immune and non-immune cells. Amongst them, monocytes/macrophages play important roles in modulating adaptive immune responses [35, 37–39].

Recent studies on cell-mediated immunity have demonstrated a functional expression of TRPV1 during immune activation responses [4, 40, 41]. TRPV1 has been found to play an active role in macrophage function and survival. In a sepsis model of cecal ligation and puncture (CLP), LPS-stimulated TRPV1 KO (*Trpv1*^{-/-}) mice exhibited decreased bacterial clearance and phagocytosis compared to CLP WT (wild-type) mice. Similarly, treatment with a TRPV1 antagonist resulted in dysfunctional phagocytosis in macrophages. TRPV1 deletion has been found to be associated with impaired macrophage-defense mechanisms [41–43]. Additionally, TRPV1 activation has been shown to facilitate microglial migration by increasing the intramitochondrial Ca²⁺ concentration. Furthermore, microglia derived from TRPV1-KO mice showed delayed Ca²⁺ influx compared to those from wild-type mice. Moreover, the regulation of TRPV1 has been reported to modulate NF-κB activation [44–46]. Therefore, it appears that modulation of TRPV1 may contextually regulate host immune activation and inflammatory responses [6, 15, 19, 23, 24, 41, 42, 47–53].

CHIKV-infection-associated immune responses in the host macrophages have been reported recently [34, 35, 38, 39, 54, 55]. However, the potential involvement of TRPV1 during CHIKV infection in host macrophages has not been investigated. Therefore, in the present study, the possible role of TRPV1 during CHIKV infection and replication in macrophages was explored. Moreover, CHIKV-induced production of inflammatory cytokines, subsequent Ca²⁺ influx, and the involvement of NF-κB (p65) associated with TRPV1-regulated macrophage responses were investigated.

The current study might have implications for TRPV1-driven regulation of CHIKV infection and the associated altered immune responses of host macrophages, and it might have implications for other viral infections as well.

Materials and methods

Cell lines and virus

The RAW 264.7 (ATCC® TIB-71™) mouse monocyte/macrophage cell line was maintained in Roswell Park Memorial Institute 1640 medium (RPMI-1640; PAN Biotech, Aidenbach Germany) supplemented with antibiotics, including penicillin (100 U/ml) and streptomycin (0.1 mg/ml), 2.0 mM L-glutamine (Himedia Laboratories Pvt. Ltd., Mumbai, India), and 10% heat-inactivated fetal bovine serum (FBS; PAN Biotech, Aidenbach Germany) at 37 °C in a humidified incubator with 5% CO₂. Vero cells (an African green monkey kidney epithelial cell line), were maintained in Dulbecco's modified Eagle's medium (DMEM; Himedia) with the same supplements and conditions listed above [35, 39, 56].

The Indian outbreak strain of CHIKV (strain DRDE-06, accession no. EF210157.2) and Vero cells were kind gifts from Dr. Manmohan Parida, Defence Research and Development Establishment (DRDE), Gwalior, India.

Antibodies, reagents, and drugs

The mouse anti-CHIKV-nsP2 monoclonal antibody used in this study was developed by us [56]. The anti-CHIKV-E2 monoclonal antibody was a kind gift from Dr. Manmohan Parida, DRDE, Gwalior, India. Rabbit polyclonal antibody for extracellular TRPV1 with a specific blocking peptide (TRPV1, NSLPMESTPHKSRGS) was purchased from Alomone Laboratories (Jerusalem, Israel). Phospho-NF-κB (p65) (Ser536), anti-mouse Alexa Fluor 647, anti-rabbit Alexa Fluor 488, and Fluo-4 AM were obtained from Invitrogen (Carlsbad, CA, USA). Mouse and rabbit IgG1 isotype controls were procured from Abgenex India Pvt. Ltd. (Bhubaneswar, India). Saponin and bovine serum albumin fraction V (BSA) were purchased from Merck Millipore (Billerica, MA, USA). The TRPV1 channel modulatory drugs 5'-IRTX and RTX were obtained from Alomone Laboratories (Jerusalem, Israel). 5'-IRTX and RTX were used as functional modulators of TRPV1, and these modulators do not affect the expression levels of TRPV1 [4, 57].

MTT assay

An MTT assay was performed to assess cellular cytotoxicity and the viability of RAW 264.7 cells after treatment

with the TRPV1 modulators 5'-IRTX and RTX, using an EZcount™ MTT Cell Assay Kit (Himedia Laboratories Pvt. Ltd., Mumbai, India) as described earlier [35, 39]. In brief, RAW 264.7 cells were seeded in a flat-bottom, polystyrene-coated, 96-well plate at a density of 5×10^3 /well. After 24 h, the medium was removed, and the cells were washed three times with 1X PBS. Each specific modulator was diluted to the desired concentration and applied to each well in triplicate. DMSO was used as a solvent control. After 24 h of treatment, the cells were treated with 10% MTT (v/v) dissolved in complete RPMI medium. Cells were left in the incubator at 37°C for 2 h to form formazan crystals. The medium was then carefully removed, and 100 µl of solubilization buffer is added to each well, followed by incubation for 15 min at room temperature (RT). Absorbance was measured at 550 nm using a microplate reader (Bio-Rad, Hercules, CA, USA), and the percentage of viable cells was calculated in comparison to the control cells of the same plate in triplicate.

CHIKV infection in macrophages

RAW 264.7 cells were infected with CHIKV (DRDE-06) at multiplicity of infection (MOI) of 5 as described earlier [35, 39]. Briefly, cells were seeded in a 6-well plate, and after 20 h, at a monolayer confluency of 60%-70%, the cells were washed three times with 1X PBS, infected with CHIKV in serum-free medium (SFM), and incubated for 2 h at 37 °C with manual shaking every 15 minutes. The virus inoculum was removed by washing with 1X PBS, and the cells were maintained at 37°C in RPMI-1640 medium. The infected cells and the supernatants were collected at different time points and subjected to further processing according to the assay. Further, the CHIKV-infected and mock-infected cells were examined under a microscope (200X magnification), and images were taken at different times postinfection to observe the cytopathic effect (CPE).

To assess the effect of TRPV1 modulators on CHIKV infection, RAW 264.7 cells were pre-treated with specific modulators for 2 h prior to infection, during CHIKV infection, and after infection until harvesting. DMSO was used as a solvent control. The remaining protocol was followed as described above.

Plaque assay

For determination of virus titers, a plaque assay was performed as described earlier [58]. Vero cells were seeded in a 24-well plate at a concentration of 0.15×10^6 cells per well and were infected using different dilutions of cell culture supernatants for 90 min. After infection, Vero cells were overlaid with complete DMEM containing methylcellulose (2% w/v) and maintained in an incubator at 37° C. After the

development of visible plaques in 3-4 days, the cells were fixed, washed gently with distilled water, and stained with crystal violet. The plaques were counted manually under white light.

Flow cytometry (FC)

For quantification of CHIKV infection and other cell markers, a flow cytometric assay was performed as described previously [35, 39]. In brief, mock- and CHIKV- infected RAW 264.7 cells were harvested by scraping and were subjected to FC staining. For TRPV1 staining, cells were stained with primary α -TRPV1 for 30 minutes on ice. After incubation, excess unbound antibody was removed by washing with FACS buffer (1X PBS, 1% BSA, 0.01% NaN₃). Then, secondary fluorochrome-conjugated AF488 was added and incubated for 30 minutes, followed by washing with FACS buffer. Rabbit IgG was used as an isotype control.

For intracellular staining (ICS) of CHIKV antigens and pNF- κ B (p65), RAW 264.7 cells were harvested by scraping and immediately fixed with 4% paraformaldehyde (PFA) for 10 min at RT. Next, the cells were suspended in FACS buffer and stored at 4°C. For ICS, the cells were first permeabilized in permeabilization buffer (0.5% BSA + 0.1% saponin + 0.01% NaN₃ + 1X PBS), followed by blocking with 1% BSA (in permeabilization buffer) for 30 min at RT. Then, the cells were washed with permeabilization buffer, incubated with anti-CHIKV-nsP2, E2, or pNF- κ B (p65) antibodies. After incubation, cells were washed twice in permeabilization buffer, followed by incubation with Alexa Fluor 647-conjugated chicken anti-mouse IgG (H + L) secondary antibody or Alexa Fluor 488-conjugated chicken anti-rabbit IgG (H + L) secondary antibody, as appropriate. After two washes with permeabilization buffer, the cells were suspended in FACS buffer and stored at 4°C. Both the primary and secondary antibodies were diluted in permeabilization buffer. Mouse IgG or rabbit IgG, as appropriate, was used as an isotype control for ICS. To prevent nonspecific binding of Fc receptors on macrophages, FcR blocking reagent (Miltenyi Biotec, Bergisch Gladbach, Germany) was used at a dilution of 1:20.

Finally, the cells were acquired using a BD FACS Calibur™ flow cytometer (BD Biosciences) and analyzed using CellQuest Pro software (BD Biosciences). Approximately ten thousand cells were acquired per sample.

Western blot

Protein expression was examined by Western blot analysis as described earlier [35, 39]. Mock- and CHIKV-infected RAW 264.7 cells were harvested at 8 h postinfection (hpi) and lysed with RIPA buffer (150 mM NaCl, 1% NP-40, 0.5% sodium deoxycholate, 0.1% SDS, 50 mM Tris, pH

8.0) supplemented with a protease inhibitor and phosphatase inhibitor cocktail (Roche, Mannheim, Germany). An equal amount of protein (30 µg) per well was subjected to 10% SDS-PAGE and blotted on to a polyvinylidene fluoride (PVDF) membrane (Millipore, MA, USA). After blocking with 3% BSA, overnight incubation at 4°C with primary antibodies against E2, nsP2, TRPV1, β-actin and GAPDH was carried out. The antibodies on the PVDF membrane were detected by chemiluminescence (Immobilon Western Chemiluminescent HRP Substrate [Millipore] or SuperSignal West Femto Reagent [Thermo Scientific, Waltham, MA, USA] using Bio-Rad Gel Doc with Quantity One software (Bio-Rad). For band intensity quantification, Western blot images were analyzed using Quantity One 1-D analysis software while normalizing to the corresponding loading control.

Real-time RT-PCR

For quantitative RT-PCR, the supernatant of CHIKV-infected RAW 264.7 cells treated with 5'-IRTX or RTX as described above was collected at 12 hpi, and 140 µl of supernatant was used to extract viral RNA using a QIAamp Viral RNA Mini Kit (QIAGEN, Hilden, Germany) as per the manufacturer's protocol [59]. The extracted viral RNA was quantified, and 1 µg was used to prepare cDNA using a PrimeScript 1st Strand cDNA Synthesis Kit (Takara, Kusatsu, Japan) and random hexamers. This cDNA was used to amplify the E1 gene by RT-PCR (Applied Biosystems QuantStudio 3, using the primers F (5'-TGCCGTCACAGT TAAGGACG-3' and R (5'-CCTCGCATGACATGTCCG -3') and a MESA GREEN qPCR MasterMix Plus for SYBR Assay No ROX (Eurogentec, Belgium). A standard curve for Ct values was prepared using six tenfold serial dilutions of the E1 gene cloned in the plasmid pBiEx [60, 61]. Percentage of copy number/ml for experimental samples was calculated from the corresponding Ct values. All samples were tested in triplicate.

Time-of-addition assay

A time-of-addition assay was performed to determine which stage of viral life cycle is affected by the TRPV1 modulators [62]. In brief, TRPV1 modulators were added to the host RAW 264.7 cells at different time points relative to the addition of virus. In this study, four different conditions were set up. In the "pre-during-post" setup (i), the TRPV1 modulators were added 2 h prior to infection, during CHIKV infection, and after infection (0 hpi). In the "pre-during" setup (ii), the TRPV1 modulators were added 2 h prior to infection and during CHIKV infection only (no TRPV1 modulators were added after infection). Finally, in the "post" setup, the TRPV1 modulators were added after infection only, either

at 0 hpi (iii) or at 4 hpi (iv). The supernatants were collected at 12 hpi in each of the four conditions. Viral RNA in the supernatant was quantified by qRT-PCR by amplifying the viral E1 gene.

Calcium imaging

Resting RAW 264.7 cells were cultured on sterile coverslips. After 20 hours, cells were loaded with the Ca²⁺-sensitive dye Fluo-4 AM (Invitrogen) for 45 min at 37 °C. Then, the cells were washed twice with 1X PBS to remove the excess dye and placed in an incubator for 30 min for de-esterification. The cells were placed in a live cell chamber, and images were acquired every 5 s. The Fluo-4 AM signal was acquired using a Zeiss LSM800 confocal microscope [4, 63], and images were analyzed using the ImageJ software. The intensity profile was represented with a pseudo-scale, and the time-lapse kinetics of intracellular calcium were plotted using the GraphPad Prism 7.0 software (GraphPad Software Inc., San Diego, CA, USA).

Confocal microscopy

RAW 264.7 cells were seeded on sterile coverslips and infected with CHIKV at an MOI of 5 as described above. At 8 and 12 hpi, cells were fixed in 4% PFA for 15 min. For permeabilization, cells were treated with blocking buffer (3% BSA in 1X PBS) + 0.2% Triton X-100 for 10 min and washed three times with 1X PBS. Blocking was carried out for 1 hour. The cells were then incubated with a monoclonal antibody (mAb) against phospho-NF-κB-p65 (Ser536) for 1 h at RT. After washing, the cells were incubated with AF594-conjugated anti-mouse antibody for 1 h at RT. Then, the coverslips were mounted with antifade (Invitrogen) to reduce photobleaching. Fluorescence microscopic images were acquired using a Leica TCS SP5 confocal microscope (Leica Microsystems, Heidelberg, Germany) using a 63X objective and images were analysed using the ImageJ software.

ELISA

Sandwich ELISA was performed to analyze the cytokine levels in cell culture supernatants using a BD OptEIA™ Sandwich ELISA Kit for TNF and IL-6 (BD Biosciences) according to the manufacturer's instructions [4, 35, 39]. The cytokine concentrations in the test samples were calculated in comparison with the corresponding standard curve, which was constructed using different concentrations of the recombinant cytokines in pg/mL.

Statistical analysis

Statistical analysis was performed using the GraphPad Prism 7.0 software (GraphPad Software Inc., San Diego, CA, USA). Data are presented as the mean \pm SD. Comparisons between the groups were performed by one-way ANOVA or two-way ANOVA with the Bonferroni post-hoc test. The data presented are representative of at least three independent experiments. Statistical significance is represented by asterisks (*) for p -value(s) and is marked correspondingly in the figures (*, $p < 0.05$; **, $p < 0.01$; ***, $p < 0.001$).

Results

CHIKV upregulates TRPV1 expression in macrophages.

TRPV1 has been shown to play a pivotal role in different inflammatory and autoimmune diseases [15, 16, 24, 49, 64–67]. Recently, TRPV1 has been shown to play a role in different viral infections [25–30]. Moreover, it has been reported that CHIKV infection induces robust inflammatory responses in macrophages [32, 35, 68, 69]. Hence, the specific role of TRPV1 during CHIKV infection in a macrophage cell line was studied. For this, RAW 264.7 cells were infected with CHIKV [35, 39], and the infected cells were analyzed by flow cytometry (FC) to detect viral proteins (nsP2 and E2) and TRPV1 expression at 8 and 12 hpi. As reported earlier, the highest percentage of positive cells for CHIKV antigens was observed at 8 hpi (nsP2, 7.74 ± 1.01 ; E2, 14.66 ± 1.09), followed by a marginal decrease towards 12 hpi (nsP2, 4.87 ± 1.01 ; E2, 11.15 ± 0.85) (Fig. 1A). To determine whether the expression of TRPV1 is altered during CHIKV infection, both infected and mock-infected cells were subjected to FC analysis. It was found that the percentage of cells that were positive for TRPV1 was 51.13 ± 1.32 at 8 hpi and 64.79 ± 0.52 at 12 hpi, which was higher than in the mock-infected control (8 hpi, 43.147 ± 1.48 ; 12 hpi, 47.22 ± 1.58) (Fig. 1B). Simultaneous detection of viral protein (nsP2 or E2) and TRPV1 could not be done due to technical limitations. TRPV1 is closely associated with cholesterol in the cell membrane [70–73], and treatment with saponin forms transient pores due to removal of cholesterol, leading to membrane loss and hence loss of the TRPV1 expression signal (data not shown) [71, 74–77]. Taken together, it appears that CHIKV infection may upregulate TRPV1 expression (1.18-fold at 8 hpi and 1.37-fold at 12 hpi) in host macrophages in a time-dependent manner.

The specificity of the TRPV1 antibody in RAW 264.7 cells was tested using a control blocking peptide antigen [4]. For this purpose, RAW 264.7 cells were stained with anti-TRPV1 antibody in the presence or absence of the blocking

peptide. As reported earlier, it was found that the percentage of cells that were positive for TRPV1 decreased in a dose-dependent manner from 42.21 ± 3.90 to 7.75 ± 2.74 ($p < 0.001$) in the presence of 1X control blocking peptide antigen, and it decreased further to 2.03 ± 0.69 ($p < 0.001$) in the presence of 3X control blocking peptide antigen, confirming the specificity of the TRPV1 antibody in RAW 264.7 cells (Supplementary Fig. 1).

TRPV1 regulates CHIKV infection

The altered expression of TRPV1 during CHIKV infection prompted us to look at whether TRPV1 plays a regulatory role during CHIKV infection. For this, the TRPV1 activator RTX and the inhibitor 5'-IRTX were used in this study. Both RTX and 5'-IRTX are highly specific modulators of TRPV1 and have been used previously in various studies [4, 78]. In order to determine the cellular cytotoxicity of TRPV1 modulators, MTT assay was carried out using different concentrations of RTX (0.08 μ M to 10 μ M) and 5'-IRTX (0.625 μ M to 160 μ M). DMSO was used as a solvent control. It was observed that approximately 97% of the RAW 264.7 cells were viable at a 0.625 μ M concentration of 5'-IRTX, and nearly 100% of the cells were viable at a concentration range of 0.08 μ M to 5 μ M RTX (Fig. 2A). Similar observations have been reported previously [79–81]. Hence, for further experiments, the same concentration, 0.625 μ M, was selected for both TRPV1 modulators, RTX and 5'-IRTX.

In order to determine whether TRPV1 modulates CHIKV infection in macrophages, RAW 264.7 cells were infected with CHIKV in the presence of 5'-IRTX, RTX, or DMSO alone. The TRPV1 modulators were added to the cells 2 h prior to the infection and were maintained during infection until the cells were harvested at 8 hpi or 12 hpi. As expected, a cytopathic effect (CPE) was observed in CHIKV-infected macrophages (membrane blebbing, rounding off, and detachment) at both 8 hpi and 12 hpi (Fig. 2B) [35]. Quantitation of CPE revealed higher CPE in RTX-treated cells and significantly lower CPE in 5'-IRTX-treated cells when compared to the CHIKV + DMSO control (Fig. 2B). Additionally, FC analysis was carried out to estimate the infectivity of CHIKV in the presence of TRPV1 modulators by determining the percentage of positive cells. Upon treatment with 5'-IRTX, the percentage of cells that were positive for CHIKV antigens decreased significantly at 8 hpi (nsP2, 6.46 ± 0.72 ; E2, 8.32 ± 1.41) compared to the CHIKV + DMSO control (nsP2, 9.71 ± 0.86 ; E2, 16.45 ± 3.87) (Fig. 2C), whereas in the presence of RTX, the percentage of cells that were positive for the CHIKV nsP2 antigen increased, and no such significant increase in the CHIKV E2 antigen was observed at 8 hpi (nsP2, 14.04 ± 1.38 ; E2, 17.86 ± 2.05) (Fig. 2C). Similarly, Western blot analysis showed that expression

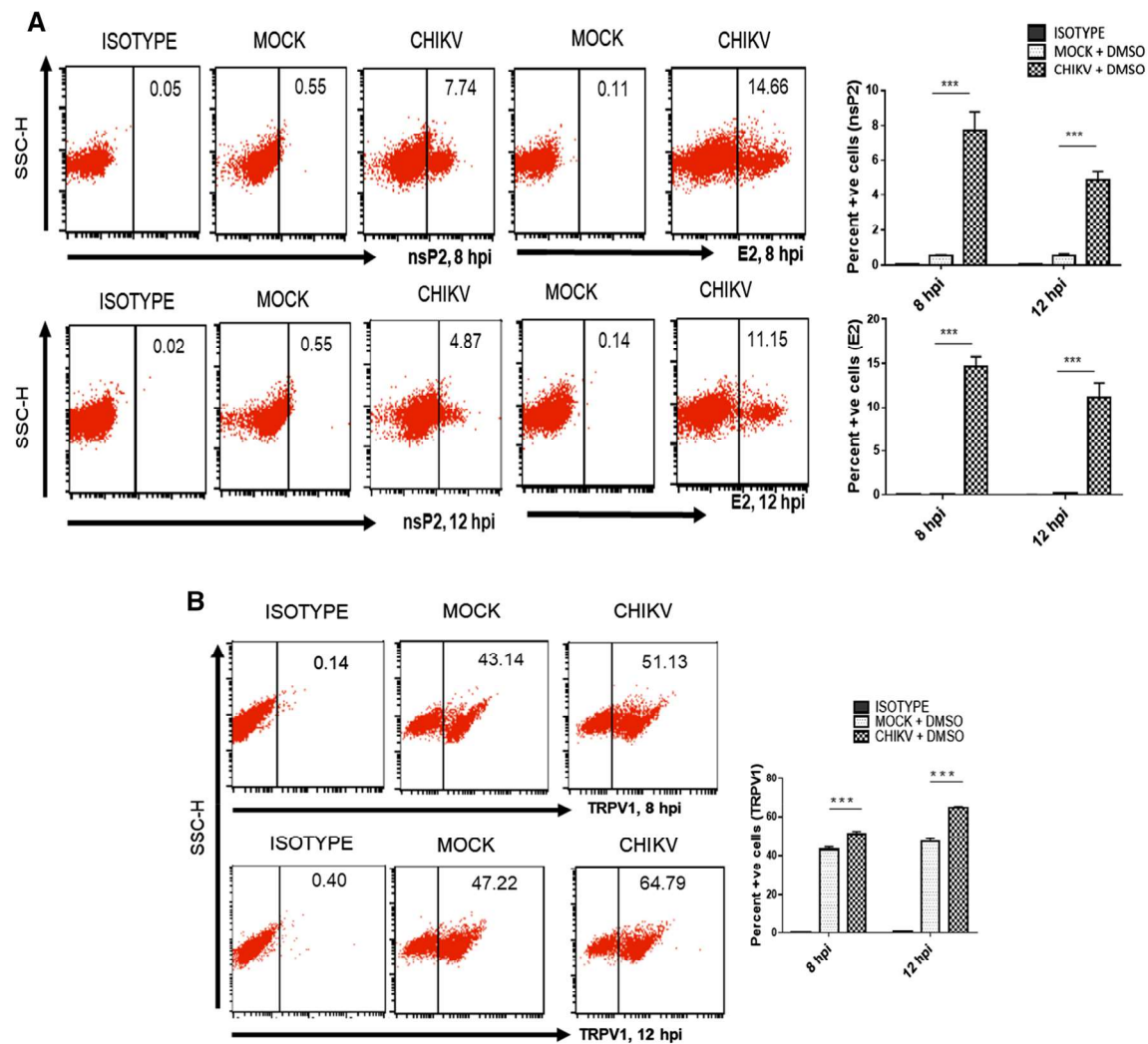


Fig. 1 CHIKV upregulates TRPV1 expression in macrophages. Macrophages (RAW 264.7 cells) were infected with CHIKV at an MOI of 5 and analyzed at 8 hpi and 12 hpi. (A) Flow cytometry (FC) dot-plot analysis with a representative bar diagram showing the percentage of cells positive for the viral proteins nsP2 and E2. (B) FC analysis and

representative bar diagram depicting TRPV1 expression in CHIKV-infected RAW 264.7 cells. Data represent the mean \pm SD of three independent experiments. Differences between groups with a p -value less than 0.05 were considered statistically significant (ns, non-significant; *, $p < 0.05$; **, $p < 0.01$; ***, $p < 0.001$).

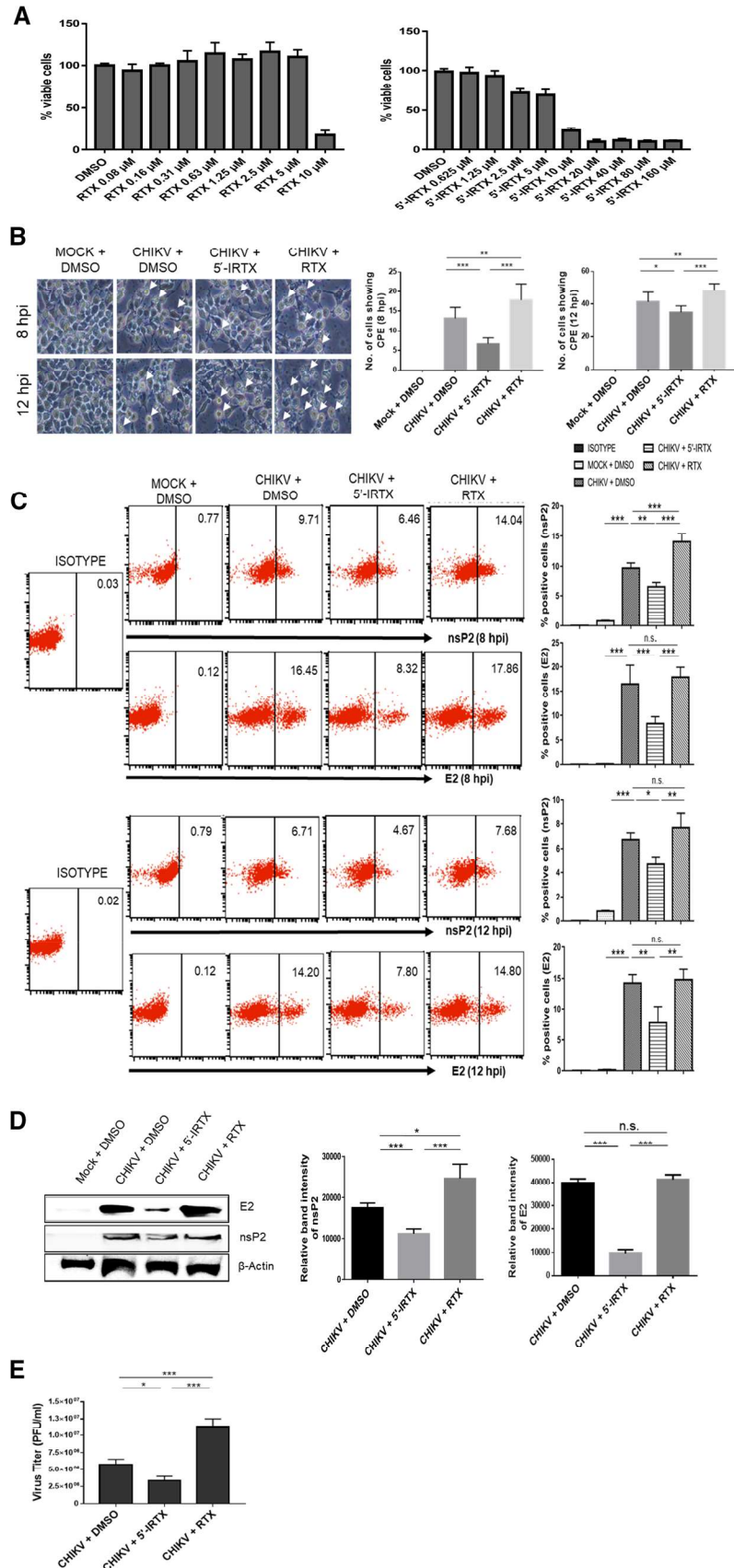
of E2 and nsP2 significantly decreased in 5'-IRTX-treated cells compared to the CHIKV + DMSO control. However, in RTX-treated cells, only nsP2 expression was found to increase significantly, which is in agreement with the FC data (Fig. 2D). Taken together, the results suggest that TRPV1 may regulate CHIKV infection in macrophages.

Subsequently, the expression of TRPV1 was assessed in the presence of TRPV1 modulators after CHIKV infection, and a significant change was observed only in the CHIKV + DMSO cells relative to the mock + DMSO cells (Supplementary Fig. 2). However, no significant change was observed between the CHIKV + DMSO control and CHIKV-infected macrophages treated with TRPV1 modulators (Supplementary Fig. 2A-C). Western blot analysis

also showed a similar trend (Supplementary Fig. 2C), as the modulators possibly affect mostly the function of TRPV1 [4, 57]. Similarly, no such changes in TRPV1 expression were observed in mock-treated cells (Supplementary Fig. 2D)

Finally, to assess the effect of TRPV1 modulators, a plaque assay was performed to quantify the release of infectious virus particles. Cell-free supernatants were collected from the above experiments, and it was found that upon treatment with 5'-IRTX, the viral titer decreased to $3.33 \times 10^6 \pm 6.66 \times 10^5$ (0.57-fold) compared to the CHIKV + DMSO control (Fig. 2E). On the other hand, upon treatment with RTX, the viral titer increased to $1.13 \times 10^7 \pm 1.15 \times 10^6$ (1.96 fold) compared to the CHIKV + DMSO control ($5.77 \times 10^6 \pm 7.69 \times 10^5$) (Fig. 2E).

Fig. 2 TRPV1 regulates CHIKV infection. RAW 264.7 cells were treated with either DMSO or with a TRPV1 modulator, 5'-IRTX or RTX. (A) Bar diagram showing the percentage of viable RAW 264.7 cells treated with different concentrations of RTX and 5'-IRTX with respect to the solvent control (DMSO), as determined by MTT assay. (B) Cells treated with TRPV1 modulators, 5'-IRTX or RTX. RAW 264.7 cells were infected with CHIKV at an MOI of 5 and observed under a bright-field microscope at a magnification of 200X for a possible cytopathic effect (CPE). Infected cells showed considerable CPE, indicated by white arrows, with membrane blebbing, rounding off, and detachment. The bar diagram represents the quantitative measurement of the cells showing CPE at 8 hpi (left panel) and 12 hpi (right panel). (C) Representative FC dot plot depicting the percentage of cells positive for the viral proteins nsP2 and E2 at 8 and 12 hpi with 5'-IRTX or RTX treatment. Bar diagram showing the percentage of cells positive for the viral proteins nsP2 and E2 for mock + DMSO, CHIKV + DMSO, CHIKV + 5'-IRTX, and CHIKV + RTX. (D) Western blot analysis showing the relative levels of the viral proteins E2 and nsP2. The bar diagram shows the relative band intensities of nsP2 and E2. (E) Bar diagram showing the viral titer (PFU/ml), determined by plaque assay from CHIKV-infected macrophages at 12 hpi with 5'-IRTX or RTX treatment. The data represent the mean \pm SD of three independent experiments. Differences between groups with a *p*-value less than 0.05 were considered statistically significant (ns, non-significant; *, *p* < 0.05; **, *p* < 0.01; ***, *p* < 0.001).



This result indicates that TRPV1 may regulate CHIKV infection.

TRPV1 modulates early stages of the CHIKV life cycle

To determine whether TRPV1 has a regulatory role in the CHIKV life cycle, the viral titers in the supernatants after viral adsorption (containing unbound virus) were measured in the presence of 5'-IRTX or RTX. Interestingly, it was observed that there was a significantly higher titer of virus particles, $3.02 \times 10^5 \pm 2.7 \times 10^4$ PFU/ml (32% more than DMSO only), in the left-over supernatant in the presence of the TRPV1 inhibitor 5'-IRTX when compared to the DMSO control ($2.28 \times 10^5 \pm 1.01 \times 10^4$). Conversely, there was a significantly lower titer of virus particles, $1.35 \times 10^5 \pm 1.5 \times 10^4$ PFU/ml (40.77% less than DMSO only) during CHIKV infection in the presence of the TRPV1 activator RTX in the left-over supernatant when compared to the DMSO control (Fig. 3A). These results suggest that the efficiency of viral adsorption and/or entry is decreased by treatment with 5'-IRTX and increased by treatment with RTX.

A time-of-addition experiment, as described in [Materials and methods](#), showed that the addition of TRPV1 modulators at different time points profoundly affected the viral copy number at 12 hpi (Fig. 3B). CHIKV infection in the presence of 5'-IRTX markedly reduced infection in the "pre-during-post" (i) (13.79%) and "pre-during" (ii) (47.29%) experiments compared to the corresponding CHIKV + DMSO controls. A non-significant change in infection was observed when the modulators were added at 0 hpi (iii) or 4 hpi (iv). Moreover, CHIKV infection was enhanced markedly in the presence of RTX in the "pre-during-post at 0 hpi" (i) (130%) and "pre-during" (ii) (110%) experiments as compared to the corresponding CHIKV + DMSO controls. No significant change in infection was observed when RTX was added at 0 hpi (iii) or 4 hpi (iv) (Fig. 3B). Together, these findings indicate that the functional modulation of TRPV1 might alter the susceptibility of macrophages to infection by regulating the early stages of the CHIKV life cycle.

TRPV1 modulates the CHIKV-induced cytokine response in host macrophages

CHIKV is known to induce pro-inflammatory cytokines in host macrophages [34, 35, 39, 54, 69]. Hence, cell culture supernatants were collected at both 8 hpi and 12 hpi to assess the effect of 5'-IRTX and RTX on the release of TNF and IL-6. Interestingly, in RTX-treated CHIKV-infected macrophages, the levels of both TNF and IL-6 were significantly higher than in the DMSO control. Surprisingly, in the presence of 5'-IRTX, the levels of both TNF and IL-6 increased despite the reduction in CHIKV infection (Fig. 4). However, TNF and IL-6 levels did not change significantly

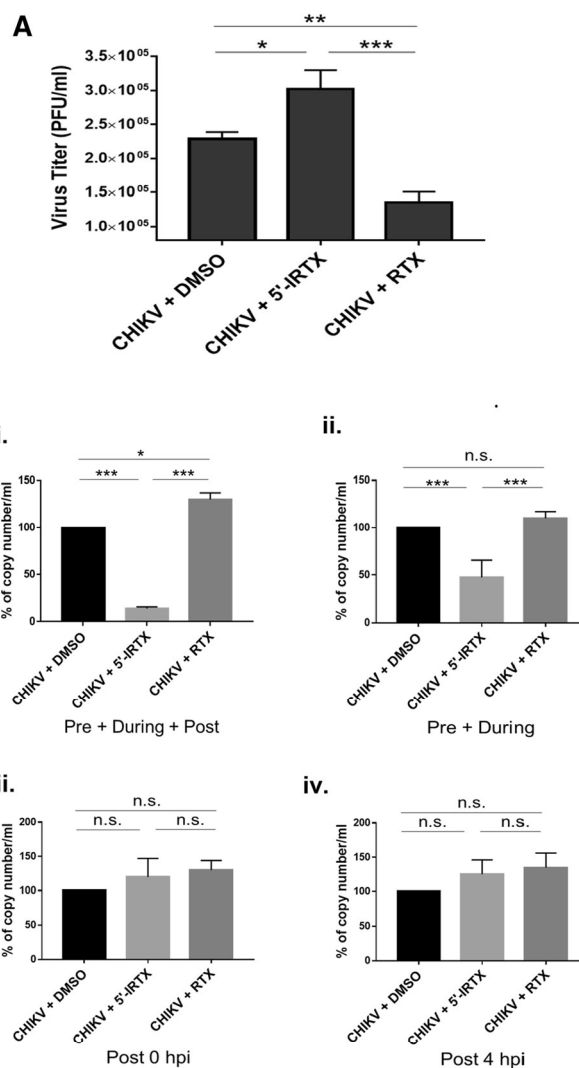


Fig. 3 TRPV1 modulates early stages of the CHIKV life cycle. RAW 264.7 cells were pre-treated with TRPV1-specific modulators (5'-IRTX/RTX) for 2 h prior to infection. After adsorption of CHIKV to RAW 264.7 cells, the remaining supernatant containing unbound virus was collected and a plaque assay was performed. (A) Bar diagram showing the virus titer (PFU/ml) remaining in the supernatant of 5'-IRTX or RTX treated CHIKV-infected macrophages. (B) CHIKV infection was carried out in RAW 264.7 cells by adding TRPV1 modulators (5'-IRTX and RTX) at the following stages of CHIKV infection: "pre + during + post at 0 hpi" (i), "pre + during" (ii), "post" at 0 hpi (iii) and "post" at 4 hpi (iv). qRT-PCR was performed using CHIKV E1 gene-specific primers, and data are expressed as a percentage of copy number/ml normalized to CHIKV + DMSO. Data represent the mean \pm SD of three independent experiments. Differences between groups with a *p*-value less than 0.05 were considered statistically significant (ns, non-significant; *, *p* < 0.05; **, *p* < 0.01; ***, *p* < 0.001).

in mock-infected cells treated with 5'-IRTX or RTX (Supplementary Fig. 3). This suggests that CHIKV-infected macrophages produce a robust pro-inflammatory cytokine response, which was found to be markedly elevated upon

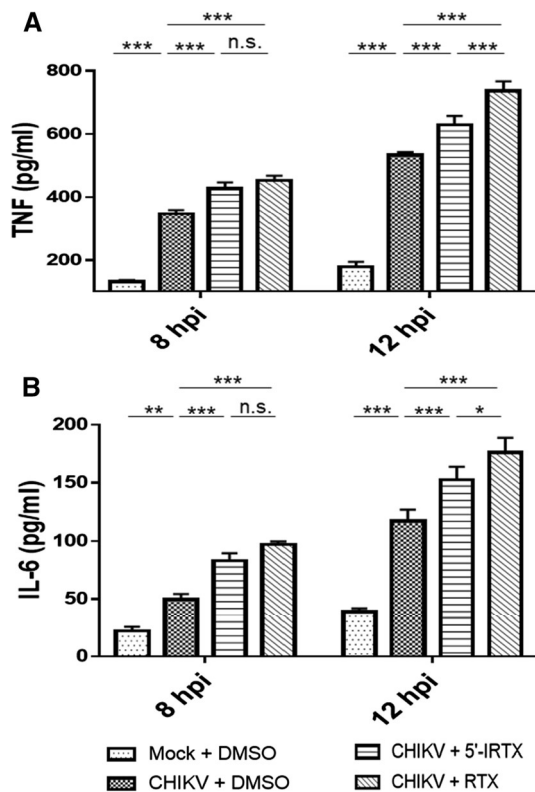


Fig. 4 TRPV1 modulates the CHIKV-induced cytokine response in host macrophages. RAW 264.7 cells were infected with CHIKV at an MOI of 5. The supernatant was collected at 8 and 12 hpi, and sandwich ELISA was performed to determine the level of cytokines. Bar diagram showing the amount of secreted (pg/ml) (A) TNF and (B) IL-6 in mock-treated and 5'-IRTX- or RTX-treated CHIKV-infected macrophages. Data represent the mean \pm SD of three independent experiments. Differences between groups with a p -value less than 0.05 were considered statistically significant (ns, non-significant; * $p < 0.05$; ** $p < 0.01$; *** $p < 0.001$).

RTX treatment, and unexpectedly, increased pro-inflammatory cytokine levels were also observed in 5'-IRTX-treated CHIKV-infected macrophages.

pNF- κ B (p65) expression and nuclear localization during CHIKV infection in macrophages treated with TRPV1 modulators

Nuclear factor kappa-light-chain-enhancer of activated B cells (NF- κ B) is a protein complex that controls diverse cellular functions as a potential transcription factor, regulating cell survival and cytokine and chemokine production. "Its phosphorylated form" (pNF- κ B) acts as a central mediator of inflammation that responds to a large variety of inflammatory diseases [21, 82, 83]. An immunofluorescence assay was performed to examine the expression and localization of pNF- κ B (p65). It was observed that, in CHIKV-infected macrophages, pNF- κ B (p65) expression and nuclear

localization increased at 8 hpi and 12 hpi as compared to the mock-infected control (Fig. 5A). The level of pNF- κ B (p65) was found to increase further in the presence of either of the TRPV1 modulators (Fig. 5A and B). For quantification, fluorescence intensity of pNF- κ B is presented in scatter plots (Fig. 5B). Interestingly, after CHIKV + 5'-IRTX treatment, the pNF- κ B levels increased compared to the CHIKV + DMSO control at both 8 and 12 hpi. Moreover, the pNF- κ B levels reached their highest peak after CHIKV + RTX treatment. The results of flow cytometry analysis and confocal microscopy showed a similar trend (Fig. 5C), showing that nuclear localization of pNF- κ B in CHIKV-infected macrophages is further elevated in RTX-treated CHIKV-infected macrophages. Unprecedentedly, the pNF- κ B levels were also increased in 5'-IRTX-treated CHIKV-infected macrophages.

TRPV1 modulates Ca^{2+} influx during CHIKV infection in macrophages

TRPV1 is a non-selective calcium (Ca^{2+})-permeable cation channel. Here, the functional contribution of TRPV1 to Ca^{2+} influx was assessed during CHIKV infection in macrophages. For this purpose, a live-cell Ca^{2+} imaging experiment was carried out using the Ca^{2+} -sensitive dye Fluo 4-AM [4]. Upon addition of the Ca^{2+} -solution only, no increase in Fluo-4 intensity was observed, indicating that there was no change in intracellular Ca^{2+} levels. Upon addition of 5'-IRTX, there was a reduction in Fluo-4 intensity. Interestingly, in the presence of CHIKV, there was a marked increase in Fluo-4 intensity, indicating robust Ca^{2+} influx. Next, the effect of CHIKV + 5'-IRTX was evaluated, and it was observed that there was a decrease in Fluo-4 intensity. With RTX, both in presence or absence of CHIKV, the Fluo-4 intensity increased (Fig. 6A and B). RTX is a specific and well-known inducer of calcium influx via TRPV1 channels [67, 85–87]. The area under the curve (AUC) was estimated from the baseline ($Y = 1$) for peaks both above and below the baseline (Fig. 6B). The AUC values for the following experimental conditions were determined: calcium solution (-99.28 a.u.), 5'-IRTX (-55.6 a.u.), RTX (+128.2 a.u.), CHIKV + DMSO (+94.03 a.u.), CHIKV + 5'-IRTX (-14.14 a.u.), and CHIKV + RTX (+179.4 a.u.). Together, these results suggest a functional role of TRPV1 in regulating intracellular Ca^{2+} influx during CHIKV infection in macrophages.

Discussion

Transient receptor potential vanilloid 1 (TRPV1) is a member of the TRP family of channels, which have recently been found to play a functional role in a number of immune cells, including macrophages, T cells, NK cells, and dendritic cells

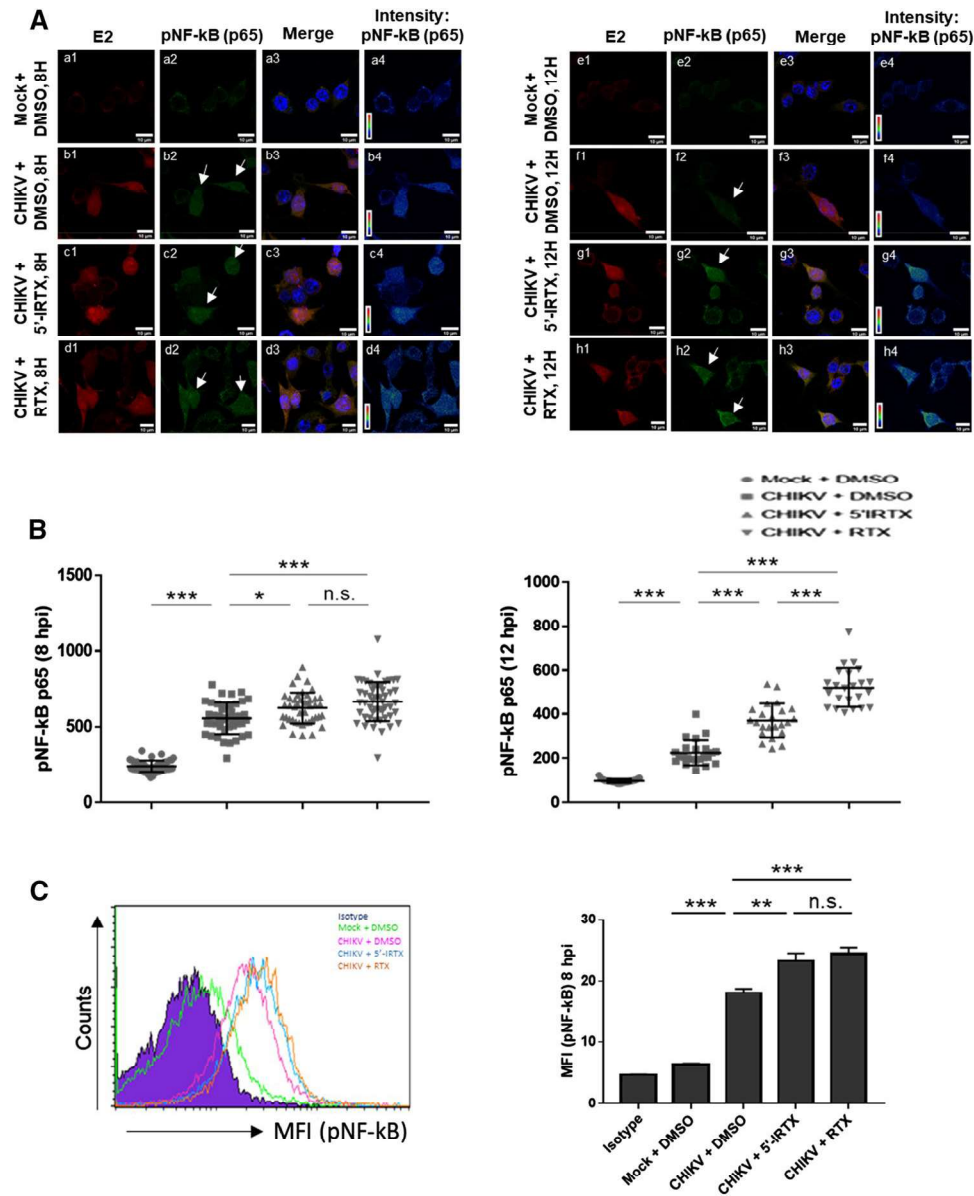


Fig. 5 pNF-κB (p65) expression and nuclear localization during CHIKV infection in macrophages treated with TRPV1 modulators. RAW 264.7 cells were infected with CHIKV at an MOI of 5, and nuclear localization of pNF-κB (p65) was examined by confocal microscopy at both 8 hpi (left panel) and 12 hpi (right panel). Mock-treated and 5'-IRTX- or RTX-treated CHIKV-infected macrophages were stained with a monoclonal antibody against CHIKV E2 (red) (a1, b1, c1, d1 and e1, f1, g1, h1). The immunofluorescence images show the nuclear localization of pNF-κB (p65) (green) (a2, b2, c2, d2 and e2, f2, g2, h2) in CHIKV-infected macrophages compared to mock-infected. Nuclei were stained with DAPI (a3, b3, c3, d3 and e3, f3, g3, h3). pNF-κB levels in rainbow scale (a4, b4, c4, d4 and e4, f4, g4, h4). Mock-infected cells were used as negative control. (B) Scatter plot depicting pNF-κB (p65) intensity at 8 hpi (left panel) and 12 hpi (right panel) in 5'-IRTX- or RTX-treated CHIKV-infected macrophages. (C) Representative FC histogram plot depicting MFI for transcription factor pNF-κB (p65) at 8 hpi with 5'-IRTX or RTX treatment. Bar diagram showing MFI for pNF-κB (p65) for mock + DMSO, CHIKV + DMSO, CHIKV + 5'-IRTX, and CHIKV + RTX. Data represent the mean \pm SD of three independent experiments. Differences between groups with a p -value less than 0.05 were considered statistically significant (ns, non-significant; * $p < 0.05$; ** $p < 0.01$; *** $p < 0.001$).

[4, 19, 40, 88, 89]. CHIKV has been known to infect and persist in macrophages serving as major reservoirs for the virus [32, 35, 39, 68]. The present study provides the first evidence that TRPV1 channels might regulate CHIKV infection in macrophages. This study also highlights an important

role of TRPV1 in the initial surge of Ca^{2+} influx, modulation of pro-inflammatory cytokine responses, altered NF-κB (p65) expression, and nuclear localization during CHIKV infection in macrophages.

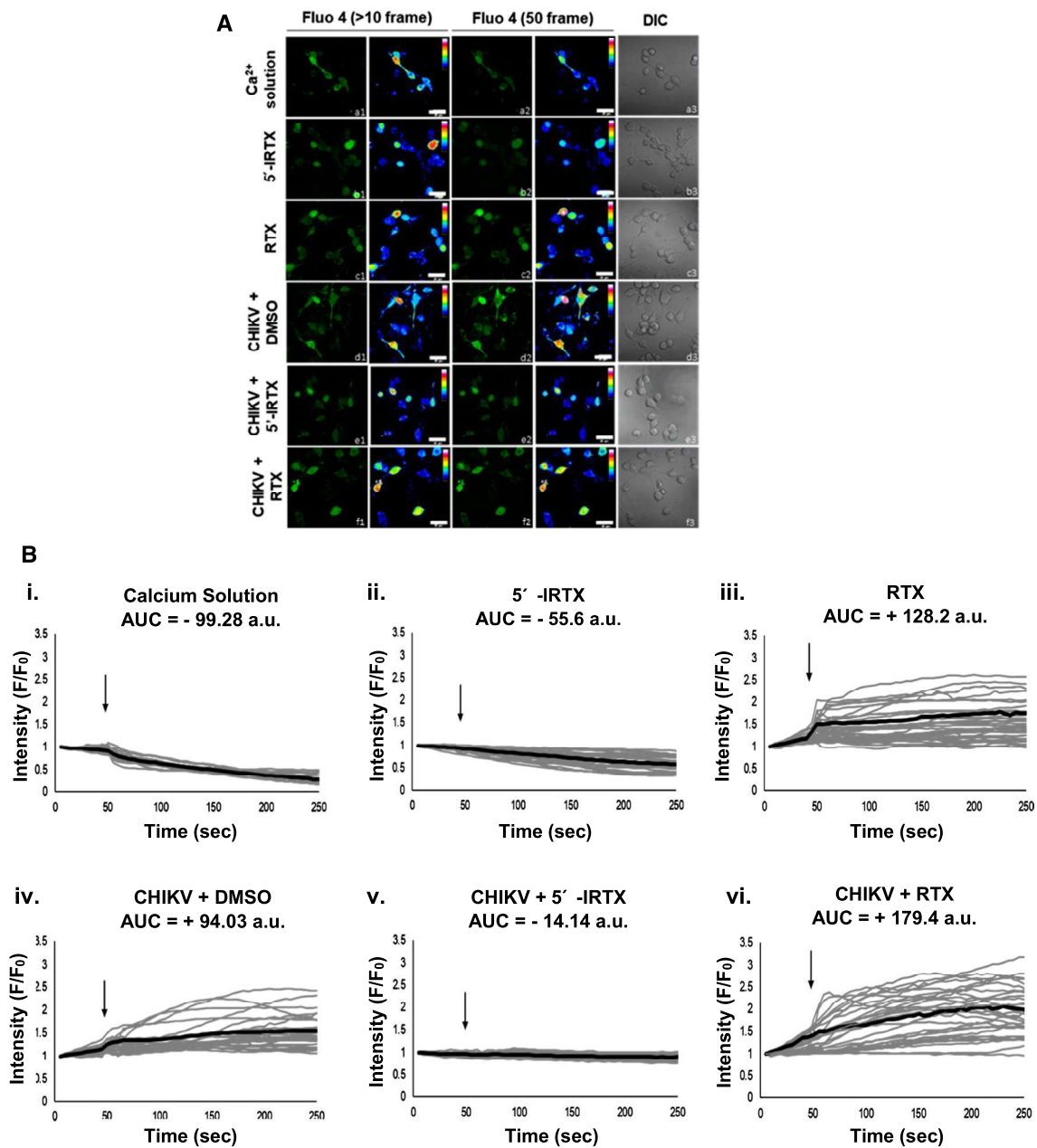


Fig. 6 TRPV1 modulates Ca²⁺ influx during CHIKV infection in macrophages. (A) RAW 264.7 cells were treated with the calcium-sensitive dye Fluo-4 AM. Fluo-4 (>10 frame) refers to the fluorescence before addition of reagent at the 10th frame, and fluo-4 (50 frame) refers to the fluorescence level at the 50th frame. The treatment conditions from top to bottom are mock + Ca²⁺ solution (a1, a2, a3), TRPV1 inhibitor (5'-IRTX) only (b1, b2, b3), TRPV1 activator (RTX) only (c1, c2, c3), CHIKV + DMSO (d1, d2, d3), CHIKV + 5'-IRTX (e1, e2, e3), and CHIKV + RTX (f1, f2, f3). The fluo-

rescence intensities are represented in pseudo 16 colour (Black and white represent the lowest and highest intracellular Ca²⁺ levels, respectively). (B) Time-lapse kinetics of intracellular calcium influx. The intensity (F/F₀) of each cell is represented in grey lines along with average in black lines for each experimental setup. The black arrows indicate the time of addition of (i) Ca²⁺ solution, (ii) 5'-IRTX, (iii) RTX, (iv) CHIKV, (v) CHIKV + 5'-IRTX, and (vi) CHIKV + RTX. The data are representative of three independent experiments.

Several viruses have been shown to upregulate TRPV1 expression in host cells, including respiratory syncytial virus, measles virus, human rhinovirus, and varicella-zoster virus [26, 27, 29]. In the current study, it was demonstrated for the first time that the alphavirus CHIKV also

has a similar effect. CHIKV-infected macrophages showed increased levels of TRPV1 expression at both 8 and 12 hpi. Upon treatment with 5'-IRTX or RTX, which are functional modulators of TRPV1, CHIKV infection in macrophages was found to be significantly decreased or increased,

respectively. However, the level of TRPV1 expression did not change in CHIKV-infected macrophages treated with TRPV1 modulators, as these are functional modulators, which modulate the functional activity of TRPV1 rather than affecting TRPV1 expression [4, 57]. As expected, when cells were treated with 5'-IRTX, the viral titer decreased, whereas upon RTX treatment, the viral titer increased considerably. Our study highlights a possible regulatory role of TRPV1 during CHIKV infection in macrophages. However, further investigation is needed to understand the mechanistic relationships between TRPV1, CHIKV infection, and host cell immunity.

TRPV1 has been found to play a pro-inflammatory and nociceptive role in various diseases and injury states, e.g., diabetic neuropathy, cancer, arthritis, airway hypersensitivity, fecal incontinence, non-erosive reflux disease (NERD), gastro-oesophageal reflux disease (GERD), and urinary bladder infection [16, 18, 23, 90–92]. Accordingly, it appears that TRPV1 might work as a pathological marker for various altered physiological processes. However, recent reports have also suggested a differential role of TRPV1. For example, i.e., ablation of TRPV1 expression has been found to enhance the pro-inflammatory response. In particular, abrogation of TRPV1 results in an increased pro-inflammatory response in the cardiovascular system and in cases of endotoxin and sepsis, dermatitis, malaria, salt hypertension, airway hypersensitivity, and renal inflammation [41, 42, 47, 50, 51, 84, 93–95]. In accordance with those observations, in the current study, we also observed a rise in the pro-inflammatory response despite downregulation of CHIKV infection in the presence of the TRPV1 inhibitor 5'-IRTX. To understand these apparent discrepancies, the expression and nuclear localization of NF- κ B (p65) were investigated. NF- κ B, especially p65, is the best-studied subunit and plays an important role during cellular activation and subsequent transcription of pro-inflammatory cytokines [96–98]. pNF- κ B (p65) is known to be translocated from cytoplasm to the nucleus during cellular activation [83, 99]. Immunofluorescence assays showed that nuclear translocation of pNF- κ B (p65) was induced in CHIKV-infected macrophages compared to uninfected cells, and this was further elevated in the presence of TRPV1 modulators. Both 5'-IRTX- and RTX-treated CHIKV-infected macrophages showed enhanced nuclear localization of NF- κ B compared to the CHIKV + DMSO control. The observation that inhibition of TRPV1 leads to higher pNF- κ B expression has been reported previously [47, 84]. This in general may suggest that both constitutive activation and constitutive inhibition of TRPV1 might affect the status of the cell and induce nuclear translocation of NF- κ B. These observations might explain the apparently paradoxical increase in pro-inflammatory cytokines found in TRPV1-inhibited CHIKV-infected macrophages as well,

where the functional deficiency of TRPV1 might also lead to inflammatory responses, as reported earlier [41, 42, 93].

Recent reports have suggested that TRP channels contribute to a number of host–virus interactions. There is ample evidence that numerous TRP channels, such as TRPV1, TRPV4, TRPA1, TRPM8, TRPML1 TRPML2, and TRPML3, contribute to various phases of the viral life cycle, including binding and entry, replication, and egress [26, 29, 100, 101]. TRPV1 in particular has been associated with various stages of the viral life cycle, including binding, entry, and replication, in the case of a number of different viruses, including respiratory syncytial virus (RSV), measles virus (MV), human rhinovirus (HRV), hepatitis C virus (HCV), herpes simplex virus (HSV) and varicella-zoster virus (HZV) [25–30]. However, no such role of TRPV1 in CHIKV infection in macrophages had been described. In order to determine whether TRPV1 affects the early stages of the viral life cycle, we measured the viral titer remaining in the supernatant after infection. A high level of inhibition in the early stages of the viral life cycle was observed in CHIKV + 5'-IRTX-treated cells, whereas a marked increase in the early stages of viral life cycle was found in CHIKV + RTX-treated cells. Similarly, in a time-of-addition assay, the TRPV1 modulators were most effective in the "pre-during-post" setup, followed by the "pre-during" setup, further confirming that TRPV1 modulators might regulate the early stages of viral infection. Taken together, the data suggest that CHIKV infection in macrophages may be regulated by the functional activity of TRPV1, affecting the early stages of the viral life cycle.

Viruses are adept at tailoring the calcium concentration in host cells to meet their own requirements for viral adsorption, infection, spread, and persistence. It is well established that virus adsorption onto host cells is immediately accompanied by calcium influx at the plasma membrane [102–106]. As TRP channels are Ca²⁺-permeable channels, we further explored the possibility of differential calcium influx during CHIKV infection with TRPV1 modulators. In this study, it was found that CHIKV infection led to an increase in intracellular Ca²⁺ levels. Moreover, CHIKV + RTX increased the intracellular Ca²⁺ levels further. Concurrently, in the case of CHIKV + 5'-IRTX, the Ca²⁺ influx decreased, suggesting that the TRPV1 channel might play a crucial role in Ca²⁺ influx during viral infection.

In summary, the present study provides evidence that TRPV1 channel expression is induced during CHIKV infection of macrophages. Our current understanding of the relationship between TRPV1 and CHIKV infection in macrophages is schematically summarized in the working model shown in Figure 7. TRPV1 may effectively regulate CHIKV infection in host macrophages, primarily affecting the early stages of the viral life cycle, which might have

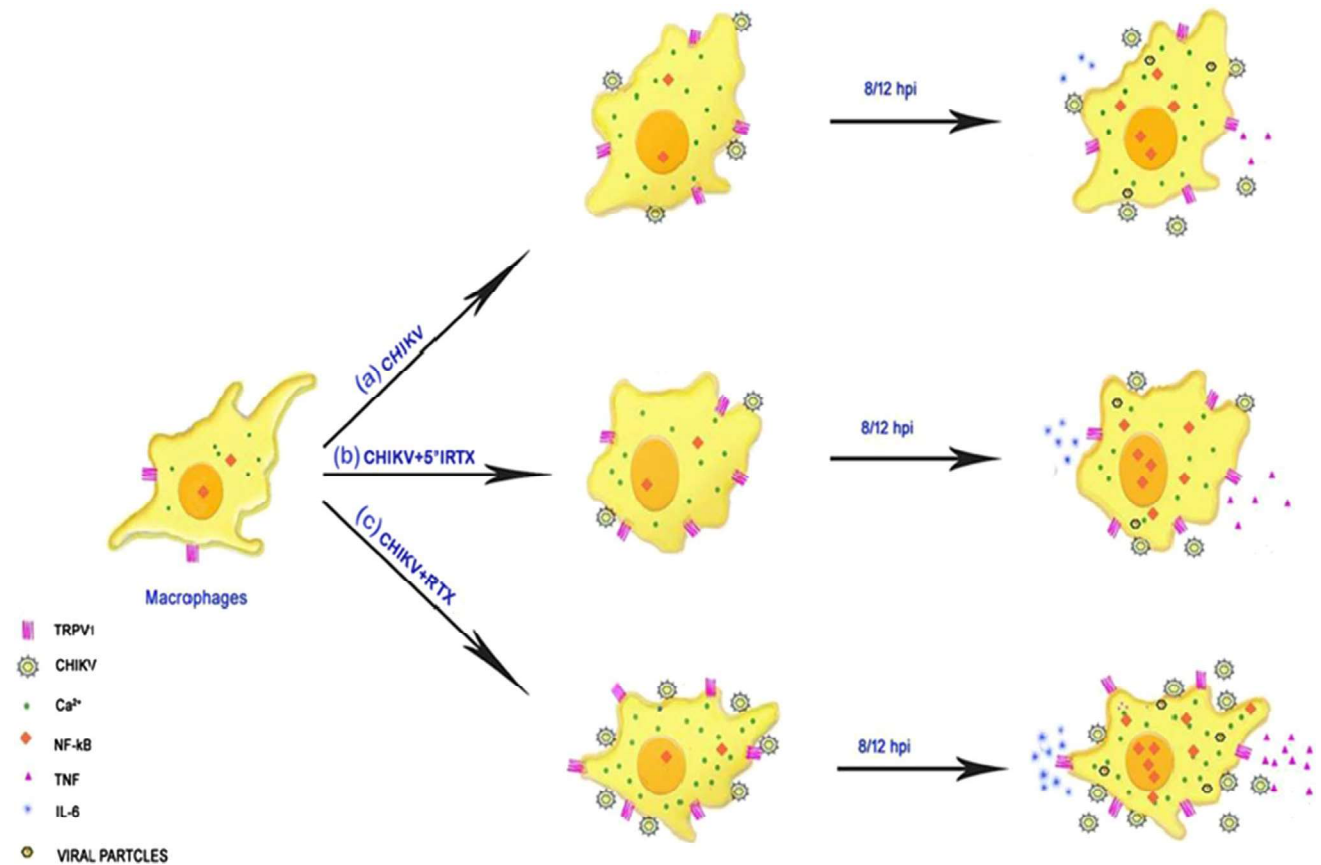


Fig. 7 Proposed working model depicting the functional role of TRPV1 in CHIKV-infected macrophages. (A) Upon CHIKV infection, TRPV1 channels get activated, facilitating Ca^{2+} influx in macrophages and entry of host cells. (B) Upon treatment with the TRPV1 inhibitor 5-IRTX, the TRPV1 channel gets inactivated and, subsequently, less Ca^{2+} enters the cell, leading to a lower rate of virus

entry into host cells. Intriguingly, secretion of the pro-inflammatory cytokines TNF and IL-6 increased compared to CHIKV-infected cells without inhibitor. (C) Upon treatment with the TRPV1 activator RTX, the TRPV1 channel gets activated, which induces Ca^{2+} influx and increases virus entry into host macrophages, resulting in a higher pro-inflammatory cytokine response.

implications for the future design of anti-CHIKV strategies. These findings might also have broader implications for understanding the role of TRP channels in the case of other viruses as well.

Acknowledgements We are thankful to Dr. Manmohan Parida, DRDE, Gwalior, India, for kindly providing the virus strain (DRDE-06), Vero cell line, and E2 antibody. We are also thankful to the flow cytometry facility and the confocal facility of NISER and ILS for their support.

Author contributions Conceptualization: P Sanjai Kumar, Soma Chattopadhyay, Subhasis Chattopadhyay; Methodology: P Sanjai Kumar, Tapas K. Nayak, Chandan Mahish, Subhransu S. Sahoo, Anukrishna R, Saikat De, Ankita Datey, Ram P. Sahu, Chandan Goswami, Soma Chattopadhyay, Subhasis Chattopadhyay; Formal analysis and investigation: P Sanjai Kumar, Soma Chattopadhyay, Subhasis Chattopadhyay; Writing - original draft preparation: P Sanjai Kumar, Soma Chattopadhyay, Subhasis Chattopadhyay; Writing - review and editing: P Sanjai Kumar, Tapas K. Nayak, Chandan Mahish, Subhransu S. Sahoo, Anukrishna R, Saikat De, Ankita Datey, Ram P. Sahu, Chandan Goswami, Soma Chattopadhyay, Subhasis Chattopadhyay; Funding acquisition: Soma Chattopadhyay, Subhasis Chattopadhyay; Resources: Soma Chattopadhyay,

Subhasis Chattopadhyay; Supervision: Soma Chattopadhyay, Subhasis Chattopadhyay

Funding This study was partly funded by CSIR, India grant no. 37 (1542)/12/EMR-II, 37(1675)/16/EMR-II, DST FIST grant no. SR/FST/LSI-652/2015 and DST-SERB, India grant no. EMR/2016/000854. It was supported by Institute of Life Sciences, Bhubaneswar, under the Department of Biotechnology and National Institute of Science Education and Research, HBNI, Bhubaneswar, under the Department of Atomic Energy, Government of India.

Compliance with ethical standards

Conflict of interest The authors declare that they have no conflict of interest. The funding sponsors had no role in the design of the study; in the collection, analysis, or interpretation of data; in the writing of the manuscript; or in the decision to publish the results.

References

- Tominaga M, Tominaga T (2005) Structure and function of TRPV1. *Pflugers Arch* 451:143–150. <https://doi.org/10.1007/s00424-005-1457-8>
- Ortiz-Rentería M, Juárez-Contreras R, González-Ramírez R et al (2018) TRPV1 channels and the progesterone receptor Sig-1R interact to regulate pain. *Proc Natl Acad Sci*. <https://doi.org/10.1073/pnas.1715972115>
- Choi JY, Lee HY, Hur J et al (2018) TRPV1 blocking alleviates airway inflammation and remodeling in a chronic asthma murine model. *Allergy Asthma Immunol Res* 10:216–224. <https://doi.org/10.4168/aair.2018.10.3.216>
- Majhi RK, Sahoo SS, Yadav M et al (2015) Functional expression of TRPV channels in T cells and their implications in immune regulation. *FEBS J* 282:2661–2681. <https://doi.org/10.1111/febs.13306>
- Yang F, Ma L, Cao X et al (2014) Divalent cations activate TRPV1 through promoting conformational change of the extracellular region. *J General Physiol* 143:91–103. <https://doi.org/10.1085/jgp.201311024>
- Ramirez G, Coletto L, Sciorati C et al (2018) Ion channels and transporters in inflammation: special focus on TRP channels and TRPC6. *Cells* 7:70. <https://doi.org/10.3390/cells7070070>
- Ramsey IS, Delling M, Clapham DE (2006) An introduction to TRP channels. *Annu Rev Physiol* 68:619–647. <https://doi.org/10.1146/annurev.physiol.68.040204.100431>
- Gees M, Colsoul B, Nilius B (2010) The role of transient receptor potential cation channels in Ca²⁺ signaling. *Cold Spring Harbor Perspect Biol* 2:a003962–a003962. <https://doi.org/10.1101/cshperspect.a003962>
- Vay L, Gu C, McNaughton PA (2012) The thermo-TRP ion channel family: Properties and therapeutic implications. *Br J Pharmacol* 165:787–801. <https://doi.org/10.1111/j.1476-5381.2011.01601.x>
- Venkatachalam K, Montell C (2007) TRP channels. *Ann Rev Biochem* 76:387–417. <https://doi.org/10.1146/annurev.biochem.75.103004.142819>
- Smami T, Shapovalov G, Skryma R et al (2015) Functional and physiopathological implications of TRP channels. *Biochimica et Biophysica Acta - Molecular Cell Research* 1853:1772–1782. <https://doi.org/10.1016/j.bbamer.2015.04.016>
- Pla AF, Gkika D (2013) Emerging role of TRP channels in cell migration: From tumor vascularization to metastasis. *Front Physiol*. <https://doi.org/10.3389/fphys.2013.00311>
- Sukumaran P, Schaar A, Sun Y, Singh BB (2016) Functional role of TRP channels in modulating ER stress and Autophagy. *Cell Calcium* 60:123–132. <https://doi.org/10.1016/j.ceca.2016.02.012>
- Lishko PV, Procko E, Jin X et al (2007) The Ankyrin repeats of TRPV1 bind multiple ligands and modulate channel sensitivity. *Neuron* 54:905–918. <https://doi.org/10.1016/j.neuron.2007.05.027>
- Devesa I, Planells-Cases R, Fernández-Ballester G et al (2011) Role of the transient receptor potential vanilloid 1 in inflammation and sepsis. *J Inflamm Res* 4:67–81. <https://doi.org/10.2147/JIR.S12978>
- Tsuji F, Aono H (2012) Role of transient receptor potential vanilloid 1 in inflammation and autoimmune diseases. *Pharmaceuticals* 5:837–852. <https://doi.org/10.3390/ph5080837>
- Fernandes ES, Fernandes MA, Keeble JE (2012) The functions of TRPA1 and TRPV1: moving away from sensory nerves. *Br J Pharmacol* 166:510–521. <https://doi.org/10.1111/j.1476-5381.2012.01851.x>
- Facer P, Casula MA, Smith GD et al (2007) Differential expression of the capsaicin receptor TRPV1 and related novel receptors TRPV3, TRPV4 and TRPM8 in normal human tissues and changes in traumatic and diabetic neuropathy. *BMC Neurol* 7:1–12. <https://doi.org/10.1186/1471-2377-7-11>
- Omari SA, Adams MJ, Geraghty DP (2017) TRPV1 channels in immune cells and hematological malignancies, 1st edn. Elsevier Inc.
- Marrone MC, Morabito A, Giustizieri M et al (2017) TRPV1 channels are critical brain inflammation detectors and neuropathic pain biomarkers in mice. *Nat Commun*. <https://doi.org/10.1038/ncomms15292>
- Yoshida A, Furube E, Mannari T et al (2016) TRPV1 is crucial for proinflammatory STAT3 signaling and thermoregulation-associated pathways in the brain during inflammation. *Sci Rep* 6:1–11. <https://doi.org/10.1038/srep26088>
- Felix A, Rosa E a Gestão Documental Como Suporte Ao Governo Eletrônico : Caso Da Secretaria De Estado Da Saúde De Santa Catarina (Ses / Sc). 36–50
- Silva RO, Bingana RD, Sales TMAL et al (2018) Role of TRPV1 receptor in inflammation and impairment of esophageal mucosal integrity in a murine model of nonerosive reflux disease. *Neurogastroenterol Motil* 30:1–8. <https://doi.org/10.1111/nmo.13340>
- Toledo-Mauriño JJ, Furuzawa-Carballeda J, Villeda-Ramírez MA et al (2018) The transient receptor potential vanilloid 1 is associated with active inflammation in ulcerative colitis. *Mediators Inflamm* 2018:1–7. <https://doi.org/10.1155/2018/6570371>
- Kitagawa Y, Tamai I, Hamada Y et al (2013) Orally administered selective TRPV1 antagonist, JTS-653, attenuates chronic pain refractory to non-steroidal anti-inflammatory drugs in rats and mice including post-herpetic pain. *J Pharmacol Sci* 122:128–137. <https://doi.org/10.1254/jphs.12276FP>
- Abdullah H, Heaney LG, Cosby SL, McGarvey LPA (2014) Rhinovirus upregulates transient receptor potential channels in a human neuronal cell line: implications for respiratory virus-induced cough reflex sensitivity. *Thorax* 69:46–54. <https://doi.org/10.1136/thoraxjnl-2013-203894>
- Han SB, Kim H, Hyun Cho S et al (2016) Transient receptor potential vanilloid-1 in epidermal keratinocytes may contribute to acute pain in herpes zoster. *Acta Dermato-Venereologica* 96:319–322. <https://doi.org/10.2340/00015555-2247>
- Cabrera JR, Viejo-Borbolla A, Alcamí A, Wandosell F (2016) Secreted herpes simplex virus-2 glycoprotein G alters thermal pain sensitivity by modifying NGF effects on TRPV1. *J Neuroinflamm* 13:1–9. <https://doi.org/10.1186/s12974-016-0677-5>
- Omar S, Clarke R, Abdullah H et al (2017) Respiratory virus infection up-regulates TRPV1, TRPA1 and ASIC3 receptors on airway cells. *PLoS ONE* 12:1–21. <https://doi.org/10.1371/journal.pone.0171681>
- Harford TJ, Rezace F, Scheraga RG et al (2018) Asthma predisposition and respiratory syncytial virus infection modulate transient receptor potential vanilloid 1 function in children's airways. *J Allergy Clin Immunol* 141:414–416. <https://doi.org/10.1016/j.jaci.2017.07.015> (e4)
- Alhmda Y, Selimovic D, Murad F et al (2017) Hepatitis C virus-associated pruritus: etiopathogenesis and therapeutic strategies. *World J Gastroenterol* 23:743–750. <https://doi.org/10.3748/wjg.v23.i5.743>
- Dupuis-Maguiraga L, Noret M, Brun S et al (2012) Chikungunya disease: Infection-associated markers from the acute to the chronic phase of arbovirus-induced arthralgia. *PLoS Neglected Trop Dis*. <https://doi.org/10.1371/journal.pntd.0001446>
- Silva LA, Dermody TS (2017) Chikungunya virus: epidemiology, replication, disease mechanisms, and prospective intervention strategies. *J Clin Investig* 127:737–749

34. Tanabe ISB, Tanabe ELL, Santos EC, Martins WV (2018) Cellular and molecular immune response to Chikungunya virus infection. *Front Cell Infect Microbiol* 8:1–15. <https://doi.org/10.3389/fcimb.2018.00345>
35. Nayak TK, Mamidi P, Kumar A et al (2017) Regulation of viral replication, apoptosis and pro-inflammatory responses by 17-aag during chikungunya virus infection in macrophages. *Viruses*. <https://doi.org/10.3390/v9010003>
36. Subudhi BB, Chattopadhyay S, Mishra P, Kumar A (2018) Current strategies for inhibition of Chikungunya infection. *Viruses* 10
37. Franken L, Schiwon M, Kurts C (2016) Microreview Macrophages: sentinels and regulators of the immune system. *Cell Microbiol* 18:475–487. <https://doi.org/10.1111/cmi.12580>
38. Pratheek BM, Suryawanshi AR, Chattopadhyay S, Chattopadhyay S (2015) In silico analysis of MHC-I restricted epitopes of Chikungunya virus proteins: Implication in understanding anti-CHIKV CD8+ T cell response and advancement of epitope based immunotherapy for CHIKV infection. *Infect Genetics Evolut*. <https://doi.org/10.1016/j.meegid.2015.01.017>
39. Nayak TK, Mamidi P, Sahoo SS et al (2019) P38 and JNK mitogen-activated protein kinases interact with Chikungunya virus non-structural protein-2 and regulate TNF induction during viral infection in macrophages. *Front Immunol* 10:1–15. <https://doi.org/10.3389/fimmu.2019.00786>
40. Bertin S, Aoki-Nonaka Y, De Jong PR et al (2014) The ion channel TRPV1 regulates the activation and proinflammatory properties of CD4+T cells. *Nat Immunol* 15:1055–1063. <https://doi.org/10.1038/ni.3009>
41. Khalil M, Alliger K, Weidinger C et al (2018) Functional role of transient receptor potential channels in immune cells and epithelia. *Front Immunol* 9:1–7
42. Fernandes ES, Liang L, Smilie S-J et al (2012) TRPV1 deletion enhances local inflammation and accelerates the onset of systemic inflammatory response syndrome. *J Immunol* 188:5741–5751. <https://doi.org/10.4049/jimmunol.1102147>
43. Clark N, Keeble J, Fernandes ES et al (2007) The transient receptor potential vanilloid 1 (TRPV1) receptor protects against the onset of sepsis after endotoxin. *FASEB J* 21:3747–3755. <https://doi.org/10.1096/fj.06-7460com>
44. Han SS, Keum YS, Chun KS, Surh YJ (2002) Suppression of phorbol ester-induced NF- κ B activation by capsaicin in cultured human promyelocytic leukemia cells. *Arch Pharmacol Res* 25:475–479. <https://doi.org/10.1007/BF02976605>
45. Miyake T, Shirakawa H, Nakagawa T, Kaneko S (2015) Activation of mitochondrial transient receptor potential vanilloid 1 channel contributes to microglial migration. *GLIA* 63:1870–1882. <https://doi.org/10.1002/glia.22854>
46. Sappington RM, Calkins DJ (2008) Contribution of TRPV1 to microglia-derived IL-6 and NF κ B translocation with elevated hydrostatic pressure. *Invest Ophthalmol Vis Sci* 49:3004–3017. <https://doi.org/10.1167/iovs.07-1355>
47. Wang Y, Wang DH (2009) Aggravated renal inflammatory responses in TRPV1 gene knockout mice subjected to DOCA-salt hypertension. *Am J Physiol-Renal Physiol* 297:F1550–F1559. <https://doi.org/10.1152/ajprenal.00012.2009>
48. Tsuji F, Murai M, Oki K et al (2010) Effects of SA13353, a transient receptor potential vanilloid 1 agonist, on leukocyte infiltration in lipopolysaccharide-induced acute lung injury and ovalbumin-induced allergic airway inflammation. *J Pharmacol Sci* 112:487–490. <https://doi.org/10.1254/jphs.092955C>
49. Hsieh WS, Kung CC, Huang SL et al (2017) TDAG8, TRPV1, and ASIC3 involved in establishing hyperalgesic priming in experimental rheumatoid arthritis. *Sci Rep* 7:1–14. <https://doi.org/10.1038/s41598-017-09200-6>
50. Fernandes ES, Brito CXL, Teixeira SA et al (2014) TRPV1 antagonism by Capsazepine modulates innate immune response in mice infected with plasmodium berghei ANKA. *Mediators Inflamm*. <https://doi.org/10.1155/2014/506450>
51. Helyes Z, Elekes K, Nemeth J et al (2007) Role of transient receptor potential vanilloid 1 receptors in endotoxin-induced airway inflammation in the mouse. *Am J Physiol Lung Cell Mol Physiol* 292:L1173–L1181. <https://doi.org/10.1152/ajplung.00406.2006>
52. White JPM, Urban L, Nagy I (2011) TRPV1 function in health and disease. 130–144
53. Gouin O, L'Héroudelle K, Lebonvallet N et al (2017) TRPV1 and TRPA1 in cutaneous neurogenic and chronic inflammation: pro-inflammatory response induced by their activation and their sensitization. *Protein Cell* 8:644–661. <https://doi.org/10.1007/s13238-017-0395-5>
54. Fox JM, Diamond MS (2016) Immune-mediated protection and pathogenesis of Chikungunya virus. *J Immunol*. <https://doi.org/10.4049/jimmunol.1601426>
55. Kulkarni SP, Ganu M, Jayawant P et al (2017) Regulatory T cells and IL-10 as modulators of chikungunya disease outcome: a preliminary study. *Eur J Clin Microbiol Infect Dis* 36:2475–2481. <https://doi.org/10.1007/s10096-017-3087-4>
56. Chattopadhyay SS, Kumar A, Mamidi P et al (2014) Development and characterization of monoclonal antibody against non-structural protein-2 of chikungunya virus and its applications. *J Virol Methods* 199:86–94. <https://doi.org/10.1016/j.jviro.2014.01.008>
57. Elokely K, Velisetty P, Delemotte L et al (2016) Understanding TRPV1 activation by ligands: insights from the binding modes of capsaicin and resiniferatoxin. *Proc Natl Acad Sci* 113:E137–E145. <https://doi.org/10.1073/pnas.1517288113>
58. Kumar A, Mamidi P, Das I et al (2014) A Novel 2006 Indian outbreak strain of chikungunya virus exhibits different pattern of infection as compared to prototype strain. *PLoS ONE*. <https://doi.org/10.1371/journal.pone.0085714>
59. Saswat T, Kumar A, Kumar S et al (2015) High rates of co-infection of dengue and chikungunya virus in Odisha and Maharashtra, India during 2013. *Infect Genetics Evol* 35:134–141. <https://doi.org/10.1016/j.meegid.2015.08.006>
60. Raghavendhar S, Patel AK, Kabra SK et al (2019) Virus load and clinical features during the acute phase of Chikungunya infection in children. *PLoS ONE* 14:1–10. <https://doi.org/10.1371/journal.pone.0211036>
61. Bartholomeusz A, Locarnini S (2006) Associated with antiviral therapy. *Antiviral Therapy* 55:52–55. <https://doi.org/10.1002/jmv>
62. C A-U, Chen M, Hotta H (2018) Time-of-addition and temperature-shift assays to determine particular step(s) in the viral life cycle that is blocked by antiviral substances(s). *Bio-protocol* 8:1–12. <https://doi.org/10.21769/BioProtoc.2830>
63. Sahoo SS, Majhi RK, Tiwari A et al (2019) Transient Receptor Potential Ankyrin1 channel is endogenously expressed in T cells and is involved in immune functions. *Biosci Rep*. <https://doi.org/10.1042/bsr20191437>
64. Lapointe TK, Basso L, Iftinca MC et al (2015) TRPV1 sensitization mediates postinflammatory visceral pain following acute colitis. *Am J Physiol* 309:G87–G99. <https://doi.org/10.1152/ajpgi.00421.2014>
65. Lawton SK, Xu F, Tran A et al (2017) N-Arachidonoyl dopamine modulates acute systemic inflammation via nonhematopoietic TRPV1. *J Immunol (Baltimore, Md: 1950)* 199:1465–1475. <https://doi.org/10.4049/jimmunol.1602151>
66. Bassi MS, Gentile A, Iezzi E et al (2019) Transient receptor potential vanilloid 1 modulates central inflammation in multiple sclerosis. *Front Neurol* 10:1–8. <https://doi.org/10.3389/fneur.2019.00030>

67. Westlund KN, Kochukov MY, Lu Y, McNearney TA (2010) Impact of central and peripheral TRPV1 and ROS levels on proinflammatory mediators and nociceptive behavior. *Mol Pain*. <https://doi.org/10.1186/1744-8069-6-46>
68. Labadie K (2010) Chikungunya disease in nonhuman primates leads to long-term viral persistence in macrophages. *J Clin Invest* 120:1–13. <https://doi.org/10.1172/JCI40104.894>
69. Venugopalan A, Ghorpade RP, Chopra A (2014) Cytokines in acute chikungunya. *PLoS ONE*. <https://doi.org/10.1371/journal.pone.0111305>
70. Picazo-Juárez G, Romero-Suárez S, Nieto-Posadas AS et al (2011) Identification of a binding motif in the S5 helix that confers cholesterol sensitivity to the TRPV1 ion channel. *J Biol Chem* 286:24966–24976. <https://doi.org/10.1074/jbc.M111.237537>
71. Sudji IR, Subburaj Y, Frenkel N et al (2015) Membrane disintegration caused by the steroid saponin digitonin is related to the presence of cholesterol. *Molecules* 20:20146–20160. <https://doi.org/10.3390/molecules201119682>
72. Frenkel N, Makky A, Sudji IR et al (2014) Mechanistic investigation of interactions between steroidal saponin digitonin and cell membrane models. *J Phys Chem B* 118:14632–14639. <https://doi.org/10.1021/jp5074939>
73. Mitra S, Dungan SR (2001) Cholesterol solubilization in aqueous micellar solutions of quillaja saponin, bile salts, or nonionic surfactants. *J Agric Food Chem* 49:384–394. <https://doi.org/10.1021/jf000568r>
74. Szoke É, Börzsei R, Tóth DM et al (2010) Effect of lipid raft disruption on TRPV1 receptor activation of trigeminal sensory neurons and transfected cell line. *Eur J Pharmacol* 628:67–74. <https://doi.org/10.1016/j.ejphar.2009.11.052>
75. Liu M, Huang W, Wu D, Priestley JV (2006) TRPV1, but not P2X3, requires cholesterol for its function and membrane expression in rat nociceptors. *Eur J Neurosci* 24:1–6. <https://doi.org/10.1111/j.1460-9568.2006.04889.x>
76. Ságghy É, Szoke É, Payrits M et al (2015) Evidence for the role of lipid rafts and sphingomyelin in Ca²⁺-gating of Transient Receptor Potential channels in trigeminal sensory neurons and peripheral nerve terminals. *Pharmacol Res* 100:101–116. <https://doi.org/10.1016/j.phrs.2015.07.028>
77. Saha S, Ghosh A, Tiwari N et al (2017) Preferential selection of Arginine at the lipid-water-interface of TRPV1 during vertebrate evolution correlates with its snorkeling behaviour and cholesterol interaction. *Sci Rep*. <https://doi.org/10.1038/s41598-017-16780-w>
78. Jeong JH, Lee DK, Liu S, et al (2018) Activation of temperature-sensitive TRPV1-like receptors in ARC POMC neurons reduces food intake. 1–24
79. Baboota RK, Singh DP, Sarma SM, et al (2014) Capsaicin Induces “Brite” Phenotype in Differentiating 3T3-L1 Preadipocytes. 9:1–12. <https://doi.org/https://doi.org/10.1371/journal.pone.0103093>
80. Takahashi N, Matsuda Y, Yamada H, et al (2014) Epithelial TRPV1 Signaling Cell Proliferation. 1141–1147. <https://doi.org/https://doi.org/10.1177/0022034514552826>
81. To I (2009) Transient Receptor Potential Vanilloid-1 Signaling as a Regulator of Human Sebocyte Biology. <https://doi.org/https://doi.org/10.1038/jid.2008.258>
82. Tak PP, Firestein GS (2001) NF-κB in defense and disease NF-κB : a key role in inflammatory diseases. 107:7–11
83. Lawrence T (2009) The nuclear factor NF-kappaB pathway in inflammation. *Cold Spring Harbor perspectives in biology* 1:1–10. <https://doi.org/10.1101/cshperspect.a001651>
84. Wang Y, Wang DH (2013a) Role of the transient receptor potential vanilloid type 1 channel in renal inflammation induced by lipopolysaccharide in mice. *Am J Physiol* 304:R1–R9. <https://doi.org/10.1152/ajpregu.00163.2012>
85. Tóth A, Blumberg PM, Chen Z, Kozikowski AP (2004) Design of a high-affinity competitive antagonist of the Vanilloid receptor selective for the calcium entry-linked receptor population. *Mol Pharmacol* 65:282–291. <https://doi.org/10.1124/mol.65.2.282>
86. Kárai LJ, Russell JT, Iadarola MJ, Oláh Z (2004) Vanilloid receptor 1 regulates multiple calcium compartments and contributes to Ca²⁺-induced Ca²⁺ release in sensory neurons. *J Biol Chem* 279:16377–16387. <https://doi.org/10.1074/jbc.M310891200>
87. Grant ER, Dubin AE, Zhang SP et al (2002) Simultaneous intracellular calcium and sodium flux imaging in human vanilloid receptor 1 (VR1)-transfected human embryonic kidney cells: a method to resolve ionic dependence of VR1-mediated cell death. *J Pharmacol Exp Ther* 300:9–17. <https://doi.org/10.1124/jpet.300.1.9>
88. Assas BM, Wakid MH, Zakai HA et al (2016) Transient receptor potential vanilloid 1 expression and function in splenic dendritic cells: a potential role in immune homeostasis. *Immunology* 147:292–304. <https://doi.org/10.1111/imm.12562>
89. Kim HS, Kwon HJ, Kim GE et al (2014) Attenuation of natural killer cell functions by capsaicin through a direct and TRPV1-independent mechanism: capsaicin-induced NK cell dysfunction. *Carcinogenesis* 35:1652–1660. <https://doi.org/10.1093/carcin/bgu091>
90. Szitter I, Pozsgai G, Sandor K et al (2010) The role of transient receptor potential vanilloid 1 (Trpv1) receptors in dextran sulfate-induced colitis in mice. *J Mol Neurosci* 42:80–88. <https://doi.org/10.1007/s12031-010-9366-5>
91. Messegue A, Planells-Cases R, Ferrer-Montiel A (2006) Physiology and pharmacology of the vanilloid receptor. *Curr Neuropharmacol* 4:1–15. <https://doi.org/10.2174/157015906775202995>
92. Alawi K, Keeble J (2010) The paradoxical role of the transient receptor potential vanilloid 1 receptor in inflammation. *Pharmacol Ther* 125:181–195. <https://doi.org/10.1016/j.pharmthera.2009.10.005>
93. Wang Y, Wang DH (2013b) TRPV1 ablation aggravates inflammatory responses and organ damage during endotoxic shock. *Clin Vaccine Immunol* 20:1008–1015. <https://doi.org/10.1128/CVI.00674-12>
94. Zhao JF, Ching LC, Kou YR et al (2013) Activation of TRPV1 prevents OxLDL-induced lipid accumulation and TNF-α-Induced inflammation in macrophages: role of liver X receptor α. *Mediators Inflamm*. <https://doi.org/10.1155/2013/925171>
95. Zhong B, Rubinstein J, Ma S, Wang DH (2018) Genetic ablation of TRPV1 exacerbates pressure overload-induced cardiac hypertrophy. *Biomed Pharmacother* 99:261–270. <https://doi.org/10.1016/j.biopha.2018.01.065>
96. Palomer X, Coll T, Davidson MM, et al (2010) The p65 subunit of NF-κB binds to PGC-1α, linking inflammation and metabolic disturbances in cardiac cells. 449–458. <https://doi.org/https://doi.org/10.1093/cvr/cvq080>
97. Pollock N, Taylor G, Jobe F, Guzman E (2019) Modulation of the transcription factor NF-κB in antigen-presenting cells by bovine respiratory syncytial virus small hydrophobic protein. 1587–1599. <https://doi.org/https://doi.org/10.1099/jgv.0.000855>
98. Gutierrez H, Davies AM (2011) Regulation of neural process growth, elaboration and structural plasticity by NF-κB. *Trends Neurosci* 34:316–325. <https://doi.org/10.1016/j.tins.2011.03.001>
99. Liu T, Zhang L, Joo D, Sun S (2017) NF-κB signaling in inflammation. <https://doi.org/10.1038/sigtrans.2017.23>
100. Doñate-Macián P, Jungfleisch J, Pérez-Vilaró G et al (2018) The TRPV4 channel links calcium influx to DDX3X activity and viral infectivity. *Nat Commun* 9:1–13. <https://doi.org/10.1038/s41467-018-04776-7>
101. Rinkenberger N, Schoggins JW (2018) Mucolipin-2 cation channel increases trafficking efficiency of endocytosed viruses. *mBio* 9:1–16. <https://doi.org/https://doi.org/10.1128/mBio.02314-17>
102. Zhou Y, Frey TK, Yang JJ (2009) Viral calciomics: interplays between Ca²⁺ and virus. *Cell Calcium* 46:1–17. <https://doi.org/10.1016/j.ceca.2009.05.005>

103. Apaire-marchais V, Ogliaastro M, Chandre F, et al (2016) Minireview Virus and calcium : an unexpected tandem to optimize insecticide efficacy. 8:168–178. <https://doi.org/10.1111/1758-2229.12377>
104. Chen X, Cao R, Zhong W (2020) Host calcium channels and pumps in viral infections. *Cells* 9(1):94
105. Ueda M, Daidoji T, Anariwa D, Yang C-S, Ibrahim MS, Ikuta K, Nakaya T (2010) Highly pathogenic H5N1 avian influenza virus induces extracellular Ca²⁺ influx, leading to apoptosis in avian cells. *J Virol* 84(6):3068–3078
106. Taverner WK, Jacobus EJ, Christianson J, Champion B, Paton AW, Paton JC, Weiheng S, Cawood R, Seymour LW,

Lei-Rossmann J (2019) Calcium influx caused by ER stress inducers enhances oncolytic adenovirus enadenotucirev replication and killing through PKC α activation. *Mol Ther Oncolytics* 15:117–130

Publisher's Note Springer Nature remains neutral with regard to jurisdictional claims in published maps and institutional affiliations.

Affiliations

P. Sanjai Kumar¹ · Tapas K. Nayak^{1,2} · Chandan Mahish¹ · Subhransu S. Sahoo¹ · Anukrishna Radhakrishnan¹ · Saikat De² · Ankita Datey² · Ram P. Sahu¹ · Chandan Goswami¹ · Soma Chattopadhyay² · Subhasis Chattopadhyay¹ 

P. Sanjai Kumar
sanjai27112009@gmail.com

Tapas K. Nayak
tapas.sbsniser@gmail.com

Chandan Mahish
chandan.mahish@niser.ac.in

Subhransu S. Sahoo
subhransusahoo87@gmail.com

Anukrishna Radhakrishnan
anukrishna.r@niser.ac.in

Saikat De
ashirbadsaikatde@gmail.com

Ankita Datey
dateyankita@gmail.com

Ram P. Sahu
ramprasad.sahu@niser.ac.in

Chandan Goswami
chandan@niser.ac.in

¹ School of Biological Sciences, National Institute of Science Education & Research, Bhubaneswar, HBNI, Jatni, Khurda, Odisha 752050, India

² Infectious Disease Biology, Institute of Life Sciences, (Autonomous Institute of Department of Biotechnology, Government of India), Nalco Square, Bhubaneswar, Odisha 751023, India

Elevation of TRPV1 expression on T cells during experimental immunosuppression

P Sanjai Kumar^{1,#}, Tathagata Mukherjee^{1,#}, Somlata Khamaru¹, Dalai Jupiter Nanda Kishore¹, Saurabh Chawla¹, Subhransu Sekhar Sahoo¹, Subhasis Chattopadhyay^{1,*}

¹ School of Biological Sciences, National Institute of Science Education and Research, Bhubaneswar, HBNI, Jatni, Khurda, Odisha 752050, India; sanjai27112009@gmail.com, tathagatam007@gmail.com, somlata.khamaru@niser.ac.in, djn.kishore@gmail.com, saurabhchawla@niser.ac.in, subhransusahoo87@gmail.com

Equal contribution

* Correspondence: Subhasis Chattopadhyay: subho@niser.ac.in

Abstract:

An intracellular rise in calcium (Ca^{2+}) is an essential requisite underlying T cell activation and its associated pro-inflammatory cytokine production. Transient receptor potential vanilloid channel (TRPV1) is a thermo-sensitive, polymodal gated and permeable to cations such as Ca^{2+} . It has been reported that TRPV1 expression increases during T cell activation. However, the possible involvement of TRPV1 during immunosuppression of T cells has not been studied yet. Here, we investigated the possible role of TRPV1 in FK506 or B16F10-culture supernatant (B16F10-CS) driven experimental immunosuppression in T cells. Intriguingly, it was found that TRPV1 expression is further elevated during immunosuppression compared to ConA or TCR activated T cells. Similarly, in B16F10 tumor-bearing mice, the TRPV1 expression was upregulated in T cells as compared to control mice, *in vivo*. Moreover, we observed an immediate rise in intracellular Ca^{2+} levels in FK506 and B16F10-CS treated T cells as compared to ConA or TCR treated T cells. Likewise, in B16F10 tumor-bearing mice, the basal intracellular calcium level was upregulated in T cells as compared to control mice, *in vivo*. To further investigate the possible mechanism of such rise in intracellular Ca^{2+} levels, TRPV1 specific functional inhibitor, 5 μ -iodoresiniferatoxin (5 μ -IRTX) was used in calcium influx studies. It was observed that the total intracellular Ca^{2+} levels decreased significantly in presence of 5 μ -IRTX for either the FK506 or B16F10-CS as well as with ConA or TCR stimulated T cells, indicating the functional role of TRPV1 channels in FK506 or B16F10-CS mediated increase in intracellular Ca^{2+} levels. The current findings highlight an essential role of the TRPV1 channel in upregulating intracellular calcium levels during both immune-activation and immunosuppression. This study might also have broad implications in the context of other immune-suppressive diseases as well.

Keywords: B16F10-CS, FK506, Immunosuppression, TRPV1

1. Introduction:

Transient receptor potential channels (TRP) belong to a superfamily of ion channels that are thermo-sensitive, polymodal gated and permeable to cations (Gees et al., 2010; Nilius, 2007; Samanta, Hughes, & Moiseenkova-Bell, 2018). Transient receptor potential vanilloid channels (TRPV1) are reported to have a regulatory role in various T cell processes including differentiation, proliferation and activation (Amantini et al., 2017; Majhi et al., 2015). Activation of TRPV1, via ligand binding, significantly increases TCR mediated Ca^{2+} influx and downstream signaling pathways (Majhi *et al.*, 2015; Bujak *et al.*, 2019). TRPV1 is distributed widely in immune cells and are involved in various inflammatory conditions such as in inflammatory bowel disease (IBD), cutaneous neurogenic inflammation, chronic obstructive pulmonary disease (COPD), allergic asthma, brain inflammation, arthritis, auto-immune diseases, hypersensitivity and colitis (Bassi et al., 2019; Silva et al., 2018) and various viral infections as well (Bassi et al., 2019; Kumar et al., 2020; Omar et al., 2017; Omari et al., 2017; Silva et al., 2018).

Free Ca^{2+} ions serve as a second messenger of cells including different immune cells such as T and B lymphocytes and macrophages regulating various physiological processes like differentiation, gene transcription and effector function (Oh-hora & Rao, 2008; Vig & Kinet, 2009). Receptor-mediated activation of different immune cells has been reported to upregulate intracellular Ca^{2+} levels (Vig & Kinet, 2009). Abnormality in Ca^{2+} signaling or unavailability in immune cells may lead to various immunological disorders like severe combined immunodeficiency (SCID) and Wiskott–Aldrich syndrome (WAS) (Feske, 2007) or hamper proper activation of naive T cell and effector function (Birnbaum et al., 1984; Nakabayashi et al., 1992; Watman, et al., 1988) respectively. Different intracellular signaling members of T cells like PKC, NFAT, NF- κ B, calmodulin-dependent kinase, JNK require Ca^{2+} for their function (Ando et al., 2014; Komada et al., 1996; Vig & Kinet, 2009).

Concanavalin A (ConA), a plant lectin (carbohydrate-binding protein), extracted from Jack Bean (*Canavalia ensiformis*), acts as a mitogen for T cell (Mackler et al., 1972) and can increase intracellular Ca^{2+} concentration required for IL-2R expression and IL-2 production (Komada et al., 1996). ConA binds to the mannose moieties of glycoproteins and glycolipids, including the T cell receptor (TCR) and is responsible for nonspecific T cell proliferation (Ando et al., 2014). On the other hand, T cell activation via TCR stimulation with anti-CD3 and anti-CD28 is more specific proliferation which also results in the rise of intracellular Ca^{2+} levels (Pang et al., 2012). Collectively, ConA or TCR induced increase of intracellular Ca^{2+} involves PLC/InsP₃, which releases Ca^{2+} from intracellular compartments like the endoplasmic reticulum and then opens plasma membrane residing Ca^{2+} channels like calcium release-activated calcium channel (CRAC) and different TRP channels (Pang *et al.*, 2012; Majhi *et al.*, 2015).

FK506 (tacrolimus), a clinical immunosuppressive agent, binds calcineurin and impede pro-inflammatory cytokine production by T cells (Almawi et al., 2001; Annett et al., 2020; Sakuma et al., 2000). FK506 binds to FK506 binding protein (FKBP) and forms complex

FK506-FKBP. FK506 binds to FK506 binding protein (FKBP) and forms FK506-FKBP complex (Bultynck et al., 2000). FKBP is reported as important modulators of intracellular Ca^{2+} . FKBP regulates intracellular ryanodine and IP_3 receptor Ca^{2+} release channels (Bultynck et al., 2000; Cameron et al., 1995; MacMillan, 2013). Recently, it has been reported that FK506 induces Ca^{2+} influx via TRPA1 channels (Bultynck et al., 2000; Kita et al., 2019).

B16F10, a mouse melanoma cell line, has been widely used as a transplantable murine melanoma model (Burghoff et al., 2014; Chen et al., 2019; Langer et al., 2006; Overwijk & Restifo, 2001). Additionally, it has also been reported to secrete various soluble factors from B16F10 derived tumors, suppressing lymphocyte activation *in vitro* (Sun et al., 2015, 2013, 2011). B16F10 derived soluble factors, such as interleukin-10 (IL-10), transforming growth factor-beta (TGF- β), vascular endothelial growth factor (VEGF), play an important role in immunosuppression. These soluble factors are known to develop an immunosuppressive network spanning from the primary tumor site to secondary lymphoid organs and peripheral vessels (Yang & Carbone, 2004; Zou, 2005). Tumor microenvironment milieu enriched with these soluble factors induces immune cells to become immunosuppressive and hinders T cell activation associated with antitumor responses (Kusmartsev & Gabrilovich, 2002; Kusmartsev et al., 2004). Additionally, tumor-released extracellular vesicles from the supernatant of malignant effusions or tumor cells such as B16F10 and ascites of cancer patients are also reported to induce immunosuppression. Immune cells such as T cells, B cells, neutrophils and macrophages can take up these tumor-released extracellular vesicles and induce an immunosuppressive environment (Chen et al., 2019; Gao et al., 2018; Wen et al., 2018; Zhou et al., 2016).

The functional role of TRPV1 in cell-mediated immunity (CMI) and its role towards an increase in intracellular Ca^{2+} has been reported (Bertin *et al.*, 2014; Majhi *et al.*, 2015; Kumar *et al.*, 2020). Moreover, a number of immunosuppressive agents, such as rapamycin, tacrolimus and cyclosporin has also been reported to induce intracellular rise in Ca^{2+} (Bielefeldt, Sharma, Whiteis, Yedidag, & Abboud, 1997; Bultynck et al., 2000; Cameron, Steiner, Roskams, et al., 1995; Cameron, Steiner, Sabatini, et al., 1995; Kanoh et al., 1999; D. MacMillan & McCarron, 2009; Van Acker et al., 2004). Based on these previous findings, we hypothesized that TRPV1 may also be contributing towards the intracellular rise in Ca^{2+} levels, subsequent immunosuppressive downstream signaling and cellular responses. Therefore, in the present study, the possible role of TRPV1 during experimental immunosuppression was explored. Moreover, FK506 or B16F10-CS driven regulation in T cell activation, inflammatory cytokines response and subsequent Ca^{2+} influx was investigated. The current study might have importance in understanding the TRPV1 driven FK506 or B16F10-CS induced immunosuppression in T cells, and it might have implications in various immunosuppressive diseases as well.

2. Materials and Methods:

2.1 Mice

6 to 8 weeks old both male and female C57BL/6 mice from the National Institute of Science Education and Research (NISER), Bhubaneswar were used for experimentation. All protocols were approved by the Institutional Animal Ethics Committee (IAEC), NISER following Committee for the Purpose of Control and Supervision of Experiments on Animals, CPCSEA guidelines (IAEC protocol no. AH-112).

2.2 Antibodies, reagents and drugs

FK506 (Cat. no. F4679-5MG), Concanavalin A (ConA) (Cat. no. C0412-5MG), 5 α -IRTX (Cat. no. I9281-1MG) were purchased from Sigma Aldrich (St. Louis, MO, USA); anti-mouse CD25 (Cat. no. 553866), OptEIA kits for IL-2 (Cat. no.555148), IFN- γ (Cat. no.555138), TNF (Cat. no. 558534) for sandwich ELISA were from BD Biosciences, SJ, CA, USA.; anti-mouse CD69 (Cat. no. 35-0691-U100), anti-mouse CD90.2 (Cat. no. 20-0903-U100) from Tonbo Biosciences, San Diego, CA, USA; anti-mouse TRPV1 (Cat. no. ACC-029) from Alomone Laboratories (Jerusalem, Israel); anti-mouse CD3 (Cat. no. 40-0032-U500) and anti-mouse CD28 (Cat. no. 40-0281-U500) [functional assay grade] were procured from Tonbo Biosciences, San Diego, CA, USA. Secondary anti-rabbit Alexa Fluor 488 and T cell isolation kit (Dynabeads™ Untouched™ Mouse T Cells Kit, Cat. no. 11413D) were procured from Invitrogen, Carlsbad, CA USA. RPMI-1640 cell culture medium and FBS were purchased from PAN Biotech, Aiden Bach, Germany; DMEM cell culture medium, 10X RBC lysis buffer, 10X PBS, L-glutamine, penicillin, streptomycin was from Himedia Laboratories, Mumbai, Maharashtra, India.

2.3 T cell isolation, purification and cell culture

Spleens were collected from C57BL/6 mice and splenocytes were isolated as mentioned previously (Sahoo *et al.*, 2018). In brief, spleens were mechanically dispersed with a syringe plunger (Dispovan) and passed through a 70 μ M cell strainer (SPL Life Sciences, Korea). After centrifugation, RBCs were lysed using RBC lysis buffer, washed with 1X PBS, centrifuged and resuspended in RPMI-1640 medium supplemented with 10% FBS, 2 mM L-glutamine, 100 U/mL penicillin, and 0.1 mg/mL streptomycin. T cells were then purified using Mouse Untouched T cell isolation kit as per manufacturer protocol. Briefly, splenocytes were incubated with biotinylated antibodies for 20 mins following resuspension in isolation buffer (2% FBS, 2 mM EDTA in 1X PBS). Cells were then washed with excess isolation buffer, centrifuged and incubated for 15 minutes with streptavidin-conjugated magnetic beads and then placed in a magnet for 2 minutes. Purity of T cells was $\geq 95\%$ measured using flow cytometry (BD FACSCalibur™ flow cytometer, BD Biosciences).

B16F10 (ATCC® CRL-6475™) cells were cultured in DMEM supplemented with 10% FBS, 2 mM L-glutamine, 100 U/mL penicillin, and 0.1 mg/mL streptomycin and maintained as per ATCC protocol. For B16F10 culture supernatant (B16F10-CS) collection, 1×10^6 B16F10

cells were seeded in a T-75 cell culture flask (SPL Life Sciences, Korea). When the confluency reaches around 60-70%, culture medium was replaced with fresh medium and allowed to grow for 24 hours. Culture medium was then collected, centrifuged, filtered through 0.22 μ M filter and stored at -80°C till further use. Purified T cells [1.0×10^6 cells per well in a 48 well cell culture plate (SPL Life Sciences, Korea), 1 mL total volume] were then stimulated with either ConA (5 μ g/mL) or anti-CD3 (plate-bound) and anti-CD28 (soluble) (2 μ g/mL each) following pretreatment with FK506 (1 hour) or B16F10-CS inside a humidified incubator with 5% CO₂ and 37°C temperature. After 36 hours, cells were harvested, stained and analyzed via flow cytometry. Cell culture supernatants were collected and stored at -20°C for ELISA.

2.4 B16F10 subcutaneous injection

B16F10 cells in the logarithmic growth phase ($\leq 50\%$ confluency) were harvested and suspended in ice-cold HBSS buffer. After counting, 2×10^5 cells/mouse were injected in the right flank of wild type C57BL/6 mice. From 14th day, tumor growth was periodically monitored in an interval of every second day (Overwijk & Restifo, 2001). On 21st day, the mice were sacrificed and spleen was harvested for further processing.

2.5 7-AAD staining

Purified mouse T cells were incubated with different doses of B16F10-CS, 5 μ -IRTX and FK506 for 36 hours. Next, cells were harvested and washed with 1X PBS, followed by incubation with 7-AAD for 15 minutes at RT. Cells were then acquired in BD LSRFortessaTM (BD Biosciences) and analyzed via FlowJo V10.7.1. 7-AAD negative cells were considered as live cells (Nayak et al., 2017; Sahoo et al., 2018).

2.6 Flow Cytometry

Flow cytometric staining of T cell was performed as per the method reported previously (Majhi *et al.*, 2015; Sahoo *et al.*, 2018, 2019). Cells were harvested, washed with 1X PBS, resuspended in FACS staining buffer (1% BSA, 0.01% NaN₃ in 1X PBS) and incubated with fluorochrome-conjugated antibodies for 30 minutes on ice in dark and then washed twice with FACS staining buffer. For TRPVI staining only, secondary fluorochrome-conjugated AF488 was added and incubated for 30 minutes, followed by washing with FACS buffer. Cells were then fixed and acquired using the BD FACSCaliburTM flow cytometer or BD LSRFortessaTM (BD Biosciences) and analyzed via Flowjo V10.7.1.

2.7 Enzyme-linked Immunosorbent Assay (ELISA)

Sandwich ELISA was performed to quantitate the cytokine levels in cell culture supernatants. ELISA for IL-2, IFN- γ and TNF were performed using BD OptEIA ELISA kits as per manufacturer's protocol (Kumar et al., 2020; Sahoo et al., 2019). The cytokine concentration in supernatants was estimated by comparing the corresponding standard curve using different concentrations of the recombinant cytokines in pg/ml.

2.8 Ca²⁺ influx

Ca²⁺ influx in purified splenic T cells was performed as reported elsewhere (Kume & Tsukimoto, 2019; Majhi et al., 2015; Sahoo et al., 2019) Here in brief, purified splenic T cells were loaded with Ca²⁺ sensitive dye (Fluo-4 AM, 2 μM) for 60 minutes at 37°C. Next, T cells were washed twice with 1X PBS and placed inside the incubator for another 30 minutes for de-esterification. The cell suspension was added to RIA vials and then treated as per the experimental conditions and acquired by Flow cytometer. Such values were plotted for fluorescence signal relative to starting signal as (F/F₀).

To estimate the intracellular Ca²⁺ contributed by the TRPV1 channel, we performed a minor modification to the Fluo-4 AM staining protocol. The minor modification has been detailed below. First, the T cells were loaded with Ca²⁺ sensitive dye (Fluo-4 AM, 2 μM) along with FK506, B16F10-CS, ConA or TCR for 60 minutes at 37 °C, as per the experimental conditions (instead of adding the above reagents, during acquiring). Additionally, another similar set-up of T cells were pre-treated with 5 μM-IRTX for 15 minutes before addition of the FK506, B16F10-CS, ConA or TCR for 60 minutes at 37 °C, as per the experimental conditions. Next, T cells were washed twice with 1X PBS and placed inside an incubator for another 30 minutes for de-esterification. The cell suspension was added to the RIA vials for the measurement of accumulated intracellular Ca²⁺ levels. The cells were acquired in flow cytometer. The rationale behind the idea was to test whether the treatment with these reagents (FK506, B16F10-CS, ConA or TCR) lead to rise in intracellular Ca²⁺ over time whereas T cells pre-treated with 5 μM-IRTX (Kumar et al., 2020; Majhi et al., 2015) may regulate intracellular Ca²⁺ in T cells.

2.9 Statistical Analysis

Statistical analysis was performed using the GraphPad Prism 7.0 software (GraphPad Software Inc., San Diego, CA, USA). Data are represented as Mean ± SEM. The comparison between the groups was performed by one-way ANOVA or student's t-test with the sidak posthoc test. Data presented are representative of at least three independent experiments. Statistical significance is represented by asterisks (*) for p-value(s) and is marked correspondingly in the figures (**p*< 0.05, ***p*<0.01, ****p*<0.001)

3. Results

3.1 Upregulation of TRPV1 during immune-activation and immunosuppression

A number of TRP channels are known to be expressed on T cells including TRPV1, TRPV4, TRPA1, TRPM8 (Acharya et al., 2020; Bertin et al., 2014; Majhi et al., 2015; Sahoo et al., 2019). To determine the expression of TRPV1 channels in mouse splenic purified resting T cells, we performed Flow cytometry, using specific antibodies against TRPV1. It was observed that the TRPV1 percent positive cells were 17.86 ± 1.34 as compared to isotype control (0.02 ± 0.01) (Supplementary Figure 1, A). Further, the specificity of the TRPV1 antibody in T cells was

tested by using control blocking peptide antigen. For that, T cells were stained with anti-TRPV1 antibody in the presence or absence of the blocking peptide. It was observed that the percentage of positive cells for TRPV1 was markedly reduced in a dose-dependent manner from 17.86 ± 1.34 to 1.46 ± 0.11 in the presence of 1X control blocking peptide antigen and further reduced to 0.74 ± 0.09 in the presence of 3x control blocking peptide antigen. These results indicate that TRPV1 is expressed on T cells and the anti-TRPV1 antibody is highly specific towards TRPV1 expressed on T cells (Supplementary Figure 1, A).

7-aminoactinomycin D (7-AAD) is a fluorescent intercalator that undergoes a spectral shift upon association with DNA. It is one of the widely used cell viability dye (Nayak et al., 2017; Sahoo et al., 2018). In order to determine the cellular cytotoxicity of 5 β -IRTX, FK506 and B16F10-CS in purified mouse T cells, we performed 7-AAD staining. It was observed that upto 96% of the cells were 7-AAD negative for 5 β -IRTX in a concentration range of 2.5 μ M to 20 μ M. Similarly, approximately upto 96% of the cells were 7-AAD negative for FK506 in a concentration range of 1.25 μ g/ml to 20 μ g/ml. Likewise, approximately upto 95% of the cells were 7-AAD negative for B16F10-CS in a range of 5% to 40% w.r.t. total media volume (Figure 1, A). In all the experiments, heat-killed purified T cells were used as a positive control. For further experiments, we have chosen concentration with upto 95% viability. Accordingly, we have chosen 10 μ M 5 β -IRTX, 5 μ g/ml FK506 and 20 % of B16F10-CS.

TRPV1 has been attributed in functional activation and regulation of T cells (Bertin et al., 2014; Majhi et al., 2015; Omari et al., 2017). Recently, TRPV1 has also been reported to play an active role in various inflammatory and autoimmune diseases (Bassi et al., 2019). To determine the status of T cell activation during immunosuppressive treatment with either FK506 or B16F10-CS, T cell activation markers including CD69 and CD25 were analyzed via Flow cytometry. For immunosuppression, T cells were treated with either FK506 or B16F10-CS for 1 hour prior to the addition of either ConA or TCR. It was observed that in T cells treated with FK506 or B16F10 in presence of ConA, CD69 decreased significantly to 24.2 ± 5.36 and 34.37 ± 3.85 respectively as compared to control ConA activated cells (60.23 ± 9.64). Similarly, treatment with FK506 or B16F10 in presence of TCR stimulations, CD69 decreased significantly to 8.19 ± 1.93 and 19.43 ± 2.45 respectively as compared to control TCR activated cells (41.43 ± 3.37) (Figure 1, B). These results indicate that CD69 significantly decreases in FK506 or B16F10-CS treated T cells stimulated with ConA or TCR.

Correspondingly, in FK506 or B16F10-CS treated T cells, stimulated with ConA, CD25 decreased significantly to 13.51 ± 10.65 and 18.18 ± 12.94 respectively as compared to control ConA activated cells (56.03 ± 13.51). Similarly, FK506 or B16F10-CS treated T cells stimulated with TCR, CD25 decreased significantly to 5.03 ± 2.92 and 20.87 ± 5.31 respectively as compared to control TCR activated cells (31.44 ± 4.21) (Figure 1, C). These results indicate that

CD25 significantly decreases in FK506 or B16F10-CS treated T cells stimulated with ConA or TCR.

T cell activation is accompanied by proliferation of T cells. To ascertain whether immunosuppressed T cell's stimulation via either ConA or TCR leads to reduced proliferation, we performed T cell proliferation assay via CFSE staining. It has been observed that 84.53 ± 1.33 % of cells proliferated in presence of ConA. In T cells pre-treated with FK506 or B16F10-CS and later stimulated with ConA, we found that 0.32 ± 0.18 % of cells and 16.5 ± 6.09 % of cells proliferated, respectively. Similarly, it has been observed that 71.1 ± 3.74 % of cells proliferated in presence of TCR. In T cells pre-treated with FK506 or B16F10-CS and later stimulated with TCR, we found that 0.62 ± 0.22 % of cells and 7.62 ± 0.83 % of cells proliferated, respectively (Figure 1, D). These results indicate that immunosuppression via either FK506 or B16F10-CS attenuates T cell proliferation.

Subsequently, the expression of TRPV1 was assessed in immunosuppressed T cells. Intriguingly, TRPV1 expression levels significantly increased in T cells treated with FK506 or B16F10-CS (26.9 ± 1.11 or 23.97 ± 1.04) as compared to resting T cells (16.5 ± 0.52). Moreover, the TRPV1 expression further increased in FK506 or B16F10-CS treated T cells with ConA or TCR stimulation. FK506 or B16F10-CS treated T cells stimulated with ConA or TCR, the TRPV1 expression was 34.53 ± 0.86 or 33.77 ± 0.85 respectively as compared to control ConA activated T cells (28.83 ± 1.19). Similarly, in TCR activated FK506 or B16F10-CS treated T cells, the TRPV1 expression was 33.97 ± 0.77 or 36.1 ± 1.31 respectively as compared to control TCR activated T cells (30.07 ± 0.20) (Figure 1, E). Interestingly, the current findings indicate that the TRPV1 expression also increases significantly in FK506 or B16F10-CS treated T cells as compared to resting T cells, which were further elevated in FK506 or B16F10-CS treated T cells and later stimulated with either ConA or TCR as compared to ConA or TCR activation alone.

3.2 Modulation of cytokine response in immunosuppressed T cells

ConA or TCR mediated activation is known to induce robust pro-inflammatory cytokines production in T cells (Majhi et al., 2015; Sahoo et al., 2019, 2018). Conversely, immunosuppressed (FK506 or B16F10-CS treated) T cells stimulated by ConA or TCR show attenuation of pro-inflammatory cytokine response (Almawi et al., 2001; Chen et al., 2019; Sun et al., 2015). Hence, cell culture supernatant were collected at 36 hours to assess the release of cytokines IFN- γ , IL-2 and TNF as studied elsewhere (Majhi et al., 2015; Sahoo et al., 2019, 2018).

For IFN- γ , upon treatment with immunosuppressive FK506 or B16F10-CS T cells, stimulated with ConA, the IFN- γ levels decreased to 486 ± 91.31 pg/ml and 657.5 ± 130.8 pg/ml respectively as compared to control ConA activated cells (6265 ± 752 pg/ml). Similarly, upon

treatment with immunosuppressive FK506 or B16F10-CS, T cells stimulated with TCR, the IFN- γ levels decreased to 388.3 ± 111 pg/ml and 704.8 ± 106.7 pg/ml as compared to control TCR activated cells (5472 ± 827 pg/ml) (Supplementary Figure 2 A). These results indicate that both FK506 and B16F10-CS stimulated with Con A or TCR show decreased production of T cell effector cytokine IFN- γ as compared to ConA or TCR activated T cells.

For IL-2, upon treatment with immunosuppressive FK506 or B16F10-CS T cells stimulated with ConA, the IL-2 levels decreased to 181.5 ± 44.29 pg/ml and 295.3 ± 58.97 pg/ml respectively as compared to control ConA activated cells (14081 ± 1740 pg/ml). Similarly, upon treatment with FK506 or B16F10-CS, T cells activated with TCR, the IL-2 levels decreased to 140.8 ± 13.38 pg/ml and 318.8 ± 72.85 pg/ml as compared to control TCR activated cells (12199 ± 565.7 pg/ml) (Supplementary Figure 2, B). These results indicate that both FK506 and B16F10-CS stimulated with Con A or TCR show decreased production of T cell activation cytokine IL-2 as compared to ConA or TCR activated T cells.

For TNF, upon treatment with immunosuppressive FK506 or B16F10-CS, T cells activated with Con A, the TNF levels decreased to 609.3 ± 76.57 pg/ml and 590 ± 55.5 pg/ml respectively as compared to control ConA activated cells (1230 ± 57.36 pg/ml). Similarly, upon treatment with immunosuppressive FK506/B16F10-CS, T cells activated with TCR, the TNF levels decreased to 608.5 ± 35.71 pg/ml and 576.8 ± 43.57 pg/ml as compared to control TCR activated cells (1380 ± 37.38 pg/ml) (Supplementary Figure 2, C). These results indicate that both FK506 and B16F10-CS stimulated with Con A or TCR show decreased production of pro-inflammatory cytokine TNF as compared to ConA or TCR activated T cells. Together these results suggest that the pro-inflammatory cytokines decreased in ConA or TCR stimulated T cells treated with FK506 or B16F10-CS.

3.3 Modulation of intracellular Ca^{2+} via TRPV1 channel

5 $\mu\text{-}$ IRTX is a potent and specific functional inhibitor of TRPV1 channel and can block TRPV1 directed Ca^{2+} influx (Kumar et al., 2020; Majhi et al., 2015). Here, the intracellular Ca^{2+} levels were assessed by using the Ca^{2+} sensitive dye Fluo-4 AM (Majhi et al., 2015; Sahoo et al., 2019). Accordingly, T cells were pre-treated with 5 $\mu\text{-}$ IRTX to determine any change in accumulated intracellular Ca^{2+} during various experimental conditions. Pre-treatment of T cells with TRPV1 functional inhibitor, 5 $\mu\text{-}$ IRTX led to reduced calcium influx and subsequently lowers intracellular Ca^{2+} in T cells compared to their corresponding controls. In T cells, treated with FK506, the intracellular Ca^{2+} levels increased markedly compared to resting T cells. Similarly, in T cells, treated with FK506 and stimulated with either ConA or TCR, the Ca^{2+} levels also increased. Further, pre-treatment with 5 $\mu\text{-}$ IRTX, leads to marked decrease in accumulated Ca^{2+} levels in T cells (Figure 2). Moreover, in T cells, treated with B16F10-CS, the Ca^{2+} levels also increased compared to resting T cells. Further, pre-treatment with 5 $\mu\text{-}$ IRTX, led to decrease in accumulated Ca^{2+} levels in T cells. Further, in T cells, treated with B16F10-CS

and stimulated with either ConA or TCR, the Ca^{2+} levels modestly elevated as compared to its corresponding ConA or TCR controls. Further, pre-treatment with 5 μM -IRTX, led to marked decrease in accumulated Ca^{2+} levels in T cells (Figure 2). As a positive control, the maximum increase in intracellular Ca^{2+} levels were depicted with ionomycin (positive control) (Figure 2, inset). These results highlight that the TRPV1 channel might be acting as a major contributor in elevating intracellular Ca^{2+} levels during both immune-activation and immunosuppression.

3.4 Modulation of TRPV1 expression and intracellular Ca^{2+} levels in B16F10-tumor bearing mice, *in vivo*

B16F10, a mouse melanoma cell line, has been injected subcutaneously as described in material and methods. In order to ascertain the modulation of TRPV1 expression and consequent rise in intracellular Ca^{2+} levels in splenic T cells isolated from B16F10-tumor bearing mice, we performed Flow cytometry and calcium influx studies. It has been observed that TRPV1 expression levels significantly increased in T cells isolated from B16F10-tumor bearing mice as compared to control mice (Figure 3, A). Next, we assessed whether the increase in TRPV1 expression levels has also led to the concurrent rise in intracellular Ca^{2+} levels. We found that the basal intracellular Ca^{2+} levels also increased in T cells isolated from B16F10-tumor bearing mice as compared to control mice (Figure 3, B). These results indicate that TRPV1 expression increases in T cells isolated from B16F10-tumor bearing mice and consequently the basal intracellular Ca^{2+} levels were also increased as compared to control mice, *in vivo*.

4. Discussion

TRPV1 is a member of vanilloid group of TRP family and has been attributed in functional expression in a range of immune cells including T cells, macrophages, dendritic cells and NK cells (Assas et al., 2016; Kim et al., 2014; Majhi et al., 2015; Omari et al., 2017). The contributing role of TRPV1 towards Ca^{2+} influx has been very well accredited in T cell development and activation. Moreover, a number of immunosuppressive agents, such as rapamycin, tacrolimus and cyclosporin has also been reported to induce intracellular rise in Ca^{2+} (Bielefeldt et al., 1997; Bultynck et al., 2000; Cameron, Steiner, Roskams, et al., 1995; Cameron, Steiner, Sabatini, et al., 1995; Kanoh et al., 1999; D. MacMillan & McCarron, 2009; Van Acker et al., 2004). However, the role of TRPV1 in calcium influx induced by immunosuppressive agents is not well studied. The current study provides the first evidence that the TRPV1 may also contribute towards FK506 or B16F10-CS driven rise in intracellular calcium associated to immunosuppression of T cells. This study further highlights the modulation of T cell activation, pro-inflammatory cytokine responses and modulation of intracellular Ca^{2+} levels.

TRPV1 is functionally expressed on T cells. TRPV1 has been reported to be upregulated during T cell activation and its associated immune responses (Bertin *et al.*, 2014; Majhi *et al.*, 2015). Moreover, TRPV1 has also been reported to be actively involved in various inflammatory

conditions and pathophysiology (Bujak et al., 2019; Kumar et al., 2020; Majhi et al., 2015; Omari et al., 2017). Upon T cell activation via ConA or TCR, CD69 and CD25 increased significantly. As reported earlier, TRPV1 expression levels increased in activated T cells. Similarly, upon treatment with immunosuppressive FK506 or B16F10-CS, CD69 and CD25 decreased significantly. Unprecedentedly, TRPV1 expression has further increased significantly in immunosuppressed T cells as compared to resting T cells. Furthermore, TRPV1 expression has also been found to be significantly upregulated in FK506 or B16F10-CS treated immunosuppressed T cells stimulated with either ConA or TCR as compared to activated T cells. Moreover, B16F10 tumor-bearing mice also displayed a significant increase in TRPV1 expression levels in T cells. This in general may suggest that during immunosuppressive environment, TRPV1 expression is upregulated in T cells during both *in vitro* and *in vivo*.

T cell activation and suppression are associated with robust cytokine response (Almawi et al., 2001; Majhi et al., 2015; Sahoo et al., 2019, 2018; Sakuma et al., 2000). Upon T cell activation, pro-inflammatory cytokines like IFN- γ , IL-2 and TNF get upregulated. However, T cells treated with immunosuppressive FK506 or B16F10-CS, and stimulated in presence of ConA or TCR, the pro-inflammatory cytokine responses are downregulated. Similar decreasing trend in cytokine response was also reported by others as well (Chen et al., 2019; Sun et al., 2015).

Intracellular Ca^{2+} plays a pivotal role in cell signaling. Modulation of intracellular Ca^{2+} levels is marked with various cellular responses including activation, migration, differentiation and suppression (Aghdasi et al., 2001; Cameron et al., 1995; Feske, 2007; Komada et al., 1996; MacMillan, 2013; Oh-hora & Rao, 2008; Pang et al., 2012; Vig & Kinet, 2009; Wille et al., 2013). T cell activation is marked with rise in intracellular calcium and so as immunosuppression as well. Hence, modulation of TRPV1 channel via 5 μM -IRTX has been used to validate the contribution of TRPV1 channel towards the FK506 or B16F10-CS driven accumulated intracellular Ca^{2+} levels in T cells. 5 μM -IRTX is widely used as a functional inhibitor of TRPV1 channel and acts as a functional blocker of TRPV1-mediated Ca^{2+} influx (Kumar et al., 2020; Majhi et al., 2015). In FK506 treated T cells, stimulated with either ConA or TCR, the accumulated intracellular Ca^{2+} levels markedly increased and pre-treatment with 5 μM -IRTX led to marked decrease in accumulated intracellular Ca^{2+} levels. In B16F10-CS treated T cells, a modest increase in accumulated intracellular Ca^{2+} levels were observed as compared to resting T cells. Further, in other experimental conditions such as, B16F10-CS treated T cells, both in presence or absence of ConA or TCR stimulation, showed a modest increase in accumulated intracellular Ca^{2+} levels as compared to ConA or TCR control. This might be due to the various secreted soluble factors in B16F10-CS released which may regulate increased Ca^{2+} levels (Sun et al., 2015, 2013, 2011; Yang & Carbone, 2004; Zou, 2005). Moreover, B16F10-tumor bearing mice also displayed a significant increase in basal calcium levels in T cells. This in general may suggest that during immunosuppressive environment, the basal calcium levels is upregulated in T

cells during both *in vitro* and *in vivo*. These findings indicate that the TRPV1 channel might be acting as a major contributor in elevating intracellular Ca^{2+} levels in T cells. Mechanistically, Ca^{2+} has been reported to activate CaMKK2 which further induces an immunosuppressive microenvironment. Moreover, deletion of CaMKK2 has been reported to attenuate tumor growth, *in vivo* (Racioppi et al., 2019). Further studies are warranted for detailed mechanisms underlying the possible association between elevated calcium and immunosuppressive microenvironment.

In brief, the present study provides evidence that the TRPV1 channel expression is induced on T cells during both immune-activation and immunosuppression. Interestingly, it was found that during immunosuppression, the TRPV1 channel expression and intracellular Ca^{2+} levels in T cells are further elevated. Moreover, the heightened elevation of intracellular Ca^{2+} during experimental immunosuppression was found to be regulated by TRPV1 channel. The current understanding of TRPV1 in T cell activation or suppression is schematically summarized as a proposed working model in figure 4. These findings might also have broad implication to understand the role of TRPV1 channel in various immunosuppressive diseases as well.

Acknowledgement

We are thankful to Dr. Chandan Goswami, SBS/NISER, Bhubaneswar, India, for the necessary advices for the work. We are also thankful to the Animal House Facility and Flow Cytometry Facility of NISER for their support.

Funding

This study was partly funded by CSIR, India grant no. 37(1675)/16/EMR-II to SC and DST FIST grant no. SR/FST/ LSI-652/2015 to SBS/NISER. It was supported by National Institute of Science Education and Research, HBNI, Bhubaneswar, under Department of Atomic Energy, Government of India.

Conflict of interest

The authors declare that they have no conflict of interest. The funding sponsors had no role in the design of the study; in the collection, analysis, or interpretation of data; in the writing of the manuscript; or in the decision to publish the results.

Author Contributions

Conceptualization: P Sanjai Kumar, Tathagata Mukherjee, Subhasis Chattopadhyay; Methodology: P Sanjai Kumar, Tathagata Mukherjee, Somlata Khamaru, Dalai Jupiter Nanda Kishore, Subhransu Sekhar Sahoo; Formal analysis and investigation: P Sanjai Kumar, Tathagata Mukherjee, Subhasis Chattopadhyay; Writing - original draft preparation: P Sanjai Kumar, Tathagata Mukherjee, Subhasis Chattopadhyay; Writing - review and editing: P Sanjai Kumar, Tathagata Mukherjee, Somlata Khamaru, Dalai Jupiter Nanda Kishore, Subhransu S. Sahoo,

Subhasis Chattopadhyay; Funding acquisition: Subhasis Chattopadhyay; Resources: Subhasis Chattopadhyay; Supervision: Subhasis Chattopadhyay

References:

- Acharya, T. K., Tiwari, A., Majhi, R. K., & Goswami, C. (2020). TRPM8 channel augments T cell activation and proliferation. *Cell Biology International*, (November). <https://doi.org/10.1002/cbin.11483>
- Aghdasi, B., Ye, K., Resnick, A., Huang, A., Ha, H. C., Guo, X., ... Snyder, S. H. (2001). Physiologic Regulator of the Cell Cycle. *Proceedings of the National Academy of Science*, 98(5), 2425–2430.
- Almawi, W. Y., Assi, J. W., Chudzik, D. M., Jaoude, M. M. A., & Rieder, M. J. (2001). Inhibition of cytokine production and cytokine-stimulated T-cell activation by FK506 (Tacrolimus)1. *Cell Transplantation*, 10(7), 615–623. <https://doi.org/10.3727/000000001783986387>
- Amantini, C., Farfariello, V., Cardinali, C., Morelli, M. B., Marinelli, O., Nabissi, M., ... Santoni, G. (2017). The TRPV1 ion channel regulates thymocyte differentiation by modulating autophagy and proteasome activity. *Oncotarget*, 8(53), 90766–90780. <https://doi.org/10.18632/oncotarget.21798>
- Ando, Y., Yasuoka, C., Mishima, T., Ikematsu, T., Uede, T., Matsunaga, T., & Inobe, M. (2014). Concanavalin A-mediated T cell proliferation is regulated by herpes virus entry mediator costimulatory molecule. *In Vitro Cellular and Developmental Biology - Animal*, 50(4), 313–320. <https://doi.org/10.1007/s11626-013-9705-2>
- Annett, S., Moore, G., & Robson, T. (2020). FK506 binding proteins and inflammation related signalling pathways; basic biology, current status and future prospects for pharmacological intervention. *Pharmacology & Therapeutics*, 215, 107623. <https://doi.org/10.1016/j.pharmthera.2020.107623>
- Assas, B. M., Wakid, M. H., Zakai, H. A., Miyan, J. A., & Pennock, J. L. (2016). Transient receptor potential vanilloid 1 expression and function in splenic dendritic cells: A potential role in immune homeostasis. *Immunology*, 147(3), 292–304. <https://doi.org/10.1111/imm.12562>
- Bassi, M. S., Gentile, A., Iezzi, E., Zagaglia, S., Musella, A., Simonelli, I., ... Buttari, F. (2019). Transient receptor potential vanilloid 1 modulates central inflammation in multiple sclerosis. *Frontiers in Neurology*, 10(JAN), 1–8. <https://doi.org/10.3389/fneur.2019.00030>
- Bertin, S., Aoki-Nonaka, Y., De Jong, P. R., Nohara, L. L., Xu, H., Stanwood, S. R., ... Raz, E. (2014). The ion channel TRPV1 regulates the activation and pro-inflammatory properties of CD4+T cells. *Nature Immunology*, 15(11), 1055–1063. <https://doi.org/10.1038/ni.3009>
- Bielefeldt, K., Sharma, R. V., Whiteis, C., Yedidag, E., & Abboud, F. M. (1997). Tacrolimus (FK506) modulates calcium release and contractility of intestinal smooth muscle. *Cell Calcium*, 22(6), 507–514. [https://doi.org/10.1016/S0143-4160\(97\)90078-6](https://doi.org/10.1016/S0143-4160(97)90078-6)
- Birx, D. L., Berger, M., & Fleisher, T. A. (1984). The interference of T cell activation by calcium channel blocking agents. *The Journal of Immunology*, 133(6).

- Bujak, J. K., Kosmala, D., Szopa, I. M., Majchrzak, K., & Bednarczyk, P. (2019, October 16). Inflammation, Cancer and Immunity—Implication of TRPV1 Channel. *Frontiers in Oncology*, Vol. 9, p. 1087. Frontiers Media S.A. <https://doi.org/10.3389/fonc.2019.01087>
- Bultynck, G., De Smet, P., Weidema, A. F., Ver Heyen, M., Maes, K., Callewaert, G., ... De Smedt, H. (2000). Effects of the immunosuppressant FK506 on intracellular Ca²⁺ release and Ca²⁺ accumulation mechanisms. *Journal of Physiology*, 525(3), 681–693. <https://doi.org/10.1111/j.1469-7793.2000.t01-1-00681.x>
- Burghoff, S., Gong, X., Viethen, C., Jacoby, C., Flögel, U., Bongardt, S., ... Schrader, J. (2014). Growth and metastasis of B16-F10 melanoma cells is not critically dependent on host CD73 expression in mice. *BMC Cancer*, 14(1), 898. <https://doi.org/10.1186/1471-2407-14-898>
- Cameron, A. M., Steiner, J. P., Roskams, A. J., Ali, S. M., Ronnettt, G. V., & Snyder, S. H. (1995). Calcineurin associated with the inositol 1,4,5-trisphosphate receptor-FKBP12 complex modulates Ca²⁺ flux. *Cell*, 83(3), 463–472. [https://doi.org/10.1016/0092-8674\(95\)90124-8](https://doi.org/10.1016/0092-8674(95)90124-8)
- Cameron, A. M., Steiner, J. P., Sabatini, D. M., Kaplin, A. I., Walensky, L. D., & Snyder, S. H. (1995). Immunophilin FK506 binding protein associated with inositol 1,4,5-trisphosphate receptor modulates calcium flux. *Proceedings of the National Academy of Sciences of the United States of America*, 92(5), 1784–1788. <https://doi.org/10.1073/pnas.92.5.1784>
- Chen, Y.-Q., Li, P.-C., Pan, N., Gao, R., Wen, Z.-F., Zhang, T.-Y., ... Wang, L.-X. (2019). c. *Journal for ImmunoTherapy of Cancer*, 7(1), 178. <https://doi.org/10.1186/s40425-019-0646-5>
- Feske, S. (2007). Calcium signalling in lymphocyte activation and disease. *Nature Reviews Immunology*, 7(9), 690–702. <https://doi.org/10.1038/nri2152>
- Gao, R., Ma, J., Wen, Z., Yang, P., Zhao, J., Xue, M., ... Pan, N. (2018). Tumor cell-released autophagosomes (TRAP) enhance apoptosis and immunosuppressive functions of neutrophils. *OncoImmunology*, 7(6), 1–11. <https://doi.org/10.1080/2162402X.2018.1438108>
- Gees, M., Colsoul, B., & Nilius, B. (2010). The role of transient receptor potential cation channels in Ca²⁺ signaling. *Cold Spring Harbor Perspectives in Biology*, 2(10), a003962–a003962. <https://doi.org/10.1101/cshperspect.a003962>
- Kanoh, S., Kondo, M., Tamaoki, J., Shirakawa, H., Aoshiba, K., Miyazaki, S., ... Nagai, A. (1999). Effect of FK506 on ATP-induced intracellular calcium oscillations in cow tracheal epithelium. *American Journal of Physiology - Lung Cellular and Molecular Physiology*, 276(6 20-6), 891–899. <https://doi.org/10.1152/ajplung.1999.276.6.l891>
- Kim, H. S., Kwon, H. J., Kim, G. E., Cho, M. H., Yoon, S. Y., Davies, A. J., ... Kim, Y. K. (2014). Attenuation of natural killer cell functions by capsaicin through a direct and TRPV1-independent mechanism: Capsaicin-induced NK cell dysfunction. *Carcinogenesis*, 35(7), 1652–1660. <https://doi.org/10.1093/carcin/bgu091>
- Kita, T., Uchida, K., Kato, K., Suzuki, Y., Tominaga, M., & Yamazaki, J. (2019). FK506 (tacrolimus) causes pain sensation through the activation of transient receptor potential ankyrin 1 (TRPA1) channels. *The Journal of Physiological Sciences*, 69(2), 305–316. <https://doi.org/10.1007/s12576-018-0647-z>
- Komada, H., Nakabayashi, H., Hara, M., & Izutsu, K. (1996). Early calcium signaling and calcium requirements for the IL-2 receptor expression and IL-2 production in stimulated lymphocytes. *Cellular Immunology*, 173(2), 215–220. <https://doi.org/10.1006/cimm.1996.0270>
- Kumar, P. S., Nayak, T. K., Mahish, C., Sahoo, S. S., & Radhakrishnan, A. (2020). Inhibition of

- transient receptor potential vanilloid 1 (TRPV1) channel regulates chikungunya virus infection in macrophages. *Archives of Virology*, 1(0123456789), 17–19.
<https://doi.org/10.1007/s00705-020-04852-8>
- Kume, H., & Tsukimoto, M. (2019). TRPM8 channel inhibitor AMTB suppresses murine T-cell activation induced by T-cell receptor stimulation, concanavalin A, or external antigen re-stimulation. *Biochemical and Biophysical Research Communications*, 509(4), 918–924.
<https://doi.org/10.1016/j.bbrc.2019.01.004>
- Kusmartsev, S., & Gabrilovich, D. I. (2002, August 1). Immature myeloid cells and cancer-associated immune suppression. *Cancer Immunology, Immunotherapy*, Vol. 51, pp. 293–298. <https://doi.org/10.1007/s00262-002-0280-8>
- Kusmartsev, S., Nefedova, Y., Yoder, D., & Gabrilovich, D. I. (2004). Antigen-Specific Inhibition of CD8 + T Cell Response by Immature Myeloid Cells in Cancer Is Mediated by Reactive Oxygen Species . *The Journal of Immunology*, 172(2), 989–999.
<https://doi.org/10.4049/jimmunol.172.2.989>
- Langer, F., Amirkhosravi, A., Ingersoll, S. B., Walker, J. M., Spath, B., Eifrig, B., ... Francis, J. L. (2006). Experimental metastasis and primary tumor growth in mice with hemophilia A. *Journal of Thrombosis and Haemostasis* □: *JTH*, 4(5), 1056–1062.
<https://doi.org/10.1111/j.1538-7836.2006.01883.x>
- Mackler, B. F., Wolstencroft, R. A., & Dumonde, D. C. (1972). Concanavalin a as an inducer of human lymphocyte mitogenic factor. *Nature New Biology*, 239(92), 139–142.
<https://doi.org/10.1038/newbio239139a0>
- MacMillan, D., & McCarron, J. G. J. (2009). Regulation by FK506 and rapamycin of Ca²⁺ release from the sarcoplasmic reticulum in vascular smooth muscle: the role of FK506 binding proteins and mTOR. *British Journal of Pharmacology*, 158(4), 1112–1120.
<https://doi.org/10.1111/j.1476-5381.2009.00369.x>
- MacMillan, Debbi. (2013). FK506 binding proteins: Cellular regulators of intracellular Ca²⁺ signalling. *European Journal of Pharmacology*, 700(1–3), 181–193.
<https://doi.org/10.1016/j.ejphar.2012.12.029>
- Majhi, R. K., Sahoo, S. S., Yadav, M., Pratheek, B. M., Chattopadhyay, S., & Goswami, C. (2015). Functional expression of TRPV channels in T cells and their implications in immune regulation. *FEBS Journal*, 282(14), 2661–2681. <https://doi.org/10.1111/febs.13306>
- Nakabayashi, H., Komada, H., Yoshida, T., Takanari, H., & Izutsu, K. (1992). Lymphocyte calmodulin and its participation in the stimulation of T lymphocytes by mitogenic lectins. *Biology of the Cell*, 75(1), 55–59. [https://doi.org/10.1016/0248-4900\(92\)90124-J](https://doi.org/10.1016/0248-4900(92)90124-J)
- Nayak, T. K., Mamidi, P., Kumar, A., Singh, L. P. K., Sahoo, S. S., Chattopadhyay, S., & Chattopadhyay, S. (2017). Regulation of viral replication, apoptosis and pro-inflammatory responses by 17-aag during chikungunya virus infection in macrophages. *Viruses*, 9(1).
<https://doi.org/10.3390/v9010003>
- Nilius, B. (2007). TRP channels in disease. *Biochimica et Biophysica Acta - Molecular Basis of Disease*, 1772(8), 805–812. <https://doi.org/10.1016/j.bbadis.2007.02.002>
- Oh-hora, M., & Rao, A. (2008, June 1). Calcium signaling in lymphocytes. *Current Opinion in Immunology*, Vol. 20, pp. 250–258. Elsevier Current Trends.
<https://doi.org/10.1016/j.coi.2008.04.004>
- Omar, S., Clarke, R., Abdullah, H., Brady, C., Corry, J., Winter, H., ... Cosby, S. L. (2017). Respiratory virus infection upregulates TRPV1, TRPA1 and ASIC3 receptors on airway cells. *PLoS ONE*, 12(2), 1–21. <https://doi.org/10.1371/journal.pone.0171681>

- Omari, S. A., Adams, M. J., & Geraghty, D. P. (2017). TRPV1 Channels in Immune Cells and Hematological Malignancies. In *Advances in Pharmacology* (1st ed., Vol. 79, pp. 173–198). Elsevier Inc. <https://doi.org/10.1016/bs.apha.2017.01.002>
- Overwijk, W. W., & Restifo, N. P. (2001). B16 as a Mouse Model for Human Melanoma. *Current Protocols in Immunology*, 39(1), Unit 20.1. <https://doi.org/10.1002/0471142735.im2001s39>
- Pang, B., Shin, D. H., Park, K. S., Huh, Y. J., Woo, J., Zhang, Y. H., ... Kim, S. J. (2012). Differential pathways for calcium influx activated by concanavalin A and CD3 stimulation in Jurkat T cells. *Pflugers Archiv European Journal of Physiology*, 463(2), 309–318. <https://doi.org/10.1007/s00424-011-1039-x>
- Racioppi, L., Nelson, E. R., Huang, W., Mukherjee, D., Lawrence, S. A., Lento, W., ... McDonnell, D. P. (2019). CaMKK2 in myeloid cells is a key regulator of the immune-suppressive microenvironment in breast cancer. *Nature Communications*, 10(1), 1–16. <https://doi.org/10.1038/s41467-019-10424-5>
- Sahoo, S. S., Majhi, R. K., Tiwari, A., Acharya, T., Kumar, P. S., Saha, S., ... Chattopadhyay, S. (2019). Transient receptor potential ankyrin1 channel is endogenously expressed in T cells and is involved in immune functions. *Bioscience Reports*, 39(9), BSR20191437. <https://doi.org/10.1042/BSR20191437>
- Sahoo, S. S., Pratheek, B. M., Meena, V. S., Nayak, T. K., Kumar, P. S., Bandyopadhyay, S., ... Chattopadhyay, S. (2018). VIPER regulates naive T cell activation and effector responses: Implication in TLR4 associated acute stage T cell responses. *Scientific Reports*, 8(1), 1–9. <https://doi.org/10.1038/s41598-018-25549-8>
- Sakuma, S., Kato, Y., Nishigaki, F., Sasakawa, T., Magari, K., Miyata, S., ... Goto, T. (2000). FK506 potently inhibits T cell activation induced TNF- α and IL-1 β production in vitro by human peripheral blood mononuclear cells. *British Journal of Pharmacology*, 130(7), 1655–1663. <https://doi.org/10.1038/sj.bjp.0703472>
- Samanta, A., Hughes, T. E. T., & Moiseenkova-Bell, V. Y. (2018). Transient receptor potential (TRP) channels. In *Subcellular Biochemistry* (Vol. 87, pp. 141–165). Springer New York. https://doi.org/10.1007/978-981-10-7757-9_6
- Silva, R. O., Bingana, R. D., Sales, T. M. A. L., Moreira, R. L. R., Costa, D. V. S., Sales, K. M. O., ... Souza, M. H. L. P. (2018). Role of TRPV1 receptor in inflammation and impairment of esophageal mucosal integrity in a murine model of nonerosive reflux disease. *Neurogastroenterology and Motility*, 30(8), 1–8. <https://doi.org/10.1111/nmo.13340>
- Sun, L. X., Li, W. D., Lin, Z. Bin, Duan, X. S., Xing, E. H., Jiang, M. M., ... Lu, J. (2015). Cytokine production suppression by culture supernatant of B16F10 cells and amelioration by Ganoderma lucidum polysaccharides in activated lymphocytes. *Cell and Tissue Research*, 360(2), 379–389. <https://doi.org/10.1007/s00441-014-2083-6>
- Sun, L. X., Lin, Z. Bin, Duan, X. S., Lu, J., Ge, Z. H., Li, M., ... Li, W. D. (2013). Ganoderma lucidum polysaccharides counteract inhibition on CD71 and FasL expression by culture supernatant of B16F10 cells upon lymphocyte activation. *Experimental and Therapeutic Medicine*, 5(4), 1117–1122. <https://doi.org/10.3892/etm.2013.931>
- Sun, L. X., Lin, Z. Bin, Duan, X. S., Lu, J., Ge, Z. H., Li, X. J., ... Li, W. D. (2011). Ganoderma lucidum polysaccharides antagonize the suppression on lymphocytes induced by culture supernatants of B16F10 melanoma cells. *Journal of Pharmacy and Pharmacology*, 63(5), 725–735. <https://doi.org/10.1111/j.2042-7158.2011.01266.x>
- Van Acker, K., Bultynck, G., Rossi, D., Sorrentino, V., Boens, N., Missiaen, L., ... Callewaert,

- G. (2004). The 12 kDa FK506-binding protein, FKBP12, modulates the Ca²⁺-flux properties of the type-3 ryanodine receptor. *Journal of Cell Science*, *117*(7), 1129–1137. <https://doi.org/10.1242/jcs.00948>
- Vig, M., & Kinet, J. P. (2009, January 17). Calcium signaling in immune cells. *Nature Immunology*, Vol. 10, pp. 21–27. <https://doi.org/10.1038/ni.f.220>
- Watman, N. P., Crespo, L., Davis, B., Poiesz, B. J., & Zamkoff, K. W. (1988). Differential effect on fresh and cultured T cells of PHA-induced changes in free cytoplasmic calcium: Relation to IL-2 receptor expression, IL-2 production, and proliferation. *Cellular Immunology*, *111*(1), 158–166. [https://doi.org/10.1016/0008-8749\(88\)90060-3](https://doi.org/10.1016/0008-8749(88)90060-3)
- Wen, Z. F., Liu, H., Gao, R., Zhou, M., Ma, J., Zhang, Y., ... Wang, L. X. (2018). Tumor cell-released autophagosomes (TRAPs) promote immunosuppression through induction of M2-like macrophages with increased expression of PD-L1. *Journal for ImmunoTherapy of Cancer*, *6*(1), 1–16. <https://doi.org/10.1186/s40425-018-0452-5>
- Wille, A. C. M., Chaves-Moreira, D., Trevisan-Silva, D., Magnoni, M. G., Boia-Ferreira, M., Gremski, L. H., ... Veiga, S. S. (2013). Modulation of membrane phospholipids, the cytosolic calcium influx and cell proliferation following treatment of B16-F10 cells with recombinant phospholipase-D from *Loxosceles intermedia* (brown spider) venom. *Toxicon*, *67*, 17–30. <https://doi.org/10.1016/j.toxicon.2013.01.027>
- Yang, L., & Carbone, D. P. (2004). Tumor-host immune interactions and dendritic cell dysfunction. *Advances in Cancer Research*, *92*, 13–27. [https://doi.org/10.1016/S0065-230X\(04\)92002-7](https://doi.org/10.1016/S0065-230X(04)92002-7)
- Zhou, M., Wen, Z., Cheng, F., Ma, J., Li, W., Ren, H., ... Wang, L. (2016). Tumor-released autophagosomes induce IL-10- producing B cells with suppressive activity on T lymphocytes via TLR2-MyD88-NF- κ B signal pathway. *OncoImmunology*, *5*(7), 1–14. <https://doi.org/10.1080/2162402X.2016.1180485>
- Zou, W. (2005, April 18). Immunosuppressive networks in the tumour environment and their therapeutic relevance. *Nature Reviews Cancer*, Vol. 5, pp. 263–274. <https://doi.org/10.1038/nrc1586>

FIGURES CAPTIONS

FIGURE 1 Upregulation of TRPV1 during immune-activation and immunosuppression.

(A) T cells viability upon treatment with different concentrations of either (i) FK506, (ii) B16F10-CS or (iii) 5 μ -IRTX, as assessed by 7-AAD staining. FC dot-plot depicting T cell activation markers (B) CD69 and (C) CD25 along with its corresponding bar diagram. (D) Histogram representing T cell proliferation as determined by CFSE staining along with its corresponding bar diagram. (E) FC dot-plot showing TRPV1 expression in T cells along with its corresponding bar diagram. Representative data of three independent experiments are shown. $P < 0.05$ was considered as statistically significant difference between the groups (ns, non-significant; * $p < 0.05$; ** $p < 0.01$; *** $p < 0.001$).

FIGURE 2 Modulation of intracellular Ca²⁺ via TRPV1 channel.

T cells were incubated with calcium sensitive dye, Fluo-4 AM as mentioned in material and methods and acquired via Flow cytometry (FC). Fluo-4 intensity representing intracellular Ca²⁺ has been expressed as percentage normalized to resting control. The various experimental conditions were pre-treated with 5 μ IRTX, followed by treatment as per experimental conditions. The inset depicts the rise in intracellular Ca²⁺ levels in ionomycin treated T cells. Representative data is of three independent experiments.

FIGURE 3 Modulation of TRPV1 expression and intracellular Ca²⁺ levels in B16F10-tumor bearing mice, *in vivo*. Splenic T cells were isolated from tumor bearing mice and analyzed via FC. (A) FC dot-plot depicting TRPV1 expression on T cells along with its corresponding bar diagram. (B) Basal intracellular Ca²⁺ levels in B16F10-tumor bearing mice as compared to control mice. Fluo-4 intensity representing intracellular Ca²⁺ has been expressed as percentage normalized to resting T cells of control mice. Representative data of three independent experiments are shown. $P < 0.05$ was considered as statistically significant difference between the groups (ns, non-significant; * $p < 0.05$; ** $p < 0.01$; *** $p < 0.001$).

Figure 4 Model depicting functional expression of TRPV1 and intracellular calcium levels in activated and immuno-suppressed T cells.

Resting T cells maintain low levels of cytosolic Ca²⁺ and basal levels of TRPV1 expression. (A) Upon activation with either ConA or TCR, both cytosolic Ca²⁺ and TRPV1 are upregulated

significantly along with robust effector cytokine responses. (B) Upon treatment with immunosuppressive FK506 or B16F10-CS, both cytosolic Ca^{2+} and TRPV1 expression increases significantly. (C) T cells during experimental immunosuppression (treated with FK506/B16-CS) and stimulated either by ConA or TCR, although shows decreased cytokine response, may show significantly higher cytosolic Ca^{2+} and TRPV1 expression.

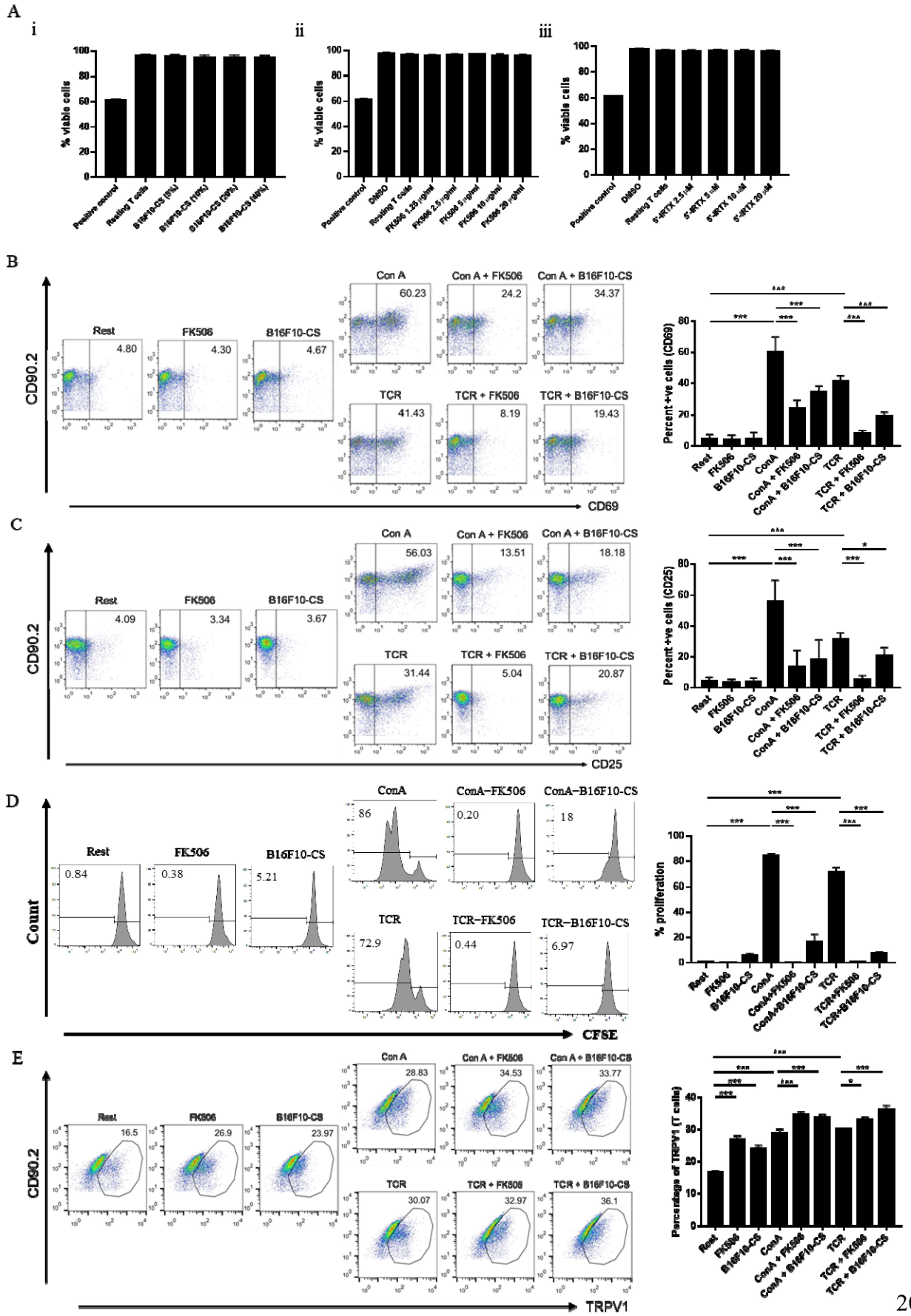


FIGURE 1: Upregulation of TRPV1 during immune-activation and immunosuppression.

(A) T cells viability upon treatment with different concentrations of either (i) FK506, (ii) B16F10-CS or (iii) 5 μ M-IRTX, as assessed by 7-AAD staining. FC dot-plot depicting T cell activation markers (B) CD69 and (C) CD25 along with its corresponding bar diagram. (D) Histogram representing T cell proliferation as determined by CFSE staining along with its corresponding bar diagram. (E) FC dot-plot showing TRPV1 expression in T cells along with its corresponding bar diagram. Representative data of three independent experiments are shown. $P < 0.05$ was considered as statistically significant difference between the groups (ns, non-significant; * $p < 0.05$; ** $p < 0.01$; *** $p < 0.001$).

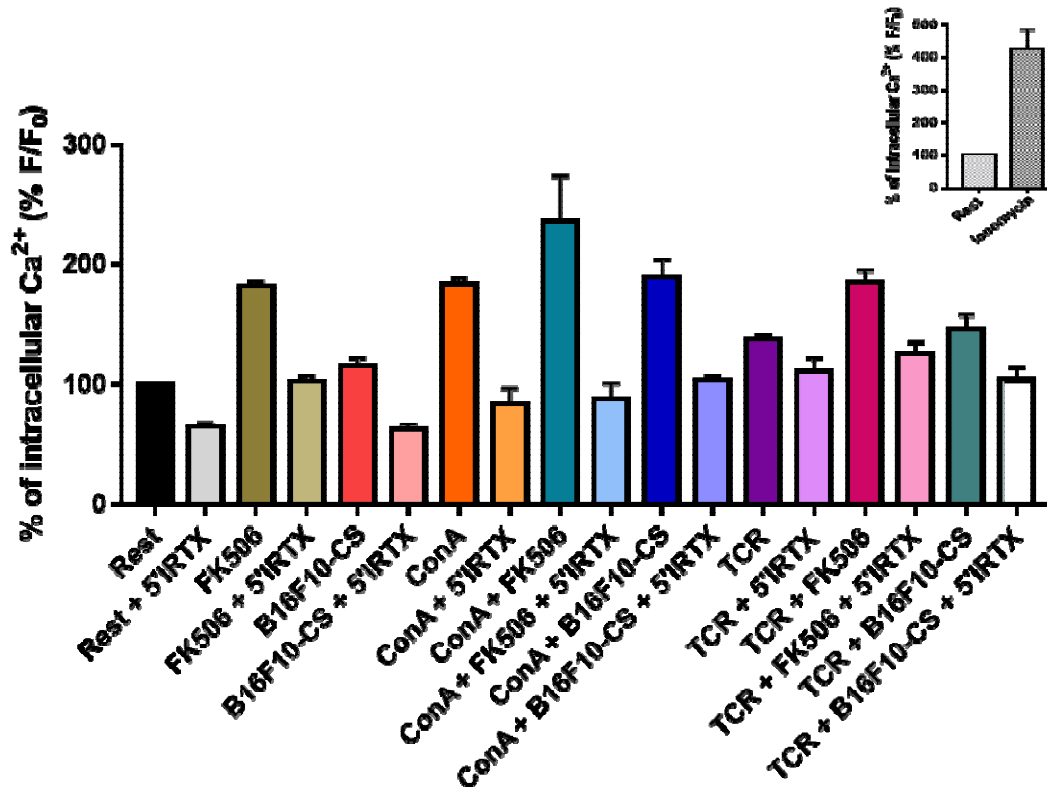


FIGURE 2: Modulation of intracellular Ca²⁺ via TRPV1 channel.

T cells were incubated with calcium sensitive dye, Fluo-4 AM as mentioned in material and methods and acquired via Flow cytometry (FC). Fluo-4 intensity representing intracellular Ca²⁺ has been expressed as percentage normalized to resting control. The various experimental conditions were pre-treated with 5 μ M-IRTX, followed by treatment as per experimental conditions. The inset depicts the rise in intracellular Ca²⁺ levels in ionomycin treated T cells. Representative data is of three independent experiments.

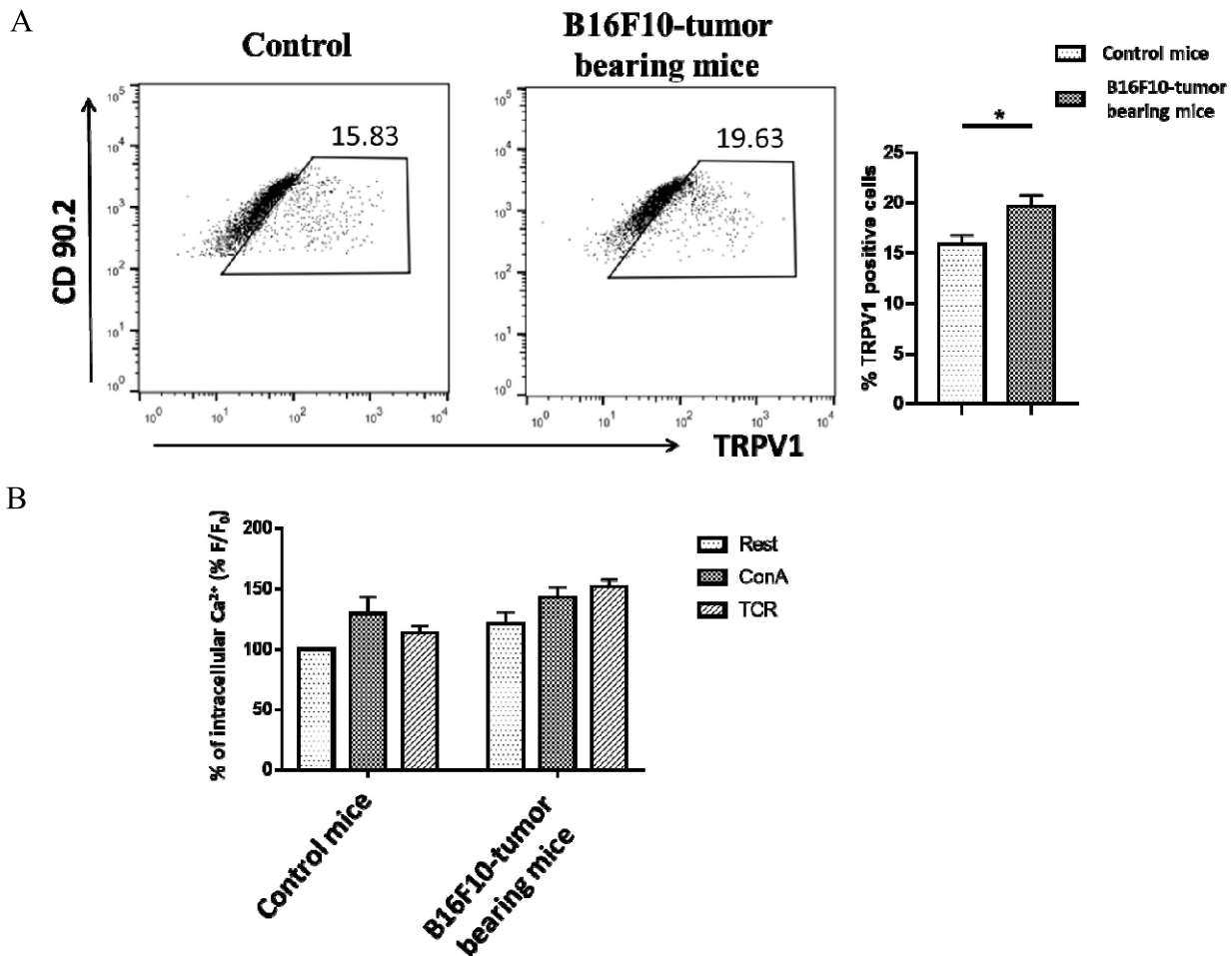


FIGURE 3: Modulation of TRPV1 expression and intracellular Ca^{2+} levels in B16F10-tumor bearing mice, *in vivo*. Splenic T cells were isolated from tumor bearing mice and analyzed via FC. (A) FC dot-plot depicting TRPV1 expression on T cells along with its corresponding bar diagram. (B) Basal intracellular Ca^{2+} levels in B16F10-tumor bearing mice as compared to control mice. Fluo-4 intensity representing intracellular Ca^{2+} has been expressed as percentage normalized to resting T cells of control mice. Representative data of three independent experiments are shown. $P < 0.05$ was considered as statistically significant difference between the groups (ns, non-significant; * $p < 0.05$; ** $p < 0.01$; *** $p < 0.001$).

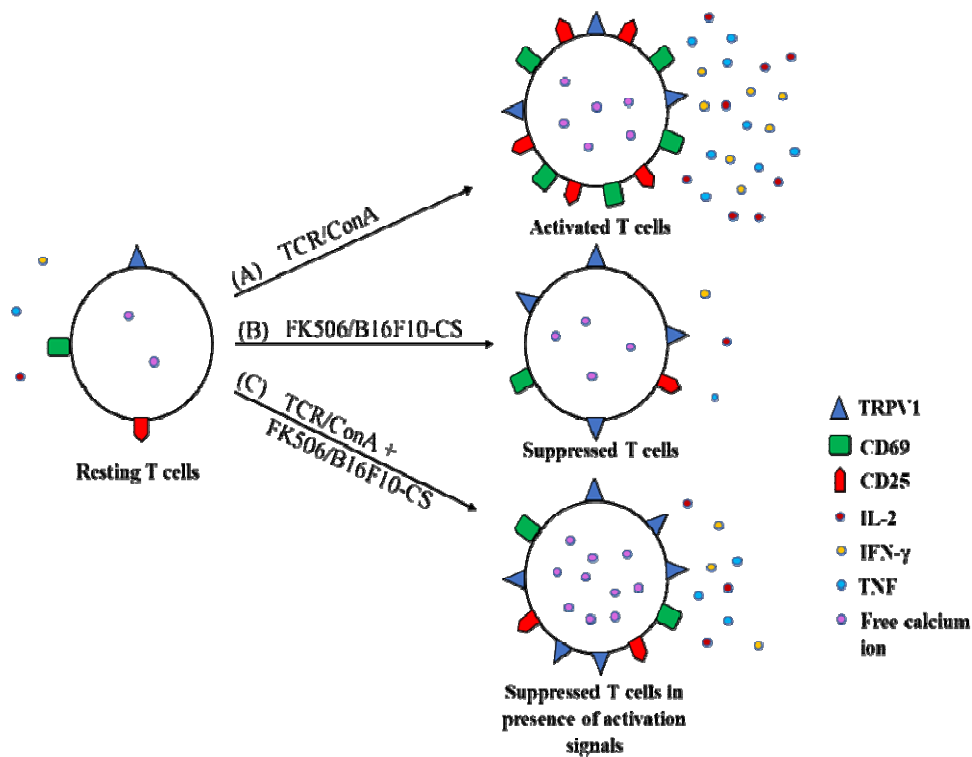


Figure 4: Model depicting functional expression of TRPV1 and intracellular calcium levels in activated and immuno-suppressed T cells. Resting T cells maintain low levels of cytosolic Ca^{2+} and basal levels of TRPV1 expression. (A) Upon activation with either ConA or TCR, both cytosolic Ca^{2+} and TRPV1 are upregulated significantly along with robust effector cytokine responses. (B) Upon treatment with immunosuppressive FK506 or B16F10-CS, both cytosolic Ca^{2+} and TRPV1 expression increases significantly. (C) T cells during experimental immunosuppression (treated with FK506/B16-CS) and stimulated either by ConA or TCR, although shows decreased cytokine response, may show significantly higher cytosolic Ca^{2+} and TRPV1 expression.

Research Article

Transient receptor potential ankyrin1 channel is endogenously expressed in T cells and is involved in immune functions

Subhransu Sekhar Sahoo^{1,*}, Rakesh Kumar Majhi^{1,*}, Ankit Tiwari^{1,†}, Tusar Acharya^{1,†}, P. Sanjai Kumar^{1,‡}, Somdatta Saha^{1,‡}, Abhishek Kumar^{2,3},  Chandan Goswami¹ and Subhasis Chattopadhyay¹

¹School of Biological Sciences, National Institute of Science Education and Research, HBNI, Bhubaneswar, Jatni, Khurda 752050, Odisha, India; ²Institute of Bioinformatics, International Technology Park, Bangaluru 560066, India; ³Manipal Academy of Higher Education (MAHE), Manipal 576104, Karnataka, India

Correspondence: Subhasis Chattopadhyay (subho@niser.ac.in) or Chandan Goswami (chandan@niser.ac.in)



Transient receptor potential channel subfamily A member 1 (TRPA1) is a non-selective cationic channel, identified initially as a cold sensory receptor. TRPA1 responds to diverse exogenous and endogenous stimuli associated with pain and inflammation. However, the information on the role of TRPA1 toward T-cell responses remains scanty. *In silico* data suggest that TRPA1 can play an important role in the T-cell activation process. In this work, we explored the endogenous expression of TRPA1 and its function in T cells. By reverse transcription polymerase chain reaction (RT-PCR), confocal microscopy and flow cytometry, we demonstrated that TRPA1 is endogenously expressed in primary murine splenic T cells as well as in primary human T cells. TRPA1 is primarily located at the cell surface. TRPA1-specific activator namely allyl isothiocyanate (AITC) increases intracellular calcium ion (Ca^{2+}) levels while two different inhibitors namely A-967079 as well as HC-030031 reduce intracellular Ca^{2+} levels in T cells; TRPA1 inhibition also reduces TCR-mediated calcium influx. TRPA1 expression was found to be increased during $\alpha\text{CD3}/\alpha\text{CD28}$ (TCR) or Concanavalin A (ConA)-driven stimulation in T cells. TRPA1-specific inhibitor treatment prevented induction of cluster of differentiation 25 (CD25), cluster of differentiation 69 (CD69) in ConA/TCR stimulated T cells and secretion of cytokines like tumor necrosis factor (TNF), interferon γ (IFN- γ), and interleukin 2 (IL-2) suggesting that endogenous activity of TRPA1 may be involved in T-cell activation. Collectively these results may have implication in T cell-mediated responses and indicate possible role of TRPA1 in immunological disorders.

*These authors contributed equally as co-first authors.

†These authors contributed equally as co-second authors.

‡These authors contributed equally as co-third authors.

Received: 22 May 2019
Revised: 02 August 2019
Accepted: 21 August 2019

Accepted Manuscript Online:
05 September 2019
Version of Record published:
20 September 2019

Introduction

Transient receptor potential cation channel subfamily A member 1 (TRPA1) is the only member of the mammalian ‘ankyrin’ type subfamily of TRP channels [1]. TRPA1 is a calcium ion (Ca^{2+})-permeable non-selective cation channel that is expressed in a set of nociceptive/thermo-receptive neurons that can detect noxious cold temperatures below 17°C. It is often co-expressed with the heat-sensitive channel, transient receptor potential cation channel subfamily transient receptor potential vanilloid1 (TRPV1) rather than with the cold-sensitive channel TRPM8. Initial reports suggested that the large influx of Ca^{2+} at lower temperatures (such as at 10°C) is primarily due to the direct activation of this channel by cold stimuli [2,3]. Apart from low temperature as a stimulus, TRPA1 also acts as a nociceptive receptor that detects noxious chemicals that can cause tissue damage. TRPA1 also acts as a mediator of inflammatory pain generated by either noxious cold or chemical irritants [4,5].

Ca²⁺ channels are an integral part of T-cell activation, differentiation, and formation of an immunological synapse between mature CD4⁺ T cells and Antigen-Presenting Cells (APC), and even exocytosis of vesicles in cytotoxic T cells. It also influences cytokine release patterns which in turn affect T-cell functions like the development of anergy, maturation, and differentiation of naïve T cells into Th1 and Th2 cells [6]. In agreement with these reports, abnormality in Ca²⁺-signaling results in several immunological disorders such as SCID and Wiskott–Aldrich syndrome (WAS) [6]. T-cell motility is also regulated by Ca²⁺ in consortium with protein kinase C (PKC) which regulates the rearrangement of actin cytoskeleton in them. Activation of several transcription factors such as NFAT, NF-κB, calmodulin-dependent kinase, JNK, and others are known to be involved in T-cell regulation and require Ca²⁺ [7]. Moreover, recently a strategic usage of cation channel blockers toward T-cell activation, cytokine secretion, and proliferation has been demonstrated [8]. Transient receptor potential (TRP) channels act as Ca²⁺-permeable channels and thereby regulate Ca²⁺ homeostasis. So far, few members of the TRP family have been identified, by us and other groups, that are endogenously expressed in T cells and regulate T-cell functions [9,10].

Endogenous inflammatory agents such as Reactive Oxygen Species (ROS) induce the production of 4-hydroxy-2-nonenal (HNE) that directly activates TRPA1 [9]. Nitrated fatty acids and prostaglandins like 15d-PGJ2 are released at the site of inflammation, and such compounds can also directly activate TRPA1 [10,11]. It is also known that lymphoma and inflammation associated itch is mediated by a Th2 cell-derived cytokine, interleukin (IL)-31 (IL-31), that directly interacts with its receptor IL-31RA located on TRPV1⁺/TRPA1⁺ sensory nerves in skin [12]. These compounds can also play a role in T-cell activation. In addition, lipopolysaccharide (LPS, a noxious by-product of Gram-negative bacteria) activates TRPA1 via a TLR4-independent mechanism and thereby generates a rapid nociceptive response and neurogenic inflammation [13]. In this work, we have probed the expression, localization of TRPA1 channel in T cells and also characterized the function of TRPA1 toward T-cell activation.

Materials and methods

Bioinformatics analysis

TRPA1 gene input was made into Search Tool for the Retrieval of Interacting Genes/Proteins (STRING 10) [14] web tool for exploring protein–protein interactions with the confidence score higher than 0.7 with the top interacting partners; Kyoto Encyclopaedia of Genes and Genomes (KEGG) and Gene Ontology annotations were deduced for TRPA1 interacting partners using g:profiler webserver [15].

Reagents

The TRPA1 channel modulatory drugs allyl isothiocyanate (AITC, activator), A-967079 (inhibitor), and HC-030031 (another inhibitor) were obtained from Sigma–Aldrich (St. Louis, MO, U.S.A.). Concanavalin A (ConA) was purchased from HiMedia (India). Knockout validated rabbit polyclonal antibody against the first extracellular loop (747–760 aa) of hTRPA1 and its specific blocking peptide (NSTGIINETS DHSE) were purchased from Alomone Laboratories (Jerusalem, Israel; Cat. no: ACC-037). The other rabbit polyclonal antibody against the N-terminus of TRPA1 was procured from Novus Biologicals (Centennial, CO, U.S.A.; Cat. no: NB110-40763). The Ca²⁺-sensitive dye Fluo-4AM was procured from Molecular Probes (Eugene, OR, U.S.A.). Calcium chelating agents BAPTA-AM (1,2-bis(2-aminophenoxy)ethane-N,N,N',N'-tetraacetic acid tetrakis (acetoxymethyl ester)) and EGTA (ethylene glycol-bis(β-aminoethyl ether)-N,N,N',N'-tetraacetic acid) were procured from Sigma (St. Louis, MO, U.S.A.). TRIzol was purchased from Life Technologies (Carlsbad, CA, U.S.A.). Verso cDNA synthesis kit was obtained from Thermo Scientific (Waltham, MA, U.S.A.). SYBR Green for reverse transcription polymerase chain reaction (RT-PCR) was procured from Life Technologies (Carlsbad, CA, U.S.A.). The RT-PCR primers for TRPA1 and GAPDH were obtained from IDT (Coralville, IO, U.S.A.). Anti-mouse cluster of differentiation 25 (CD25)-PE, cluster of differentiation 69 (CD69)-PE, and anti-human CD3-PE as well as functional grade (azide-free) anti-CD3 and anti-CD28 mAbs were obtained from BD Biosciences (San Jose, CA, U.S.A.). CD3/CD28 T-cell activation beads were purchased from Thermo Fisher (Gibco). The CD90.2-APC antibody was from Tonbo Biosciences (San Diego, CA, U.S.A.). The sequences of the primers used in the study are mentioned below:

TRPA1 Forward: 5'- GTC CAG GGC GTT GTC TAT CG - 3'
 TRPA1 Reverse: 5'- CGT GAT GCA GAG GAC AGA AT - 3'
 GAPDH Forward: 5'- CCG CAT CTT CTT GTG CAG TG- 3'
 GAPDH Reverse: 5'- CCC AAT ACG GCC AAA TCC GT- 3'.

Isolation and culture of T cells

T cells were isolated and cultured as described previously [16]. Briefly, murine spleen cells were obtained from 6- to 8-week-old BALB/c mice as per the approval of the Institutional Animal Ethics Committee (IAEC protocol no. NISER/SBS/IAEC/AH-39). Single cell suspension was made by passing the suspended splenocytes through a 70- μ m cell strainer. T cells were purified from the non-adherent splenocyte population by using BD IMag™ Mouse T Lymphocyte Enrichment Set – DM according to the manufacturer's instructions. The isolated cells were cultured in a 24-well polystyrene cell culture plate (3×10^6 cells/well) with RPMI (PAN Biotech, Aidenbach, Germany) supplemented with 10% FBS (PAN Biotech). The percentage purity of the purified T cells was above 95% in each case. All the experiments were performed at approximately 36 h after plating the cells as most of the primary T cells were found to be activated during 36–48 h after ConA or TCR treatment (data not shown). Primary murine T cells were activated with either a combination of plate-bound α -CD3 (2 μ g/ml) and soluble α -CD28 (2 μ g/ml), or with ConA (4 μ g/ml) alone for 36 h before experiments. Similarly, human peripheral blood mononuclear cell (hPBMC)-derived T cells were purified by Human T cell isolation kit from Invitrogen (Invitrogen Dynal AS, Oslo, Norway) according to manufacturer's instructions. Treatment of T cells was carried out with selective TRPA1 activator AITC (100 μ M) and inhibitor A-967079 (100 μ M) with or without ConA or α -CD3/CD28.

RNA isolation and RT-PCR

Approximately 5×10^6 T cells were used for RNA isolation. For positive control, spinal cord tissue from mice was used. RNA isolation was done using TRIzol reagent according to the manufacturer's instructions. Nanodrop readings were taken and 1 μ g of RNA was converted into cDNA using verso cDNA synthesis kit as per the mentioned protocol. RT-PCRs were performed for TRPA1 and GAPDH in ABI7500 system (Applied Biosystems, Foster City, CA, U.S.A.) using 2 \times SYBR Green Mix following the reaction gene expression was visualized in 1% agarose gel.

Flow cytometry

Flow cytometry analysis of T cells was performed as described previously [16]. For probing TRPA1 expression, cells were stained with the TRPA1-specific antibody mentioned before and subsequently flow cytometric analysis was performed as described previously [16,17]. For evaluating the profile of immune markers, mouse T cells were incubated with anti-CD25-PE, CD69-PE and CD90.2-APC mAbs dissolved in FACS buffer (1 \times PBS, 1% BSA, and 0.05% sodium azide) for 30 min on ice and then washed further. Stained cells were washed twice with the same FACS buffer before the line-gated acquisition of approximately 10000 cells. hPBMC-derived T cells were stained with anti-human CD3 antibody and were acquired with FACS Calibur (BD Biosciences). Data were analyzed using CellQuest Pro software (BD Biosciences). The percentages of cells expressing the markers are represented in dot-plots while the MFI values represent the expression levels of the markers per cell.

Immunofluorescence analysis and microscopy

Immunofluorescence analysis of T cells was performed as described previously [16]. For immunocytochemical analysis, immediately after harvesting, T cells were diluted in PBS and fixed with paraformaldehyde (final concentration 2%). After fixing the cells with paraformaldehyde, immunostaining was done by two procedures: in first case cell permeabilization was not performed as the antibody detecting TRPA1 recognizes an extracellular region of TRPA1. In other cases, the cells were permeabilized with 0.1% Triton X-100 in PBS (5 min). Subsequently, the cells were blocked with 5% BSA for 1 h. The primary antibody was used at 1:400 dilution. In some experiments, blocking peptides were used to confirm the specificity of the immunoreactivity. The ratio of blocking peptides with specific antibody was 1:1 (in concentration). Another rabbit polyclonal antibody (procured from Novus Biologicals) detecting epitope present in the N-terminal cytoplasmic domain of TRPA1 was used (1:1000 dilution) in some experiments to confirm the endogenous expression of TRPA1 in T cells. All primary antibodies were incubated overnight at 4 $^{\circ}$ C in PBST buffer (PBS supplemented with 0.1% Tween-20). AlexaFluor-488 labeled anti-rabbit antibody (Molecular Probes) was used as secondary antibody and at 1:1000 dilutions. All images were acquired on a confocal laser scanning microscope (LSM-780, Zeiss) with a 63 \times objective and analyzed with the Zeiss LSM image examiner software followed by compilation using Adobe Photoshop.

Ca²⁺ imaging

Ca²⁺ imaging of primary murine splenic T cells was performed as described previously with minor modifications [16,18]. In brief, primary murine splenic T cells were loaded with Ca²⁺-sensitive dye (Fluo-4 AM, 2 μ M for 30 min). Ca²⁺-chelation experiment was performed by treating the cells with 5 μ M BAPTA-AM for 1 h and extracellular Ca²⁺

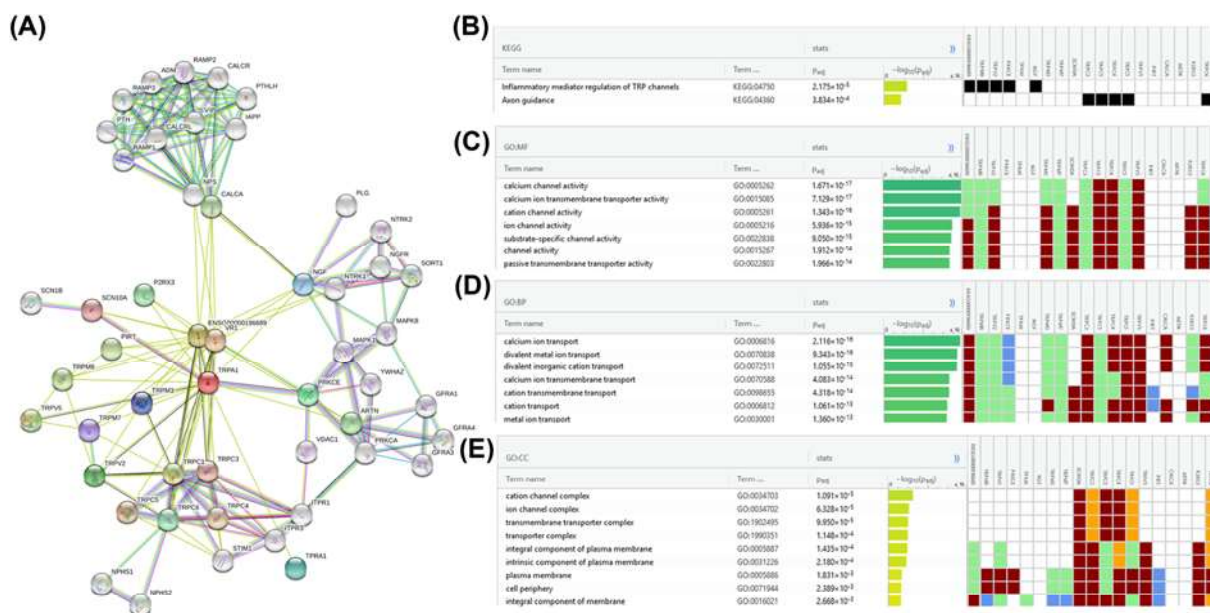


Figure 1. Possible involvement of TRPA1 in immuno-functions based on protein interaction data

(A) Overview of protein–protein interaction partners of TRPA1. The interaction network suggests that TRPA1 may be involved in inflammatory processes based on KEGG (B) and GO annotations MF (C), BP (D) and CC (E). Abbreviations: BP, biological process; CC, cellular component; MF, molecular function.

was chelated with 5 μM EGTA for 1 h. The cell suspension was added to the live cell chamber for Ca^{2+} imaging and images were acquired at every 5-s intervals. The cells were stimulated with specific agonists alone or in a combination of agonists and antagonists and CD3/CD28 T-cell activation beads as described. Fluo-4 AM signal was acquired using a Zeiss microscope (LSM 780) and Olympus microscope (FV3000) and with the same settings. The images were analyzed using LSM software and Fiji. The intensities specific for Ca^{2+} -loaded Fluo-4 are represented in artificial rainbow color with a pseudo scale (red indicating the highest level of Ca^{2+} and blue indicating the lowest levels of Ca^{2+}). For quantification of the changes in the intracellular Ca^{2+} levels, fluorescence intensity of T cells present in view field was measured before and just after adding the drugs. Such values were plotted for relative changes.

Enzyme-linked immunosorbent assay

Supernatants from the respective experiments were collected and stored at -80°C . Enzyme-linked immunosorbent assay (ELISA) for different T-cell effector cytokines tumor necrosis factor (TNF), IL-2, and interferon- γ (IFN γ) were performed using BD Biosciences Sandwich ELISA kits (San Jose, CA, U.S.A.) as per the manufacturer's instructions. The readings were acquired using a microplate reader (Bio-Rad iMARK) at 450 nm.

Statistical tests

The primary data were imported into R software for statistical analysis. The ANOVA test was performed for dataset comprising more than two experimental groups. To check the reliability and significance. Student's *t* test was performed in GraphPad Prism 7 to derive significance of the calcium imaging data with two experimental groups. The *P*-value of <0.05 was considered statistically significant. Data presented here are representative of three independent experiments. The significance values are as follows: ****, $P \leq 0.0001$; ***, P between 0 and 0.001; **, P between 0.001 and 0.01; *, P between 0.01 and 0.05; ns, P above 0.05.

Results

Gene set enrichment analysis reveals that TRPA1 has immune function

Protein–protein interaction patterns of TRPA1 were examined using STRING11 [14] with confidence cut-off score (>0.7) (Figure 1A). These proteins interacting with TRPA1 were evaluated for their roles using gene set enrichment analysis via g:Profiler webserver [15]. This computational analyses suggests that TRPA1 is potentially associated with

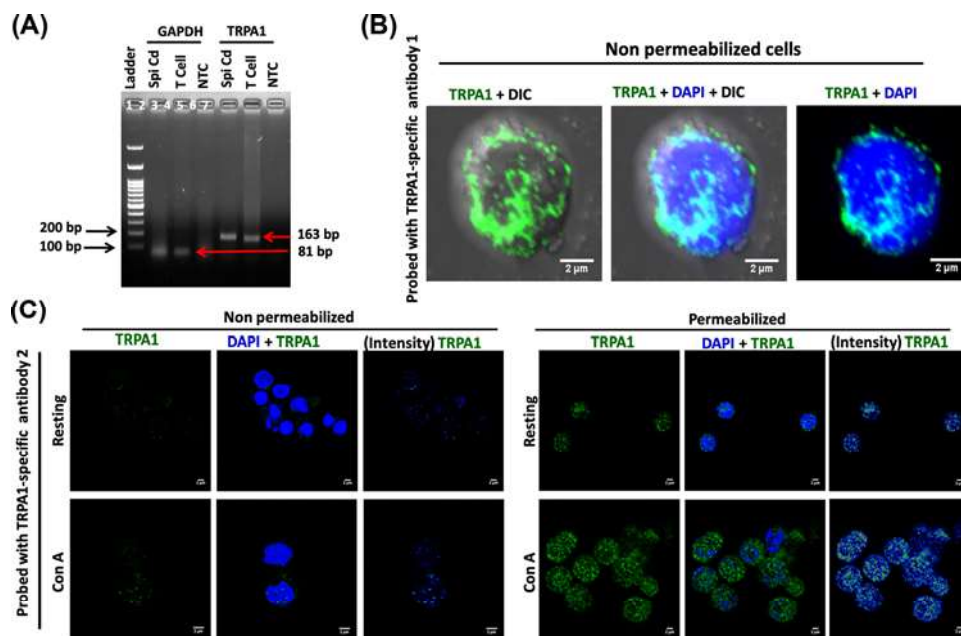


Figure 2. Endogenous expression of TRPA1 primary murine T cells

(A) RT-PCR for TRPA1 and GAPDH from mRNA isolated from T cell. Total mRNA isolated from mouse spinal cord is used as a positive control and no-template control (NTC) is used as negative control. (B) Immunolocalization of TRPA1 in the surface of unpermeabilized T cells. (C) Immunodetection of TRPA1 in T cell by using another antibody recognizing the epitope present in the N-terminal cytoplasmic domain. In permeabilized cells this antibody detects TRPA1 at low levels in resting condition and modest level in ConA-treated condition. This antibody does not detect TRPA1 in non-permeabilized T cells as its epitope at N-terminus is located in intracellular region.

immune function associated processes along with typical function as of ion channels (Figure 1B–E). This indicates that TRPA1 might possibly be involved in regulation of immune system. Hence, this imposed further experimental evaluation.

TRPA1 is expressed endogenously in primary murine and human T cells

Expression of TRPA1 at mRNA level in T cells was confirmed by RT-PCR (Figure 2A). The surface expression of specific ion channels is critical for signaling events. Therefore we used a specific antibody (from Alomone labs) for which the epitope is present at the extracellular loop-1 of TRPA1 (i.e., present outside the cell surface). This antibody allowed us to probe the surface expression of TRPA1 (in unpermeabilized cells) and as well as total TRPA1 expression (in Triton X-100-permeabilized cells). This antibody detected endogenous TRPA1 signal at the surface of unpermeabilized T cells (Figure 2B). To confirm the endogenous expression of TRPA1 in T cell, we used another antibody (Novus Biologicals) raised against epitope present in the N-terminal cytoplasmic domain of TRPA1. This antibody detects TRPA1 modestly in resting T cells and strongly in ConA (a lectin that acts as a mitogen and results in T-cell activation) activated T cells, but after permeabilization (Figure 2C, right-hand side). This antibody does not detect TRPA1 in unpermeabilized T cells, indicating specificity of the antibody (Figure 2C, left-hand side). Taken together, the data strongly suggest that TRPA1 is endogenously expressed in murine T cells.

Next, we probed surface as well as total expression of TRPA1 in murine T cells that are at resting (naïve) stage and/or activated with either ConA or by T-cell receptor (TCR) stimulation with α -CD3/ α -CD28 antibodies [19,20].

Confocal microscopy of unpermeabilized cells revealed that TRPA1 is endogenously expressed in resting and activated T cells as distinct clusters that are primarily located at the cell surface (Figure 3A(i)). Notably, the TRPA1 signal was blocked upon pre-incubating the antibodies with their antigenic peptide confirming the specificity of the antibody used (Figure 3A(i),B). The intracellular localization of TRPA1 was almost minimal as there was no significant difference in its expression in surface versus in whole cell (in resting conditions) (Figure 3A,C). However, all the T cells do not express TRPA1 at resting state. Flow cytometry results confirmed that the expression level of TRPA1 was increased in ConA-activated and in TCR-activated T cells (Figure 3B,C).

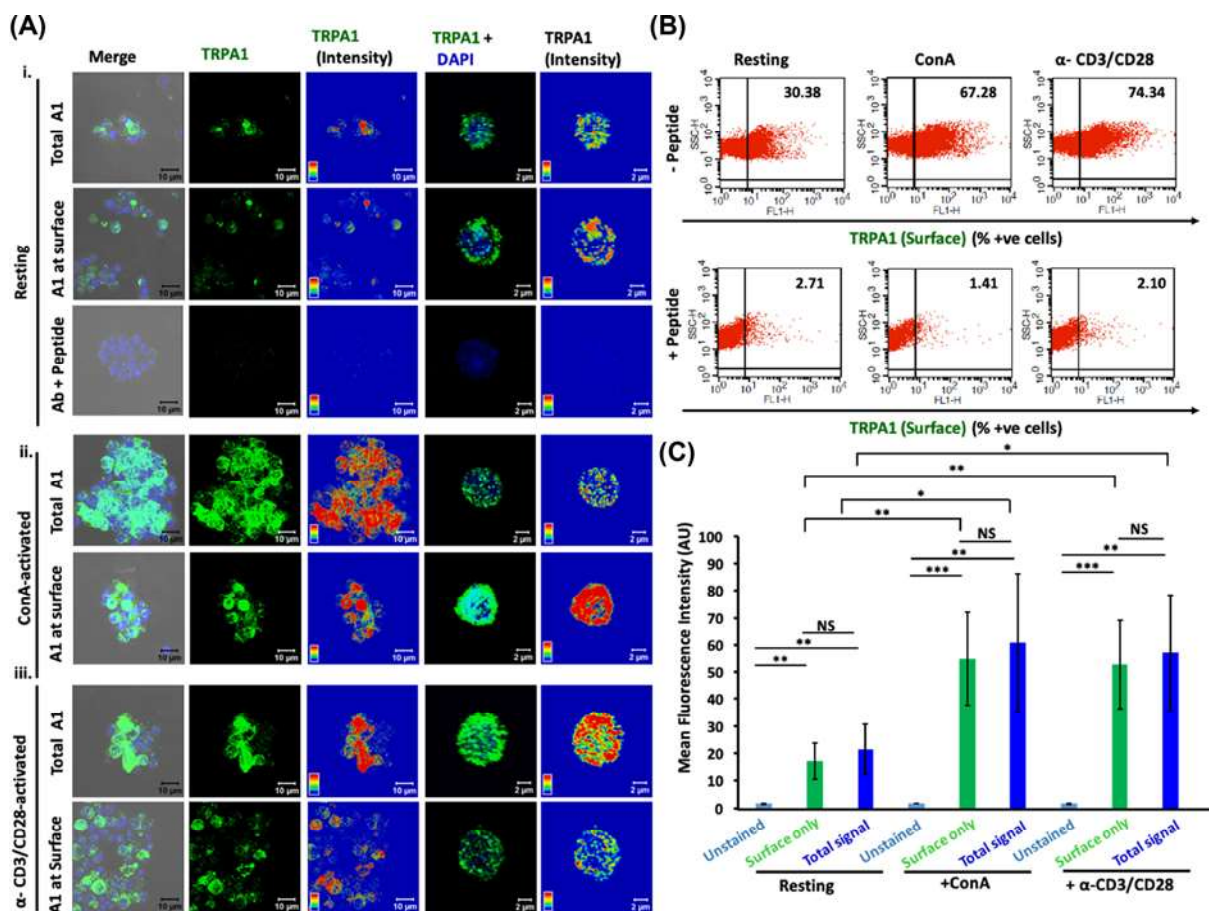


Figure 3. TRPA1 expression increases during murine T-cell activation

(A) Expression of TRPA1 is increased in activated T cells compared with the resting conditions. TRPA1 present at the surface only (in non-permeabilized cells) and in whole cell (in permeabilized cells) were probed. Triton X-100 permeabilized cells when stained with TRPA1-specific antibody pre-incubated with its antigenic peptide results in loss of TRPA1 signal, indicating the specificity of the antibody. Confocal images of purified CD3⁺ murine T cells stained with antibody detecting the extracellular loop of TRPA1 are shown. Both surface level and total expression of TRPA1 in resting cells (i), in ConA-activated cells (ii), and in α -CD3/ α -CD28-activated T cells (iii) are shown. Fluorescence intensity of the TRPA1 signal is indicated in rainbow scale (right panels). (B) Dot-plot values indicating the percentage of cells expressing TRPA1 at the surface. The number of TRPA1⁺ cells are much higher in activated conditions. This staining is completely blocked when the same antibody is pre-treated with its specific blocking peptide. (C) Mean fluorescence intensity determined by flow cytometry analysis reveal that ConA-activated and α -CD3/ α -CD28-activated T cells have higher levels of TRPA1 than the resting T cells. The difference in TRPA1 expression level (both in surface as well in whole cell) between resting stage with ConA-activated or α -CD3/ α -CD28-activated T cells are significant. The *P*-values are: ns, non-significant; *, <0.05; **, <0.01; ***, <0.001.

Similar to murine T cells, hPBMC-derived T cells also show TCR and ConA activation driven increased expression of TRPA1 (Figure 4A). The Z-section images showed an increase in TRPA1 at the surface on T-cell activation by ConA or TCR (Figure 4B). Moreover, we have also studied the expression of TRPA1 in resting and activated hPBMC-derived T cells and found that percent positive cells for TRPA1 was increased in activated T cells as compared with resting T cell (Figure 4C). However, we did not observe any marked change in the MFI of TRPA1 in hPBMC-derived T cell in resting and activated cells (Figure 4D). These qualitative and quantitative data strongly suggest that TRPA1 is endogenously expressed in T cells and increased surface expression of TRPA1 correlates with T-cell activation process.

TRPA1 activation induces increased Ca²⁺ level in T cells

In order to explore if the TRPA1 present in T cells are functional, we performed Ca²⁺-imaging experiments (Figure 5). For that purpose, we have used purified mouse T cells loaded with Fluo-4 AM. Live cell imaging revealed that

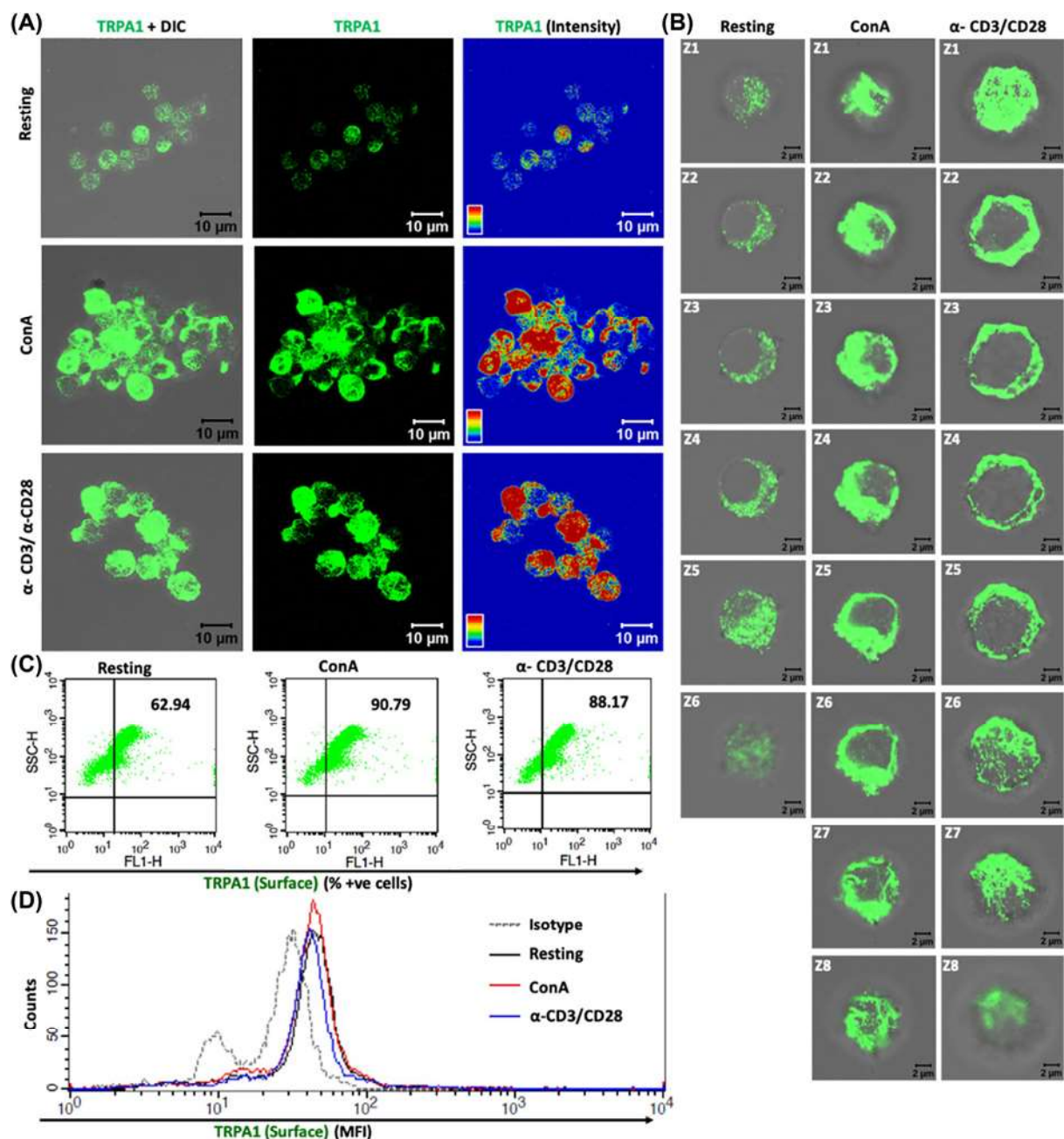


Figure 4. Human T cells show increased surface expression of TRPA1 upon activation

(A) Confocal imaging revealed that TRPA1 is endogenously expressed in purified CD3⁺ human T cells and TRPA1 expression increases in activated T cells. (B) Optical sections (Z1–Z8) of T cells reveal that TRPA1 is present mostly at or near the cell surface both in resting and in activated conditions. (C) Flow cytometry dot-plot values indicate that approximately 60% of human T cells are TRPA1⁺ under resting conditions while approximately 90% cells are TRPA1⁺ in immunologically activated state. (D) MFI for TRPA1 of hPBMC-derived T cells in resting, ConA, and TCR stimulated cells.

in the absence of any stimuli, there is no increase in Fluo-4 intensity in majority of the cells with respect to time. However, upon stimulation by TRPA1 activator AITC, intracellular Ca²⁺ level increases in most of the T cells (Figure 5A). This AITC-mediated increase in Ca²⁺ level was effectively blocked by TRPA1-specific inhibitors A-967079, and HC-030031 (Figures 5 and 6). Calcium chelation experiments with BAPTA-AM as well as by EGTA (present in extracellular media) suggest that TRPA1 regulates Ca²⁺ influx from both extracellular and intracellular reserves (Figure 6). Similarly, the level of intracellular Ca²⁺ goes down after adding the inhibitor in activator (AITC) treated cells (Figure

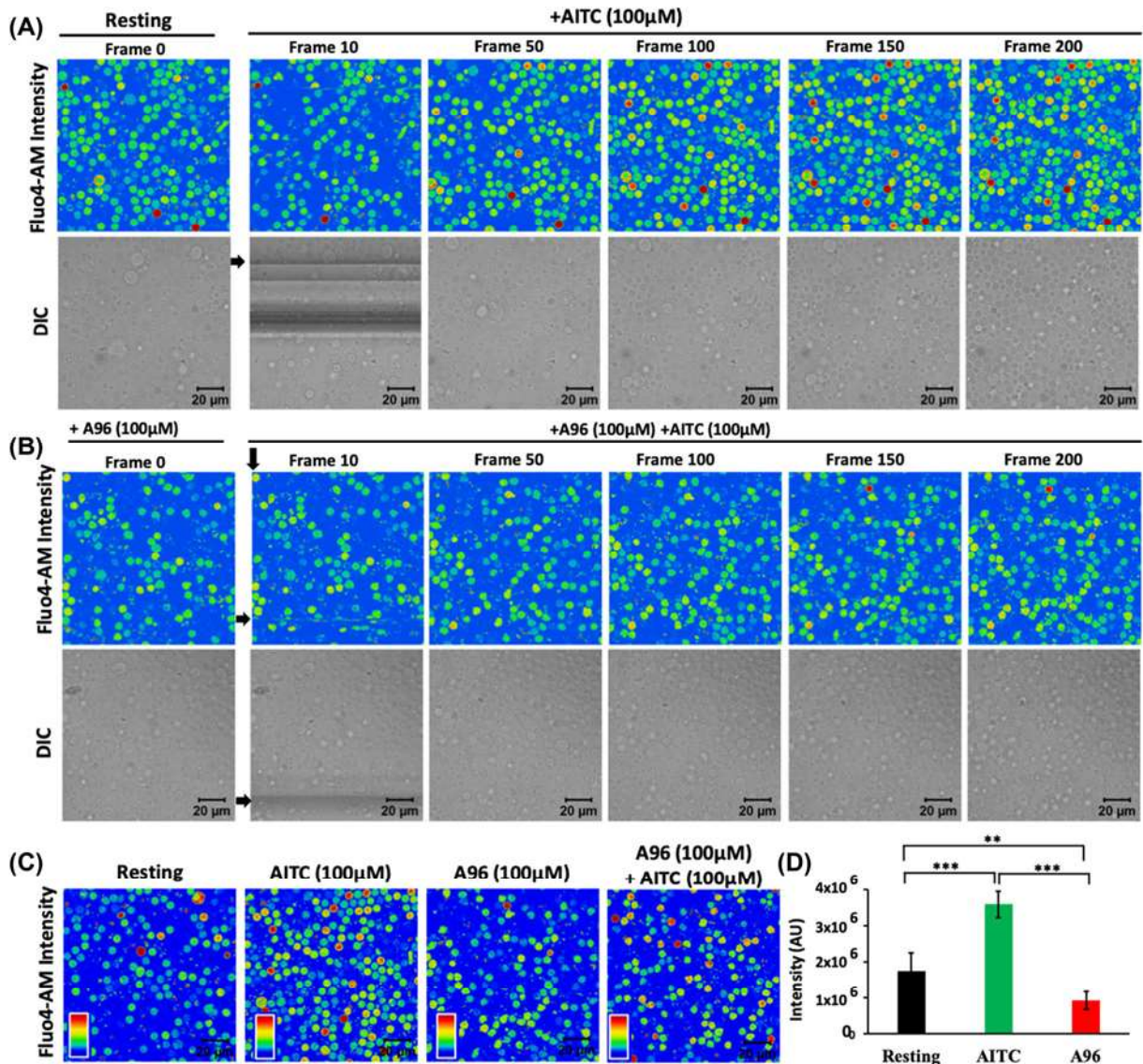


Figure 5. TRPA1 activation induces increase in intracellular Ca^{2+} levels in murine T cells

(A,B) Fluorescence intensity images derived from time-series imaging of view fields containing multiple cells loaded with Ca^{2+} -sensing dye Fluo 4-AM are depicted here. The time difference between each frame is 5 s. The cells were treated with different pharmacological agents at the 10th frame (F10). Activation of TRPA1 by its specific activator AITC (100 μM) causes increment in the Ca^{2+} level (A) which can be blocked by pre-incubating the cells with TRPA1-specific inhibitor A967079 (A96; 100 μM) for 30 min (B). (C) Fluo 4 intensity of T cells at resting stage or incubated with AITC (100 μM), A96 (100 μM), or combination of AITC (100 μM) and A96 (100 μM) for 12 h is shown. (D) Quantification of Fluo-4 intensity from six random fields after acquisition of 200 frames (~1000 s) of two independent experiments is depicted. AITC (100 μM) treatment significantly increases Ca^{2+} levels, while A96 (100 μM) treatment reduces intracellular Ca^{2+} levels below that of resting T cells. The *P*-values are: ns, non-significant; *, <0.05; **, <0.01; ***, <0.001.

6F). To confirm all these effects quantitatively, we compared the level of Ca^{2+} in T cells just before and after adding the TRPA1 modulatory drugs (Figure 6G). The analysis clearly suggests the changes in the fluorescence intensity in quick time. This confirmed that functional TRPA1 is expressed in T cells.

TRPA1 regulates TCR-mediated Ca^{2+} -influx during T-cell activation

TCR-mediated T-cell stimulation leads to increase in intracellular Ca^{2+} levels in T cells which is critical for optimum T-cell activation. As we have observed that TRPA1 activation initiates Ca^{2+} influx in T cells; hence we studied the effect

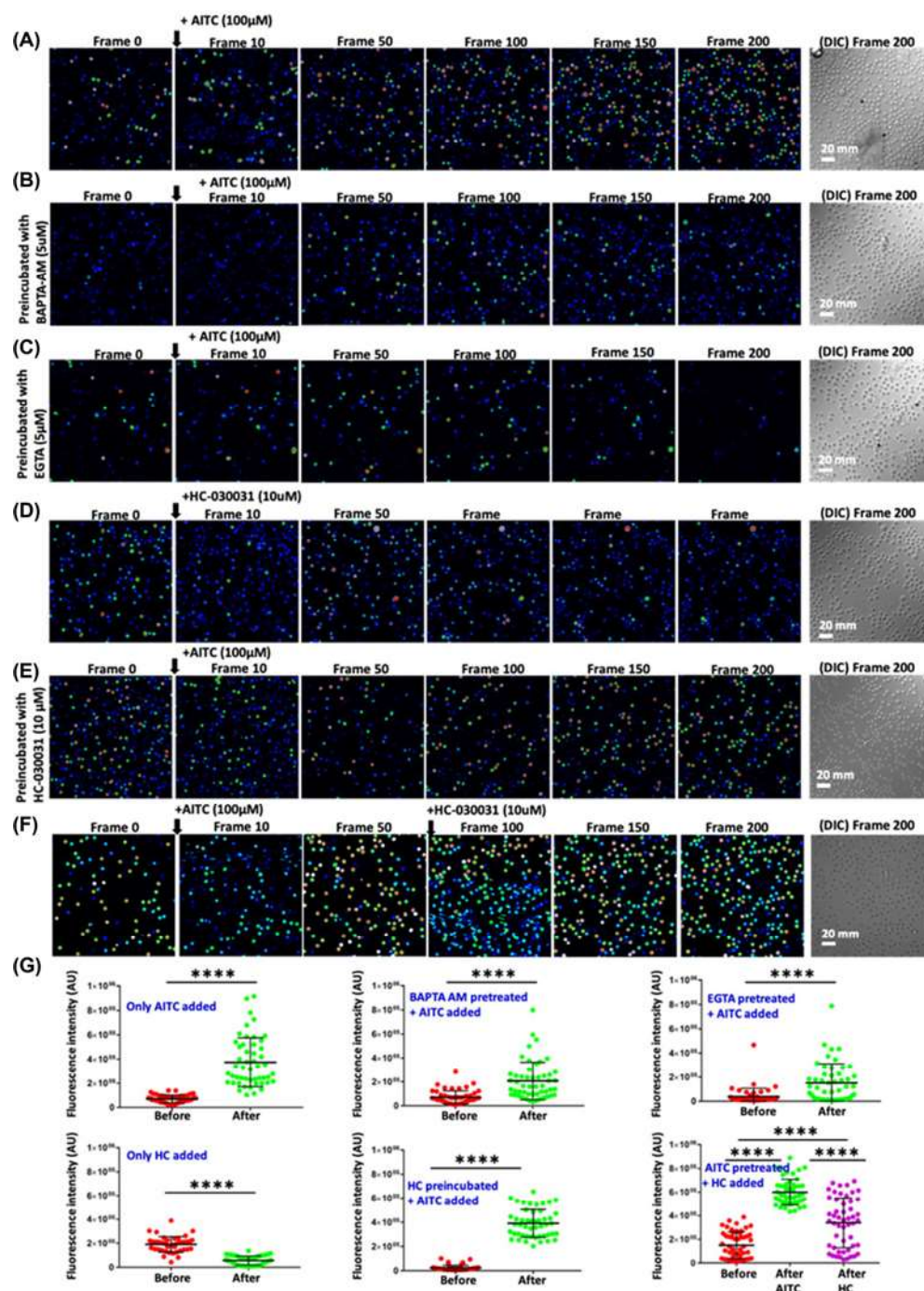


Figure 6. TRPA1 activation-induced increase in intracellular Ca^{2+} can be altered by Ca^{2+} -chelators and channel inhibitors
 Fluorescence intensity images derived from time-series imaging of view fields containing multiple cells loaded with Ca^{2+} -sensing dye Fluo 4-AM are depicted here. The time difference between each frame is 5 s. Untreated cells at resting stage or pre-incubated with specific Ca^{2+} -chelators or TRPA1 blocker. Activation of TRPA1 by AITC at the 10th frame causes increment in the Ca^{2+} level (A) which can be reduced by pre-incubating the cells with BAPTA-AM (intracellular Ca^{2+} -chelator) (B) or with extracellular Ca^{2+} -chelator (EGTA) (C). Application of HC-030031, another inhibitor of TRPA1 results in reduced intracellular level of Ca^{2+} (D). Application of AITC on population preincubated with HC-030031 fails to increase the basal Ca^{2+} levels (E). Application of HC-030031 after AITC results in initial rise (due to activation) followed by reduction (due to inhibition) in the basal Ca^{2+} levels (F). In each case, the DIC image represents the number and morphology of cells in the view-field at the end of the experiments (200th frame). (G) Quantification of basal Ca^{2+} levels in multiple cells before and after addition of TRPA1 modulatory agents. The maximum time gap between these two measurements is ~ 5 s. **** indicates P -value < 0.0001 . For more details see Supplementary Movies.

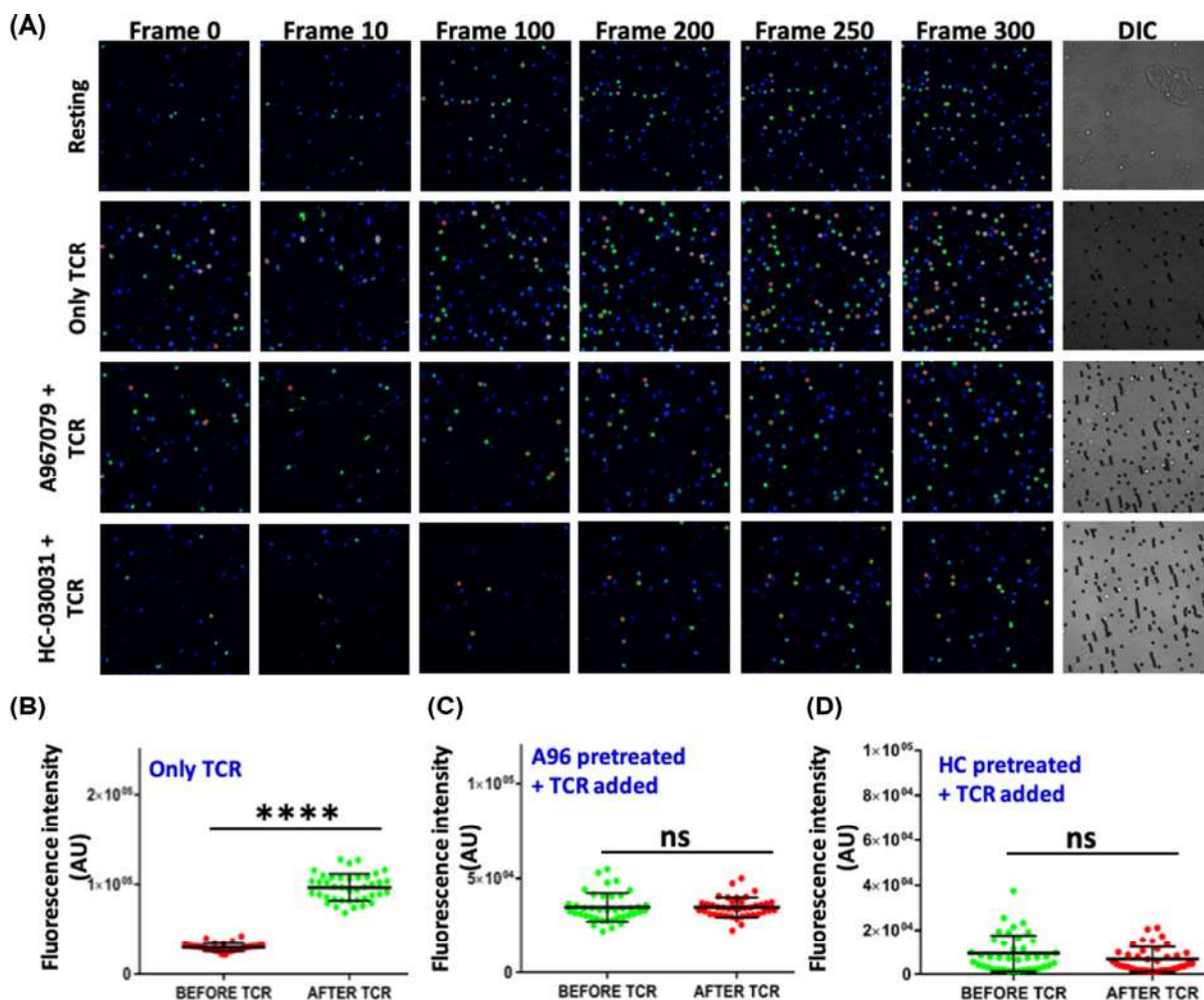


Figure 7. TRPA1 regulates TCR mediated Calcium influx

(A) Representative images in rainbow scale shows addition of α -CD3/CD28 (TCR) beads elevates Ca^{2+} levels in murine T cells compared with the resting T cells. Reduced Ca^{2+} levels observed in T cells treated with TRPA1 inhibitors A967079 and HC-030031 upon TCR-mediated stimulation. (B) Graph showing elevated calcium levels in T-cell population after addition of TCR beads. (C,D) Graph shows no significant change in calcium levels in A967079 and HC-030031 treated T cells after TCR beads treatment, respectively. **** $P < 0.0001$.

of TRPA1 inhibition in Ca^{2+} influx during TCR-mediated stimulation. TCR stimulation increased intracellular Ca^{2+} levels (Figure 7A,B), while TRPA1 inhibition by A-967079 and HC-030031 significantly reduced the TCR-mediated Ca^{2+} influx in T cells (Figure 7A,C,D).

TRPA1 is involved in ConA/TCR-mediated T-cell activation and effector cytokine secretion

In order to explore the role of TRPA1 in T-cell activation, we have activated the cells either by ConA or via TCR stimulation and probed for the expression of activation markers, namely CD25 and CD69 in the purified murine T cell (CD90^{2+}) population. The expression of these markers was probed after ConA treatment with or without TRPA1 channel modulators (Figure 8). Flow cytometric evaluation revealed a shift in the T-cell population expressing CD25 upon T-cell activation (in resting condition, $3.495 \pm 0.95\%$; in ConA-activated condition, $73.795 \pm 0.82\%$; in TCR-activated condition, $59.075 \pm 1.14\%$). Notably, in the presence of TRPA1 inhibitor (A-967079, $100 \mu\text{M}$), T-cell activation by ConA or TCR was significantly inhibited (Figure 8A,C). In this condition (after treatment with both ConA and A-967079), $27.87 \pm 0.41\%$ of the cells express CD25. Similar down-regulation was seen when cells were treated with TCR in combination with A-967079, where only $30.495 \pm 1.08\%$ T cells are found to be CD25^+ .

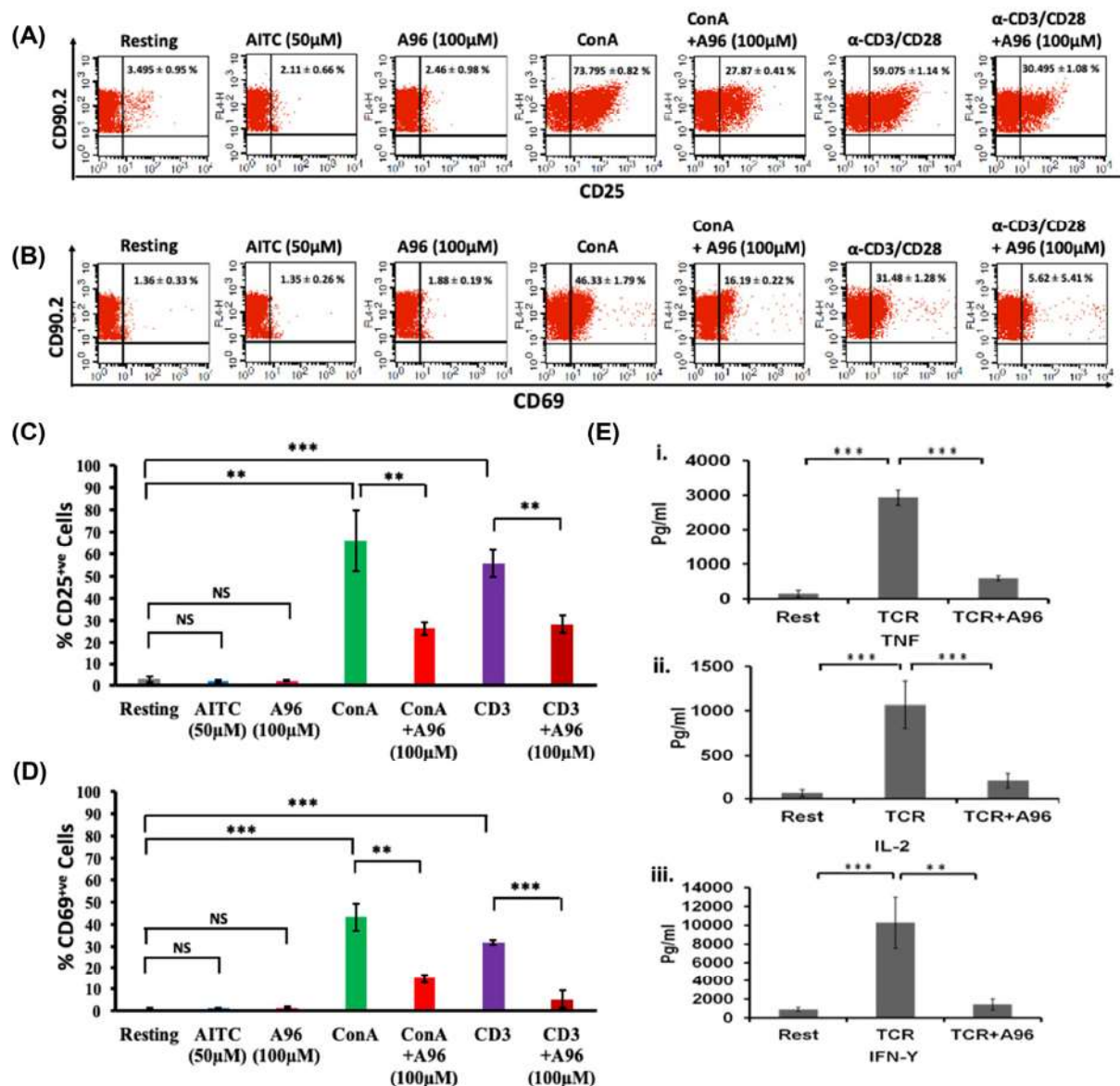


Figure 8. Pharmacological inhibition of endogenous TRPA1 blocks T-cell activation

(A,B) T-cell activation markers CD25 and CD69 were analyzed by flow cytometry after incubating the cells with TRPA1 modulators for 36 h. Inhibition of TRPA1 by A96 (100 μM) reduces the ConA-mediated activation. Treatment of murine T cells with AITC (50 μM) or A96 (100 μM) alone do not increase the % of CD25⁺ cells or % of CD69⁺ cells. The average number ± SD values of CD25⁺ or CD69⁺ cells are mentioned in the upper right corner of each dot-plot. Representative dot plots of three independent experiments are shown. (C,D) T cells treated with A96 (100 μM) along with ConA (5 μg/ml) or plate-bound α-CD3 (2 μg/ml) and soluble α-CD28 (2 μg/ml) have reduced percentage of CD25⁺ or CD69⁺ cells. The corresponding levels/intensity of CD25 or CD69 expression (determined from MFI values) in response incubation with indicated modulators are shown (n=3). (E) Graphical bars represent the concentration (in pg/ml) of effector cytokines TNF (i), IL-2 (ii), IFNγ (iii) released from T cells at approximately after 36 h. Incubation of TRPA1 inhibitor A96 (100 μM) along with plate-bound α-CD3 (2 μg/ml) and soluble α-CD28 (2 μg/ml) resulted in significant reduction in the release of cytokines TNF, IL-2 and IFNγ. The P-values are: ns, non-significant; **, <0.01; ***, <0.001 (n=3 independent experiments).

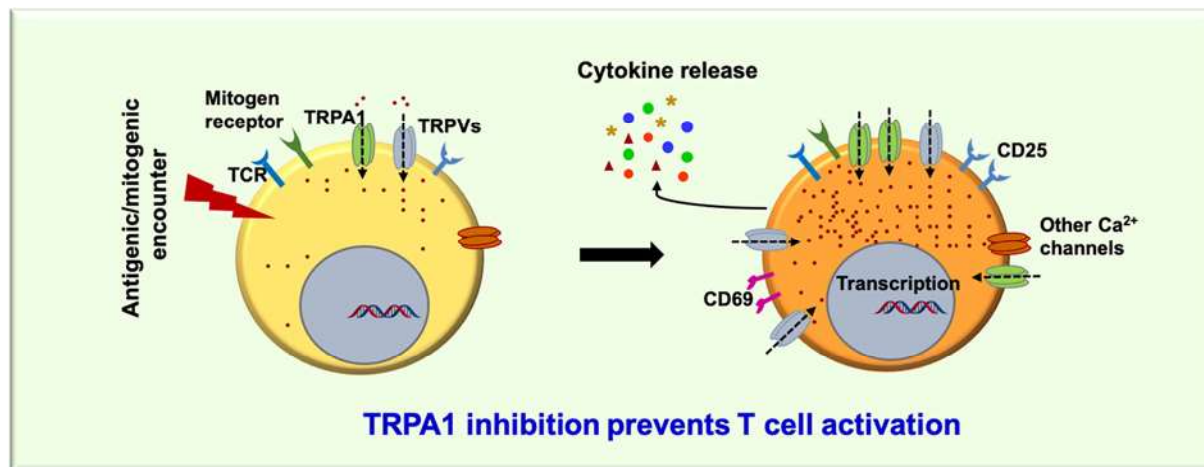


Figure 9. A proposed model for the expression and involvement of TRPA1 in T-cell activation

Both percentage of T cells and level of TRPA1 per cell increases during T-cell activation. TRPA1 activation mediates Ca^{2+} -influx to the cell. Inhibition of endogenous TRPA1 activity reduces the T-cell activation and release of certain cytokines. However, further investigation are needed to explore how TRPA1 regulates T-cell activation and cytokine release during T-cell activation process.

In a similar manner, TRPA1 inhibitor (A-967079) also reduced CD69 expression. The effect of TRPA1 inhibitor on CD69 expression was also reflected by the percentage of CD69 positive cells (in resting condition, $1.36 \pm 0.33\%$; in ConA-activated condition, $46.33 \pm 1.79\%$; in TCR-activated $31.48 \pm 1.28\%$) which was reduced after treating with the inhibitor (in combination of ConA and A-967079, $16.19 \pm 0.22\%$; in TCR and A-967079 combination, $5.62 \pm 5.41\%$) (Figure 8B,D).

T-cell activation involves an increased level of secretion of several effector cytokines like TNF, $\text{IFN}\gamma$, and IL-2. We explored the role of TRPA1 in the production of these cytokines by analyzing the culture supernatants by ELISA (Figure 8E). TCR-stimulation induced high levels of TNF (resting condition: 151.8 ± 94.88 pg/ml; TCR-mediated activated condition: 2931.98 ± 220.85 pg/ml) while inhibition of TRPA1 by A-967079 blocked the effect of these stimulators on TNF production (TCR + A-967079 combination: 597.74 ± 71.83 pg/ml) (Figure 8E). TRPA1 inhibition also blocked IL-2 secretion (resting: 62 ± 37.91 pg/ml; TCR: 1067.4 ± 267.003 pg/ml; TCR + A-967079 combination: 200.33 ± 83.25 pg/ml) (Figure 8E). Moreover $\text{IFN}\gamma$ production was down-regulated by A-967079 treatment (resting: 912.83 ± 216.20 pg/ml; TCR: 10279.5 ± 2702.65 pg/ml; TCR + A-967079 combination: 1421.72 ± 599.3 pg/ml) (Figure 8E).

Taken together, the results indicate that TRPA1 is expressed in T cells and may positively regulate T-cell activation and effector cytokine release.

Discussion

T-cell activation involves several distinct signaling events, and the influx of Ca^{2+} is vital during this process. However, so far only a few Ca^{2+} channels have been detected in T cells, whereas the identity of the major Ca^{2+} channels present in T cells is unknown. In addition, the mode of regulation of these channels and their exact role in the context of T-cell functions are mostly unknown. Although expression of TRPA1 in the peripheral sensory neurons and its involvement in the neural excitation has been widely demonstrated, limited information is currently available about the expression and role of TRPA1 in non-neuronal cells. In this work, the endogenous expression of TRPA1 in primary murine and human T cell was observed by using two different TRPA1 specific antibodies. Expression of TRPA1 was found to be mostly predominant at the surface of these cells rather than being present in intracellular regions. We also provided evidence for the functional role of TRPA1 in immune functions. Flow cytometric analysis coupled with confocal imaging conclusively suggested enhanced expression of TRPA1 (both at surface level and in total) in activated T cells as compared with resting conditions. TRPA1 activation by specific ligands leads to increased intracellular Ca^{2+} concentration in purified murine T cells, confirming that this channel is present in a functional form in resting T cells. Moreover TRPA1 inhibition down-regulated the Ca^{2+} influx during TCR-mediated T-cell stimulation.

TRPA1 can be activated by several means and also by endogenous factors. Though TRPA1 has been initially considered as a 'cold-activated ion channel', its true thermosensitive nature is debatable. For example, it has been shown

that TRPA1 is not directly gated by cold but rather gated by increased intracellular Ca^{2+} levels as a consequence of cooling [21]. Recently TRPA1 has been demonstrated as a sensor of noxious heat ($\geq 45^\circ\text{C}$) in association with two other heat sensors TRPV1 and TRPM3 [22]. Notably, animals where both TRPV1 and TRPA1 were knocked out, still continued to sense noxious heat, indicating that these channels are not essential and in the absence of TRPV1 and TRPA1, some other ion channel/s take/s up their function [22]. Further, it has been demonstrated that pharmacological inhibition of TRPA1 by HC030031 (100 μM) shows the same effect as TRPA1 knockout mice [22]. In these cases, at least in neuronal systems, any increase in neuronal firing or heat avoidance is observed in mice lacking TRPA1. This suggests that TRPV1 and TRPA1 act in synergistic manner, rather than TRPA1 inhibiting TRPV1 as proposed recently [23].

In this work, we demonstrated that functional TRPA1, a non-selective cation channel is expressed in the human and murine T cells. Our results suggest that TRPA1 plays an important role relevant to T-cell activation, much similar to that of two other heat sensors namely TRPV1 and TRPV4 reported by us earlier [16]. TRPA1 modulation by different endogenous factors are likely to play a major role in this process. The functional expression of TRPA1 in murine and human CD4^+ T cells has also been shown to regulate T-cell activation and having anti-inflammatory role as reported recently [23]. However, in contrast with these findings, so far majority of the previous reports have suggested a pro-inflammatory role of TRPA1 toward immune activation and/or inflammation [24]. TRPA1 has been considered as one of the critical regulators of neurogenic inflammation and neuropeptide release [25]. It has also been reported that TRPA1 is associated with inflammation and puritogen responses in dermatitis [26]. A recent paper has shown that both TRPV1 and TRPA1 are pro-inflammatory in nature and act in a similar manner (not antagonistic manner as claimed) [23] in DSS-induced colitis using TRPA1 and TRPV1 knockout mice [27]. The association of TRP channels toward inflammation and immunogenic responses has been largely found to be positively regulated during the immune-physiology of the cellular and systemic responses. TRPA1 has been reported to contribute to the inflammation-induced pain and is also associated with experimental colitis in mice models [26-30]. Taken together, our data are in line with majority of reports showing TRPA1 as a pro-inflammatory regulator.

Inhibition of TRPA1 by its specific inhibitor reduces TCR- and ConA-driven mitogenic activation of T cells. This suggests that TRPA1 might be involved in the signaling pathways toward T-cell activation. Thus, inhibiting TRPA1 activity has profound inhibitory effects on CD25 and CD69 expression together with the secretion of signature effector cytokines such as TNF, $\text{IFN}\gamma$, and IL-2. TNF production is associated with several pro-inflammatory responses [31]. Additionally TNF is shown to be a major mediator of different inflammatory disease conditions like colitis and rheumatoid arthritis (RA) [32,33]. TRPA1 channel expression is found to be increased in peripheral blood leukocytes of RA patients and associated with pain [34]. Moreover, it has been shown that TRPA1 facilitates TNF-directed inflammatory responses in various pathophysiological conditions and blockade of TRPA1 receptors may be beneficial in reducing TNF-induced chronic pain [35,36]. Functional role of $\text{IFN}\gamma$ as a signature Th1 cytokine is also implicated in pro-inflammatory responses and disease conditions like colitis [37]. However, there are some reports which suggest an anti-inflammatory role of $\text{IFN}\gamma$ in the mouse model of colitis as well [38,39]. Apparently, these reports may indicate that these cytokines may differentially regulate inflammatory responses in different disease conditions. Interestingly, we have found that during *in vitro* TCR activation the induction of signature Th1 and pro-inflammatory cytokines like IL-2, $\text{IFN}\gamma$, and TNF could be down-regulated by the TRPA1 specific inhibitor, A-967079. TRPA1^{-/-} CD4^+ T cells have been recently reported to produce higher IL-2 and $\text{IFN}\gamma$ but not TNF during TCR stimulation [23]. This difference with our data could be due to difference in the type of cells used or a complicated consequence of TRPA1 knockdown triggering compensatory roles by other ion channels in knockout animals. Also T cells derived from colitis-induced animals can be very different from naïve T cells isolated from healthy individuals.

Moreover, ConA and TCR stimulated induction of T-cell activation markers like CD25 and CD69 were also found to be down-regulated in presence of A-967079. TRPA1 inhibition not only prevents T-cell activation in the general CD3^+ T cells, but also in subsets of T cells like CD4^+ and CD8^+ T cells (data not shown). This role of TRPA1 in T-cell activation could be primarily due to its role in regulating intracellular Ca^{2+} levels in T cells. TRPA1 upon activation by its specific activator (AITC) was found to increase the Ca^{2+} levels, while two different inhibitors namely A-967079 and HC-030031 are able to reduce the intracellular Ca^{2+} levels. Therefore, it seems that during T-cell activation, TRPA1 becomes functional and shows augmented expression and executes immune-regulatory functions, whereas, inhibition of this channel inhibits T-cell activation. Recent report demonstrating the activation of TRPA1 by specific microRNA can also be relevant for T-cell activation [40]. While our current work confirms the functional expression of TRPA1 channel and its requirement toward T-cell activation, the involvement of this ion channel in T-cell activation process associated with inflammatory diseases needs further investigation (Figure 9).

In brief, our current findings demonstrated an *in vitro* T-cell activation directed functional expression and requirement of TRPA1 in T cells. This is in line with the earlier reports of inflammatory responses associated with the function of TRPA1 in various physiological systems. The current observation might have implication in the immunogenic and inflammatory role of T cell responses as well.

Acknowledgments

We gratefully acknowledge the support from the Imaging Facility, Flow Cytometry Facility of NISER and the Animal House Facilities of NISER and ILS, Bhubaneswar. AK is thankful to DBT-Ramalingaswami re-entry faculty fellowship programme (BT/HRD/35/02/2006).

Competing Interests

The authors declare that there are no conflict of interests associated with the manuscript.

Funding

The work was partly supported by the Council of Scientific and Industrial Research, Government of India [grant number 37/1675/16/EMR-II (to S.C.)], Department of Biotechnology, Government of India [grant number BT/PR8004/MED/30/988/2013 (to C.G.)] and Department of Science and Technology (SERB), Government of India [grant number SR/SO/040/2012 (to C.G.)].

Data Availability

All data generated during the present study are included in this published article.

Author Contribution

S.S.S., R.K.M., C.G., and S.C. conceived the idea and designed all the experiments. S.S.S., R.K.M., T.A., A.T., S.S., and P.S.K. performed all the experiments. S.S.S., R.K.M., A.T., T.A., S.S., P.S.K., A.K., C.G., and S.C. analyzed the data. S.S.S., R.K.M., C.G., and S.C. wrote the manuscript. C.G. and S.C. communicated the manuscript.

Abbreviations

AITC, allyl isothiocyanate; APC, antigen-presenting cell; BAPTA-AM, 1,2-bis(2-aminophenoxy)ethane-N,N,N',N'-tetraacetic acid tetrakis (acetoxymethyl ester); Ca²⁺, calcium ion; CD25, cluster of differentiation 25; CD69, cluster of differentiation 69; ConA, Concanavalin A; EGTA, ethylene glycol-bis(β-aminoethyl ether)-N,N,N',N'-tetraacetic acid; ELISA, enzyme-linked immunosorbent assay; hPBMC, human peripheral blood mononuclear cell; IFN γ , interferon- γ ; IL, interleukin; RA, rheumatoid arthritis; RT-PCR, reverse transcription polymerase chain reaction; TNF, tumor necrosis factor; TRPA1, transient receptor potential channel subfamily A member 1; TRPV, transient receptor potential cation channel subfamily vanilloid transient receptor potential Ankyrin1.

References

- 1 Wu, L.J., Sweet, T.B. and Clapham, D.E. (2010) International Union of Basic and Clinical Pharmacology. LXXVI. Current progress in the mammalian TRP ion channel family. *Pharmacol. Rev.* **62**, 381–404, <https://doi.org/10.1124/pr.110.002725>
- 2 Story, G.M., Peier, A.M., Reeve, A.J., Eid, S.R., Mosbacher, J., Hricik, T.R. et al. (2003) ANKTM1, a TRP-like channel expressed in nociceptive neurons, is activated by cold temperatures. *Cell* **112**, 819–829, [https://doi.org/10.1016/S0092-8674\(03\)00158-2](https://doi.org/10.1016/S0092-8674(03)00158-2)
- 3 Doerner, J.F., Gisselmann, G., Hatt, H. and Wetzel, C.H. (2007) Transient receptor potential channel A1 is directly gated by calcium ions. *J. Biol. Chem.* **282**, 13180–13189, <https://doi.org/10.1074/jbc.M607849200>
- 4 Kwan, K.Y. and Corey, D.P. (2009) Burning cold: involvement of TRPA1 in noxious cold sensation. *J. Gen. Physiol.* **133**, 251–256, <https://doi.org/10.1085/jgp.200810146>
- 5 Bandell, M., Story, G.M., Hwang, S.W., Viswanath, V., Eid, S.R., Petrus, M.J. et al. (2004) Noxious cold ion channel TRPA1 is activated by pungent compounds and bradykinin. *Neuron* **41**, 849–857, [https://doi.org/10.1016/S0896-6273\(04\)00150-3](https://doi.org/10.1016/S0896-6273(04)00150-3)
- 6 Feske, S. (2007) Calcium signalling in lymphocyte activation and disease. *Nat. Rev. Immunol.* **7**, 690–702, <https://doi.org/10.1038/nri2152>
- 7 Vig, M. and Kinet, J.P. (2009) Calcium signaling in immune cells. *Nat. Immunol.* **10**, 21–27, <https://doi.org/10.1038/ni.f.220>
- 8 Petho, Z., Balajthy, A., Bartok, A., Bene, K., Somodi, S., Szilagyi, O. et al. (2016) The anti-proliferative effect of cation channel blockers in T lymphocytes depends on the strength of mitogenic stimulation. *Immunol. Lett.* **171**, 60–69, <https://doi.org/10.1016/j.imlet.2016.02.003>

- 9 Trevisani, M., Siemens, J., Materazzi, S., Bautista, D.M., Nassini, R., Campi, B. et al. (2007) 4-Hydroxynonenal, an endogenous aldehyde, causes pain and neurogenic inflammation through activation of the irritant receptor TRPA1. *Proc. Natl. Acad. Sci. U.S.A.* **104**, 13519–13524, <https://doi.org/10.1073/pnas.0705923104>
- 10 Cruz-Orengo, L., Dhaka, A., Heuermann, R.J., Young, T.J., Montana, M.C., Cavanaugh, E.J. et al. (2008) Cutaneous nociception evoked by 15-delta PGJ2 via activation of ion channel TRPA1. *Mol. Pain* **4**, 30, <https://doi.org/10.1186/1744-8069-4-30>
- 11 Taylor-Clark, T.E., Ghatta, S., Bettner, W. and Udem, B.J. (2009) Nitrooleic acid, an endogenous product of nitritative stress, activates nociceptive sensory nerves via the direct activation of TRPA1. *Mol. Pharmacol.* **75**, 820–829, <https://doi.org/10.1124/mol.108.054445>
- 12 Cevikbas, F., Wang, X., Akiyama, T., Kempkes, C., Savinko, T., Antal, A. et al. (2014) A sensory neuron-expressed IL-31 receptor mediates T helper cell-dependent itch: involvement of TRPV1 and TRPA1. *J. Allergy Clin. Immunol.* **133**, 448–460, <https://doi.org/10.1016/j.jaci.2013.10.048>
- 13 Meseguer, V., Alpizar, Y.A., Luis, E., Tajada, S., Denlinger, B., Fajardo, O. et al. (2014) TRPA1 channels mediate acute neurogenic inflammation and pain produced by bacterial endotoxins. *Nat. Commun.* **5**, 3125, <https://doi.org/10.1038/ncomms4125>
- 14 Szklarczyk, D., Franceschini, A., Wyder, S., Forslund, K., Heller, D., Huerta-Cepas, J. et al. (2015) STRING v10: protein-protein interaction networks, integrated over the tree of life. *Nucleic Acids Res.* **43**, D447–D452, <https://doi.org/10.1093/nar/gku1003>
- 15 Raudvere, U., Kolberg, L., Kuzmin, I., Arak, T., Adler, P., Peterson, H. et al. g:Profiler: a web server for functional enrichment analysis and conversions of gene lists (2019 update). *Nucleic Acids Res.* **47**, W191–W198, <https://doi.org/10.1093/nar/gkz369>
- 16 Majhi, R.K., Sahoo, S.S., Yadav, M., Pratheek, B.M., Chattopadhyay, S. and Goswami, C. (2015) Functional expression of TRPV channels in T cells and their implications in immune regulation. *FEBS J.* **282**, 2661–2681, <https://doi.org/10.1111/febs.13306>
- 17 Chattopadhyay, S., O'Rourke, J. and Cone, R.E. (2008) Implication for the CD94/NKG2A-Qa-1 system in the generation and function of ocular-induced splenic CD8+ regulatory T cells. *Int. Immunol.* **20**, 509–516, <https://doi.org/10.1093/intimm/dxn008>
- 18 Goswami, C., Schmidt, H. and Hucho, F. (2007) TRPV1 at nerve endings regulates growth cone morphology and movement through cytoskeleton reorganization. *FEBS J.* **274**, 760–772, <https://doi.org/10.1111/j.1742-4658.2006.05621.x>
- 19 Levine, B.L., Mosca, J.D., Riley, J.L., Carroll, R.G., Vahey, M.T., Jagodzinski, L.L. et al. (1996) Antiviral effect and *ex vivo* CD4+ T cell proliferation in HIV-positive patients as a result of CD28 costimulation. *Science* **272**, 1939–1943, <https://doi.org/10.1126/science.272.5270.1939>
- 20 Kay, J.E. (1991) Mechanisms of T lymphocyte activation. *Immunol. Lett.* **29**, 51–54, [https://doi.org/10.1016/0165-2478\(91\)90198-J](https://doi.org/10.1016/0165-2478(91)90198-J)
- 21 Zurborg, S., Yurgionas, B., Jira, J.A., Caspani, O. and Heppenstall, P.A. (2007) Direct activation of the ion channel TRPA1 by Ca²⁺. *Nat. Neurosci.* **10**, 277–279, <https://doi.org/10.1038/nn1843>
- 22 Vandewauw, I., De Clercq, K., Muller, M., Held, K., Pinto, S., Van Ranst, N. et al. (2018) A TRP channel trio mediates acute noxious heat sensing. *Nature* **555**, 662–666, <https://doi.org/10.1038/nature26137>
- 23 Bertin, S., Aoki-Nonaka, Y., Lee, J., de Jong, P.R., Kim, P., Han, T. et al. (2016) The TRPA1 ion channel is expressed in CD4+ T cells and restrains T-cell-mediated colitis through inhibition of TRPV1. *Gut*
- 24 Gouin, O., L'Herondelle, K., Lebonvallet, N., Le Gall-Ianotto, C., Sakka, M., Buhé, V. et al. (2017) TRPV1 and TRPA1 in cutaneous neurogenic and chronic inflammation: pro-inflammatory response induced by their activation and their sensitization. *Protein Cell* **8**, 644–661, <https://doi.org/10.1007/s13238-017-0395-5>
- 25 Bautista, D.M., Pellegrino, M. and Tsunozaki, M. (2013) TRPA1: a gatekeeper for inflammation. *Annu. Rev. Physiol.* **75**, 181–200, <https://doi.org/10.1146/annurev-physiol-030212-183811>
- 26 Liu, B., Escalera, J., Balakrishna, S., Fan, L., Caceres, A.I., Robinson, E. et al. (2013) TRPA1 controls inflammation and pruritogen responses in allergic contact dermatitis. *FASEB J.* **27**, 3549–3563, <https://doi.org/10.1096/fj.13-229948>
- 27 Utsumi, D., Matsumoto, K., Tsukahara, T., Amagase, K., Tominaga, M. and Kato, S. (2018) Transient receptor potential vanilloid 1 and transient receptor potential ankyrin 1 contribute to the progression of colonic inflammation in dextran sulfate sodium-induced colitis in mice: links to calcitonin gene-related peptide and substance P. *J. Pharmacol. Sci.* **136**, 121–132, <https://doi.org/10.1016/j.jphs.2017.12.012>
- 28 Miampamba, M., Chery-Croze, S., Detolle-Sarbach, S., Guez, D. and Chayvialle, J.A. (1996) Antinociceptive effects of oral clonidine and S12813-4 in acute colon inflammation in rats. *Eur. J. Pharmacol.* **308**, 251–259, [https://doi.org/10.1016/0014-2999\(96\)00306-8](https://doi.org/10.1016/0014-2999(96)00306-8)
- 29 Engel, M.A., Becker, C., Reeh, P.W. and Neurath, M.F. (2011) Role of sensory neurons in colitis: increasing evidence for a neuroimmune link in the gut. *Inflamm. Bowel Dis.* **17**, 1030–1033, <https://doi.org/10.1002/ibd.21422>
- 30 Bautista, D.M., Jordt, S.E., Nikai, T., Tsuruda, P.R., Read, A.J., Poblete, J. et al. (2006) TRPA1 mediates the inflammatory actions of environmental irritants and proalgesic agents. *Cell* **124**, 1269–1282, <https://doi.org/10.1016/j.cell.2006.02.023>
- 31 Popa, C., Netea, M.G., van Riel, P.L., van der Meer, J.W. and Stalenhoef, A.F. (2007) The role of TNF-alpha in chronic inflammatory conditions, intermediary metabolism, and cardiovascular risk. *J. Lipid Res.* **48**, 751–762, <https://doi.org/10.1194/jlr.R600021-JLR200>
- 32 Popivanova, B.K., Kitamura, K., Wu, Y., Kondo, T., Kagaya, T., Kaneko, S. et al. (2008) Blocking TNF-alpha in mice reduces colorectal carcinogenesis associated with chronic colitis. *J. Clin. Invest.* **118**, 560–570
- 33 Matsuno, H., Yudoh, K., Katayama, R., Nakazawa, F., Uzuki, M., Sawai, T. et al. (2002) The role of TNF-alpha in the pathogenesis of inflammation and joint destruction in rheumatoid arthritis (RA): a study using a human RA/SCID mouse chimera. *Rheumatology (Oxford)* **41**, 329–337, <https://doi.org/10.1093/rheumatology/41.3.329>
- 34 Pereira, I., Mendes, S.J., Pereira, D., Muniz, T.F., Colares, V.L., Monteiro, C.R. et al. (2017) Transient receptor potential ankyrin 1 channel expression on peripheral blood leukocytes from rheumatoid arthritic patients and correlation with pain and disability. *Front. Pharmacol.* **8**, 53, <https://doi.org/10.3389/fphar.2017.00053>
- 35 Fernandes, E.S., Russell, F.A., Spina, D., McDougall, J.J., Graepel, R., Gentry, C. et al. (2011) A distinct role for transient receptor potential ankyrin 1, in addition to transient receptor potential vanilloid 1, in tumor necrosis factor alpha-induced inflammatory hyperalgesia and Freund's complete adjuvant-induced monoarthritis. *Arthritis Rheum.* **63**, 819–829, <https://doi.org/10.1002/art.30150>

- 36 Koivisto, A., Chapman, H., Jalava, N., Korjamo, T., Saarnilehto, M., Lindstedt, K. et al. (2014) TRPA1: a transducer and amplifier of pain and inflammation. *Basic Clin. Pharmacol. Toxicol.* **114**, 50–55, <https://doi.org/10.1111/bcpt.12138>
- 37 Ito, R., Shin-Ya, M., Kishida, T., Urano, A., Takada, R., Sakagami, J. et al. (2006) Interferon-gamma is causatively involved in experimental inflammatory bowel disease in mice. *Clin. Exp. Immunol.* **146**, 330–338, <https://doi.org/10.1111/j.1365-2249.2006.03214.x>
- 38 Sheikh, S.Z., Matsuoka, K., Kobayashi, T., Li, F., Rubinas, T. and Plevy, S.E. (2010) Cutting edge: IFN-gamma is a negative regulator of IL-23 in murine macrophages and experimental colitis. *J. Immunol.* **184**, 4069–4073, <https://doi.org/10.4049/jimmunol.0903600>
- 39 Jin, Y., Lin, Y., Lin, L. and Zheng, C. (2012) IL-17/IFN-gamma interactions regulate intestinal inflammation in TNBS-induced acute colitis. *J. Interferon Cytokine Res.* **32**, 548–556, <https://doi.org/10.1089/jir.2012.0030>
- 40 Sheahan, T.D., Hachisuka, J. and Ross, S.E. (2018) Small RNAs, but sizable itch: TRPA1 activation by an extracellular microRNA. *Neuron* **99**, 421–422, <https://doi.org/10.1016/j.neuron.2018.07.040>